Commissariat à l'énergie atomique

e-den

A Nuclear Energy Division
Monograph

# Nuclear fuels

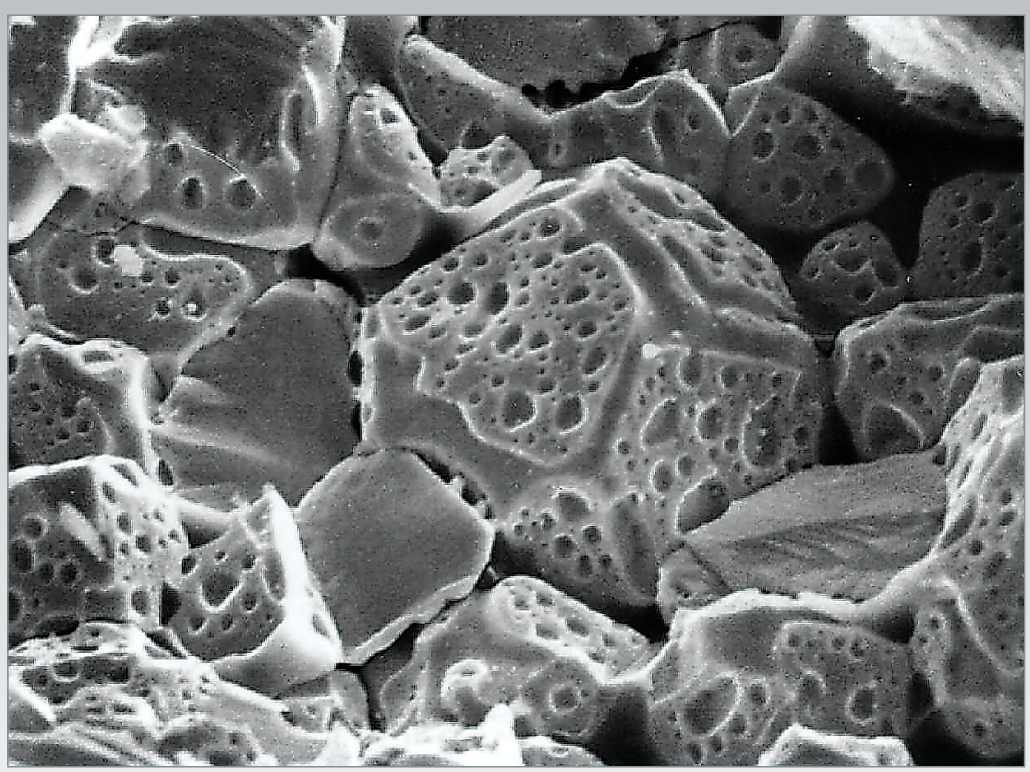

EDITIONS LE MONITEUR

**DEN Monographs**

A Nuclear Energy Division Monograph
Commissariat à l'énergie atomique,
91191 Gif-sur-Yvette Cedex (France)
Phone: + 33 (0)1 64 50 10 00



**Contributors to articles in this Monograph:**
Alain Ballagny, Jean-Luc Béchade, Bernard Bonin,
Jean-Christophe Brachet, Marc Delpech,Sylvie Dubois,
Gérard Ducros, Cécile Ferry, Michel Freyss, Didier Gilbon,
Jean-Paul Grouiller, Yannick Guérin, Daniel Iracane, Sylvie Lansiart,
Patrick Lemoine, Richard Lenain, Philippe Marsault, Bruno Michel,
Jean Noirot, Daniel Parrat, Michel Pelletier, Christophe Perrais,
Mayeul Phelip, Sylvie Pillon, Christophe Poinssot, Joëlle Vallory,
Carole Valot.

**Executive Publisher:** Philippe Pradel.

**Editorial Committee:** Bernard Bonin (Editor in chief),
Bernard Bouquin, Martine Dozol, Michaël Lecomte, Alain Vallée.

**Manager:** Fanny Bazile.

**Editor:** Jean-François Parisot.
**Layout:** Pierre Finot.

**English translation:** Jean-François Roberts

**Correspondence:** all correspondence to be addressed the Editor,
or to CEA/DEN Direction scientifique, CEA Saclay
91191 Gif-sur-Yvette Cedex (France).
Phone: + 33 (0)1 69 08 16 75



ISBN 978-2-281-11345-7
ISSN pending

Commissariat à l'énergie atomique

# e-den

A Nuclear Energy Division
Monograph

# Nuclear fuels

EDITIONS LE MONITEUR

# Foreword

*After getting off to a headlong start in the 1950s, when, for many, it embodied the hope of an inexhaustible source of energy, at a competitive cost, nuclear energy experienced, in the 1980s and 1990s, rejection by the majority public opinion, in a number of countries, in North America and Western Europe, followed by an abrupt check to its growth, and development.*

*Indeed, while the oil crises of 1973 and 1979 had heralded the launch of massive equipment programs, in a few countries hit heavily by the cost of oil imports – such as France, and Japan – they were paradoxically followed by a halt in investments in nuclear energy, in the United States initially, then in Western Europe. And yet, the strained oil markets that had prevailed only just recently, along with the first concerns as to a possibly impending depletion of natural resources should, by contrast, have bolstered such investments.*

*The reason for this interruption are doubtless manifold, though it was in part accounted for by the accidents at Three Mile Island, in 1979, and Chernobyl, in 1986, which made a considerable impact on public opinion. At the same time, pro-ecology movements, and the Green parties took up opposition to nuclear energy as one of the mainstays of their programs, widely echoed in this by the media.*

*In France, whereas the siting of nuclear power plants had – with one exception – never aroused much debate in the population, a mood of rejection emerged in the late 1980s, with the issue of nuclear waste. Faced with the increasing obstruction encountered by the French National Agency for Nuclear Waste Management (ANDRA), in its search for a site for an underground laboratory, the Government of the time decided to discontinue work on the operation, institute a one-year moratorium, and submit the issue to the Parliamentary Office for the Evaluation of Scientific and Technological Options (OPECST: Office parlementaire d'évaluation des choix scientifiques et technologiques).*

*By adopting most of the Parliamentary Office's recommendations, in particular the specification of a diversified research program, but equally with the initiation of a democratic debate, involving the populations concerned, the Act of 30 December 1991 on nuclear waste management greatly contributed to taking the heat out of the argument. Now, while it is nowadays generally agreed that long-term management of existing nuclear waste is a requisite, continuation of the French nuclear power plant program is still far from being assured: thus, the French Energy Act of 13 July 2005 simply stipulates that "the nuclear energy option is to be kept open up to 2020".*

*And yet, the coming century should involve the collective realization that meeting the energy needs of our generation may not be contemplated without taking on board respect for the environment, and preserving the rights of future generations to cover the selfsame needs. This is the concept of sustainable development, which our society, inescapably, will have to face up to.*

*The anthropic origin of global warming, due to the considerable increase in greenhouse gas releases, is no longer put in doubt nowadays. Only the consequences of that warming are still a subject for debate. Industrialized nations, being largely the root cause of the present situation, hold a particular responsibility, which should act as an incentive for them to*

*curb, in proactive fashion, emissions of such gases. Nuclear energy, exempt as it is, by its very nature, from this kind of emission, while having the capability to provide energy that is relatively plentiful, reliable, and economically competitive, should by rights be widely taken up.*

*The position in this respect is contrasted, across the world. On the one hand, some European countries, as Germany, or Belgium, have opted to phase out gradually the use of nuclear energy, even though no reversibility has been provided for, in this respect. On the other hand, countries such as China, South Korea, and, closer to France, Finland are investing heavily in development of this technology. At the same time, according to a recent statement by President George W. Bush, the United States are determined to launch, before the decade is out, programs for the construction of new nuclear power plants, a process that had been in abeyance for over 25 years.*

*In France, following the national energy debate, held in the first semester of 2003, the Strategic Orientation Act on energy, passed in June 2005, sanctioned the decision to build an EPR demonstrator reactor, to lay the ground for replacement of the power plants currently in service.*

*A number of signs are thus indicating that the "renaissance" of nuclear energy may be at hand, particularly if oil prices persistently remain pegged at levels of USD 70 per barrel, or more. Be that as it may, the future of nuclear energy, in France as in other countries, will largely depend on its ability to address, in requisite fashion, the two following concerns:*

*– the first concern has to do with social acceptance; it is essential that use of nuclear energy take place in optimum safety and security conditions, yielding a minimum amount of ultimate waste, while such waste must be perfectly controlled, in terms of its possible impact on health, and the environment;*
*– the second concern involves availability of resources; it is crucial that fuel supplies be guaranteed over the long term, by laying the ground for a switch to technology lines ensuring a better husbanding of natural fissile material, and, most importantly, less affected by market fluctuations.*

*These issues stand at the core of the remits CEA's Nuclear Energy Division is charged with. Indeed, the Division stands as a major player, in research work aimed at supporting the nuclear industry, with improvements in reactor safety, and competitiveness; providing the French Administration with options, regarding long-term nuclear waste management; and, finally, developing the nuclear systems of the future, chiefly fast-neutron reactors, affording highly promising improvements in terms of waste management, and raw material utilization.*

*As a staunch supporter of efforts to ensure the widest possible dissemination of scientific and technological knowledge, it strikes me as being of the utmost importance that such research work, drawing as it does on a wide spectrum of scientific disciplines, and often ranking as among the best of its kind worldwide, be set out, and explained to all those who wish to make up their own minds, regarding nuclear energy. Which is why I salute, with deep-felt satisfaction, the publication of these DEN Monographs, careful perusal of which will undoubtedly provide an incomparable wealth of information for their readers, of which, I hope, there will be many.*

*My thanks go to all those, researchers and engineers, who, through their contributions to this survey, have taken pains to share their experience, and knowledge.*

*Bernard BIGOT*
*High Commissioner for Atomic Energy*

# Fuel: the “consumable” in reactors

Within the core of nuclear reactors, fuel is where **fission*** processes occur, involving heavy atoms of uranium, or plutonium. Fuel provides the source for the heat which, ultimately, will allow generation of electricity, or indeed the production of energy for other applications.

Fuel is the consumable component in reactors: it is held a few years in the reactor, until it reaches its operating limits, whereas the reactors themselves have lifetimes of several decades. Over a reactor’s lifetime, fuel is the only component for which improved performance may be achieved, as and when refueling occurs. There is, further, a strong economic benefit to be gained by increasing its in-reactor dwell time, since it will yield more energy, for a comparable **cycle*** cost.

The term “fuel element” refers to the unit comprising the **fissile*** material, in the form as a rule of a stack of cylindrical pellets, and its cladding, this forming the first containment barrier for the nuclear materials. All of the design and dimensioning studies for fuel elements have the purpose of guaranteeing the resistance of that initial barrier, in the various operating situations. In the event of an accident situation, fuels are the main potential source of radioactive pollution in the environment; this aspect is, consequently, systematically taken on board in development work.

Understanding and modeling fuel in-reactor behavior involves very many areas of physics: **neutronics***, to specify the fission and transmutation nuclear reactions occurring inside the fuel; the physics of materials, to evaluate the damage caused to the crystal structure by neutrons, and, most crucially, by the dissipation of fission energy; thermics, to arrive at a precise evaluation of heat removal to the **coolant*** fluid, and to compute the evolution of the temperatures prevailing at every point; mechanics allows strains and stresses to be computed, in fuel pellets, and in the cladding, along with the risks of cladding failure; turning to thermodynamics makes it possible to evaluate the various compounds liable to be formed by the elements yielded by the fission nuclear reaction (these are known as “fission products” [FPs]: more than 10% of atoms found at the end of irradiation were not present at the beginning of the fuel’s life); solid-state chemistry considers the kinetics according to which the system, as a rule out of equilibrium conditions, evolves in nominal operating conditions, and during the various transients that may arise.

The purpose of investigation on nuclear fuels is to provide answers to two major sets of questions:

- What do we know, regarding current fuels for pressurized-water reactors (PWRs)? What are the limits for such fuels, and what is the development work that is required, if their performance is to be improved?

- What fuels will be needed for the reactors of the future?

A variety of materials have been used, or contemplated, as fuel materials, since the outset of nuclear reactor development work. Fissile **actinide*** isotopes have either been incorporated into stable metal alloys, or into refractory ceramics (oxides, nitrides, carbides, or silicides). Other, more complex materials, taking the form of cercer (ceramic–ceramic combinations) or cermet (ceramic–metal) composites, have also been investigated, and these concepts are currently being reassessed, for some of the reactors of the future. In the main, it is actinide oxides that have been used on an industrial scale, the world over, as fuel for power reactors. Metal alloys carry the drawback of a low melting temperature, moreover forming **eutectics*** that further bring that temperature down, entailing that their use be restricted to under 1,000° C. Oxides, on the other hand, are highly stable, and prove highly refractory, exhibiting melting temperatures higher than 2,500° C. Nevertheless, even though such oxides do adequately fulfill their function as fuel for the various reactors that have been around for over 40 years, they do not provide an ideal material, owing, in particular, to their relatively poor thermal conductivity. Other candidates, such as nitrides, or carbides, potentially more satisfactory in terms of thermal conductivity as they are, are nonetheless finding it very difficult to gain acceptance, since knowledge of their in-reactor behavior is, as a whole, too limited to guarantee a significant improvement, compared with oxide fuels.

In PWRs, the core consists of **assemblies*** of fuel **rods***, featuring a zirconium alloy cladding, holding uranium oxide pellets (with uranium enriched to ~ 4% U 235), or MOX pellets (mixed uranium–plutonium oxides [$(U,Pu)O_2$], with a Pu content of 5–10%). The choice of oxide as a fuel material emerged as the accepted solution for water reactors, for a variety of reasons, particularly owing to its quite satisfactory chemical compatibility with the coolant, in the event of failure of the first containment barrier.

**Burnup***, i.e. the energy extracted from fuel assemblies by the time they are discharged, has risen, over 20 years, from 33 GWd/t to 52 GWd/t. This amount remains low, considering the energy potential of the fissile material held in the fuel. The limitations are mainly of a technological character, and currently ongoing R&D is allowing these to be pushed back gradually: thus, the development, and qualification of a novel zirconium alloy (M5®, a zirconium–niobium alloy), to provide a cladding material that is more corrosion-resistant than Zircaloy 4, will make it possible to increase maximum burnup, from 52 GWd/t to 60 GWd/t. Likewise, the development, and qualification of a $UO_2$ fuel doped with chromium oxide, endowing it with better viscoplastic properties, while greatly increasing crystal grain size, should, in the longer term, make for enhanced reactor operating flexibility, while further raising burnup values.

Fuel R&D, conducted at CEA in close collaboration with its industrial partners, EDF and Areva, seeks to ensure that any evolution in fuels results in an advance with respect to nominal operation, but equally that it yields further margins as regards operating in accident conditions. Such advances entail an in-depth understanding of the physical, and chemical processes governing in-reactor fuel behavior. Such an understanding relies on modeling, duly validated by experiments.

R&D on fuels for the reactors of the future relates to a stage that is further out, the nature of the fuel considered being intimately bound up with the type of reactor involved, and relevant fuel cycle. Under the aegis of the Generation IV International Forum, which has launched investigations on new nuclear systems, priority is given to investigating fuels affording the capability to recycle part of their own waste (or even waste from previous generations), particularly the **minor actinides*** (neptunium [Np], americium [Am], curium [Cm]) yielded by the transmutation of uranium, and plutonium, during their stay inside the reactor. For that purpose, fast-neutron reactors, ensuring as they do the fission of these actinides, are the favored option.

In such fast-neutron reactors, or fast reactors (FRs), the operating conditions the fuel must meet are more severe than is the case in PWRs: **fissile*** material density has to be high, resulting in high specific power within the fuel pellet, operating temperatures higher than with PWRs, and significant damage caused by fast neutrons to metallic structures, particularly to fuel element claddings.

The situation, currently, is very much open: oxide ceramics still stand as a fuel to be reckoned with, oxide being a robust, proven material, particularly in view of its use in sodium-cooled fast reactors. However, the specifications set by fast reactors, particularly of the gas-cooled type, are an inducement to look for denser materials, exhibiting better conductivity, such as carbide or nitride ceramics, or metal alloys. These materials do afford advantages, compared to oxide, however they also involve drawbacks, which have to be weighed up. Ceramic–ceramic (cercer) or ceramic–metal (cermet) composite materials also stand out as potential candidates, however they do require major development work. Likewise, as regards cladding and structural materials, subjected as these are to a powerful neutron bombardment, the quest for high temperatures is pushing against the operating limits of known alloys, and will necessitate innovations.

With respect to such fuels of the future, the innovations concern not just the nature of the materials involved, but also the prevailing concepts, leading to a reassessment of the benefits that might accrue from a departure from conventional concepts, relying on the principle of a fuel pellet held in a cylindrical cladding. In particular, the particle fuel concept, as used in HTR reactors, has been revisited; and dimensioning studies for gas-cooled fast reactors are bringing forward some highly innovative concepts, such as macrostructured plates, in which the fissile material is inserted into a honeycomb-shaped ceramic.

The challenges relating to nuclear fuels are many. This monograph surveys the state of knowledge as regards in-reactor behavior, operating limits, and the avenues for R&D, as regards improving the performance of current fuels, and developing novel fuels for the reactors of the future.

While making no claims to exhaustiveness, the present monograph also provides illustrations from ongoing research, setting out some notable results, recently obtained.

**Yannick Guérin,**
*Fuel Research Department*

# What are the features of water reactor fuel?

## What is the purpose of a nuclear fuel?

The design goals for a nuclear fuel may be summed up by the following criteria:

- delivering the power anticipated from the reactor, throughout the planned irradiation **cycles***; the fuel must thus allow heat removal, while ensuring core reactivity in the reactor;
- confining fission products within the fuel element, in normal operating conditions, as in incident and accident conditions (within the dimensioning envelope);
- ensuring optimum utilization of fissile material, to achieve the most economical cycle cost.

This entails technical and technological requirements:

- as to the power released per unit volume (typically, this stands at around 400 W/cm$^3$ fuel, for current water reactors);
- high reliability, combined with a long lifespan: the fuel assembly, its structure, and constituent rods must be able to withstand, failure free, the entire in-reactor dwell time, currently set at 4–5 years, the aim being to achieve 6 years by 2010. The choice of constituent materials for the **assembly*** structure, and **cladding*** must thus take into account their irradiation and corrosion resistance;
- fuel imperviousness. In incident or accident situations, safety requires that nuclear materials remain confined; the fuel rod cladding forms the first containment barrier (the other two barriers being the primary circuit, and the containment enclosure);
- even though, in extreme accident conditions, cladding failures may not be prevented, and should the assembly structure become distorted, it should still be possible to ensure its ongoing cooling;
- despite such performance requirements, the fuel assembly must remain simple: simple to fabricate, simple to handle, simple to transport, simple to repair, and, after use, simple to store. There is the further requirement, in France in particular, that it should be "reprocessable," i.e. it must be possible to recover the uranium and plutonium elements still affording some energy potential.

## Ceramic fuel

In ordinary-water (light-water) reactors, the fissile material comes in the form of polycrystalline $UO_2$ oxide (or $UO_2$–$PuO_2$ oxide, in the MOX fuel case). Chemically stable, and compatible with water, these oxides prove highly resistant to high temperatures, and irradiation; the oxygen in the oxide is a weak neutron absorbent, and the oxide crystallites achieve good fission product retention, while retaining their cubic crystal structure.

The uranium oxides (UOX), or mixed uranium and plutonium oxides (MOX) used as fuel are single-phase, relatively dense (about 95% of theoretical density) polycrystalline materials, consisting of small dioxide grains a few micrometers across. Actinide dioxides exhibit a structure of the fluorite type, crystallizing in a face-centered cubic form, with respect to the actinide lattice. Such $UO_{2+x}$ or $(U_{1-y}Puy)O_2 + x$ dioxides accommodate large deviations from stoichiometry, corresponding to the presence of vacancy-, or interstitial-type point defects: $0 \leq x \leq 0.25$ for UOX, $-0.25 \leq x \leq 0.25$ for MOX, at ambient temperature. Such deviation from stoichiometry, strongly influencing as it does the properties exhibited by the fuels, must thus be specified, and adhered to during fabrication. Stoichiometric uranium dioxide ($x = 0$) allows the substitution of uranium by plutonium at crystal sites in any proportion ($0 \leq y \leq 1$), and the mixed oxide thus exists with every variation in plutonium content. However, when the oxide ceases to be stoichiometric, the possibilities for substitution become much more restricted, and, for plutonium contents higher than 40%, the oxide as a rule turns into a two-phase material. Finally, the $UO_{2+x}$ or $(U_1 - {}_yPu_y)O_2 + x$ cubic dioxide stands as one phase in the U–O–Pu system, among many others. Any large variation in oxygen content, or, more accurately, in the O/(U + Pu) ratio, results in phase changes, the most common phases being $(U_{1-y}Pu_y)_3O_8$ and $(U_{1-y}Puy)_4O_9$. These new phases may be observed during the fuel cycle, in particular as the oxygen potential varies.

## Fuel rods

The oxide is conditioned in the form of sintered pellets (with a height, and diameter of about 1 centimeter, the height being greater than the diameter).

The pellets are stacked inside a metallic cladding tube, this having the purpose of containing fission products, ensuring

mechanical support for the pellets, and allowing the removal, to the coolant fluid, of the heat generated by nuclear reactions. The unit as a whole, known as a “fuel rod”, has a length of some 4 m, with a diameter of around 1 cm.

Aside from the stacked pellets, and cladding tube, the rod comprises two welded endplugs, a plenum (or expansion chamber) to accommodate the fission gases released, and a spring, located inside the plenum, holding the fuel column in position. The rod is filled with helium, at a pressure of about 25 bars, to compensate, in part, for the outside pressure, in the primary circuit (155 bars in PWRs).

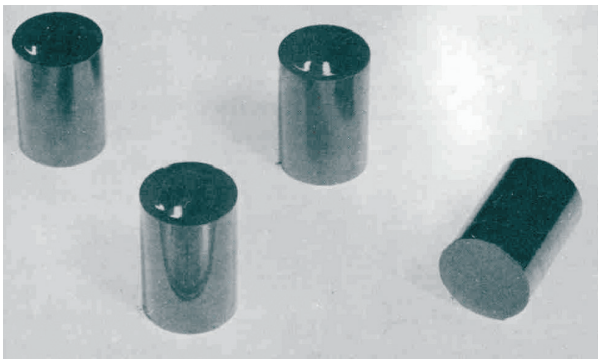

Fig. 1. Fuel pellets.

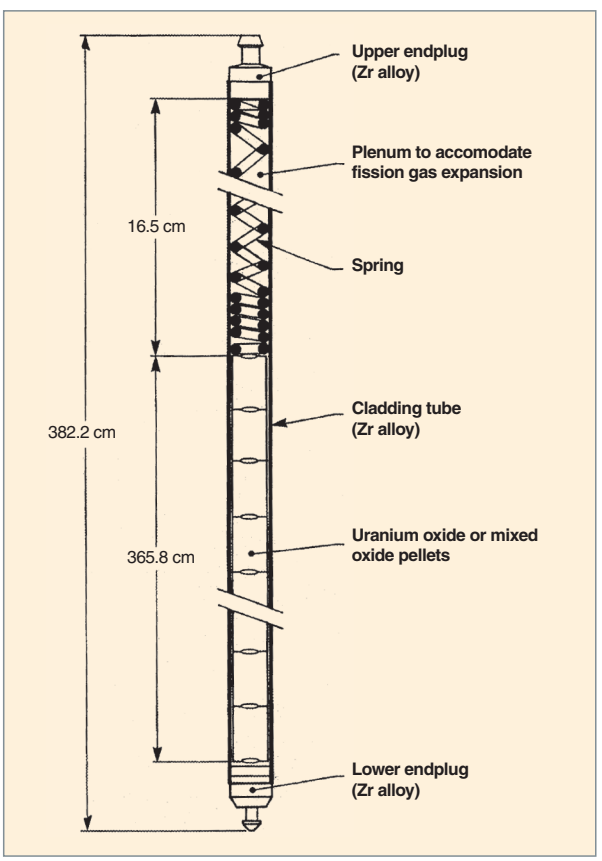


Fig. 2. Schematic of a fuel rod
(showing the dimensions for a 900-MW PWR rod).

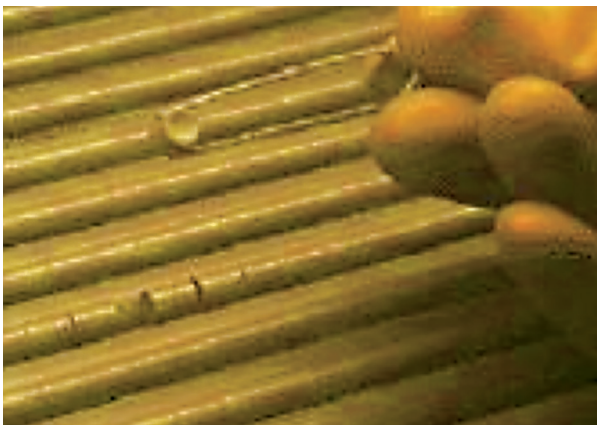

Fig. 3. MOX fuel pellets, readied for cladding.

The cladding material is a zirconium alloy, selected for its transparency to neutrons, mechanical properties, and corrosion resistance. The most commonly used alloy, to date, in PWRs, has been Zircaloy 4, however currently this is being replaced by new zirconium–niobium-based alloys, exhibiting better corrosion resistance (see chapter on “Cladding and assembly materials”).

## PWR fuel assemblies

The rods are brought together to form a “fuel **assembly***”, in which they are positioned in a square-mesh array, being held in a “structure” ensuring, in particular, mechanical support.

This geometrical layout allows the circulation of water in between rods, and thus the removal from the core of the heat generated within the reactor core. In a pressurized-water reactor, this structure is open, and water may circulate transversely across the assemblies.

**PWR*** assemblies feature a structure comprising an upper and a lower end fitting (known as the top nozzle, and bottom nozzle), and guide tubes, to which are attached the spacer grids, holding the fuel rods in place (and serving to mix the coolant fluid).

The absorber rods in the control clusters slide within the guide tubes. One guide tube is set aside to hold core instrumentation.

The grids, welded onto the guide tubes, ensure, by means of springs and dimples (see Fig. 6), fuel rod support, and spacing. They further carry vanes, allowing improved mixing of fluid streams, thus enhancing the assembly’s thermal–hydraulic performance.

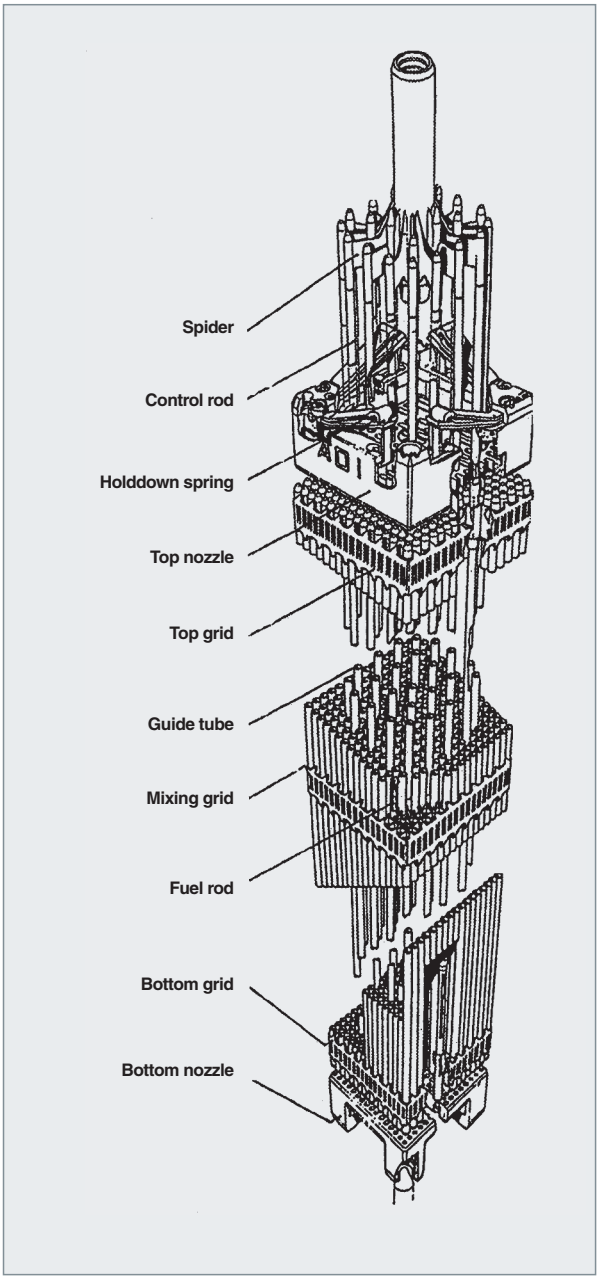


Fig. 4. Schematic of a 17 x 17 PWR fuel assembly and control bundle.

The bottom nozzle features a debris mitigation device, to catch traveling foreign bodies, which had formed, at one time, the chief cause of cladding failure. The top nozzle ensures the assembly handling function.

## BWR fuel assemblies

In a boiling-water reactor (**BWR***), by contrast to what is the case in PWRs, the assembly structure is closed, each rod bundle being enclosed in a casing, precluding any transverse exchange.

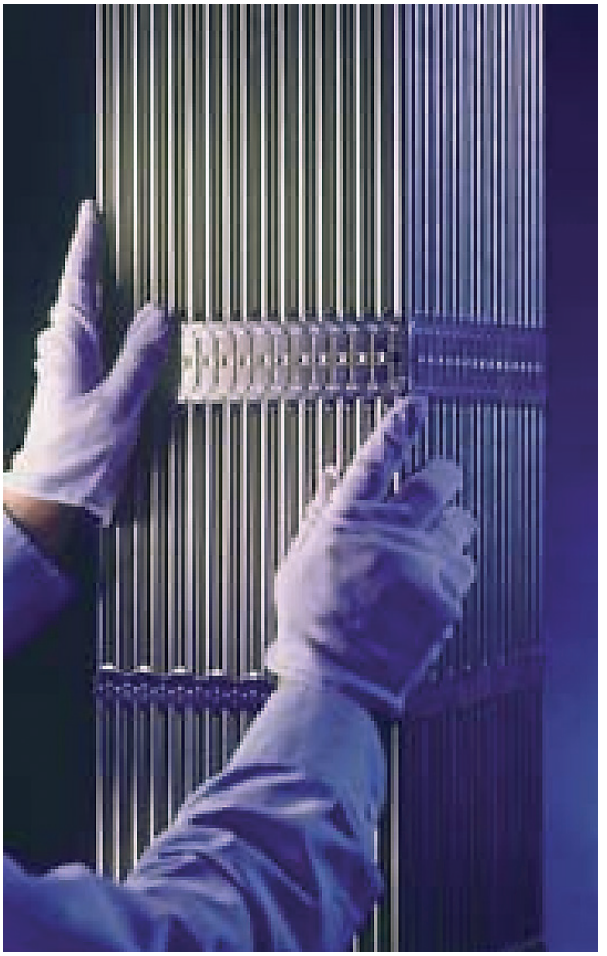

Fig. 5. Photograph of part of a PWR assembly at the control stage.

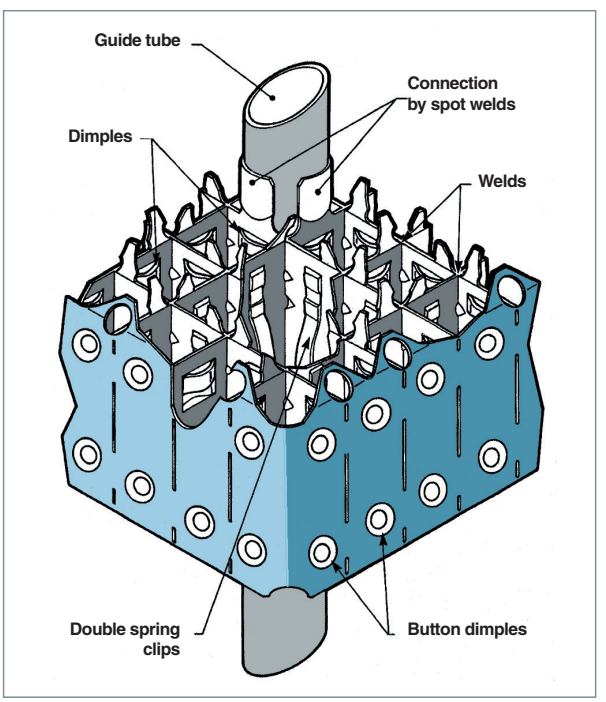


Fig. 6. Schematic of an AFA2G assembly grid (AREVA).

BWR fuel assemblies feature a casing, or box, carrying out the functions of hydraulic channel, core mechanical support, fuel handling unit, and guide for the cruciform control rods (which are inserted between four channel boxes).

The other structural components ensure similar functions to those of PWR assemblies.

**Yannick Guérin,**
*Fuel Research Department*
**and Bernard Bonin,**
*Scientific Directorate*

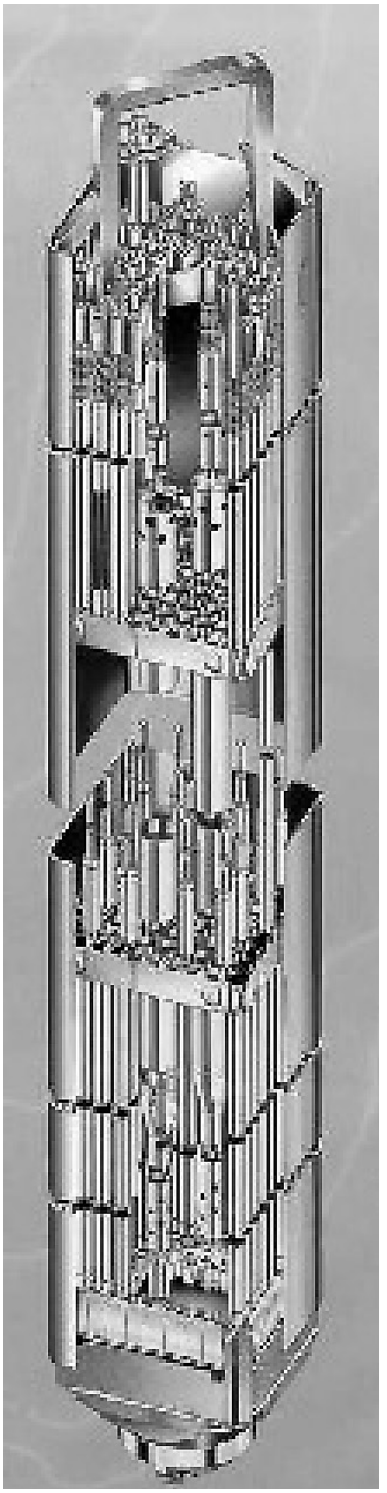

Fig. 7. Schematic of a BWR fuel assembly.

# Fabrication of water reactor fuels

Nearly all water reactor fuels (for both PWRs and BWRs) are enriched-uranium-based (3–5% U 235); in some countries – in France, in particular – mixed oxide (MOX: $UO_2$–$PuO_2$) fuels are also made, allowing the recycling of plutonium.

The fabrication of fuel elements involves a number of distinct steps:

- fabrication of the materials (zirconium alloys in particular), and components: cladding tubes, and structural components;
- preparation of the (enriched $UO_2$) or ($UO_2$ and $PuO_2$) powders;
- pellet fabrication: cylindrical pellets are pressed into shape, and subjected to **sintering***, i.e. baked into ceramic form;
- rod fabrication: the pellets are inserted, and the rod is sealed;
- completion of the assembly, and storage.

## Fabrication of $UO_2$ pellets

Oxide fuel comes in the form of cylindrical pellets, about 1 cm in height and diameter. Such pellets are fabricated by powder metallurgy, from enriched uranium oxide powder.

Uranium enrichment is carried out by way of the gaseous $UF_6$ molecule. The uranium fluoride is then turned into uranium oxide by means of a dry **conversion*** process (i.e. involving only gas-to-gas or solid–gas reactions):

$UF_6 + 2\ H_2O \rightarrow UO_2F2 + 4\ HF$ (hydrolysis)
$UO_2F_2 + H_2 \rightarrow UO_2 + 2\ HF$ (reduction)

The full process involves use of an integrated facility, comprising, at the head end, a hydrolysis reactor, followed by a rotary kiln, inside which defluorination is effected by reductive pyrolysis, resulting in the formation of uranium dioxide powder.

The powder thus obtained has a specific surface area of around 2 $m^2/g$, sufficiently small to endow it with outstanding stability (no risk of **pyrophoricity***, and little change over time in the O/U ratio), and at the same time large enough to result in good sinterability (a density of 98% may be obtained when such a powder is sintered, with no additives).

The target density, for pellets, is 95% of theoretical density; indeed, a high value is required, if adequate pellet stability is to be guaranteed (low in-reactor redensification), however, the aim is also to maintain a few percent porosity, to help the pellet accommodate its own irradiation swelling. The target density is achieved by adding to the $UO_2$ powder a pore-forming product, and a proportion of $U_3O_8$. This very fine $U_3O_8$ powder is yielded by calcination of fabrication scraps (oxidation of $UO_2$ in air at 350° C); its presence acts on pellet ultimate density, and further makes for increased mechanical strength in the compacted pellet blanks (UROX process).

Dry route $UO_2$ powder exhibits inadequate pourability, for the purposes of filling pressing dies. A granulation step must thus resorted to, involving compacting the powder at low pressure, the briquettes thus obtained then being fractured, and the granules "spheroidized," by working them in a blender. A lubricant may be added to the powder, up to a content of 0.2–0.3%, to facilitate pressing of the "green" (uncured) pellets, these exhibiting a density of 5.9–6.3 $g/cm^3$.

The green pellets are placed in molybdenum boats, and sintered for 4 hours at 1,700° C in a reducing atmosphere (hydrogen), in a continuous furnace. Subsequent to sintering, the pellets (exhibiting slight hourglassing) are rectified by grinding, to ensure a cylindrical shape, and achieve the specified diameter, to ± 10 microns or so.

To guarantee compliance with specifications, a large number of checks, be they systematic controls, or through sampling, are carried out at the end of each fabrication step:

- visual inspections: pellets must exhibit no chipping;
- dimensional controls: diameters, length, taper, dishing, chamfers;
- measurement of hydrostatic and geometric density (very low open porosity: < 0.1%);
- chemical assays: O/U, impurities, U 235 or Pu content;
- thermal stability test (24 hours' annealing at sintering temperature), to verify that any additional densification occurring during the test remains low.

Checks are also carried out to arrive at the values for certain quantities, even though they are not specified. Thus, metallographs (see Fig. 8) allow ceramic grain size to be ascertained (as a rule, around 10 µm), along with the morphology of residual porosity.

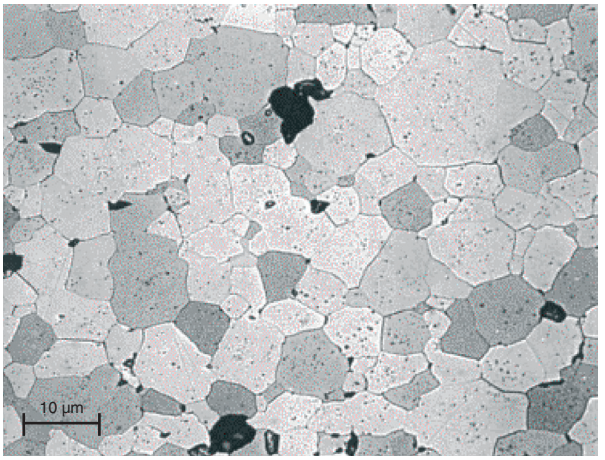


Fig. 8. Micrograph of $UO_2$ ceramic, after chemical etching, revealing grains.

## Fabrication of MOX (mixed uranium–plutonium oxide) pellets

Subsequent to the reprocessing of irradiated $UO_2$ fuel, partitioning of uranium from plutonium results in plutonium being obtained in oxide form ($PuO_2$); this plutonium oxide is obtained by calcination at 450° C of the oxalate yielded by the precipitation of plutonium nitrate by oxalic acid. The $PuO_2$ powder (see Fig. 9) exhibits a large specific surface area (> 6 $m^2/g$).

The fabrication process used in the MELOX plant, in France (and previously in Belgium), for the purposes of MOX production, is the MIMAS (MIcronized MASter Blend) process: a master blend of $UO_2$ and $PuO_2$ powders (with a $PuO_2$ content of 25–30%) is ground in a ball mill; an intimately mixed blend is thus obtained of the two, very fine powders, which are able to reagglomerate. The blend is then subjected to forced sieving, making for the guaranteed absence of large agglomerates, then diluted with $UO_2$ – fabricated either by the dry route, as outlined above, or through a wet route process, from uranyl nitrate – to achieve the target plutonium content (5–10%) (see Fig. 10).

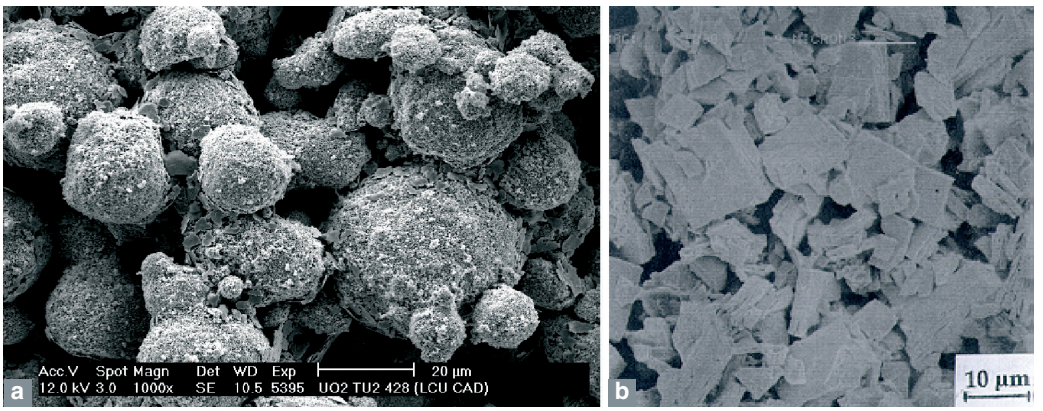


Fig. 9. SEM photographs, showing agglomerates of $UO_2$, and $PuO_2$ powders, as currently used for the fabrication of MOX fuels at the MELOX plant. a. $UO_2$ powder. b. $PuO_2$ powder.

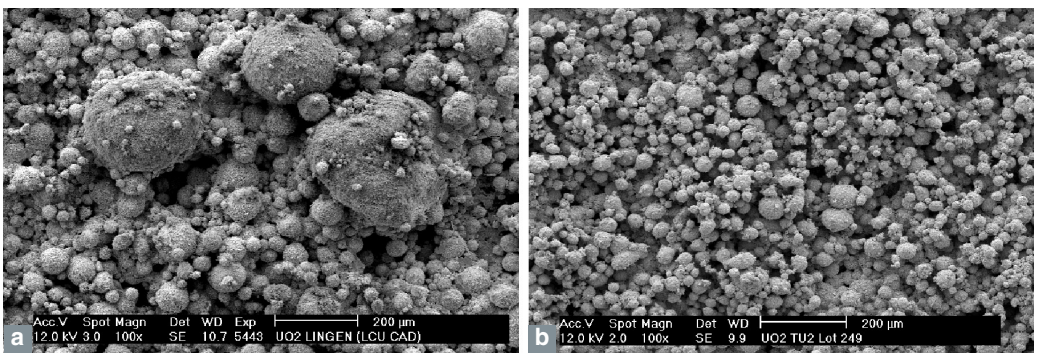


Fig. 10. SEM photographs, showing agglomerates of $UO_2$ powders. a. Dry route $UO_2$ powder (Areva ANF). b. Wet route $UO_2$ powder.

There are other processes for the fabrication of mixed uranium–plutonium oxide pellets, in particular the process involving the blending of $UO_2$ and $PuO_2$ powders directly to the desired plutonium content. In the early days of industrial fabrication, MOX pellets were produced at Cadarache by the COCA (CObroyage CAdarache: Cadarache Cogrinding) process, a straightforward adaptation of the process used for the fabrication of mixed-oxide pellets for fast-neutron reactors (Phénix and Superphénix). MOX produced in the United Kingdom uses a similar process, known as the short binderless route (SBR) process, involving the blending, and grinding of all of the powders.

The powders thus obtained are turned into pellets by pressing, a step that has recently been modeled at CEA, to minimize fabrication scrap, and the volume of powder from rectification grinding at the MELOX plant.

To limit the density gradient occurring inside the green compacts, the friction forces arising at the sides, between the powder and pressing die materials, must be brought down. Tests carried out on a number of materials show that a TiC coating allows a reduction of some 20% to be achieved, with respect to the powder–die friction coefficient.

Subsequent to pressing, MOX pellets are sintered for 4 hours at 1,700° C. By contrast to $UO_2$, MOX sintering is not carried out in a reducing atmosphere, rather in a slightly moist ($20 < H_2/H_2O < 50$) argon–hydrogen mixture, to achieve, inside the sintering furnace, an oxygen potential such as to allow a $(U,Pu)O_2$ oxide to be obtained, for which the oxygen/metal ratio is close to stoichiometric.

After sintering, as is the case with $UO_2$ pellets, MOX pellets are rectified, and inspected.

Due to the fabrication process, plutonium distribution is not uniform: microprobe observations (see Fig. 12) show that part of the plutonium is found in agglomerates for which plutonium content, higher than 20%, is close to that for the master blend. R&D is ongoing, along a number of avenues, to improve the homogeneity of plutonium distribution, through use of **sintering*** additives, such as chromium, or sulfur. See the chapter on "Advanced $UO_2$ and MOX ceramics", p. 47.

## Modeling powder compaction to achieve better control of fuel pellet shape and density

The PréCAD code describes the mechanical behavior under load of a powdered medium, according to an elastoplastic law. The acquisition of data for powders (compressibility and sinterability curves, Young's modulus, fluidity index, powder–die friction coefficient…) has made it possible to keep the code database supplied, and thus to compute density gradients inside the pellets, differential sintering shrinkage, and ultimate pellet shape (see Figure 11). It thus becomes possible to optimize the pressing cycle, to minimize the extent of hourglassing (i.e. the deviation of the sintered pellet's shape from a true cylindrical shape), and hence the volume of powders from rectification grinding.

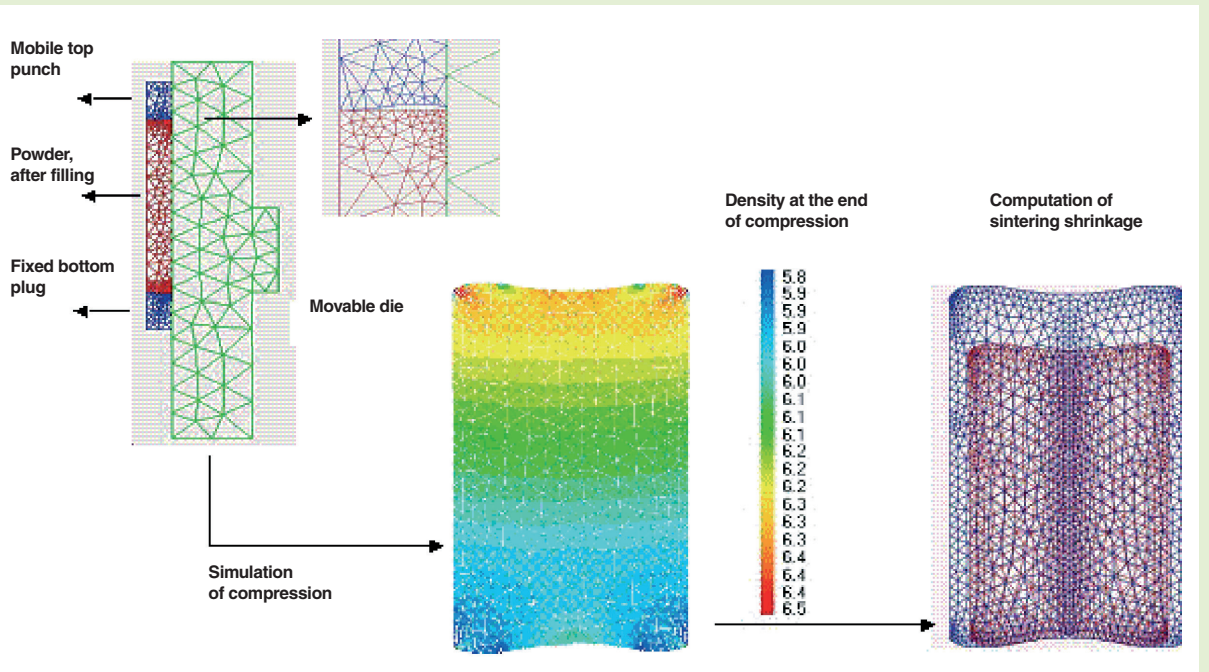


Fig. 11. An illustration of investigations on the pressing of MOX powders: the use of finite-element modeling (PréCAD code), in the single-action pressing case.

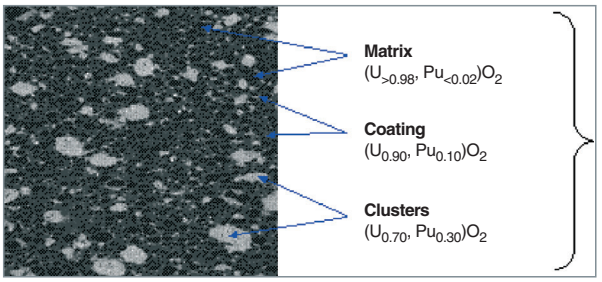


Fig. 12. Microprobe X-ray mapping of plutonium in a MOX fuel, showing regions exhibiting varying plutonium contents: $UO_2$ matrix, coating phase, and plutonium-rich clusters.

## Fabrication of claddings

The pellets are then inserted into tubes some 4 m in length, with a 9.5 mm outer diameter, sealed at both ends by welded plugs. The inside of the rods thus constructed is filled with pressurized helium (at 15–34 bars, depending on cases); for that purpose, the upper plug features a capillary pipe, which is sealed by arc welding.

The most commonly used cladding material, in PWRs, is Zircaloy 4, a zirconium alloy (transparent to neutrons) containing some tin (1.2–1.7%), together with small amounts of iron (~ 0.2%), chromium (~ 0.1%), and oxygen (~ 0.1%). These alloying elements have the purpose of enhancing mechanical strength, and resistance to water corrosion.

Cladding fabrication involves several steps. The initial ingot is fabricated by arc melting, from zirconium sponge charged with the alloying elements. Two or three melts are required to obtain homogeneous ingots. The ingot is shaped by forging in the b phase, at around 1,040° C, then heat treated, still in the b domain, and quenched, for the purposes of homogenization, and to reduce the size of precipitates.

Turning the blank into a cladding tube is effected by hot extrusion of the billet, which has first been drilled through, followed by multi-pass cold pilgering, with intermediate annealing, after each pass, in vacuum, or in an inert atmosphere, always in the a phase (at around 700° C).

As zirconium in the a phase exhibits a hexagonal crystal structure, the strains the material undergoes during the transformation steps result in texturing in the tube, this being more are less marked, depending on conditions. Such a texture has an effect on mechanical properties, and on the distribution, and orientation of zirconium hydride precipitates, in the event of cladding hydriding.

The final heat treatment makes it possible to obtain tubes in the stress-relieved state, if carried out below 500° C – this being the temperature of initial recrystallization – or in the recrystallized state, if that temperature is exceeded.

Claddings are then subjected to systematic dimensional and ultrasound controls, along with destructive inspections of sample tubes (chemical analysis, texture, mechanical properties, corrosion resistance).

Zircaloy 4 having shown its limitations, particularly with respect to corrosion resistance, new cladding materials have been developed; in particular, the M5® zirconium–niobium alloy is on its way to supplanting Zircaloy 4, owing to its much better corrosion resistance.

Quality assurance further requires the highest degree of "traceability" for materials, equipment, and operations, in other words the ability to recover the history for, and guarantee the origin of, every component in the fuel element.

### Bibliography

Y. Guérin et J. Henckes, "Conception et fabrication de combustibles à base d'uranium", *Techniques de l'ingénieur* (in press).

J.-L. Nigon and G. Le Bastard, "Fabrication des combustibles au plutonium pour les REP et les REB", *Techniques de l'ingénieur*, BN 3635.

**Yannick Guérin,**
*Fuel Research Department*

# In-reactor behaviour of $UO_2$ and MOX fuels

## Irradiation conditions during nominal operation

Most processes that arise within the fuel during irradiation are dependent on temperature, and local fission density; they are thus directly correlated with the evolution of linear power, over the various irradiation cycles.

In a PWR core, total power remains virtually constant over an **irradiation cycle***, however linear power, in a given rod, exhibits an axial variation, from the bottom to the top of the fissile column, and also varies over time. Integrating this over in-reactor dwell time, axial **burnup*** distribution by the end of irradiation is relatively uniform, over a large part of the fissile column (it is lower only in regions close to the upper and lower ends).

Fuel rods operate, in nominal conditions, with average linear powers ranging from 150 W/m to 250 W/m. An example of average linear power evolution, in a $UO_2$ rod subjected to irradiation for 5 irradiation cycles, is shown in Figure 13; the power increment, for the second cycle, is related to the assembly being moved closer to the core center; as a result of fuel burnup, average power tends thereafter, as may be expected, to decrease over time.

Nominal primary circuit water pressure stands at 155 bars, coolant core inlet temperature being about 280° C.

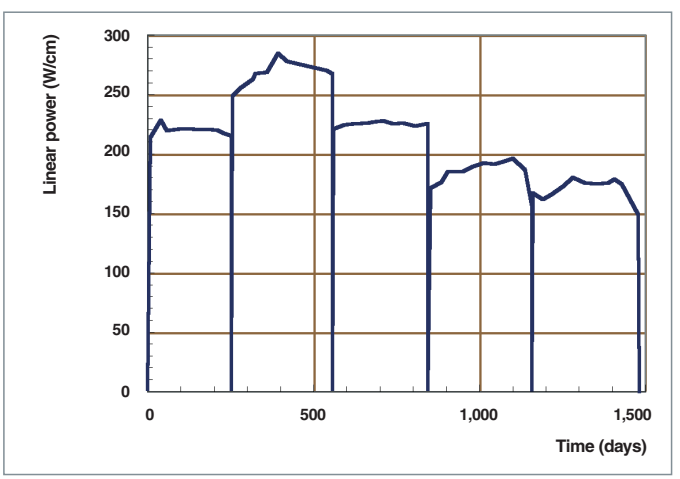


Fig. 13. An example of the evolution, as a function of time, of average linear power in a $UO_2$ fuel rod, irradiated over 5 cycles in a pressurized-water reactor.

## Heat generation, and removal

In a reactor, the main process that takes place within fuel is the fission of heavy nuclei. It is from such fissions that the entire behavior may be derived, exhibited by the material. The fissions yield several hundred types of nuclides, mostly radioactive, and short-lived, together with energy, mainly in the form of kinetic energy in fission products, but also in the form of $\beta$ and $\gamma$ radiation. Fission product kinetic energy is dissipated in the form of heat, as implantation of the fission products into the material takes place.

This implantation occurs through the "recoil" of fission products inside the material, over a distance of 5–8 micrometers (mm), and results in the formation of a large number of defects, recombination of which depends on fuel temperature. Highly energetic, the track such an implantation leaves is known as a "**fission spike***".

The distribution of such heat generation is not homogeneous across the pellet. Indeed, the generation of Pu 239 by capture, in uranium 238, of **epithermal*** neutrons is quite marked in the pellet rim, by way of the **self-shielding*** effect (for neutrons endowed with an energy corresponding to resonances, the capture **cross-section*** is so large that they are unable to reach the center of the pellet). This overconcentration of plutonium in the rim, gradually building up during irradiation, results in a drop, from rim to center, in radial power distribution.

Thermal conductivity in unirradiated oxide fuel is low. Standing at about 4.5 $Wm^{-1}K^{-1}$ at 450° C, and mainly phononic in character, this decreases, reaching a minimum (~ $2Wm^{-1}K^{-1}$) around 1,500° C, then rises again, owing to an increasing electronic contribution. Fuel thermal conductivity decreases as porosity rises. MOX fuel conductivity is some 10% lower than that of $UO_2$ fuel. In the course of irradiation, the generation of fission products, and the formation of irradiation defects further result in a gradual, but quite distinct degradation in thermal conductivity.

The energy dissipated within the material, and the heat exchange conditions prevailing with the coolant, at the cladding surface, result in high temperatures, and a steep thermal gradient inside the fuel. The temperature differential between the center of a pellet, and the rim, varying widely as it does during irradiation (under the combined effects of a number of parameters, in particular variations in power, decreased thermal conductivity, narrowing pellet–cladding gap, and the

formation of oxidized layers on the cladding surface), stands at around 500–700° C.

## The processes involved at the start of irradiation

Differential expansion, between center and rim, induces tangential tensile stresses. As any ceramic, fuel pellets exhibit brittle behavior up to a temperature of about 1,400° C; the material's rupture strength limit is, as a rule, exceeded as early as the initial power ramp, resulting in radial and transverse cracking in the pellet. Such cracking continues in the newly formed fragments. Figure 14 shows a radial section across a $UO_2$ fuel rod, irradiated over 1 cycle, exhibiting such cracking.

Moreover, under the effect of elastic stresses, induced by the temperature field, pellets take on a so-called "hourglass" shape. From the start of irradiation, the interaction of fission spikes with pores in the material generates vacancies, dispersed across the lattice. The diffusion of these vacancies to the grain boundaries results in an overall densification of the material. This densification takes the form, in particular, of a sharp drop in the density of small pores (< 2–3 µm). The extent of this process, dependent as it is on initial microstructure, on fine porosity in particular, results in a variation in density, and hence in volume, of around 1%.

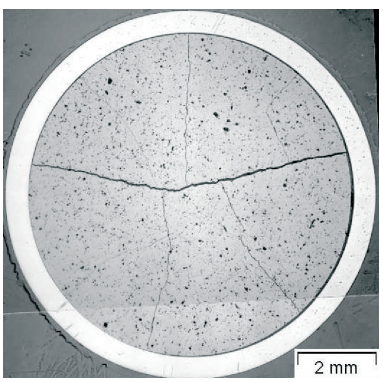


Fig. 14. Radial section of a $UO_2$ fuel rod, irradiated over 1 cycle. The onset of radial cracking may be noted, along with the not-yet-closed pellet–cladding gap, and fragment relocation.

Concurrently, the formation, by fission, of two atoms from a single heavy nucleus results in the fuel swelling. This process continues throughout irradiation. Swelling depends on irradiation conditions, temperature in particular. Indeed, all **fission products*** do not contribute equally to this swelling, rather this depends on the phase they form, or the position they take up within the matrix, in supersaturation. Moreover, some fission products are gaseous (xenon, and krypton), and may, in certain conditions, form bubbles contributing to overall pellet swelling. Under nominal irradiation conditions, such swelling stands at around 0.06–0.07% per GWd/t (i.e. per unit burnup).

The combined, opposite effects of densification, and swelling result, initially, in the material contracting, then, above about 15 GWd/t, only swelling is apparent, initial density being regained between 15 GWd/t and 30 GWd/t. This swelling of the fuel, combined with small relative displacements of the fragments formed by cracking, along with a decreased cladding diameter, due to irradiation **creep***, owing to pressure from the coolant, results in closure of the pellet–cladding gap. Increasingly extensive contact thus develops, between fuel and cladding. It is virtually complete by around 30 GWd/t. Cladding diameter thereafter rises again, depending on fuel swelling. These geometrical evolutions are shown in Figure 15.

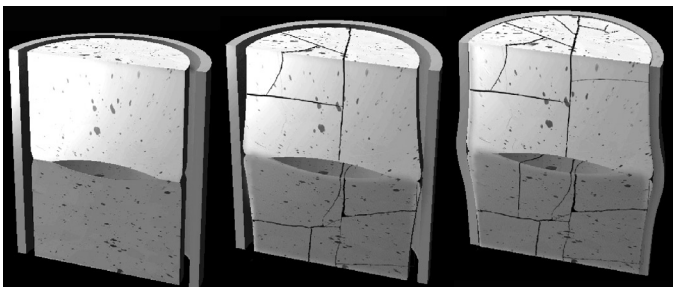

Fig. 15. Schematic representation of pellet cracking, hourglassing, and evolution of the pellet–cladding gap in the course of irradiation.

At the points of contact between fuel and cladding, there arises, on the inside surface of the cladding, a layer of zirconia, about 8 µm thick, due to diffusion of oxygen from the fuel.

Fuel "hourglassing," gap closure, and the formation of an inner zirconia layer result in the cladding and fuel bonding together, no longer coming apart, even during reactor outages.

## Fission gas behavior [1, 2]

Throughout irradiation, gaseous fission products (xenon, and krypton) are released by the ceramic to the free spaces in the rod. The initial process involved in such release is athermal diffusion, and the ejection of atoms of gaseous fission products at the free surfaces of the fuel ("knockout"), as a result of displacement cascades caused by fission product implantation. This process increases constantly, during irradiation, owing to the fuel's rising fission product content, and the evolution of free surfaces. Under nominal irradiation conditions, this is the chief fission gas release mechanism involved, up to 30 GWd/t or so. By this mechanism, only FPs generated quite close to a free surface can be ejected. These account for only a small fraction of total gaseous FPs formed within the fuel. Beyond 30 GWd/t, the gas release rate rises more swiftly, being markedly dependent on fuel temperature. Thermally activated mechanisms are then involved: diffusion mechanisms for gas atoms held in solid solution in grains, and mechanisms of release path formation, along grain boundaries. The gas release rate may then, under nominal irradiation conditions, reach values standing at around 3% of the gases generated, at 60 GWd/t, for $UO_2$ fuel, around 6% for MOX fuel (see Fig. 16); such a release rate may induce, in the rod's free spaces, pressures that may rise above 10 MPa in hot conditions, at the

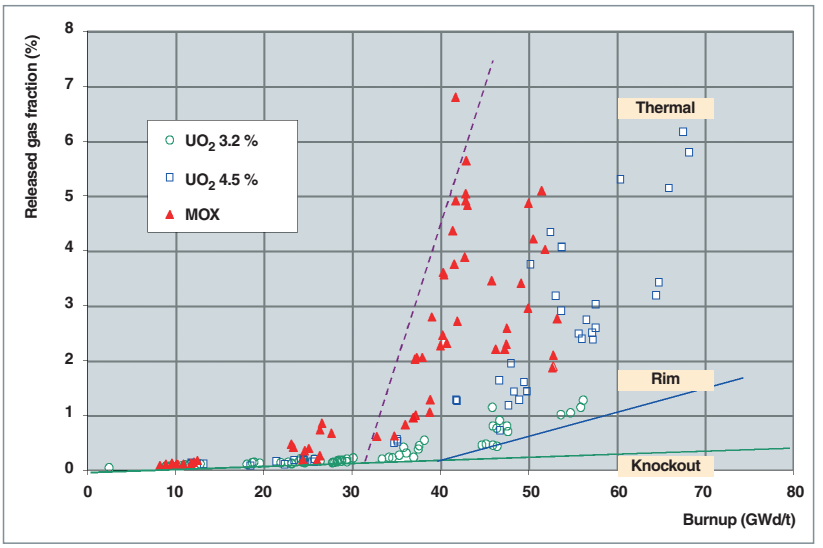


Fig. 16. Evolution, as a function of burnup, of the fraction of fission gases released, in $UO_2$ and MOX PWR rods.

end of irradiation at high burnup, meaning there is a reduced margin with respect to coolant pressure, especially for MOX fuels, which are more highly stressed than $UO_2$ fuels (higher linear power, at high burnup, and higher pellet centerline temperatures, owing to the lower thermal conductivity). This increased pressure is one of the parameters limiting fuel burnup extension. Current R&D is seeking to develop new fuel microstructures, having the ability to ensure better fission gas retention – through increased grain sizes, and/or use of additives at grain boundaries – particularly in accident conditions.

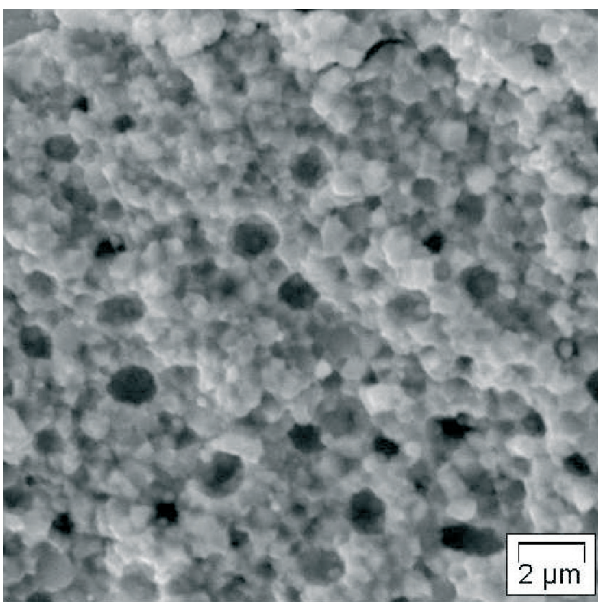


Fig. 17. Microstructure of restructured fuel (HBS). The initial grains, about 10 microns across, have been replaced by submicrometer grains, and fission gas bubbles have formed.

## Microstructural changes

Finally, once large amounts of fission products and irradiation defects have accumulated inside the material, particularly in the less hot regions in the pellet, where defect annealing is weakest, and fission product diffusion slowest, the oxide grains divide, yielding grains about 0.2 µm across, from initial grains of about 10 µm diameter [3]. As this restructuring takes place, most of the gas in the regions affected by it collects into bubbles, about 0.6 µm in diameter. Figure 17 shows a scanning electron microscope observation of a restructured region. When, in a given region, such restructuring is complete, and has only just occurred, bubble formation-induced porosity stands at around 10% of material volume. Formation also occurs of precipitates of metallic fission products. The newly formed microstructure is known as high-burnup structure (HBS). During such restructuring, fission gas release is low. This structure is found at the periphery of $UO_2$ pellets ("**rim*** effect"), owing to the low temperature, and very high fission product concentration, related to the formation, in the rim region, of plutonium through **capture*** of **epithermal*** neutrons by uranium nuclei. This process arises after 40 GWd/t.

This microstructure is also to be found in heterogeneous MOX fuel, within, and around plutonium-rich aggregates, over the outer half or so of the pellet radius (i.e. in a region amounting to three quarters of the pellet's volume). In this type of fuel, restructuring occurs much earlier on in irradiation, owing to the swift accumulation of fission products, and defects, in these fissile plutonium-rich regions. As irradiation continues, the new gases formed feed into the bubbles, which grow in size, and coalesce (see Fig. 18).

Figure 19 sets out, by way of a simplified overview, the main processes arising in irradiated fuel, and the most salient interactions between these processes.

As a whole, these evolutions affecting the fuel, despite their extensive character, in no way affect cladding integrity, in the normal operating domain.

**Jean Noirot,**
*Fuel Research Department*

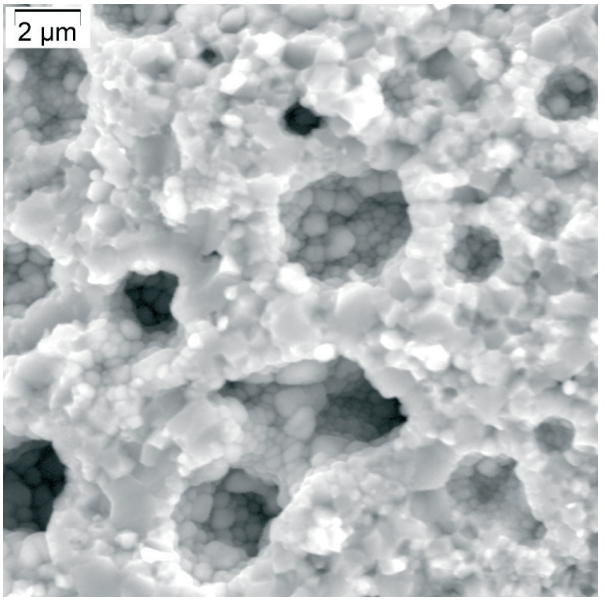


Fig. 18. Coalescence of bubbles in HBS microstructure, in a very-high-burnup (180 GWd/t) region, in a MOX fuel aggregate.

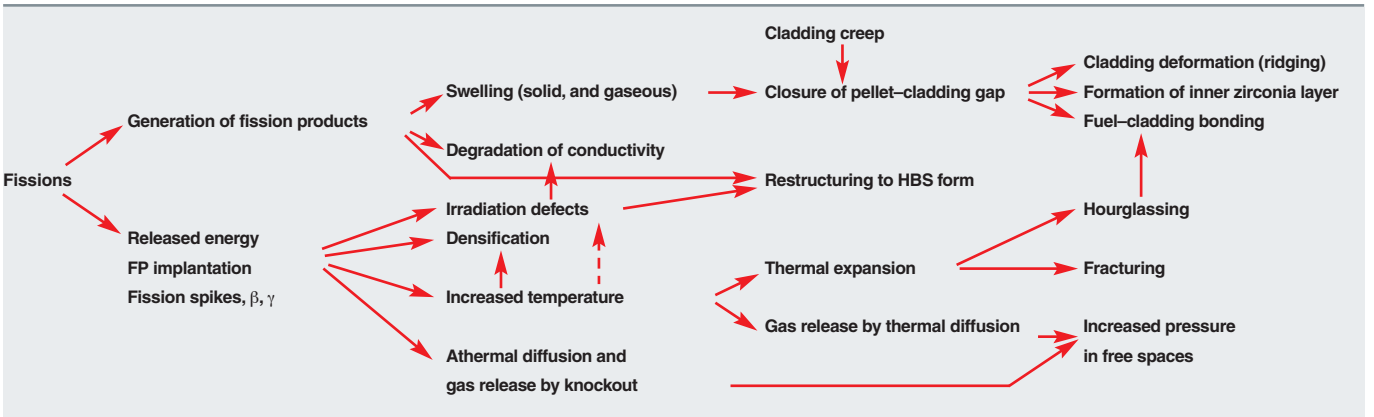


Fig. 19. The main processes arising in PWR fuel under irradiation.

## References

[1] M. Boidron, "Forts taux de combustion", SFEN meeting, 16 January 2002.

[2] Y. Guérin, J. Noirot, D. Lespiaux, C. Struzik, P. Garcia, P. Blanpain, G. Chaigne, "Microstructure evolution and in-reactor behaviour of MOX fuel", *Proceedings of the International Topical Meeting on Light Water Reactor Fuel Performance*, Park City, Utah (USA), 10–13 April 2000.

[3] J. Noirot, L. Desgranges, J. Lamontagne, "Detailed characterisations of high burn-up structures in oxide fuels" (2007), *Journal of Nuclear Materials* 372, 2–3, 318–339, January 2008; DOI: 10.1016/j.jnucmat.2007.04.037.

# Water reactor fuel behavior in loss of tightness conditions

## Cladding, the first containment barrier

The **cladding*** of a fuel rod forms the first containment barrier for nuclear fuel, during its irradiation inside a reactor. Emergence of a leak in that cladding results in:

- the transport of specific chemical elements ("fission products" [FPs]) that are stable, and radioactive (iodine, xenon, krypton…) into the reactor's primary circuit;
- deposits of long-lived isotopes (cesium, strontium, technetium…), or even, in exceptional circumstances, of alpha emitters onto the piping of the primary circuit, or of ancillary circuits;
- an increase in the overall level of irradiation for that circuit, from the level already due to **activation*** products (corrosion products, e.g. cobalt, chromium, iron in particular).

A leak thus poses a major challenge in operational terms, for a power plant operator, since it has a direct bearing on the level of radiological exposure workers are subjected to, when running the plant, or carrying out maintenance. Fortunately, such a situation arises but rarely. The reliability of light-water reactor fuel is, indeed, very high. Operational feedback shows that the overall frequency of occurrence of a leak in irradiated fuel rods is currently very low (standing at some $10^{-6}$ per year, corresponding to distinctly less than one leaking rod per year, per unit operated).

Use of a fuel rod presenting a leak is seen as forming part of normal reactor operations, when such loss of tightness arises during the cycle. This means the reactor, as a rule, continues operating, even though certain restrictions may, in some circumstances, be imposed (e.g., discontinuing load following). Defects that involve unacceptable deterioration occur rarely, in the water reactor line. It may be noted, at this point, that just two units, in France, have experienced an unscheduled operating cycle interruption due to loss of leaktightness, since Fessenheim 1, the first 900-MWe PWR in the French fleet, first went critical, in 1977.

However, in order to limit cumulated doses for operatives, restrict the level of activity stored, or discharged, and make for easier intervention conditions during unit outages, and dismantling operations, primary circuit content, with respect to certain fission products (noble gases, iodine), may not exceed a given absolute level, or vary outside a given range, during a cycle. Such thresholds, which are set by the safety authority, are specified, in the French case, in the mandatory technical operating specifications, under the rubric "Primary circuit activity". By way of example, the threshold for shutting down, within 48 hours, a French PWR reactor is set as follows:

- 100,000 MBq per tonne water, for the sum of specific activities from noble gases, in the event of a presumption of cladding failure involving high-burnup fuel;
- an increase in iodine 134 specific activity greater than 10,000 MBq/t, as compared to the I 134 "background".

The reactor is fitted with purification equipment to limit activity levels in the primary circuit. The chemical and volume control system (CVCS) features a degassing system, and a set of filters and resins, to retain **sorbed*** or dissolved FPs.

Identification of assemblies holding leaking rods is carried out through a specific inspection step, taking place during unit outages, know as "fuel sipping". A techno–economic analysis then allows a decision to be taken, as to the future of this assembly: reuse after removal of the faulty rod (repair), or final discharge.

## Causes of failure

The chief cause of failure, for a long time, was the presence of foreign bodies (debris) carried by the primary circuit fluid (see Fig. 20). Mitigation measures, at the assembly construction stage (filters mounted onto the bottom nozzle), have made it possible to achieve a marked drop, as regards this external cause. For the most part, the prime causes of failure, nowadays, relate to processes such as fretting, for PWRs (due to the cladding rubbing against the retaining springs on the grids; see the chapter on "Mechanical behavior of fuel assemblies", p. 51). Fabrication defects only figure as a marginal cause.

Any change with respect to the fuel management mode (e.g. increased burnup, or highly hybrid core configurations), or the introduction of novel fuels into reactors (new microstructures, fuels containing burnable poisons, doped fuels…) entails that the issue be reconsidered, of behavior in "nonleaktight" mode, and of the adequacy of current technical specifications. Such knowledge is gained through R&D work, in both experimental and theoretical areas.

Fig. 20. Debris trapped between two rows of fuel rods in a PWR assembly.

## Consequences of a failure

The description of the processes involved in "nonleaktight"-mode operation combines radiochemistry and thermal-hydraulics, in the very narrow (a few tens of micrometers, in hot conditions) annular fuel–cladding gaps, under high thermal gradient conditions (about 150° C). The opening up of a defect is accompanied by inflow of water from the primary, in the liquid state. What happens to that water depends, essentially, on local fuel linear power. By way of example, for PWRs:

- at low power levels (less than 120 W/cm or so), fuel surface temperature is lower than the saturation temperature of water at 155 bars. The water stays in the liquid state, gradually flooding the fuel–cladding gap. This "water plug" acts as an effective restraint on the axial migration of FPs (through gas-to-liquid diffusion, for gases; trapping for iodines), and released activity levels are low as a rule;

- at medium power levels (120–170 W/cm or so), a two-phase regime sets in, as water vaporizes on contact with the fuel, while forming a liquid film on the cladding inside surface. A radial vaporization–condensation mechanism is set up, involving intense internal agitation. Released activity levels may be high, and highly sensitive to reactor operating parameters;

- at high power levels (above 180 W/cm), the pellet–cladding gap only holds steam, and internal axial exchanges are slower. On the other hand, the release "source term" (i.e. the amount of radioactive elements liable to escape from the fuel rod) is large, being related both to power (rate of fission product formation), and pellet temperature (diffusion coefficient).

Such local thermal–hydraulic developments are modified, however, owing to two further processes:

- the ends of a rod (several tens of centimeters) always remain "cool," since they deliver but little nuclear power. Water condenses, forming a volume of liquid at these locations (in the upper **plenum***, in particular). Once pressure equilibrium with the primary circuit is reached (stopping the inflow of water), this volume will very slowly drain into the gap, by gravity and/or vaporization, causing FPs to be drawn along by the steam to the outlet, at the defect;

- **radiolysis*** of water (liquid, or steam), mainly due to FPs, gradually causes it to disappear, to be replaced by hydrogen (the oxygen essentially being absorbed into the pellet). Hydrogen may then act as a carrier gas, for the transport of gaseous FPs. It may also, in certain conditions, form precipitates in the cladding, in the form of zirconium hydrides, even to the point of causing a new leak, through "secondary hydriding," that often proves to be much larger than the primary defect (see Fig. 21).

Levels of fission products escaping from the fissile matrix are expressed, in normalized form, in terms of the release rate/birth rate, or "release-to-birth" (R/B) ratio: (number of atoms of FP i released from the fuel per second)/(number of atoms of FP i formed at radioactive equilibrium per second). Plotted on a log–log scale, as a function of the decay constant l of the substances involved, the values for gaseous isotopes, and iodines fall along two negative-slope straight lines (see Fig. 22). The height and slope of the straight line provide information as to the nature of the processes causing the escape of FPs. For instance, it has been experimentally ascertained that a $UO_2$ rod, operating with a linear power of 200 W/cm, exhibits an R/B ratio (Xe 133) of about 3%, that figure rising to 7% at 250 W/cm (see Fig. 23). Depending on the slope:

- zero slope (outflow independent of radioactive half-life): involves emission of an FP by direct recoil, subsequent to a fission event occurring very close to the fuel surface (less than 10 micrometers away);


Fig. 21. A leak due to hydriding.

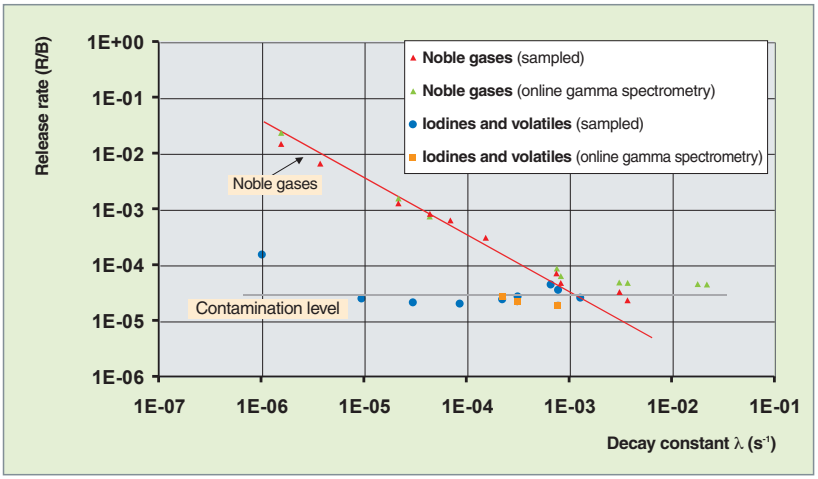


Fig. 22. An example of release rates, as measured on an experimental fuel rod at 150 W/cm.

- slope of – 0.5: diffusion mechanism;
- slope of – 1.0: sudden offgassing mechanism, of a volume of FPs that has accumulated during irradiation.

At CEA, release rates are measured experimentally during analytical irradiations in research reactors [1, 2, 3], on short, refabricated rods, instrumented in some cases (internal pressure sensors); or in experiments in high-activity laboratory cells, on fissile column segments. The associated post-irradiation investigation program is chiefly concerned with monitoring the evolution of fissile material microstructure, subsequent to changes in operating conditions: higher temperature, prevalence of oxidizing conditions, presence of aggressive radiolytic species, faster diffusion of fission products.

Concurrent with this experimental approach, modeling is carried out, at CEA, along three directions:

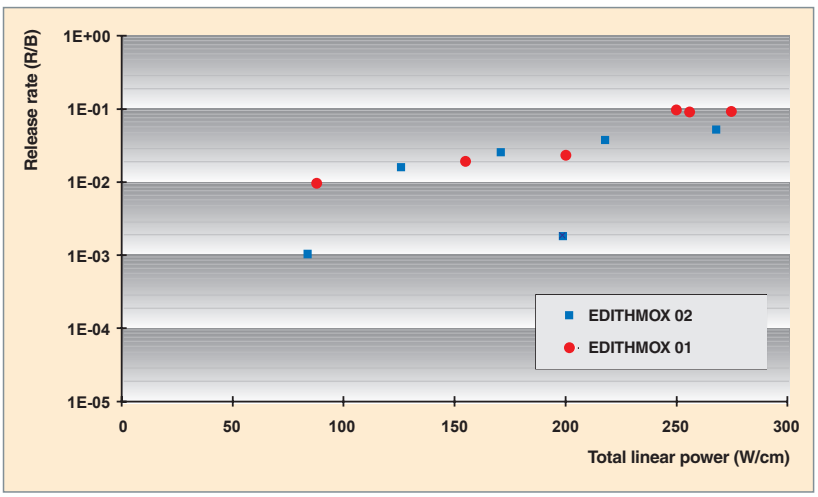


Fig. 23. An example of the evolution of the release rate, as a function of linear power (in the case of a newly fabricated MOX rod ["01"], and a high-burnup MOX rod ["02"]).

- predicting levels, for the various FPs escaping, under given irradiation conditions, by modeling the processes outlined above. The simulation tool involved (PROFIP) is used to predict the evolution of FP activity values in the primary circuit, and give the alert if there is a risk that technical specification limits will be reached;

- diagnosing the state of the cladding, during operation, on the basis of observed activity levels in the primary circuit. This operating aid tool allows an assessment to be made of the number, and seriousness of defects present inside the core; it detects their further deterioration, should it occur, as the unit is operating; and, if required, quantifies any release of fissile material. At CEA, the "Diagnosis" module in the DIADEME code is used for this;

- predicting activities for long-lived emitters, and alpha emitters lodged in ancillary circuits, and purification equipment (filters, resins). This tool allows the operator to achieve improved waste management, and gain a more global overview of the evolution of contamination in the installation, in the long run, in particular with a view to dismantling requirements. For that purpose, the "RNVL" module in the DIADEME code is used at CEA.

## References

[1]. H. Seveon, C. Leuthrot, P. Chènebault, R. Warlop, J.-P. Stora, "Release of fission products by defective pressurized water reactor fuel", *International Meeting on Nuclear Reactor Safety*, Karlsruhe (Germany), 10–13 September 1984.

[2]. D. Parrat, Y. Musante, A. Harrer. "Failed annular $UO_2$ fuel in PWR conditions: the EDITH 03 experiment", *Proceedings of the International Topical Meeting on Light Water Reactor Fuel Performance*, Portland, Oregon (USA), 2–6 March 1997.

[3]. D. Parrat, A. Harrer. "Failed high burn-up MOX fuel performance: the EDITHMOX 02 analytical irradiation", *Proceedings of the International Topical Meeting on Light Water Reactor Fuel Performance*, Park City, Utah (USA), 10–13 April 2000.

**Daniel Parrat,**
*Fuel Research Department*

# Microscopic morphology of fuel ceramic and its evolution under irradiation migration and localization of fission products in UOX and MOX matrices

Microstructural characterizations of PWR fuel, prior to irradiation, make it possible to show up the grains in the ceramic. They further show porosity, the porosity ratio and size spectrum depending on fabrication methods. Finally, characterizations may be effected of the presence of impurities, of fabrication additives, and, in the case of MOX fuel, of heterogeneities in the distribution of fissile material (plutonium-rich aggregates: see Figure 12, in the chapter on "Fabrication of water reactor fuels").

## The ceramic under irradiation

Under irradiation, this microstructure changes:

- stresses, thermal in origin, induce fracturing in the pellet, resulting in new free surfaces being formed;

- the smaller fabrication pores disappear, through the re-solution of **vacancies*** by **fission spikes*** (see the chapter on "In-reactor behavior of $UO_2$ and MOX fuels");

- the appearance of the free surfaces (newly fractured surfaces, surfaces of as-fabricated pores, pellet end surfaces) is altered by irradiation. Figure 24 shows this evolution in the end surface of a pellet, in a hollow (dishing), as observed in scanning electron microscopy (SEM). It will be noted that, from one grain to the next, i.e. depending on crystallographic orientation, the new pattern may be quite different from its neighbor. This type of surface may also be found at certain grain boundaries, a sign these are at least partly opening up.

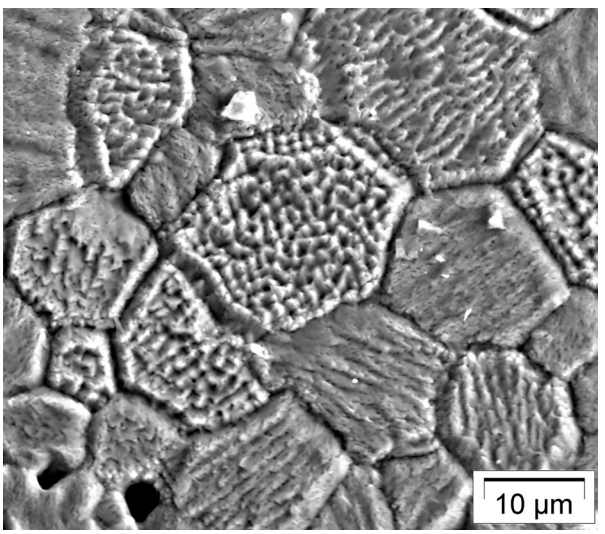


Fig. 24. Surface of dishing at the end of a pellet, evidencing the evolution of grain surfaces under irradiation, and differences in this evolution, depending on crystal orientation.

- At high temperature, i.e. when high power levels are sustained (in incident or accident situations), in-reactor crystal growth occurs. At temperatures higher than 1,800° C, there is even an onset of as-fabricated pore migration, these migrating up the temperature gradient through evaporation–condensation (vapor transport), resulting in the formation of large, highly elongated grains – so-called "columnar grains" – and even in the formation of a central void, on the pellet centerline. During normal irradiation in a PWR, however, no change in grain size is found, and the extent of the overall densification and swelling processes is not large enough to be evidenced by a measurement of grain sizes.

- Subsequent to in-grain implantation, some of the fission products remain in solid solution in the matrix. This is the case, in particular, for rare earths, such as neodymium. Other elements, proving less soluble, or even poorly soluble in $UO_2$ or $(U,Pu)O_2$, diffuse across the material, under the action of fission spikes, and temperature. Three terms are considered, as a rule, in such diffusion of fission products: the first, so-called "athermal" term is directly related to the motions of atoms in fission spikes, and thus, locally, to fission density; the second, so-called "thermal" term, corresponds to conventional diffusion, as equally observed in materials out of irradiation; the final terms is the so-called "mixed" term, relating to thermal diffusion speeded up by an increased presence of interstitials, and vacancies, in irradiation conditions. Depending on stresses in the material, the formation may occur, under irradiation, of precipitates, and gas bubbles. The presence of such particular aggregates of fission products depends on irradiation conditions, chiefly burnup, and temperature. Observation of these aggregates is mainly dependent of the means of investigation being used. This applies, in particular, to aggregates of metallic fission products – molybdenum (Mo), technetium (Tc), ruthenium (Ru), rhodium (Rh), palladium (Pd) – and of gaseous fission products, xenon (Xe), and krypton (Kr). For instance, at 1,000° C, for a fission density of $10^{19}$ fissions $\cdot$ $m^{-3}s^{-1}$, the diffusion coefficient D stands at $5 \cdot 10^{-20}$ $m^2/s$ (with the mixed term dominant), corresponding, for fuel at the end of irradiation, to characteristic distances $\sqrt{Dt}$ of around 1 micrometer.

## Bubbles and precipitates

Transmission electron microscopy (TEM) observations show the existence, within the fuel, even at low burnup, and at widely diverse irradiation temperatures, of fission gas bubbles a few nanometers across, with a number of bubbles per unit volume of $10^{23}$–$10^{24}$ bubbles/$m^3$. Xenon and krypton density, inside these bubbles, is very high, close to the density of the substance in the solid state, and pressure may be higher than 1 GPa. Nucleation of such bubbles is constant, during irradiation, while the re-solution of the gas in these nanobubbles through the action of fission spikes results in their disappearance. A dynamic equilibrium is thus involved.

The speeding up of the diffusion of fission gases held in solid solution inside grains, at high temperatures, results in that equilibrium being altered, allowing the formation of larger bubbles, with diameters greater than 100 nm, which may be observed in scanning electron microscopy (SEM), or even optical microscopy. Here again, xenon and krypton pressure, in these bubbles, is very high, well above the elastic equilibrium pressure for such cavities. The limiting temperature, beyond which such fission bubbles may be observed, falls markedly with increased burnup, i.e. chiefly as the proportion of fission products present within the material rises. This limiting temperature stands at about1 200° C around 10 GWd/t burnup, coming down to about 700° C only at 50 GWd/t. Thus, in fuel that has undergone base irradiation, but at high burnup, the formation may be observed of a region exhibiting porosity that is quite visible in SEM or optical microscopy, the boundary for which, depending as it does on burnup, is an isotherm during irradiation. Precipitates of metallic fission products are also found in these regions exhibiting intragranular bubbles, at the pellet center. Figure 25 shows the type of microstructure found in such intragranular precipitation regions at the center of a sample, as observed by SEM at Cadarache.

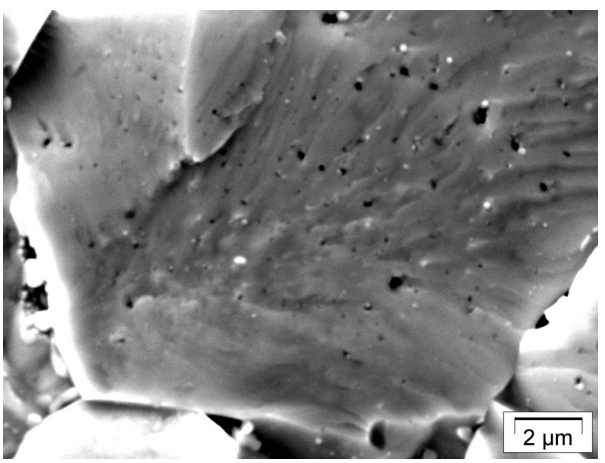


Fig. 25. Formation of bubbles, visible by SEM, in grains of high-burnup fuel, at the center of the pellet.

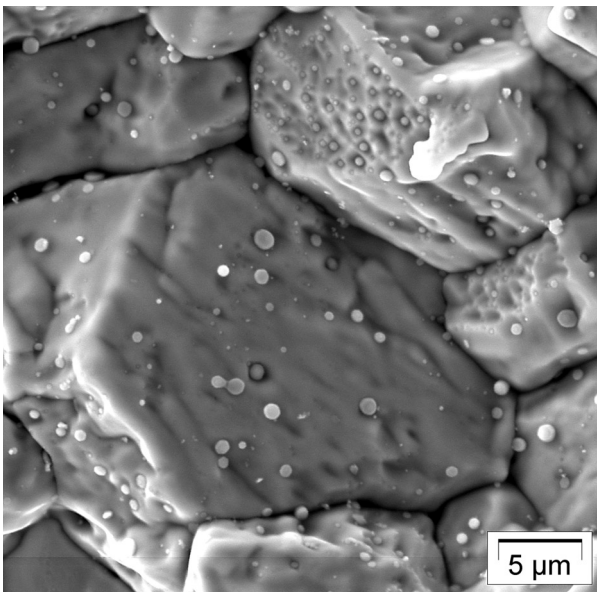


Fig. 26. Grain surfaces in a MOX fuel after irradiation. Round spots are metallic fission product precipitates.

The diffusion of fission gases held in solid solution further allows them to accumulate at grain boundaries, where diffusion even speeds up. In the same way as within grains, the formation may develop, at grain boundaries, of bubbles, and metallic precipitates. It is through such accumulation of gas at grain boundaries, and the formation of submicron escape paths, particularly at triple boundaries, that a substantial proportion of fission gases are released into the fuel rod's free spaces. Figure 26 shows grain surfaces in a homogeneous MOX fuel, irradiated to 45 GWd/t, across which many large metallic precipitates may be seen. The rounded shape of grain

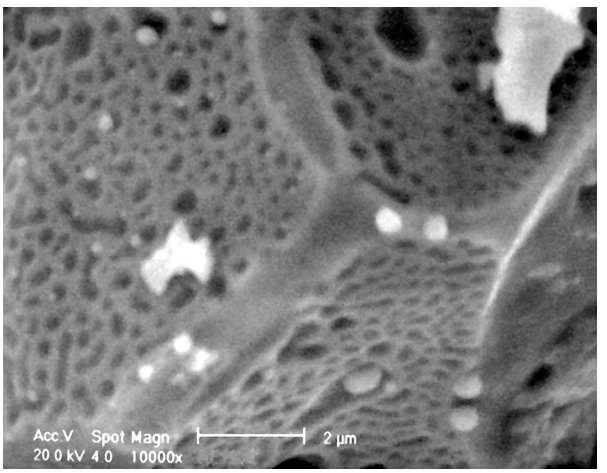


Fig. 27. The surface of a grain after a power ramp, resulting in high temperatures at the center of the fuel pellet. Bubbles have formed at the grain boundaries, some have coalesced, channels have been formed at triple boundaries. Here again, metallic precipitates may be seen.

Concurrently with developments in modeling, which is becoming increasingly physical in character (see chapter on "Modeling fuel behavior"), major advances have been achieved at CEA, with respect to the precise ascertaining of fission gas localization, through the use of complementary characterization techniques on one and the same sample [1, 2, 3, 4, 5, 6, 7]: SEM, microprobe, and ion probe (**SIMS***), along with heat treatment techniques (ADAGIO).

In particular, SIMS characterization, used with irradiated fuel, is making it possible, for the first time, to visualize, and measure fission gases held in bubbles (see Figures 28 and 29), since the fuel is abraded to a depth of several microns during the measurement. Whereas such a measurement is not feasible using a microprobe (probing to a depth of less than 1 mm), since any bubbles visible have been pierced, during sample preparation. Through this technique, it has been possible to verify that bubbles in the rim region still hold the near-totality of the fission gases generated (see Figure 29), even though the greater part of these evade microprobe detection.

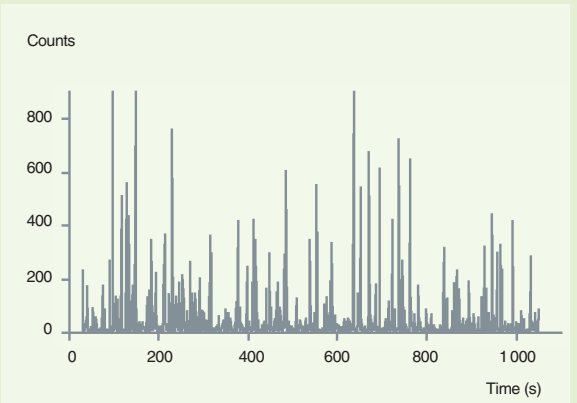


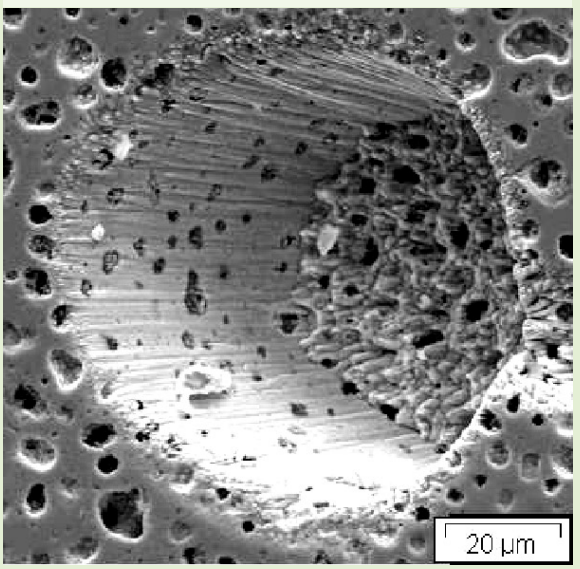


Fig. 28. An example of SIMS measurement: in-depth xenon profiles in a region of fission gas precipitation, in a $UO_2$ pellet irradiated to 60 GWd/t. Each peak corresponds to a gas bubble that has been pierced during abrasion of the fuel.

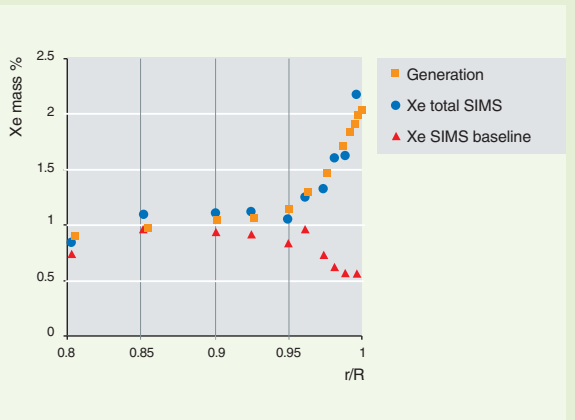


Fig. 29. Xenon concentration profiles, as measured by SIMS at the rim of a $UO_2$ pellet, irradiated to 60 GWd/t. Most of the gas escaping from the grains (the distance between squares, and triangles) is retained in the bubbles (circles).

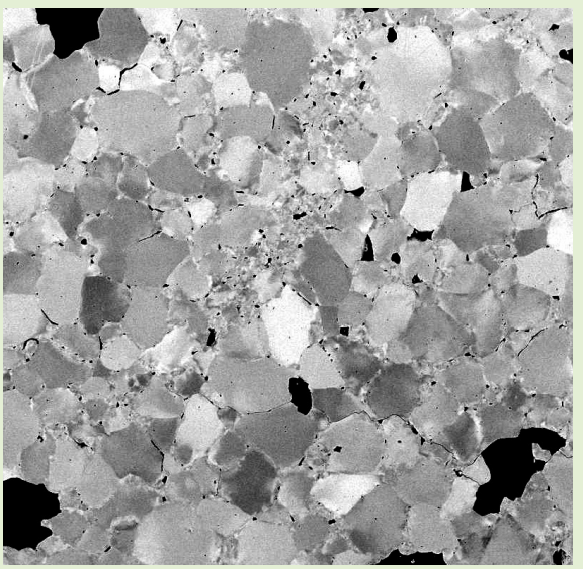

Fig. 30. SEM examination makes it possible to reveal crystal grains, and to determine a porosity spectrum, together with porosity locations, whether intragranular or at grain boundaries.

angles may be seen as an indication that triple boundaries provide an escape path for the fission gases reaching them.

At high temperatures, as during power ramps, or during simulations by means of heat treatments, outside the reactor, the speeding up of diffusion makes for a larger supply for the bubbles, which may coalesce. This is particularly spectacular at grain boundaries, where fission gases reach the extent of forming interconnected labyrinths, with, in particular, tunnels appearing at triple boundaries, these acting as release paths, for the escape of fission gases out of the pellet, into fuel rod free spaces. Figure 27 shows such a microstructure, as observed by SEM. Well formed channels may be seen, at the triple boundaries, along with the formation of intergranular bubbles lining the grain boundaries, partly interconnected, and, finally, metallic precipitates. At the same time, during fast transients, thermal stressing of the gases already present at grain boundaries may result in the latter opening up, and in the release of these gases, whereas the gas occluded inside the grains, on the other hand, is not readily released.

Comparison of SIMS measurements with prior investigations by SEM (see the example shown in Figure 28) makes it possible to arrive at an experimental value for gas pressure inside bubbles.

Carrying such investigations forward, with fuels of diverse origins, will make it possible to refine the complementarity afforded by these various techniques.

## References


[1] J. Noirot, L. Noirot, L. Desgranges, J. Lamontagne, Th. Blay, B. Pasquet, E. Muller, "Fission gas inventory in PWR high burnup fuel: experimental characterisation and modelling", *Proceedings of the International Meeting on LWR Fuel Performance*, Orlando, Florida (USA), 19–22 September 2004.

[2] J. Lamontagne, L. Desgranges, C. Valot, J. Noirot, Th. Blay, I. Roure, B. Pasquet, "Fission gas bubbles characterisation in irradiated $UO_2$ fuel by SEM, EPMA and SIMS", *Microchimica acta* 155, 1–2, 183–187, September 2006.

[3] J. Noirot, C. Gonnier, L. Desgranges, Y. Pontillon, J. Lamontagne, "LWR fuel gas characterization at CEA Cadarache LECA-STAR Hot Laboratory", IAEA TM *on Hot Cell Post-Irradiation Examination Techniques and Poolside Inspection of Water Reactor Fuel Assemblies*, Buenos Aires (Argentina), 27–30 November 2006.

[4] L. Desgranges, C. Valot, B. Pasquet, J. Lamontagne, T. Blay, I. Roure, "Quantification of total xenon concentration in irradiated nuclear fuel with SIMS and EPMA" (2007), *Nuclear Instruments and Methods in Physics Research B* (in press); DOI: 10.1016/j.nimb.2007.10.035.

[5] C. Valot, J. Lamontagne, L. Desgranges, B. Pasquet, J. Noirot, T. Blay, I. Roure, "Fission gases pressure evaluation in irradiated PWR fuels: complementarities of microanalyses techniques, SEM, EPMA and SIMS", HOTLAB 2006, Jülich (Germany), 19–21 September 2006.

[6] J. Noirot, L. Desgranges, J. Lamontagne, "Detailed characterisations of high burn-up structures in oxide fuels" (2007), *Journal of Nuclear Materials* 372, 2–3, January 2008, 318–339; DOI: 10.1016/j.jnucmat.2007.04.037.

[7] Y. Pontillon, J. Noirot, L. Caillot, E. Muller, "Direct experimental evaluation of the grain boundaries gas content in PWR fuels: new insight and perspective of the ADAGIO technique", *Proceedings of the International Meeting on LWR Fuel Performance*, San Francisco, California (USA), 30 September–3 October 2007.



**Jean Noirot,**
*Fuel Research Department*

# Modeling fuel behavior

All of the processes arising inside reactors, and surveyed in the preceding pages are subjected to modeling, the ensemble of these models being brought together in a fuel behavior code, which has the capability to compute all of the physical quantities involved, whether locally (temperatures, stresses, strains, fission gas distribution, etc.) or globally (dimensional variations, fission gas release, etc.). Such modeling is indeed indispensable, in order:

- to understand, and interpret the measurements carried out in reactors, and the findings of post-irradiation investigations (since the processes closely interact with one another);
- to predict the behavior of standard, or experimental fuel rods subjected to specific operating conditions;
- to provide pointers for investigations concerned with improving fuel performance;
- to support safety reports, demonstrating the satisfactory behavior of fuels in all operational situations.

Work on modeling the behavior of PWR fuels, initiated as it was at CEA, and around the world, several decades ago, was initially a fairly empirical affair, mostly relying on simple laws, derived from experimental findings. Gradually, codes subsequently sought to reflect, as closely as possible, the physics underlying each of the processes described, and, nowadays, the effort is being carried forward along these lines.

In the 1990s, the METEOR code [1] was developed at CEA, and is still being widely used. This is a so-called 1 1/2-D code, in other words a code effecting computations on a rod that has been segmented into n slices; each slice, divided into *p* annuli, is computed axisymmetrically, however the interactions of each slice with its neighbors are taken into account.

In this manner, modeling is effected, in particular, of:

- thermics, for every point in the rod: the radial power profile, fuel thermal conductivity at every point, its degradation under irradiation, and the influence of all relevant quantities (porosity, O/M ratio, cracking, etc.), heat transfer in the oxide–cladding gap and in the cladding, cladding waterside corrosion;
- mechanics: stresses and strains are computed, at every point, by means of a finite-element model taking on board the presence of numerous cracks in the fuel pellets, fuel densification and subsequent swelling, cladding growth, and all visco–plasticity processes in the oxide, and in the cladding;
- fission gas behavior: swelling, and release, in nominal conditions, and during operating transients, taking into account structural alterations (formation of the rim structure).

The code caters for $UO_2$, and fuel bearing a burnable **poison*** ($UO_2$ + $Gd_2O_3$); a specific effort has been concerned with developing models having the ability to cater for MOX fabricated by the MIMAS process, while taking on board the heterogeneous fissile material distribution. The code has been validated by comparing findings from computations, and from measurements, for a large number of quantities, on a large number (> 300) of both standard, and experimental fuel rods: integral quantities, such as rod and fissile column elongation, internal pressure, free space, released fission gas fraction; and more local quantities, such as axial profiles of diametral deformations, and of cladding corrosion depth, pellet density, gas bubble precipitation diameters, or rim structure thickness; or quantities measured in situ, in particular temperatures measured in reactor by means of a thermocouple positioned at pellet center.

At CEA, modeling R&D is being carried forward along two directions:

1. Increasingly physical modeling: thus the MARGARET model [2, 3, 4] is used to model fission gas behavior by taking on board all known physical processes, from the behavior of intragranular, nanometer-size gas bubbles (nucleation, growth, resolution of gas atoms by fission spikes, coalescence, and migration of gas atoms, vacancies, and bubbles) to that of intergranular, micrometer-size bubbles, before and after such bubbles have interconnected, and before and after release of the gas they hold, by percolation. Validation of such finely grained models needs must always be based, obviously, on integral quantities, such as fission gas release, but also, most importantly, on observations that are quantified at microscopic and submicroscopic scales, in particular the variations, as a function of radius, in bubble density, and size, as measured by SEM, with image analysis; and the amounts of xenon observable by microprobe, and **SIMS***.

Such modeling explores the outer reaches of current knowledge, both in theoretical and experimental terms. It makes use

of nanometer-scale characterization resources, in particular transmission electron microscopy. It draws on the return of experience from all of the experimental programs conducted under the aegis of CEA–EDF–Areva partnerships, but equally takes in recent advances in basic research on materials, such as synchrotron characterizations, or *ab initio* computation (see the following chapter).

2. The development of software platforms, with the ability to integrate, into a single architecture, the ensemble of physical models developed, for the various types of fuel. Thus the PLEIADES platform [5] (jointly developed by CEA and EDF) has the ability to cater for water reactor fuels, but equally for other fuel types (sodium- or gas-cooled fast reactor fuel, particle fuel for high-temperature reactors, or fuel plates for experimental reactors). Moreover, this finite-element, thermal–mechanical architecture has the ability to carry out, as and when required, 1-D, 2-D, or 3-D computations. The latter characteristic is required, in particular, if correct computations are to be obtained of stress and strain fields, in the pellet–cladding interaction (**PCI***) case, during a power ramp, since pellet hourglassing induces stress concentrations, at the level of interpellet spaces and radial cracks (see the chapter on "Pellet–cladding interaction", p. 41).

Finally, such a platform features a suitable software architecture, to facilitate coupling with other simulation platforms, in particular those covering thermal–hydraulics, or core neutronics. Such couplings will, in particular, allow advances to be made as regards predictions of fuel behavior in accident situations, such as a loss of primary coolant accident (see the chapter on "Fuel during a loss of primary coolant accident").

## References


[1] C. Struzik, M. Moyne, J.-P. Piron, "High Burnup Modelling of $UO_2$ and MOX fuel with METEOR/TRANSURANUS version 1.5", *International Meeting on LWR Fuel Performance, Portland*, Oregon (USA), 2–6 March 1997.

[2] L. Noirot, C. Struzik, P. Garcia, "A mechanistic fission gas behaviour model for $UO_2$ and MOX fuels", *International Seminar on Fission Gas Behaviour in Water Reactor Fuels*, Cadarache (France), 26–29 September 2000.

[3] J. Noirot, L. Noirot, L. Desgranges, J. Lamontagne, Th. Blay, B. Pasquet, E. Muller, "Fission gas inventory in PWR high burnup fuel: experimental characterization and modelling", *International Meeting on LWR Fuel Performance*, Orlando, Florida (USA), 19–22 September 2004.

[4] L. Noirot, "MARGARET: an advanced mechanistic model of fission gas behavior in nuclear fuel", *Journal of Nuclear Science and Technology*, vol. 43, No. 9, pp. 1149–1160, October 2006.

[5] D. Plancq, J.-M. Ricaud, G. Thouvenin, C. Struzik, T. Helfer, F. Bentejac, P. Thévenin, R. Masson, "PLEIADES: A unified environment for multi-dimensional fuel performance modelling", *International Meeting on LWR Fuel Performance*, Orlando, Florida (USA), 19–22 September 2004.



**Yannick Guérin,**
*Fuel Research Department*

# Modeling defects and fission products in $UO_2$ ceramic by *ab initio* computation

As has been noted in the preceding pages, aside from providing a description that is increasingly physical in character, modeling also has the ability to consider ever finer scales. Modeling fission gas behavior, which in earlier times was carried out at the scale of the grain (10 µm), is now concerned with what happens to nanometer-size bubbles, which play a key part in gas migration mechanisms. The evolution of mechanical properties in materials is directly related to what becomes of the **point defects*** generated by irradiation (essentially through displacement cascades caused by recoiling fission products [FPs], at the end of their trajectory): recombination of **vacancies*** and **interstitials***, precipitation in the form of **dislocation*** loops. What becomes of fission products, and the helium yielded by alpha decays, in particular their ability to migrate, depends on the degree to which the atoms can form a solution in the $UO_2$ crystal.

**Atomic-scale modeling**

Atomic-scale modeling makes it possible to gain an understanding, at the quantum scale, of properties of matter that depend on electronic structures (cohesion, spectroscopic, or mechanical properties). The models used all rely on the resolution of equations describing the interactions between the system's constituent nuclei, and electrons. The chief purpose of such computations is to determine the energy corresponding to the most stable geometry, for the system considered. The method selected, based on the density functional theory (DFT), is known as an *"ab initio"* method, since it only involves use of the atoms' intrinsic quantities, i.e. quantities not dependent on a parameter. *Ab initio* modeling of $UO_2$ fuel involves two main difficulties. On the one hand, actinides do not readily lend themselves to theoretical investigation, owing to their 5f electrons, which are liable to exhibit varying degrees of localization around the nuclei. The description of systems involving strongly correlated electrons is a research topic of itself. And, on the other hand, the systems that must be considered in order to take into account defects, and fission products feature complex compositions, and symmetries. Treatment of such systems, consisting moreover as they do of elements with large numbers of electrons, may be simplified, by only considering the valence electrons, these being the only ones involved in the body's chemical and cohesion properties. For uranium, this comes down to treating just 14 electrons per atom, rather than 92. At the same time, expanding electron orbitals in terms of a plane-wave basis makes it possible to arrive, fairly easily, at the equilibrium position of atoms around defects.

If advances are to be made with respect to our understanding of fuel behavior, it is thus essential that further indications be made available, as to the properties, and behavior, of matter at the atomic scale.

It is no simple thing to acquire such data by way of experiment, owing to the difficulties involved in gaining access to the relevant scales. Numerous processes are involved, and their consequences are not readily separated out for evaluation purposes. Among other investigation methods, atomic-scale modeling has been used at CEA since 1996. The purpose of such investigations is to determine precisely the mechanisms of defect and fission product formation and migration in fuel, along with the associated energies.

## *Ab initio* computation

*Ab initio* computations, as regards actinide compounds, began by using approximations such as the local density approximation (LDA), and atomic sphere approximation (ASA) [1]. Subsequently, some effective pseudopotentials were developed, for actinides, and, in particular, for uranium [2, 3]. Combining such pseudopotentials with more sophisticated exchange-correlation approximations, such as the generalized gradient approximation (GGA), made it possible to arrive at precise findings as to defect structure, and energy [4], along with fission product localization, and solubility [5]. More recently, an *ab initio* method, the projector-augmented wave (PAW) method, has allowed systems containing a hundred nonequivalent atoms or so to be modeled, and thus made it possible to investigate more complex processes, such as defect migration.

The contribution of such *ab initio* computation methods lies in their allowing the various kinds of point defects, or of fission products in the fissile material to be treated separately, and, for each of them, making it possible to determine their stability (formation energy, or incorporation energy), their effect on the crystal structure, and migration mechanisms. Such data may be used as input parameters for empirical models describing the behavior of the material under irradiation, at a macroscopic scale. The investigation of point defect behavior, and fission gas and helium solubility, as a function of deviation from stoichiometry in $UO_2$ fuel, is presented in this paper.

## Point defects in uranium dioxide

Defect modeling is carried out by considering a cell of 96 atoms (8 cells in the cubic uranium sublattice), repeated indefinitely across space to form a periodic solid body. Point defects – vacancies, and interstitials – are introduced into this supercell (see Figure 31, for the case of a uranium vacancy). The ideal case would involve being able to consider even larger cells, to ensure defects do not interact between adjacent supercells. A 96-atom supercell, however, is the maximum that may be considered with the present formalism, given currently available computing resources. Computations of total energy are carried out with respect to uranium and oxygen interstitials, and vacancies. From the energies for the system containing these defects, defect formation energies may also be determined. Experimental findings, using neutron diffraction, obtained as early as 1964 [6], show that oxygen interstitials in $UO_{2.12}$ are located at sites offset from the cube centers. However, initial *ab initio* computations have been unable to show such a distortion [3], and, consequently, in the computations presented in this paper, only the octahedral site (at the center of the oxygen cube) is considered, for interstitial defects. Moreover, for large deviations from stoichiometry, many oxygen interstitial defects form clusters [7], a situation not yet catered for by *ab initio* computations.

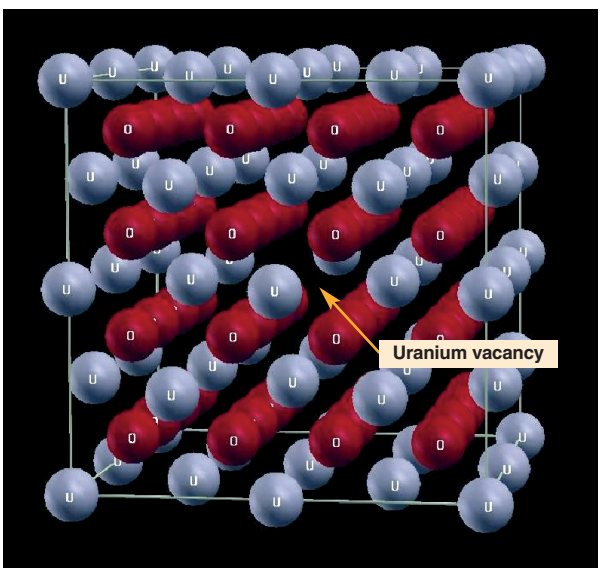


Fig. 31. The supercell considered when modeling point defects in $UO_2$, in this case, for instance, uranium vacancies. Uranium atoms are shown in blue, oxygen atoms in red. The site of the missing uranium atom (the vacancy) is marked out by the arrow.

### *Variations in the volume of the $UO_2$ cell*

For each type of vacancy, and of interstitial, atom positions in the supercell, and supercell volume were computed by minimizing stresses within the solid body. Computed variations in supercell volume show that the largest variation is due to uranium defects, these causing, in the interstitial case, significant swelling, and, in the vacancy case, contraction, to a less significant extent however. Oxygen defects do not result in any major variation.

**Crystal defects**

In crystallography, **point defects*** are defects arising in the arrangement of crystals, that only concern isolated nodes in the crystal lattice. A point defect may consist in a vacancy (a missing atom, leaving an empty position in the crystal lattice), or an interstitial (a "supernumerary" atom, sited at an intermediate location in the lattice). When an atom is displaced from its normal position, to take up an interstitial position, this generates one vacancy, and one interstitial, i.e. a so-called "**Frenkel pair***". Schottky defects are pairs of defects, arising in ionic crystals. A Schottky defect involves the association of one anionic vacancy, and one cationic vacancy.

### *Point defect formation energies in $UO_2$*

Formations energies for a vacancy, or an interstitial defect are obtained from the total energy of the system, with and without the defect involved. These energies further allow formation energies to be determined for Frenkel pairs (i.e. pairs involving one vacancy and one interstitial of the same chemical type), and Schottky defects (involving one uranium vacancy and two oxygen vacancies). *Ab initio* computations predict a greater stability of oxygen Frenkel pairs, compared to uranium Frenkel pairs or Schottky defects. They show that oxygen interstitials exhibit a negative formation energy (– 2.1 eV), with respect to gaseous oxygen. This agrees with the ready oxidation of $UO_2$, confirming that the initial oxidation stage involves the incorporation of oxygen into crystal interstitial sites [3].

### *Point defect migration mechanisms and migration energies in $UO_2$*

Atomic transport properties for a chemical element, or a defect may be arrived at by determining the most favorable migration path for it, and the associated energy barrier that has to be passed (the migration energy). Such an investigation was carried out with respect to the migration of oxygen and uranium defects in $UO_2$. In practice, to launch the computation, a migration path is set for the defect: for instance, the migration of an oxygen vacancy from one crystal site to another (see Fig. 32). The system's energy is then computed for the successive posi-

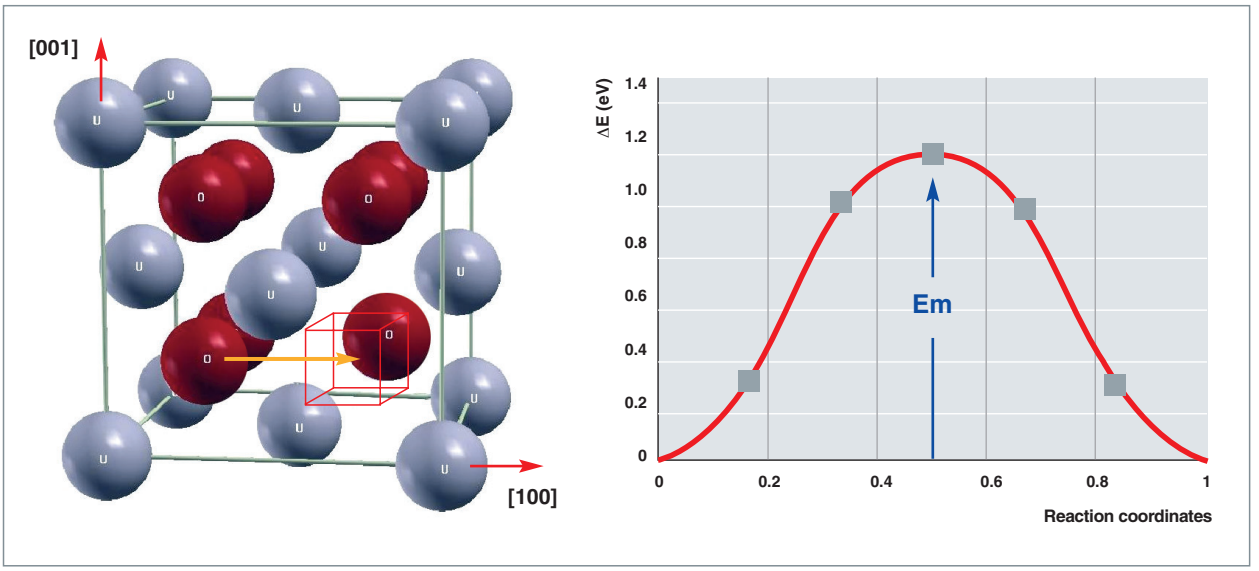


Fig. 32. Left, an example of migration path, explored for the investigation of the transport properties of oxygen defects: migration of an oxygen vacancy along crystallographic direction [100]. At right, the energy barrier D E to be overcome, as computed for the migration of this defect along this direction: the curve maximum corresponds to the migration energy Em.

tions of the defect along its trajectory, taking into account the distortion induced in the structure by the defect. The energy barrier that must be overcome for this migration may thus be determined (see Fig. 32). Migration paths along various crystallographic directions, and involving different mechanisms (vacancy, or interstitialcy) may be explored. In the case of oxygen defects in $UO_2$, *ab initio* computations show that it is a migration mechanism of the indirect interstitial type that involves the lowest migration barrier (1.1 eV). Such an approach may equally be applied to the investigation of the atomic transport of fission products, or helium. Computed migration energies may be brought together, and compared to diffusion activation energies, which can be measured experimentally.

## Fission products in uranium dioxide

*Ab initio* computation further allows the investigation of fission product and helium behavior in fuel. A study using the LDA approximation had already been carried out at CEA for helium, krypton, cesium, iodine, and strontium [8]. Incorporation of the noble gases helium and xenon was also studied, using the GGA approximation [5]. Helium and xenon incorporation energies are computed for various crystal sites: the oxygen or uranium substitution sites, and the octahedral interstitial site. In practice, these elements are introduced into a supercell, in like manner to point defects. The incorporation energies obtained allow the preferred site to be determined, for the incorporated element, and the element's solubility to be quantified, by way of the point defect model (PDM) [9]. The solution energy, as computed, takes into account the concentration of sites at which the gas may settle (vacancies), depending on oxide stoichiometry. For helium, the solution energy obtained is low (< 1 eV), regardless of stoichiometry, which means helium stands at the solubility limit in $UO_2$. The position is more clear-cut for xenon, the solution energy for which stands at around 6 eV in $UO_2$. Incorporation of xenon atoms into the crystal lattice is thus a highly unfavorable event, which agrees with experimental observations showing xenon precipitation in the form of bubbles [10]. The subsequent step in the *ab initio* investigation of fission gas behavior is to gain an understanding of diffusion mechanisms, through computation of migration energies.

## The indispensable coupling of modeling and experiment

*Ab initio* computational studies of $UO_2$ form one of the building blocks in the multiscale modeling of the effects of irradiation on nuclear fuels, a recent, leading-edge area of investigation at CEA. Bridges are being set in place, to ensure the various modeling techniques, from atomic scale to pellet scale, complement one another. This is already the case, in particular, for *ab initio* classical molecular dynamics methods, and kinetic diffusion models. Such linking must be extended, to cover kinetic Monte-Carlo modeling methods (as has been done with respect to metals [11]), and dislocation dynamics methods. At the same time, CEA is actively contributing to improvements in *ab initio* computation methods, and enhanced computing performance is making it possible to consider ever more complex systems. An increasingly finescale description of the physical–chemical properties of actinide compounds is thus becoming feasible, along with ever more realistic modeling of fuel behavior under irradiation. This

approach is beginning to be applied, at CEA, to fuels such as those intended for the reactors of the future (uranium and plutonium carbide, or nitride). Advances in modeling, however, needs must go hand in hand with breakthroughs in experimental methods. Such coupling between modeling and experiment, indeed, is indispensable, in order, on the one hand, to supply models with the empirical physical quantities required to set them up, and, on the other hand, to validate such models *post factum*.

## References


[1] T. Petit, C. Lemaignan, F. Jollet, B. Bigot, A. Pasturel, "Point defects in uranium dioxide", *Phil. Mag.* B 77, 779–786, March 1998.

[2] N. Richard, S. Bernard, F. Jollet, M. Torrent, "Plane-wave pseudopotential study of the light actinides", *Phys. Rev.* B 66, 235112, 2002.

[3] J.-P. Crocombette, F. Jollet, L.-N. Nga, T. Petit, "Plane-wave pseudopotential study of point defects in uranium dioxide", *Phys. Rev.* B 64,104107, 2001.

[4] M. Freyss, T. Petit, J.-P. Crocombette, "Point defects in uranium dioxide: ab initio pseudopotential approach in the generalized gradient approximation", *J. Nucl. Mater.* 347, 44–51, December 2005.

[5] M. Freyss, N. Vergnet, T. Petit, "Ab initio modeling of the behavior of helium and xenon in actinide dioxide nuclear fuels", *J. Nucl. Mater.* 352, 144–150, June 2006.

[6] B. T. M. Willis, *Proc. Br. Ceram.* Soc. 1, 9, 1964.

[7] A. D. Murray,, B. T. M. Willis, "A neutron diffraction study of anion clusters in non-stoichiometric uranium dioxide", *J. Solid State Chem.* 84, 52–27, January 1990.

[8] J.-P. Crocombette, "Ab initio energetics of some fission products (Kr, I, Cs, Sr and He) in uranium dioxide", *J. Nucl. Mater.* 305, 29–36, September 2002.

[9] H. J. Matzke, "Atomic transport properties in $UO_2$ and mixed oxides $(U,Pu)O_2$", *J. Chem. Soc. Faraday Trans.* II 83, 1121–1142, 1987.

[10] P. Garcia, P. Martin, G. Carlot, E. Castelier, M. Ripert, C. Sabathier, C. Valot *et al.,* "A study of xenon aggregates in uranium dioxide using X-ray absorption spectroscopy", *J. Nucl. Mater.* 352, 136–143, June 2006.

[11] C.-C. Fu, J. Dalla Torre, F. Willaime, J.-L. Bocquet, A. Barbu, "Multiscale modelling of defect kinetics in irradiated iron", *Nature Materials* 4, 68–74, January 2005.



**Michel Freyss and Carole Valot,**
*Fuel Research Department*

# Cladding and assembly materials

## What is the purpose of cladding?

In a water reactor, fuel in oxide form may not be put directly into contact with water in the primary circuit, since confinement of fission products must be ensured. In the absence of a cladding which takes on the role of first containment barrier, these fission products would be released directly into the primary circuit water. At the same time, the fuel oxide's mechanical characteristics would not allow control of fissile material geometry to be maintained.

In functional terms, cladding must thus contribute to maintaining fuel geometry inside the core, and ensure the confinement of this fuel, and of the fission products generated within it. It is further required to exhibit a good capability, with respect to removing heat produced in the rod.

From a more operational standpoint, cladding is thus required to exhibit good transparency to neutrons, satisfactory thermal conductivity, good mechanical strength, even at high temperature, high imperviousness, and good corrosion resistance in all situations, including accident situations (up to class 4).

The fuel assembly is likewise required to meet very precise specifications. In functional terms, it has to hold the rods in position, so as to guarantee core geometry, and ensure its proper functioning, in terms of neutronics, and thermal-hydraulics. From an operational standpoint, it is required to prevent rods vibrating as a result of turbulent flow in the primary coolant fluid. It must ensure such support "flexibly," throughout the fuel's in-reactor dwell time, including in incident and accident situations, e.g. in the event of an earthquake, or during unplanned fuel rod heating up, relating either to a reactivity excursion, or to a loss of primary coolant.

In water nuclear power reactors, fuel cladding, but likewise fuel assembly structural components (guide tubes, and grids: see Fig. 33), are fabricated using zirconium alloys. The main reasons guiding such a choice relate to the combination of a number of crucial properties: very low thermal neutron absorption, satisfactory mechanical properties, adequate stability of these properties under neutron flux conditions, and, finally, very high water corrosion resistance at high temperature.

The last two properties are decisive: indeed, other metals likewise exhibit a low thermal neutron **capture* cross-section*** (in particular magnesium, or aluminum, which are used for cladding purposes in research reactors), however their corrosion resistance in the presence of water is found to degrade, as soon as temperature rises. They thus may not be used in reactors where thermal efficiency dictates high temperatures, around 350° C.

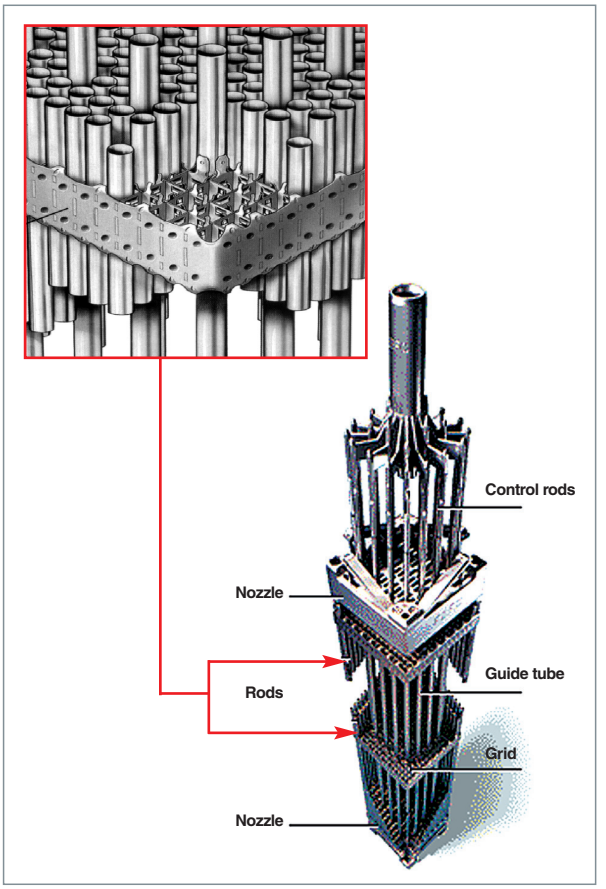


Fig. 33. Pressurized-water reactor (PWR) fuel assembly.

Industrial development of zirconium (Zr), around the 1960s, is bound up with Admiral Hyman G. Rickover's decision, in 1949, to go for zirconium alloys, in the context of the nuclear submarine program. This choice stemmed from their higher neutronic efficiency, compared to stainless steel cladding. It was only subsequently that the "Atoms for Peace" program led to the development of power reactors, derived from the military programs, and thus to an economic optimization of the alloys employed [1].

## Zirconium alloys

Pure zirconium exhibits two crystallographic structures: below 865° C, the alpha structure, of the compact hexagonal type, is thermodynamically stable. Above that temperature, the beta structure, of the body-centered cubic type, is stable. In the beta phase, all alloying additives are soluble, whereas transition metals (iron [Fe], chromium [Cr], nickel [Ni]) are practically insoluble in the alpha phase, forming intermetallic precipitates the size distribution of which influences the alloy's corrosion resistance.

Adding tin enhances mechanical strength, creep resistance in particular, however it does detract from general corrosion resistance; oxygen hardens the alloy; niobium and transition metals bring improved corrosion resistance.

## Claddings: required to exhibit good mechanical strength

The cladding is stressed under the combined effects of outside pressure from the primary circuit (about 15 MPa, in a PWR), pellet swelling, differential pellet–cladding expansion as power varies, and release of fission gases.

Currently, the evolution of the mechanical properties of Zr alloys in the presence of neutron irradiation remains a very active research domain, at CEA, in partnership with EDF and Areva NP. Investigations are addressing both in-service behavior, and the new issue of spent fuel storage. By way of illustration of this particular point, we shall provide some details of the latest findings obtained in this area, covered by a doctoral thesis at CEA [3], focusing on the work-hardening behavior of irradiated Zr alloys.

## Mechanical behavior of irradiated Zr alloys

As a consequence of irradiation, the increased concentration of defects, chiefly <a> loops, localized in the {1010} and {1120} prism planes (see Fig. 34), results in considerable hardening.

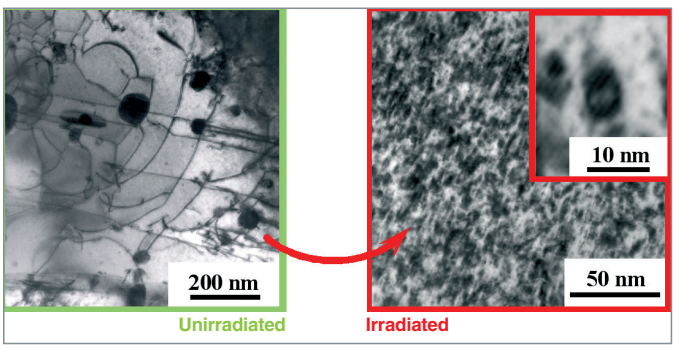


Fig. 34. Electron microscopy images of a zirconium alloy, before and after irradiation.

Thus, regardless of the alloy's nature (chemical composition), or metallurgical state, the yield point is found to rise constantly, reaching a saturation level lying around 600 MPa, for a dose of about $1 \cdot 10^{25}$ n/m², beyond which value saturation of irradiation effects occurs [2].

Figure 35 sets out this evolution of mechanical properties with irradiation.

Concurrently, the **ductility*** of Zr alloys falls constantly, from its original value (several percent) down to less than 1%, for the same irradiation dose. This evolution of uniform elongation with irradiation may be accounted for, if the particular structure of the irradiated material is taken into account: irradiation loops, forming obstacles to dislocation glide as they do [3], may be destroyed, or swept away, given sufficient applied stress, thus giving rise to the creation of a band cleared of irra-

**Composition (in wt%) of the main zirconium alloys employed in light-water reactors**

| Name of alloy | | | | |
|---|---|---|---|---|
| **Alloy constituent** | **Zircaloy-2** | **Zircaloy-4** | **Zr 1-Nb, or M5®** | **Zr 2.5-Nb** |
| **Sn** | 1.2-1.7 | 1.2-1.7 | | |
| **Fe** | 0.07-0.2 | 0.18-0.24 | | |
| **Cr** | 0.05-0.15 | 0.07-0.13 | | |
| **Ni** | 0.03-0.08 | | | |
| **Nb** | | | 1 | 2.5 |
| **O** | | 1,100 à1,400 ppm | | |

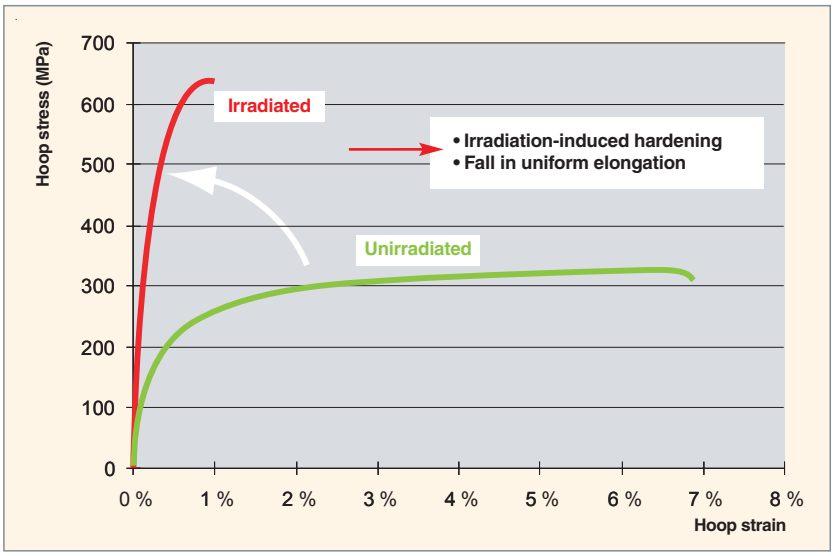


Fig. 35. Evolution of work hardening mechanical behavior, at 350° C (bursting test), of a Zr alloy, before/after irradiation ($10^{25}$ n/m²).

diation defects, forming a preferred glide region for subsequent dislocations. This is the dislocation channeling mechanism.

Once formed, such defect-free regions (the channels) result in highly localized deformation, and thus very low uniform deformation [4], as may be seen in Figure 36.

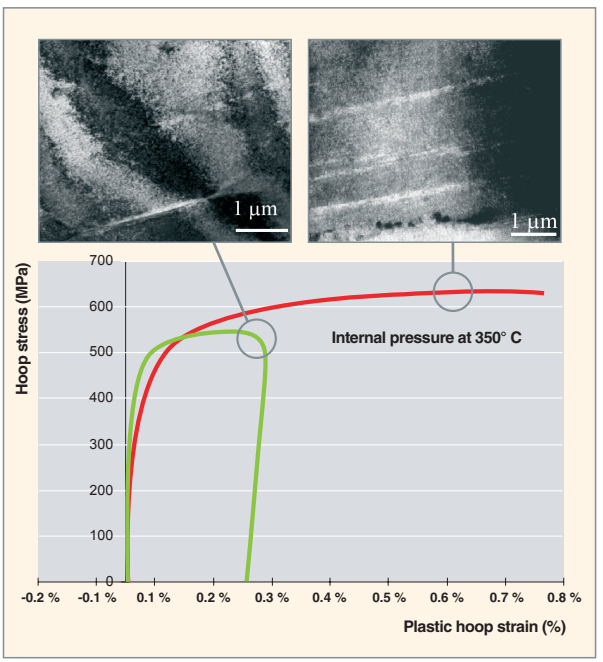


Fig. 36. Channeling, as observed during bursting tests, at two strain levels.

On the basis of such finescale analysis of the microstructure, as observed in transmission electron microscopy, along with the investigation of macroscopic behavior, involving instrumented tests of irradiated materials, using varying stress directions (internal pressure, or traction), it became possible to suggest a predictive micromechanical model, based on identified deformation mechanisms.

The modeling effort, based on heterogeneous material homogenization methods, explicitly taking into account the material's texture, and crystalline nature (slip plane, and direction), along with the irradiation microstructure (loops, and channels), made it possible, in particular, to highlight the major part played by internal stresses. Indeed, these are higher for an irradiated material than in the unirradiated material case, owing to the highly heterogeneous character of deformation (with a marked localization of deformation within channels).

Work to extend this approach, to cover the creep case, and, ultimately, deformations under neutron flux conditions, irradiation creep in particular, has presently been initiated at CEA.

## Claddings: required to prove corrosion resistant

One further point of importance is cladding corrosion resistance. Temperature, metallurgical state, irradiation, water chemistry: there are many factors influencing Zircaloy corrosion kinetics.

The aggressive agent in this respect is primary circuit water, at a temperature of some 300° C. This oxidizes zirconium according to the reaction:

$$Zr + 2H_2O \rightarrow ZrO_2 + 2H_2$$

resulting in formation of solid oxide on the metal's surface. Part of the hydrogen thus generated is incorporated into the metallic matrix, migrating under the effect of the thermal gradient to accumulate in the less hot regions, forming hydrides that are liable to cause brittleness in the cladding, as the fuel cools down. The two processes, oxidation and hydridation, are thus intimately bound up together.

Growth of the oxide layer takes place at the oxide–metal interface, due to the diffusion of oxygen ions through the oxide layer that has already formed, which thus acts as a barrier against further development of corrosion. This protective property of the superficial zirconia layer is limited, however, owing to a change in corrosion regime, associated to a phase transition

in zirconia, once the layer reaches a thickness of a few micrometers [5]. Zirconia can exist – in in-reactor conditions – in two crystallographic forms: monoclinic, and tetragonal. As the oxide layer builds up, formation of the oxide induces local stresses, placing the layer under compressive stress, which stabilizes the tetragonal form. The oxide film, at this stage, is dense, and protective. When the thickness of the layer becomes greater than 2–3 µm, that stress can no longer be sustained: the layer cracks, and the superficial zirconia transforms, switching to a porous monoclinic structure. Subsequent to this transition, the oxide layer comprises a dense, protective inner layer, exhibiting both tetragonal and monoclinic structures, overlain by a basically porous monoclinic layer.

During the initial stage of oxidation (prior to the kinetic transition), oxide thickness, as a function of time, conforms to a law of the form: $\varepsilon_1 = \varepsilon_{1.0} \cdot t^{1/n} \cdot \exp(-\Delta H_1/RT)$, with $n$ ranging between 2 and 3, depending on the nature of the alloy;

During the second stage, the effect of which is predominant in practice, the law was assimilated, as a first approximation, to a linear law, of the form: $\varepsilon_2 = \varepsilon_{2.0} \cdot t \cdot \exp(-\Delta H_2/RT)$. Thorough investigations of the oxide's structure, and of the oxidation kinetics show that the latter, in fact, involves a succession of cycles, comparable to that found for the initial stage.

In the conditions prevailing in water reactors, the oxide layer growth rate stands at some 5–20 µm/year for standard Zircaloys, much less for the new, niobium-base alloys, such as the M5® alloy, developed by Areva NP (see Fig. 39). Activation energy $\Delta H_2$ stands at 120–140 kJ · mol$^{-1}$. The particularly high value for this activation energy results in a doubling in corrosion rate, for a temperature rise of 20° C only, meaning a finescale understanding of the mechanisms involved is indispensable, if corrosion is to be kept under control.

In particular, oxide layer growth, during the cladding's in-reactor dwell time, results in the interposition of a thermal barrier of increasing thickness, between fuel and coolant, causing a rise in temperature at the metal–oxide interface, contributing to the speeding up of in-reactor oxidation kinetics, above ~ 20 µm oxide thickness (see Fig. 37). For instance, at a linear power of 20 kW · m$^{-1}$, for an oxide thickness of 40 µm, temperature at the metal–oxide interface is 20° C higher than coolant temperature, while corrosion rate is increased by a factor 2, compared to that for a new rod. The runaway character of the corrosion process (oxidation and hydridation) at high temperatures precludes an oxide thickness of more than 100 µm or so being tolerated. Moreover, above such a value, oxide spallation sets in, resulting in the release of oxide particles into the primary circuit, and the emergence of cool spots at the level of the underlying metal, thereby affecting hydride precipitation, and speeding up local fuel rod embrittlement.

Aside from temperature, other environmental parameters may significantly speed up the oxidation kinetics for Zr alloys (see

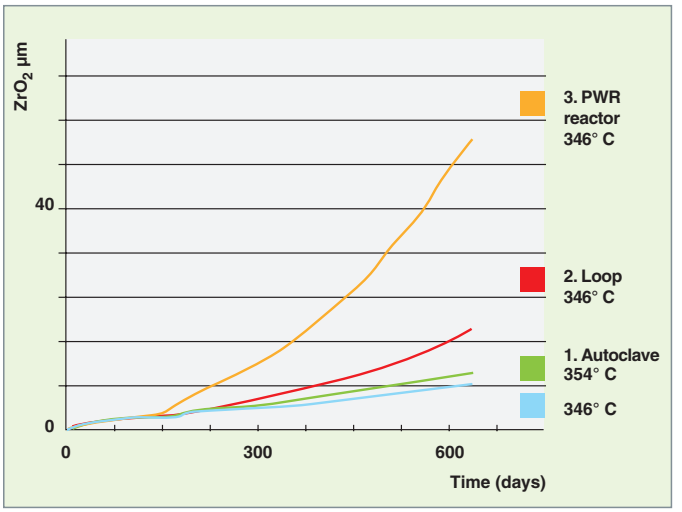


Fig. 37. Thickness of zirconia formed, as a function of time, as derived from tests carried out at CEA on Zircaloy, oxidized under a variety of corrosion conditions: 1. in autoclave (no thermal gradient, at 2 different temperatures); 2. in loop (with electric heating inside the cladding, to simulate heat flux); 3. in reactor (with heat flux, under irradiation). The influence of the various factors inducing speeding up of corrosion may be clearly seen.

Fig. 37). These include, in particular, irradiation, thermal–hydraulics (void fraction, vaporization rate, heat flux), and primary circuit water chemistry (lithium [Li] and boron [B] contents). The latter is closely monitored, both in order to control the reactor's neutronic behavior, and to keep cladding and structural corrosion in check. Addition of boric acid – a neutron absorber – in the primary circuit results in lower pH, which is counteracted by addition of LiOH, which speeds up corrosion. The effect of **radiolysis*** is counterbalanced by addition of $H_2$, acting as a catalyst on the recombination of free radicals.

These points are covered more extensively in monograph DEN M3, dealing with corrosion (in press).

Alloying elements (Fe, Cr) form ordered secondary phases ($ZrCr_2$), which end up incorporated into the zirconia, as the oxide layer is formed (see Fig. 38). These phases, present as they are in an unoxidized state in the inner, dense zirconia layer, restrict oxidation kinetics, probably through an anodic protection mechanism, shielding the matrix.

The improvement brought about by the additive niobium probably involves a different mechanism: in the case of Zr–Nb alloys, in certain conditions, segregation of niobium in the Nb5+ state is found to occur at the zirconia–oxidizing medium interface, over a thickness of a few nanometers. This segregated layer may limit corrosion by acting on water molecule splitting kinetics, at the outer surface of the oxide layer.

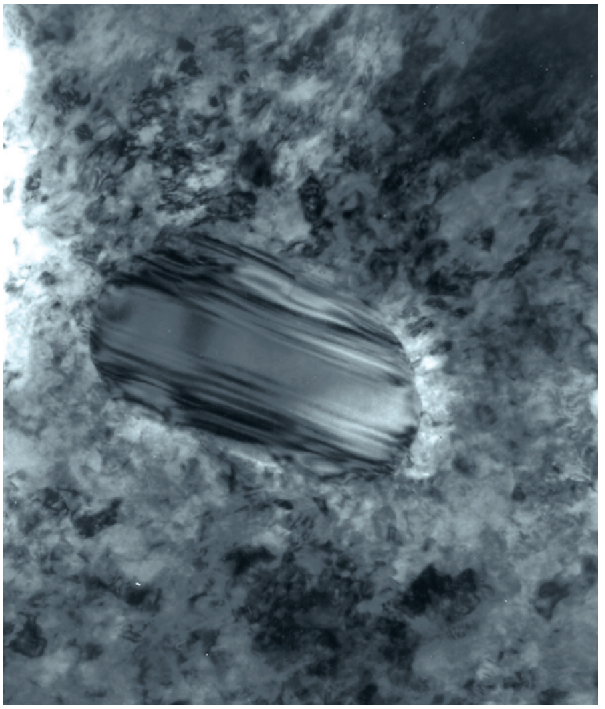

Fig. 38. Intermetallic Zr(Fe,Cr)2 precipitate, observed in transmission electron microscopy, in the dense inner oxide layer (from reference [7]).

Overall, the new M5® alloy exhibits much improved corrosion resistance, compared with earlier Zircaloy grades (see Fig. 39). Such improvement, achieved without impairing cladding mechanical quality, allows a higher operating temperature to be contemplated, along with longer in-reactor dwell times.

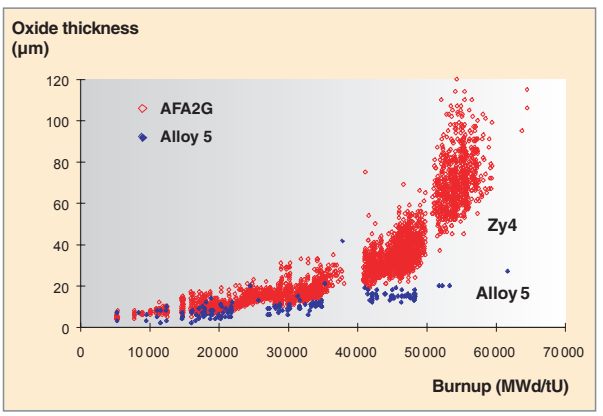


Fig. 39. Oxide thicknesses on $UO_2$ fuel Zy-4 rods [6]. Speeding up of corrosion is found at high burnups, or long dwell times. The benefit afforded by the new M5® alloy is apparent.

## References


[1] C. Lemaignan, *Science des matériaux pour le nucléaire*, "Génie atomique" Series, EDP Sciences, 2004.

[2] D. L. Douglass, "The metallurgy of zirconium", *Atomic Energy Review Supplement*, International Atomic Energy Agency, 1971.

[3] F. Onimus, "Approche expérimentale et modélisation micromécanique du comportement des alliages de zirconium irradiés", Paris École centrale (ECP) doctoral thesis, December 2003.

[4] C. Régnard, B. Verhaeghe, F. Lefebvre-Joud, C. Lemaignan, "Activated slip systems and localized straining of irradiated alloys in circumferential loadings", ASTM STP 1423 (2002), *Zirconium in the nuclear industry, 13th International Symposium*, Annecy (France), 10–14 June 2001, 384–399.

[5] P. Bossis, G. Lelièvre, P. Barberis, X. Iltis et F. Lefebvre, "Multi-scale characterisation of the metal-oxide interface of Zr alloys", ASTM STP 1354 (2000), *Zirconium in the nuclear industry, 12th International Symposium*, Toronto (Canada), 15–18 June 1998, 918–945.

[6] M. Boidron, SFEN Seminar, "Forts taux de combustion", 16 January 2002.

[7] C. Lemaignan, "Corrosion of zirconium alloy components in light water reactors", in B. M. Gordon (ed.), "Corrosion in the Nuclear Power Industry", in *Corrosion*, ASM Handbooks, vol.13, 13C *Corrosion: Environments and Industries*, 2006, 415–420.



**Didier Gilbon and Jean-Luc Béchade**
*Nuclear Materials Department*
**and Bernard Bonin,**
*Scientific Directorate*

# Pellet-cladding interaction

## The phenomena involved in pellet–cladding interaction (PCI)

In nominal operating conditions, pellet temperature stands at about 1,000° C at the center, 400–500° C at the periphery. Under the effect of this thermal gradient, the pellet fragments into wedges and segments, which may be seen after cooling (see Fig. 40). The pellet further takes on an hourglass shape, which leaves its imprint on the cladding, once contact occurs, in the form of primary ridges, likewise visible after cooling, owing to the irreversible deformation induced.

Pellet–cladding contact occurs, on the one hand, owing to a reduction in cladding diameter, due to creepdown caused by pressure from the coolant, and, on the other hand, increased pellet diameter, due to thermal expansion, and swelling. Owing to hourglassing, such contact initially occurs at the level of interpellet spaces. Concurrently, a gradual relocation of pellet fragments is found to take place. Subsequently, a steady state is set up: due to pellet swelling, the cladding is subjected to tensile stress, and accommodates through irradiation **creep*** the diametral strain it is subjected to. Equilibrium hoop stress within the cladding is low (< 100 MPa), compared to creep rupture strength (> 600 MPa), and thus involves no risk of damage.

In the event of a major increase in power, temperature at the pellet center rises steeply (> 1,500° C, or even > 2,000° C, in some cases). Hourglassing is exacerbated, and volatile fission products, liable to attack the cladding, such as iodine, are released, preferentially at the level of cracks in the fuel. All conditions are thus potentially present, to trigger a process of

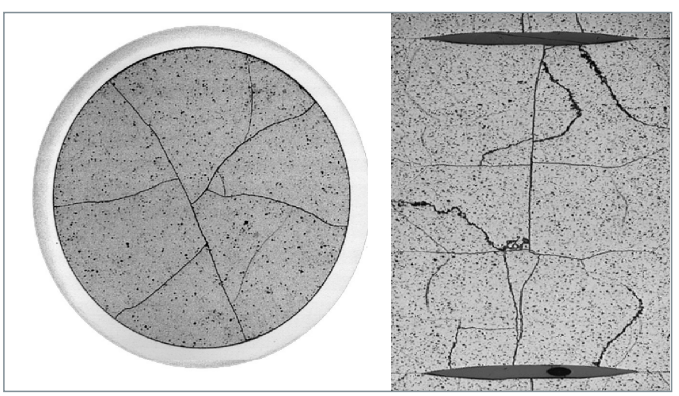

Fig. 40. Cracking in a $UO_2$ pellet, after 2 annual PWR cycles.

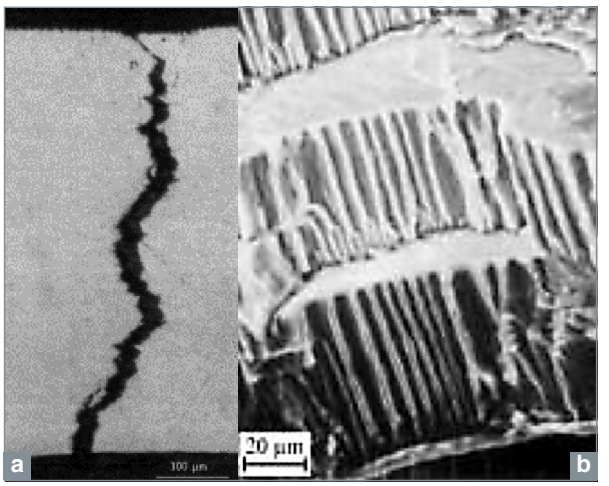


Fig. 41. Transverse section of a cladding end crack (a), and its aspect with typical pattern exhibiting quasi-cleavage planes, and ribbing (b).

stress corrosion cracking (SCC) on the inside surface of the cladding, at the interpellet plane, opposite a radial crack in the fuel pellet. Such corrosion may initiate a radial crack, resulting in a failure exhibiting a characteristic appearance (see Fig. 41).

Such a failure is found to occur, experimentally, after from one to a few minutes' holding time, at sustained high power levels. The edge crack involves little concomitant cladding deformation, and proves hard to visualize on the outside surface. Its specific morphology results in a loss of rod tightness, with respect to gaseous, and volatile fission products, however it does preclude dissemination of fuel into the coolant.

Increasing power causes thermal expansion of the pellets, but equally other processes, which may prove beneficial:

- viscoplastic deformation arises at the pellet center, close to the end dish, resulting in a realignment of radial fragments, thus reducing hourglassing;
- partial relief, through creep, of stress within the cladding curbs the increase in local loading;
- pellet cracking shows a marked evolution during the transient: there occurs, in the brittle rim region, subjected to tensile stress in hot conditions, additional multiple cracking (see Fig. 42), which may contribute to mitigating the damage initiated in the cladding, at the critical location. Circumferential

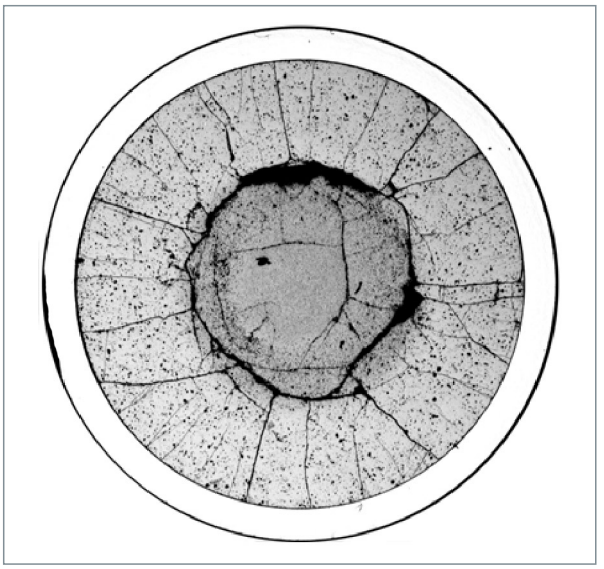

Fig. 42. Cracking in a $UO_2$ pellet subjected to 2 annual PWR cycles, followed by 12 hours at a linear power of 430 W/cm.

cracking, on the other hand, arises during the return to cooler conditions, separating the brittle region from the viscoplastic region.

Finally, a further effect, detrimental at first blush, arises during holding time at high power, all the more marked the higher the power level, the greater the burnup value, and the longer the holding time: to wit, gas swelling affecting the pellet.

Owing to the risk of cladding failure during a power transient, such pellet–cladding interaction (PCI) thus stands as a major process in the safety approach for water reactor (PWR, and BWR) fuel elements: cladding integrity – i.e. integrity of the first fission product containment barrier – must be guaranteed for all normal operational transients (class 1), and all incidental transients (class 2: probability of occurrence ≥ $10^{-2}$ per reactor, per year). To preclude such a risk, the safety approach involves restricting the authorized operating domain for reactors, in terms of maximum allowable power (by way of thresholds for neutronic protection systems), and of core maneuverability (by way of constraints regarding the kinetics of operational transients, and duration of operation at intermediate power). It is of great concern to nuclear power plant operators, obviously, that constraints as to reactor operation be lessened.

## Experimental simulation of PCI and the lessons to be drawn from it. The requirement for an experimental basis

Predicting whether cladding will retain its imperviousness, or otherwise, at the outcome of a power transient calls for precise modeling of pellet, and cladding thermomechanical behavior, which needs must be grounded on a sound basis of experimental data. Existing databases are mainly centered on fuels tested according to a protocol involving a class 2 transient, namely a so-called "power ramp." The transient is applied to a short fuel rod, refabricated from a "mother" rod that has been irradiated in a power reactor.

**What is a power ramp?**

This involves the application of a power transient, rising from an initial power rating close to that prevailing at the end of base irradiation, at a constant ramp rate (as a rule, 100 W · $cm^{-1}$ · $min^{-1}$), to reach a predetermined plateau. This high plateau is held until the experimental rod fails, or for a maximum of 12 hours, in the event of absence of failure. Experiments are carried out in a pressurized-water loop, e.g. in the OSIRIS experimental reactor, at Saclay (France) [3].

The prime purpose of power ramp tests is to specify, for a given rod design, the "technological limit," which, if not exceeded, will guarantee cladding leaktightness. Other experiments, involving in particular ramps with zero holding time, have also been carried out, for the purposes of better understanding, in particular to gain information as to the state of fuel pellets, and cladding, at the point in time when loading is at its most critical [4].

### *Transient characteristics: the role of local power*

The findings obtained show that the maximum power level reached at the end of the ramp (ramp terminal power) may be seen as a major parameter. One may thus specify, for a given rod design, within a given burnup range, a threshold power level, below which the cladding retains its imperviousness, and above which the risk of failure increases, as power rises. This power threshold has been found to lie at around 420–430 W/cm for a $UO_2$ rod, clad with Zircaloy 4, and subjected to a base irradiation of 2 annual cycles in a PWR. By way of comparison, average nominal power, for a PWR rod, stands at about 180 W/cm, and maximum power, not to be exceeded if the criterion of no fuel centerline melting is to be complied with, stands at 590 W/cm.

### *Characteristics of rod initial state: the influence of burnup**

With respect still to the same $UO_2$/Zy–4 rods, risk from PCI would appear to reach a maximum as early as the stage of strong pellet–cladding contact, typically after 2 cycles (~ 25–30 GWd/tU). The subsequent increase in burnup turns out to be somewhat beneficial: in particular, formation of the "rim" region, a small-grained, highly porous region at the pellet periphery, reduces pellet rigidity at the points of contact with cladding, lowering the risks of clad puncture. Such beneficial effects outweigh other burnup-related effects, detrimental at first blush, such as the overall rise in pellet strain, due to gas swelling, or reduced cladding plasticity. Moreover, at high burnup, the occurrence of a high-power transient becomes improbable, owing to increasing fuel specific burnup.

### *The cladding material: from Zy–4 to M5®*

The nature of the cladding material likewise influences the risk of cladding failure. The M5® alloy (a recrystallized alloy), developed for its outstanding aqueous corrosion resistance, exhibits modified mechanical properties, compared to those of the (stress-relieved) Zy–4 alloy, in particular higher irradiation creep resistance at low stress levels, and greater relief capacity under high stress. This results in a rise in the burnup value for which PCI risk reaches a maximum, and a slight increase in the failure threshold power level (~ + 20 W/cm).

### *Benefits from MOX and doped fuel*

Specific fuels were able to withstand, with no cladding failure, ramps to power levels far higher than the threshold value for standard $UO_2$ fuel (~ 420 W/cm).

- MOX [$(U,Pu)O_2$ mixed oxide] rods, base-irradiated over 2–3 annual cycles in a PWR, were successfully tested to levels close to 500 W/cm.

- A large-grained $UO_2$ fuel, obtained by chromium oxide doping, was ramped to 535 W/cm without incurring failure.

These fuels are characterized by a greater high-temperature viscoplasticity than is exhibited by $UO_2$, and denser pellet rim cracking, this being related to greater brittleness in the cool region.

## Numerical simulation of PCI

PCI modeling was initiated, at CEA, with the METEOR code, based on a 1-D axisymmetrical formulation [5], which effects a coupling of every one of the processes involved, yields an estimate of average geometric changes, and evaluates fission product behavior, along with the associated microstructural alterations.

A detailed description of local change conditions, during PCI, does however require a 3-D representation of the fuel element. For that purpose, the TOUTATIS 3-D fuel application [6] was developed, from CEA's CAST3M finite-element code. More recently, a multi-D application, ALCYONE [7], has been developed, in the context of the PLEIADES fuel computation platform [8], to allow all of the advanced models to be integrated, that have been developed in the METEOR and TOUTATIS codes.

### *A multiphysics coupling scheme*

The main processes that have to be taken into account, for the purposes of fuel behavior simulation, are set out in Figure 43.

These processes may be divided into two categories: on the one hand, physicochemistry, which is concerned with fission product behavior, and alterations in the material, at scales ranging from 1 nanometer to about 100 micrometers; and, on the other hand, thermomechanics, which evaluates geometric alterations at the scale of a fuel rod. Multiphysics coupling of the processes is effected via a convergence loop, which links the coupled thermic, mechanical, and physicochemical problems, on the basis of 4 main internal variables: displacements, temperature, stresses, and associated strains.

The mechanical behavior law, for the pellet, takes into account the various strain and creep mechanisms, coupled with the growing extent of cracking in the regions subjected to traction [9]. Cladding viscoplastic behavior under irradiation takes into account, for the various grades of the material, plasticity, creep, and irradiation effects: in particular the increase in creep rate due to the fast-neutron flux, microstructural alteration-related hardening, and axial growth, along with the anisotropy of inelastic behavior.

The chief physicochemical processes selected for consideration, for the purposes of 3-D PCI simulation, are densification, solid swelling, and gas swelling in transient conditions, the latter being directly coupled, in ALCYONE, with mechanical behavior.

In the 3-D finite-element model (see Fig. 46), only one quarter of a pellet fragment is represented, located at the axial elevation of the plane of maximum power applied during the ramp. Boundary conditions take into account fragment geometry-related symmetries, together with pellet–cladding and fragment–fragment interactions.

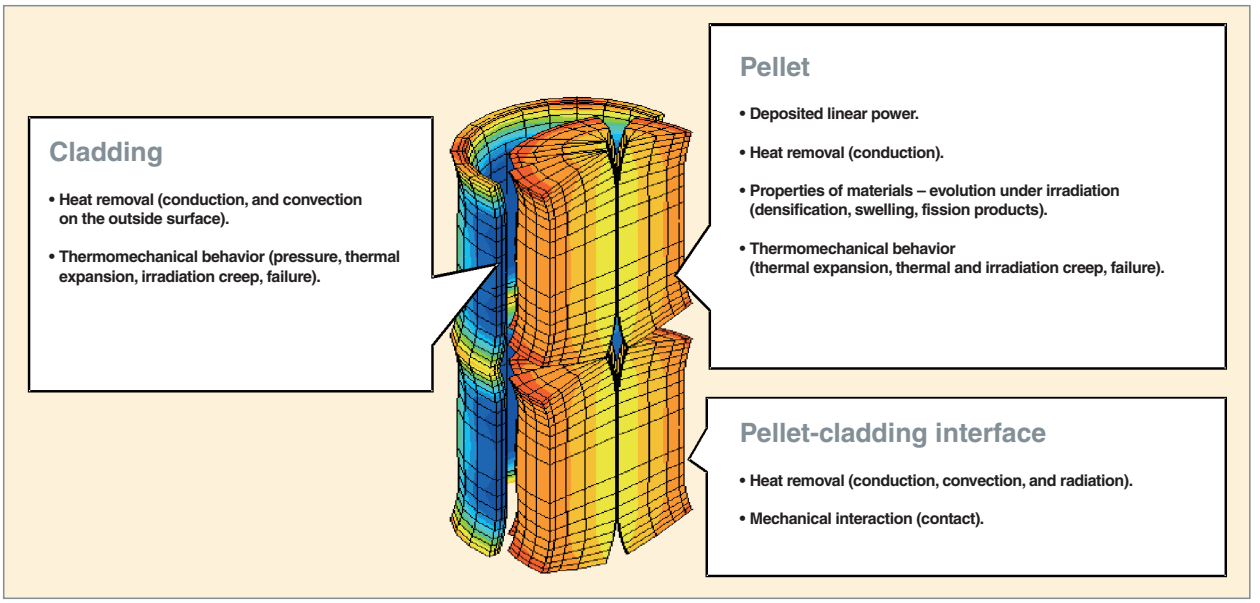


Fig. 43. Thermomechanical modeling of PWR fuel.

### *Computation of cladding external profiles before and after ramping*

The validation of simulation findings on the basis of cladding profilometry allows a verification of the model's ability to mimic the pellet–cladding interaction mechanisms causing significant residual deformation subsequent to irradiation:

- during base irradiation, computation does indeed indicate the various processes that result in pellet hourglassing, and primary ridging in the cladding;

- during the ramp, through the combined effects of thermal loading and gas swelling, computation does show increased viscoplastic strains at the pellet center, these leveling the dish, and attenuating fragment radial relocation at the inter-pellet plane, while, concurrently, contributing to an increase in pellet mid-plane diameter, inducing the secondary ridging observed in post-ramping profilometries.

Comparing findings from computation, and measurement (see Fig. 44) shows the ability of 3-D simulation to predict ridge height, and the variation in diameter, during the ramp. Such satisfactory estimation of diameter variation is one of the improvements brought about by taking into account the coupling with gas swelling, in 3-D computation.

### *Evolution of pellet fragment cracking during irradiation*

Recent developments in 3-D computation now make it possible to compute, consistently with experimental findings, the onset, and evolution (opening, and closure) of axial, radial, and circumferential cracks, arising in various planes in the pellet, as power rises, and drops, thus making for improved computations of the loads transferred to the pellet–cladding interface.

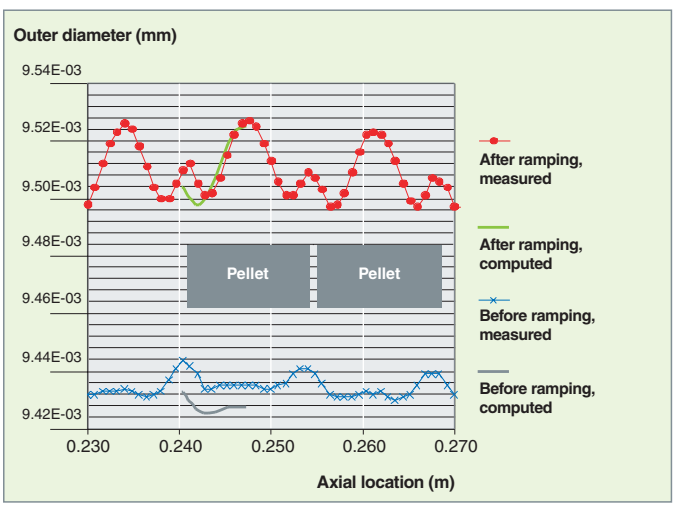


Fig. 44. Cladding outer diameters, as computed, and measured before and after ramping.

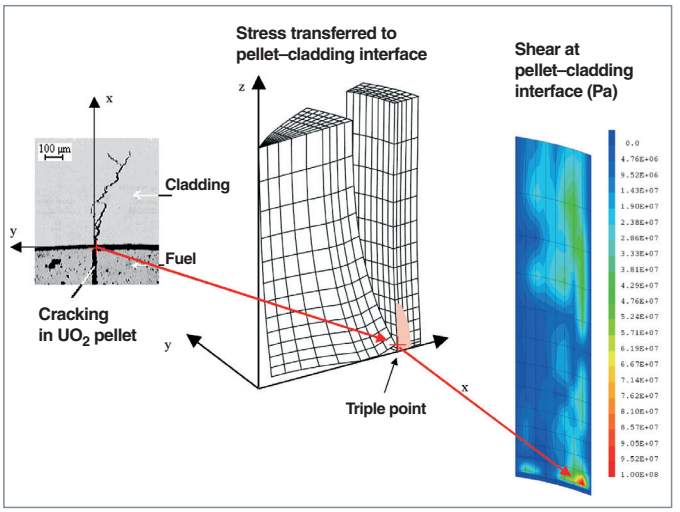


Fig. 45. Localization of shear stress at the end of a ramp transient.

### *Localization of failure during PCI*

Advances in 3-D simulation make it possible to account for the localization typical of PCI failures: maximum shear stress, imparted by the pellet to the cladding, arises at the level of the triple point where the failure occurs (see Fig. 45). Such specific localization is accounted for by the concurrence of maximum values for contact pressure, and the discontinuity in relocation displacement, at the pellet–cladding interface. These two mechanical quantities relate, respectively, to cladding puncture, and the spreading out, to the periphery, of pellet fragments.

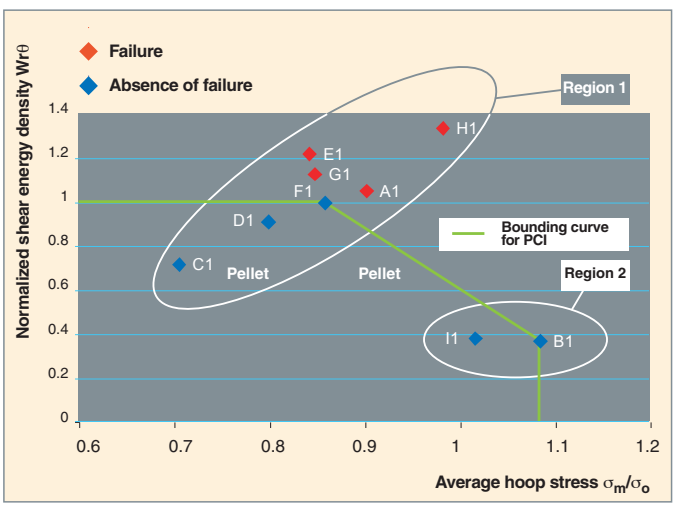


Fig. 46. Findings from ramp tests, ranged against a PCI failure criterion involving two parameters: shear energy at the pellet–cladding interface, average hoop stress.

### *Influence of the fuel on PCI behavior*

3-D simulation further shows that the shear stress transferred by the interface falls when the number of cracks at the pellet periphery rises, this accounting, in part, for the better PCI behavior exhibited by chromium oxide-doped $UO_2$ fuels. A two-parameter criterion has also been suggested. This criterion resolves PCI stress into two aspects: average hoop stress sm, and an energy parameter Wrq, corresponding to the work effected by shear forces at the pellet–cladding interface. Use of a second, interface shear-related parameter thus allows the rational classification of experimental findings obtained from power ramps for standard $UO_2$, and doped $UO_2$ fuels (see Fig. 46). A bounding curve may thus be defined, for PCI failure, common to both fuel types, that is consistent with the absence of failure of chromium oxide-doped fuels at higher power (region 2, in Figure 46).

## Towards a lifting of PCI-related operating constraints

To meet the safety requirement to guarantee the absence of PCI–SCC cladding failure, in the event of a class 1, or class 2 transient, the industrial strategy implemented for French PWRs, grounded as it is on experiment, and modeling, has proven its effectiveness. Indeed, no cladding crack due to PCI has been found in French PWRs. However, this strategy does involve some burdensome directives, with respect to core operation.

With the aim of lessening (or even, ultimately, of lifting) the mandatory PCI restrictions concerning reactor control, a remedial, chromium oxide-doped fuel has been investigated in CEA laboratories. The validation stage has yet to be passed, with an industrially fabricated product. Considering the wide variety of cases that have to be covered, and the complexity of the processes involved, the contribution due to the predictive capability of the 3-D numerical scheme developed by CEA will prove decisive, combined with the drawing up of a robust experimental basis.

### References

[1] C. Mougel, B. Verhaeghe, C. Verdeau, S. Lansiart, S. Béguin, B. Julien, "Power ramping in the OSIRIS reactor: data base analysis for standard $UO_2$ fuel with Zy-4 cladding", *International Seminar on Pellet–Clad Interaction in Water Reactor Fuels*, Aix-en-Provence (France), 9–11 March 2004.

[2] G.G. Bond *et al.*, "SGHWR fuel performance under power ramp conditions", *Journal of the British Nuclear Energy Society* 16, 1977, pp. 225–235.

[3] A. Alberman *et al.*, "Technique for power ramp tests in the ISABELLE 1 loop of the OSIRIS reactor", *Nuclear Engineering and Design* 168, 1997, pp. 293–303.

[4] C. Nonon *et al.*, "Impact of fuel microstructure on PCI behaviour",

International Atomic Energy Agency (2004), *Advanced fuel pellet materials and designs for water cooled reactors. Proceedings of a technical committee meeting held in Brussels, 20–24 October 2003*, pp. 259–277.

[5] P. Garcia, C. Struzik, M. Agard and V. Louche, "Mono-dimensional mechanical modelling of fuel rods under normal and off-normal operating conditions", *Nuclear Engineering and Design 216*, 1–3, July 2002, pp. 183–201.

[6] F. Bentejac, N. Hourdequin, "TOUTATIS: an application of the CAST3M finite element code for PCI three-dimensional modelling", *International Seminar on Pellet–Clad Interaction in Water Reactor Fuels*, Aix-en-Provence (France), 9–11 March 2004.

[7] G. Thouvenin, J.-M. Ricaud, B. Michel, "ALCYONE: the PLEIADES fuel performance code dedicated to multidimensional PWR studies", *International Meeting on LWR Fuel Performance*, Salamanca (Spain), 22–26 October 2006.

[8] D. Plancq, "PLEIADES: a unified environment for multi-dimensional fuel performance modelling", *International Meeting on LWR Fuel Performance*, Orlando, Florida (USA), 19–22 September 2004.

[9] B. Michel, J. Sercombe *et al.*, "3D fuel cracking modelling in pellet cladding mechanical interaction", *Engineering Fracture Mechanics*, 2007 (in press).

**Sylvie Lansiart and Bruno Michel,**
*Fuel Research Department*

# Avanced $UO_2$ and MOX ceramics

With a view to improving economic returns, nuclear power plant operators are looking to increased burnup of $UO_2$ and MOX fuels, involving longer in-reactor dwell times. Fuels are further required to enable flexible reactor operation, by allowing reactor power to be matched to the requirements of the power distribution grid, while retaining adequate safety margins. A first step was achieved with the development of a cladding material exhibiting higher corrosion resistance: a zirconium–niobium alloy (see the chapter on "Cladding and assembly materials"), making it possible to overcome one of the first obstacles encountered, as regards achieving increased burnup values, namely cladding external corrosion.

These goals further entail the development, and qualification of novel fuel pellet microstructures, affording better performance, with the ability, in particular, to attenuate mechanical stresses, and mitigate pellet–cladding interaction-related cladding failure risks, and further exhibiting higher fission gas retention capacity, whether in normal operating conditions or accident conditions. To meet these requirements, investigations are looking into $UO_2$ or MOX ceramics, featuring a highly controlled microstructure, in particular through the addition of doping agents at the time of sintering.

## Chromium oxide-doped $UO_2$ fuel

The prime aim, as regards enhanced $UO_2$ fuel performance, is to achieve improved reactor maneuverability, and consequently to secure availability of a fuel allowing the lessening of operating constraints dictated by PCI failure risk (see the chapter on "Pellet–cladding interaction"). To that end, investigations have looked to a material exhibiting improved mechanical properties, compared to standard $UO_2$, in particular a higher creep rate.

A second aim is to achieve enhanced fission gas retention capacity, in order to extend fuel rod burnup, while retaining adequate margins as regards internal pressure. To that end, researchers have sought to obtain large-grained microstructures, the idea being to increase the distance fission gases must travel in order to arrive at grain boundaries, this being the first stage on the path that, ultimately, ends in gases being released into the **plenum***.

Large-grained $UO_2$ microstructures may be obtained either through very lengthy sintering, which is uneconomic, or through oxidizing sintering, which would involve considerable capital costs, and a sintering cycle that is not easily mastered. A third method involves the use of sintering additives, in particular trivalent oxides such as $Cr_2O_3$ or $Al_2O_3$, complemented – or not, as the case may be – by a second additive, $SiO_2$, to form viscous phases at the grain boundaries.

A major R&D program has been carried out at CEA [1, 2, 3], in collaboration with Areva NP and EDF, for the purposes of:

- developing fabrication conditions that allow large grains to be obtained; identifying, and understanding the mechanisms resulting in larger grain size; and optimizing the relevant parameters (in particular, additive contents); it is indeed imperative that the additive cation be kept with valence 3, and sintering must thus be carried out in a moist hydrogen atmosphere, in order to maintain an adequate oxygen potential. For the same temperature (1,700° C), and same sintering time, it thus becomes feasible to obtain grain sizes of 50 µm or more, as compared to standard grains of about 10 µm (see Fig. 47);

- characterizing the pellets thus obtained, by determining, in particular, their mechanical properties (creep, plastic deformation). A significantly increased creep rate has thus been

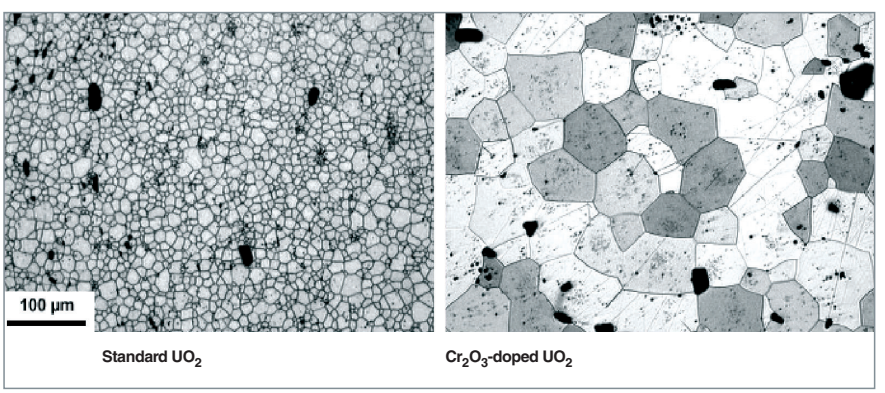


Fig. 47. Grain sizes in chromium oxide-doped $UO_2$, compared with those found in standard $UO_2$.

evidenced for doped $UO_2$ products, compared to the values obtained with standard $UO_2$ (contrary to what might have been anticipated for a large-grained product, had diffusion creep been the dominant creep mechanism, in the temperature/stress domain being considered);

- carrying out initial tests under irradiation, in experimental reactors, with the various microstructures obtained, and thus effecting an initial selection, on the basis, in particular, of a program involving thermal annealing of irradiated pellets;

- setting up initial rod irradiations in PWRs, involving chromium oxide-doped $UO_2$ (CONCERTO experiments). These rods, subjected to examinations at various burnup values, made it possible, subsequent to two irradiation cycles, to carry out power ramps, demonstrating the major gains afforded by these doped products, with respect to the PCI issue [4], since ramping to 535 W/cm was achieved with no failure occurring, i.e. with a gain of some 100 W/cm, compared to standard $UO_2$ [5].

Development of such doped products is currently carrying forward, with the irradiation of complete assemblies in PWRs, for the purposes of product qualification.

## Novel MOX microstructures

The behavior of MOX fuels contrasts with that of $UO_2$ fuels, in that it involves high rates of fission gas release (see the chapter on "In-reactor behavior of $UO_2$ and MOX fuels"). Such larger release from MOX fuels is the outcome of a harsher irradiation history than is the case for $UO_2$ rods (higher linear power levels at the end of irradiation), and a higher centerline temperature (due to slightly lower thermal conductivity); however, the specific microstructure found in MOX fabricated by the MIMAS process (see the chapter on "Fabrication of water reactor fuels"), exhibiting as it does slightly smaller grain sizes than $UO_2$, and a heterogeneous fissile material distribution [6], may equally play a part in this respect, and the issue has been addressed by in-depth investigations at CEA: the plutonium-rich aggregates are regions of very high burnup, causing restructuring of the mixed oxide: a further division of grains, and precipitation of gas bubbles, which now end up at intergranular locations, thus being immediately available for release, in the event of a power transient. In particular, at the end of reactivity insertion accident (RIA) tests, fission gas release is found to be higher in MOX fuels than in $UO_2$ fuels.

In order to regain better margins, an R&D drive was conducted at CEA, in collaboration with Areva NC, Areva NP, and EDF, to develop novel MOX microstructures, exhibiting a higher retention capacity [7, 8]. As in the case of $UO_2$, the aim is to increase grain size, however a further aim is to achieve improved homogeneity of plutonium distribution, while retain-

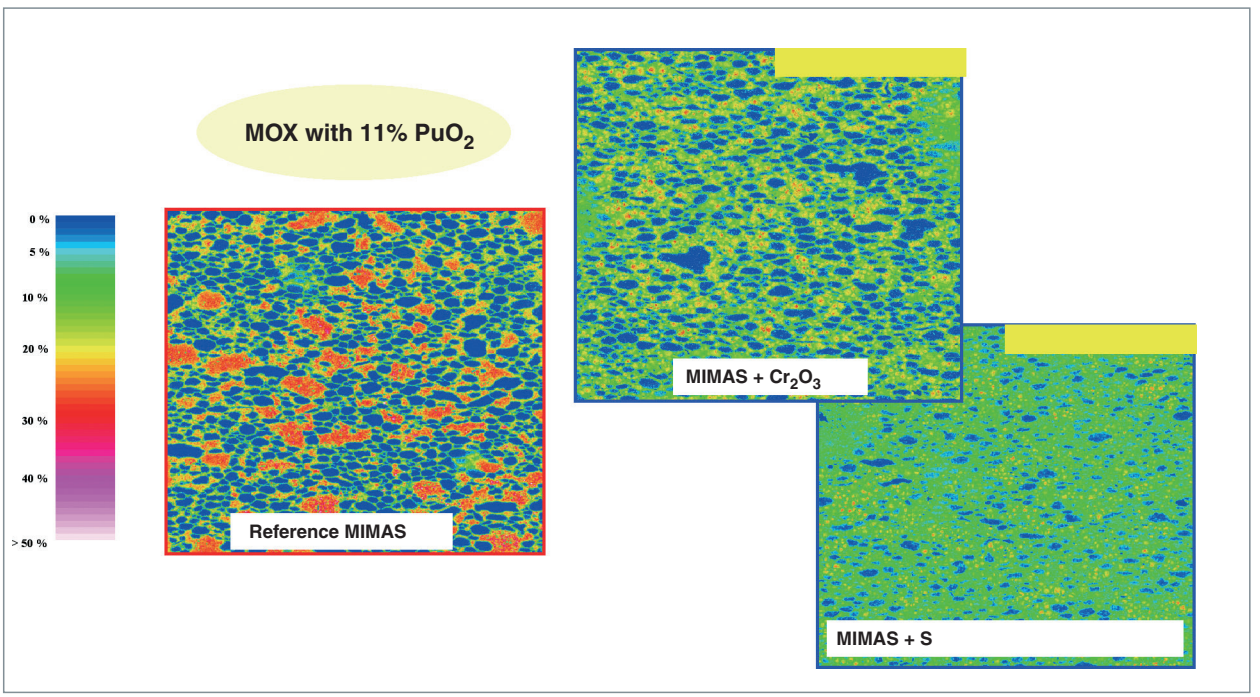


Fig. 48. Microprobe mappings of MIMAS MOX fuel featuring chromium oxide and sulfur additives, compared with a standard MOX fuel.

ing the MIMAS fabrication process, for which the MELOX plant was dimensioned.

The investigations have made it possible, in particular, to ascertain, and understand the influence of sintering additives, namely chromium oxide and sulfur, on grain growth, and on uranium and plutonium interdiffusion during sintering. It has thus been shown that, through use of these additives, gains could be achieved by a factor 2–3 in terms of grain sizes, in MOX fuel; it proves highly difficult, however, to achieve grain sizes as large as with $UO_2$: the formation of the solid $(U,Pu)O_2$ phase slows down grain growth. The findings further showed that presence of chromium, or sulfur allowed a speeding up of U and Pu interdiffusion: with the MIMAS process, it thus becomes feasible to obtain a near-homogeneous fissile material distribution (see Fig. 48).

The behavior under irradiation of these novel MOX microstructures is currently being investigated, through irradiations in experimental reactors, in particular in OSIRIS, at Saclay (France). Irradiations of rods fabricated in industrial facilities are due to be carried out in the near future, in power reactors. The crucial issue will be to ascertain that these microstructures do afford the gains anticipated, while not involving detrimental effects in other respects, in particular with regard to the satisfactory pellet–cladding interaction behavior achieved with standard MOX fuel.

## References


[1] Ph. Dehaudt, L. Caillot, G. Delette, G. Eminet, A. Mocellin, "Irradiation of $UO_2$ + x fuels in the TANOX device", IAEA, *Technical Committee Meeting on Advances in Pellet Technology for Improved Performance at High Burnup*, Tokyo (Japan), 28 October–1 November 1996.

[2] L. Bourgeois, Ph. Dehaudt, C. Lemaignan, A. Hammou, "Factors governing microstructure development of $Cr_2O_3$-doped $UO_2$ during sintering", *Journal of Nuclear Materials* 297, 2001, 313–326.

[3] S. Valin, L. Caillot, Ph. Dehaudt, Y. Guérin, A. Mocellin, C. Delafoy, A. Chotard, "Synthesis of the results obtained on the advanced $UO_2$ microstructures irradiated in the TANOX device", International Atomic Energy Agency (2004), *Advanced fuel pellet materials and designs for water cooled reactors. Proceedings of a technical committee meeting held in Brussels, 20–24 October 2003*, 175–186.

[4] Ch. Delafoy, P. Blanpain, C. Maury, Ph. Dehaudt, Ch. Nonon, S. Valin, "Advanced $UO_2$ fuel with improved PCI resistance and fission gas retention capability", *TOPFUEL 2003, International Symposium on the Nuclear Fuel Cycle*, Würzburg (Germany), 16–19 March 2003.

[5] C. Nonon, J.-C. Ménard, S. Lansiart, J. Noirot, S. Martin, G.-M. Decroix, O. Rabouille, C. Delafoix, B. Petitprez, "PCI behaviour of chromium oxide doped fuel", *International Seminar on PCI in Water Reactor Fuels*, Aix-en-Provence (France), 9–11 March 2004.

[6] G. Oudinet, I. Munoz-Viallard, M.-J. Gotta, J.-M. Becker, G. Chiarelli, R. Castelli, "On the characterization of Pu distribution in MIMAS MOX by image analysis", *International Atomic Energy Agency (2004), Advanced fuel pellet materials and designs for water cooled reactors. Proceedings of a technical committee meeting held in Brussels, 20–24 October 2003*, 221–233.

[7] P. Blanpain, L. Brunel, X. Thibault, M. Trotabas. "MOX Fuel Performance in the French PWRs: Status and Developments", *Proceedings of the International Topical Meeting on Light Water Reactor Fuel Performance*, Park City, Utah (USA), 10–13 April 2000.

[8] P. Blanpain, M. Arslan, J.-C. Bouchter, X. Thibault, "Le MOX et ses évolutions futures", SFEN Annual Convention, *Le Combustible nucléaire: de la mine au réacteur*, 13–14 June 2006.



**Yannick Guérin,**
*Fuel Research Department*

# Mechanical behavior of fuel assemblies

The fuel assembly (i.e. the unit comprising the support skeleton, and fuel rods: see Fig. 49) forms a mechanical structure that is subjected to the complex hydraulic loadings imparted to it by the coolant fluid (flow turbulence, flow redistribution within the core); loads imparted to the support components, at the boundaries, by the surrounding structures (vessel internals, upper and lower core plates); and effects due to its environment (temperature, neutron flux, primary circuit chemistry), inducing in-service alterations in its constituent materials. Stresses resulting from normal conditions, accident situations (earthquake, loss of primary coolant accident [LOCA]), handling, or pool storage must never – not at any point in the assembly's lifetime – compromise its essential functions, with respect to reactor safety. It is imperative to ensure, in particular, that the integrity of the first containment barrier is preserved, along with the fissile material distribution geometry inside the core, the ability to cool fuel elements, and the ability to insert cluster control assemblies.

With a view to improving competitiveness for the nuclear electricity generation fleet, the new fuel management modes now being implemented, or planned tend to go for increased fuel assembly burnup, and longer in-reactor dwell times. Such a trend towards longer in-reactor dwell times has an incidence on the mechanical behavior of assembly structures, owing in particular to the evolution of its various components under irradiation. At the same time, the call for ever greater safety entails improved control of situations that might result in a cladding breach, whether owing to the impact of stray debris carried by the coolant, or a speeding up of cladding wear from fretting, through the repeated chafing of vibrating rods against supports. This further entails gaining a better understanding of fuel assembly deformations liable to slow down the fall of **rod cluster control assemblies*** (RCCAs), and compiling more stringent mandatory reports to guarantee assembly mechanical behavior in accident conditions (earthquake, **LOCA***).

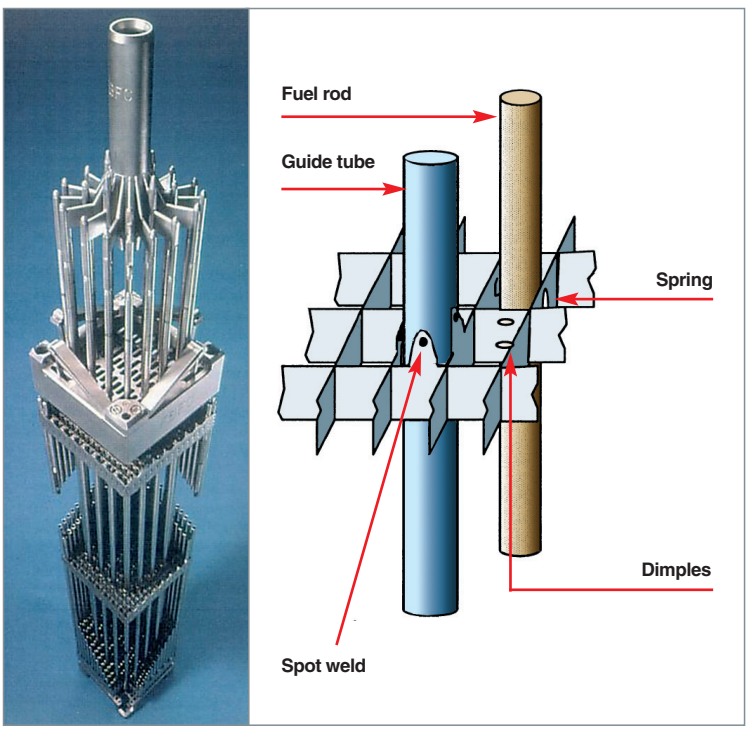


Fig. 49. Fuel assembly + rod cluster control assembly. Principle schematic of an AFA grid cell.

Mechanical design studies, for PWR fuel assemblies, are part of the manufacturer's remit. R&D studies carried out at CEA are on offer, and used to support assembly design justification. These studies rely on experimental test loop protocols, analytical experiments, and modeling of mechanical behavior. Their chief purpose is to enhance the robustness of qualification and design methodologies, and to investigate issues related to incidents arising in the fleet, for which CEA expertise has been called in.

Numerous cladding failures initiated by grid-to-rod **fretting*** processes occurred, with the deployment of "extended" management modes, in the early 2000s [1]. In the United States, punctures due to grid-to-rod fretting were found, in PWRs, to account for ~ 25% of the causes of failure in the early 1990s, rising to 90% by the end of that decade [2]. A major R&D effort was launched to mitigate these issues, and arrive at more rugged assemblies.

## Assembly mechanical behavior in normal operating conditions

Inside the core, assembly structures are subjected to a variety of stresses: compression loads, imparted by the springs in the support system, coolant fluid hydrodynamic loads on the assembly; irradiation, inducing assembly and rod growth, together with the relief, through flux creep, of stressed structures… Controlling such loads throughout the irradiation cycle is crucial, since inadequate axial support results in assembly "liftoff," while increased loading causes excessive lateral deformation of the guide tubes. The latter condition results in additional friction loads for the rod cluster control assembly, resulting in a degradation of RCCA drop kinetics.

The R&D effort carried out at CEA seeks to achieve improved preliminary evaluation of in-reactor behavior for structures involving novel designs, this entailing:

- modeling in-reactor hydraulic loadings, and associated structural deformations. Such modeling is validated through the out-of-pile experimental determination of axial, and transverse hydraulic loads, in test loops (see Fig. 50);
- ascertaining the creep laws, for component (guide tube, support system springs, grid springs) constituent materials, by means of numerous experimental irradiations, carried out in the OSIRIS reactor. These laws are then integrated into mechanical models taking into account the effects of irradiation on deformation;
- empirical evaluation of component characteristics, in the thermal–hydraulic conditions prevailing in PWRs: relief of friction loads in the support system under flow conditions, support system hysteresis curves, pressure drop at grids and nozzles (see Fig. 51);
- ascertaining the consequences of the overall deformations observed in reactor, with respect to RCCA drop kinetics, in facilities providing full-scale simulation of the PWR command line, and integrating: core plates, fuel assembly, RCCA guide, rod cluster control assembly, rod cladding, and control rod drive mechanism (see Fig. 52) [3].

Vibrations induced by in-core flow turbulence affect the fuel rods. These vibrations result in relative motion of the rod, with respect to its supports (spring and/or dimple) in the grid cell. This motion is the root cause of the fretting wear found on

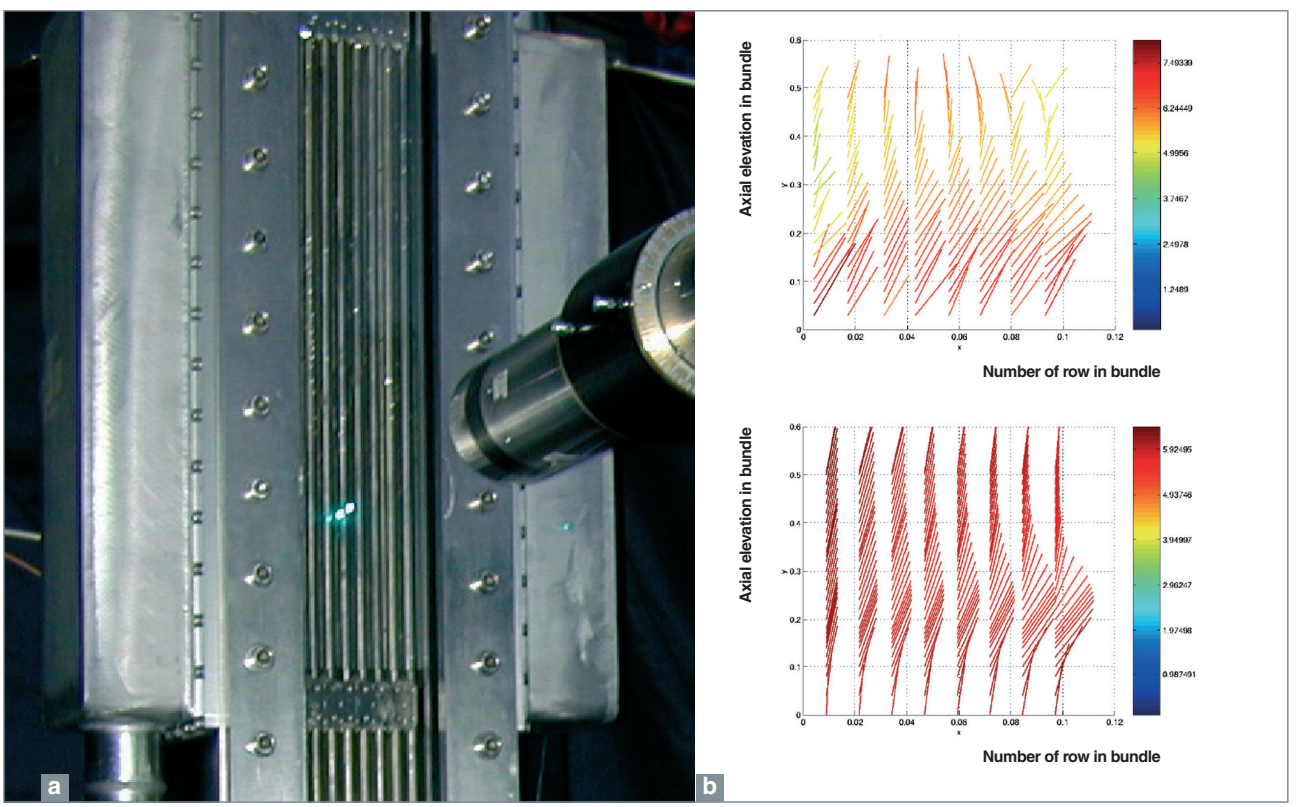


Fig. 50. Photograph of the laser velocimetry bench mounted in the dedicated experimental facility used for flow characterization, and measurements of fuel rod loadings (a). Comparison of measurements of fluid velocity fields within the bundle (top), and computations carried out using the FLICA code (bottom). Velocity fields are shown as normed vector fields (b).

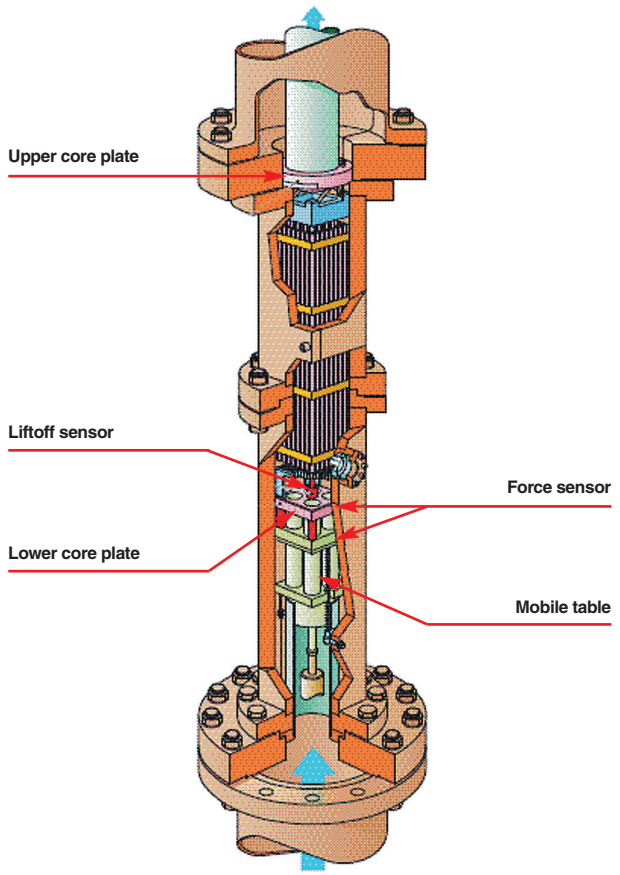


Fig. 51. Schematic of the dedicated experimental facility used for support system characterization (HERMES T/single, full-scale assembly). Illustrated: experimentally obtained hysteresis curve.

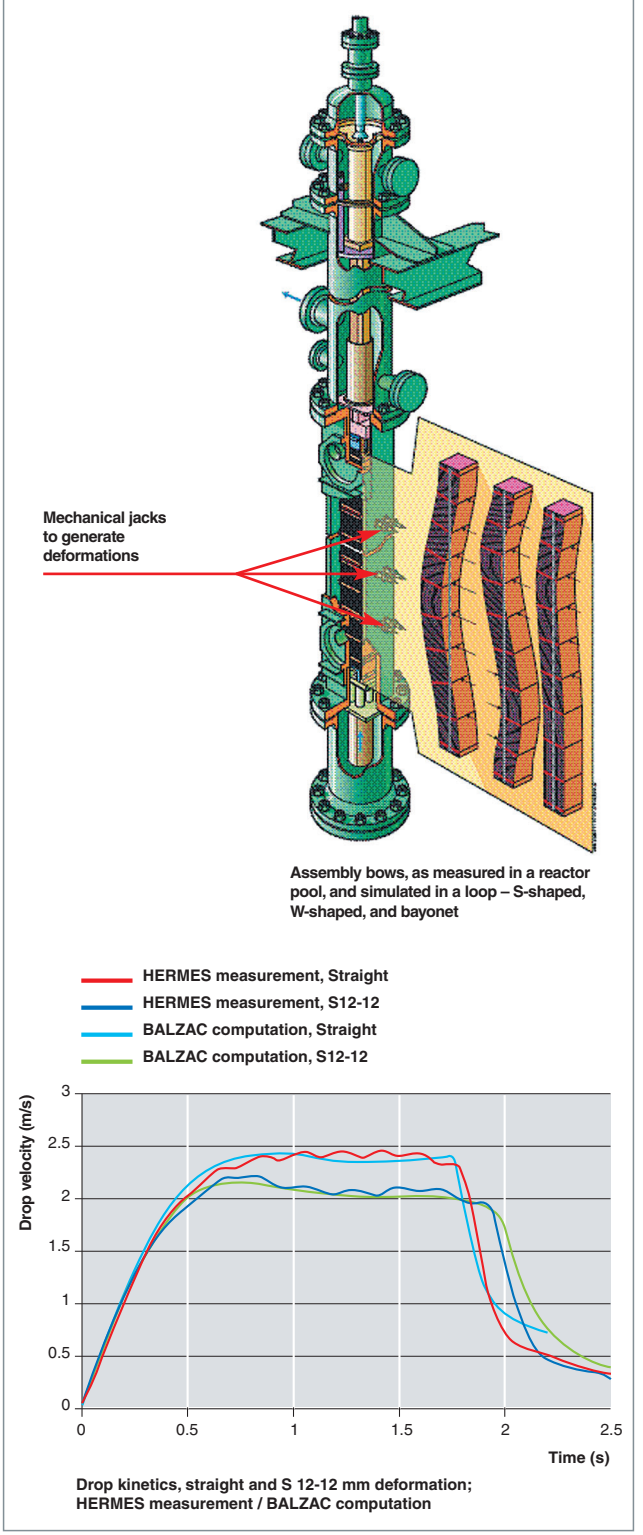


Fig. 52. Schematic of the dedicated facility used for drop kinetic measurements, under a variety of fuel assembly deformations. Illustrated: drop kinetics, as measured:
– on a nonbowed assembly (red curve);
– on an assembly exhibiting 12-mm amplitude, S-shaped bowing (blue curve), and comparison with the associated "BALZAC" modeling.

some claddings, at the level where contacts occur. The kinetics of such wear varies, depending on rod support in the grid cell, the state of the surfaces coming into contact, and rod modal characteristics.

Finally, aging during in-reactor cycles results in reduced rod restraint loads within the cell. This is due to creep or flux relief in grid springs, or dimples, rod diameter variations, and grid growth. During irradiation, alterations are also observed with respect to surface mechanical properties, these being related to the environment (primary circuit chemistry, power history), and its impact on cladding and structural materials (corrosion, hydriding, local corrosion, combined effects of mechanical wear and oxidation, or "tribocorrosion"…). Finally, irradiation induces an evolution in the fuel rod's global mechanical characteristics, e.g. structural damping, during irradiation, owing in particular to closure of the pellet–cladding gap, as a result of cladding creepdown, when subjected to external pressure from primary circuit water.

Increased in-reactor dwell times, for assemblies, may thus result in unfavorable situations, as regards wear, under the combined effects of these various aging processes.

Preliminary controls of fuel assembly endurance have led to the deployment, and improvement of experimental facilities, and test protocols, for the purposes of qualifying cladding wear resistance, with new types of supports, or involving novel materials.

At the same time, modeling tools, to model rod vibration behavior when subjected to flow turbulence, are leading to improved interpretation of findings yielded by the experimental protocols. Modeling wear, on the other hand, is a complex matter, owing to the many relevant parameters that must be integrated, and satisfactory prediction of wear, on the mere basis of computed vibration response, wear load, and Archard's law [4], would appear to be inadequate, for the purposes of addressing issues relating to assembly endurance: indeed, while mechanical wear is, as a whole, quite adequately described in terms of this law, the PWR environment, which is not taken into account here, probably influences wear kinetics in a complex fashion. For that reason, tests for qualification purposes are carried out in a representative environment, in terms of chemistry and thermal–hydraulics.

For the purposes of PWR fuel qualification, with respect to wear resistance, two approaches, one an experimental, the other a modeling approach, are implemented concurrently. The experimental protocols, and the associated models thus drawn up involve the following ingredients:

- evaluation of in-core mechanical loadings, and specification of the conditions to be implemented in order to simulate such loadings in out-of-pile test loops (HERMES). This step relies on thermal–hydraulic computations;
- evaluation, by means of computation, of the vibration response to these loadings, as characterized by the turbulent flow excitation spectrum. Modeling of fuel rod vibration response to flow turbulence, initiated in the 1990s [5], involves linear methods, using a modal basis. The vibration amplitude ($\sigma_r$) exhibited by the modal response (for mode $r$) takes the form:

$$\sigma_r(x) = F_{fluide} \times H_{structure} \times \sqrt{f_{Rr}\,\overline{\phi}_{fe}\left(f_{Rr}\right)\,a_r^2} \quad (1)$$

where $F_{\text{fluid}}$ is a characteristic constant for the flowing fluid, and $H_{\text{structure}}$ is a characteristic transfer function, for the structure's modal response.

$\overline{\phi}_{fe}\left(f_{Rr}\right)$ is the flow's turbulent excitation spectrum (a function of frequency $f_{Rr}$, i.e. of the product of vibration frequency by rod diameter, normalized by flow velocity), and $a_r$ is a modal excitation coefficient. It should be noted that turbulent excitation spectra were initially determined experimentally, through direct measurement of the loads on ideal mockups of fuel rod bundles. To narrow down the discrepancy between vibration behavior, as predicted by the standard model outlined above, and that found in test-loop vibration measurements, advances achieved with signal processing tools have been put to good use, to develop an inverse method of spectrum identification (see Fig. 53) on scaled-down, more representative assembly structures. Typically, vibration amplitudes, as measured on assembly structures, stand at a few tens of microns or so, for frequencies ranging from a few hertz, for assemblies, to several tens of hertz, for fuel rods;

- evaluation – by way of analytical experiments – of the environmental parameters influencing wear kinetics (length of test, temperature, chemistry, wear/corrosion competition…). Such investigations have the purpose, on the one hand, of evaluating the potential impact of conditions used in test loops, as regards carrying out accelerated endurance tests, and, on the other hand, of achieving, in the longer term, improved predictive capability for models used to predict in-service wear;
- construction of test mockups, representative of the fuel assembly at the various stages in its lifetime: on the basis of what is known as to grid and rod material in-reactor behavior, the evolution of rod support under irradiation may then be estimated.

Data from these investigations are integrated into the specification of the experimental wear resistance qualification protocol, for a new design, carried out in an out-of-pile facility (HERMES), in PWR thermal–hydraulic conditions [6]. This protocol has been validated, in terms of its ability to mimic fretting processes in bottom support grids, as observed in reactor [2].

The HERMES facility features a hydraulic loop, simulating PWR thermal–hydraulic conditions. The test section allows variable flow conditions to be set up around the (full-scale)

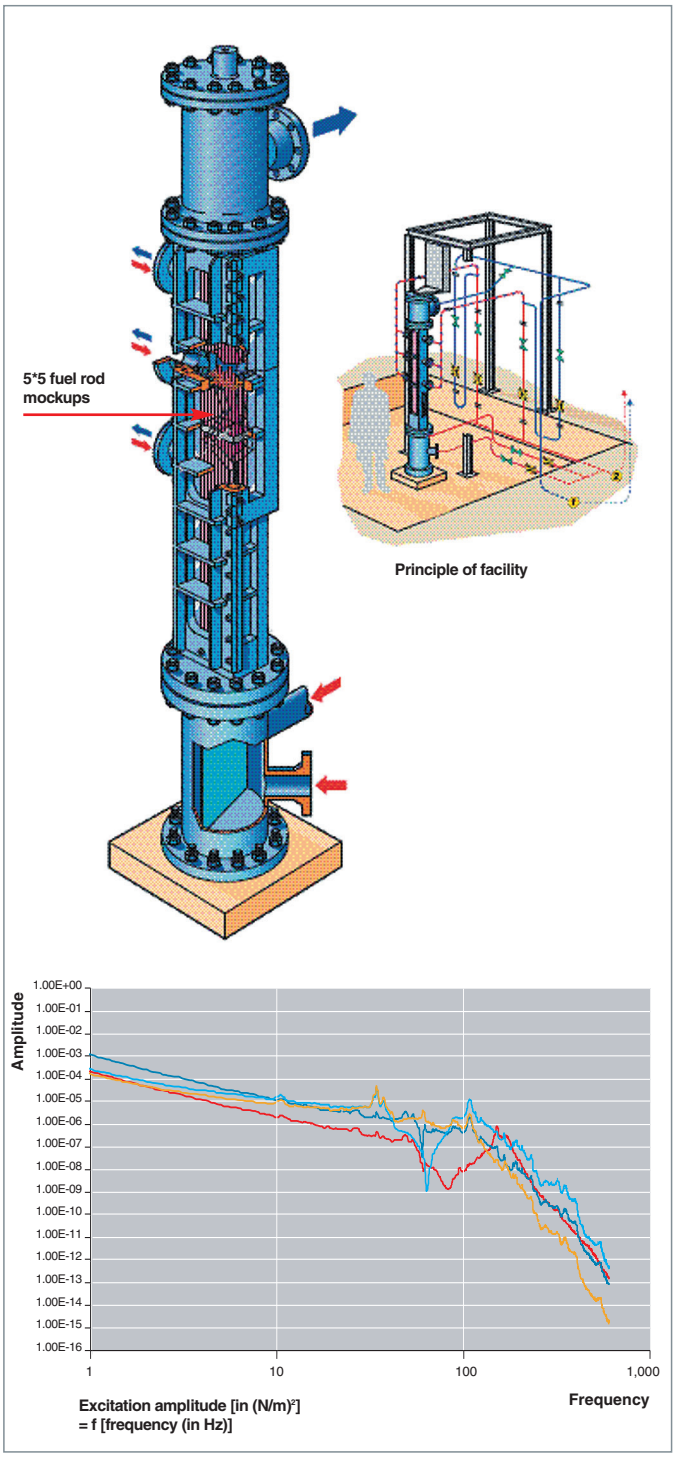


Fig. 53. Schematic of the dedicated experimental facility used for the reverse-method evaluation of turbulent flow excitation spectra (GRILLON froid). – Illustrated: frequency spectrum of loadings obtained (input data for the rod vibration response computation codes).

assembly mockup being investigated, and transverse flow redistribution processes to be simulated, as observed on the first assembly level inside cores. Such redistribution processes are involved in the preferential localization of wear at bottom support grids.

Findings from such tests show that the spring–dimple distance is the first-order influential parameter, with respect to wear. At cells where looseness is found, significant wear may develop, according to an exponential kinetics.

## Assembly mechanical behavior in accident situations

Accident studies, in the area of fuel assembly mechanics, are chiefly concerned with the computation of impact forces on the grids, in the event of an earthquake, and grid resistance to **buckling***.

The industrial models developed use, as input data, the results from seismic computations for the reactor block, yielding motions for core plates and baffles. The latter components form the interface between the fuel assemblies, and the vessel. A single core row is taken into consideration, and fuel assemblies are modeled by way of a two-beam model (i.e. one “guide tube” beam, and one “rod” beam), with stiffeners and shock absorbers at grid level. Assembly damping is determined experimentally, in facilities allowing flow effects to be taken into account. It has been shown, through use of such facilities, that the contribution to total damping due to the fluid is considerable [7] (see Fig. 54). The conditions for extrapolation of this finding to the situation for an in-reactor assembly are being investigated experimentally, and through modeling of the couplings with the fluid [8].

The impact forces thus computed are compared to the values found for grid buckling. Knowledge of buckling forces, as regards irradiated grids, has been gained, and investigated experimentally (see Figs. 55, 56) [9]. The buckling forces measured for these grids show diminished strength, compared with new grids. Such differences may be accounted for by the fact that the first-order influential parameter, with respect to grid strength, is the load due to rod support within the cell, which falls as irradiation increases.

## Conclusion

For the purposes of enhancing assembly mechanical behavior, currently ongoing design studies are chiefly concerned with deployment of a solution yielding a reduction in the amount of grid-to-rod fretting observed at the bottom support grid, on the one hand, and enhanced skeleton mechanical behavior, on the other.

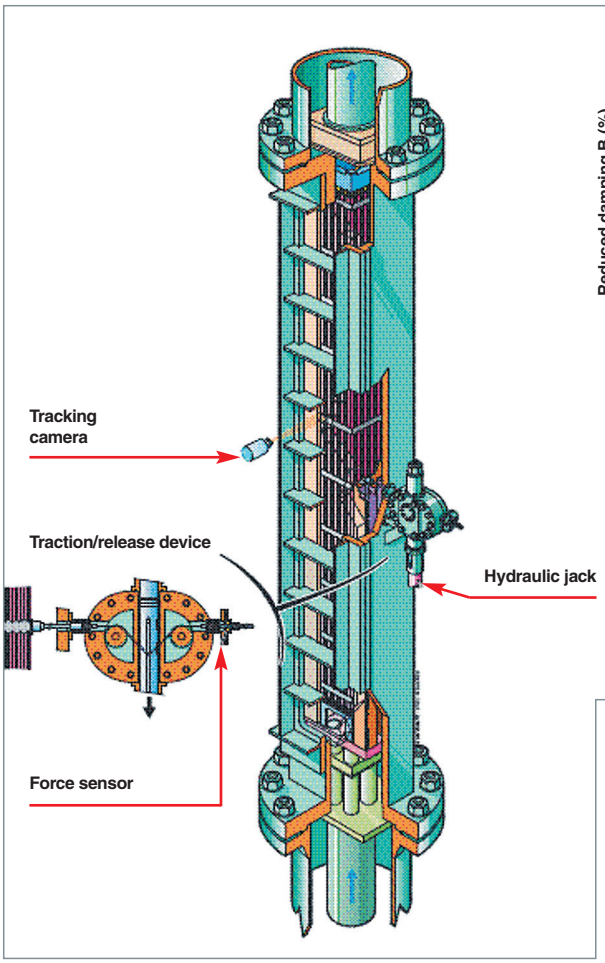


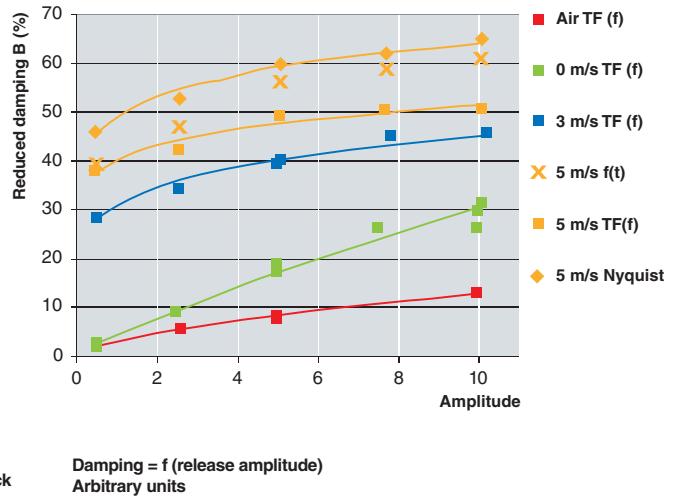


Fig. 54. Schematic of the dedicated facility used for the evaluation of fuel assembly modal characteristics in flow conditions (HERMES T). – Illustrated: the effect of flow on fuel assembly damping, for various excitation (release) amplitudes.
Evaluation of damping by the Nyquist circle method, using a parametric model adjusted in terms of the frequency domain TF (f), and temporal domain f (t). A fast flow increases damping.

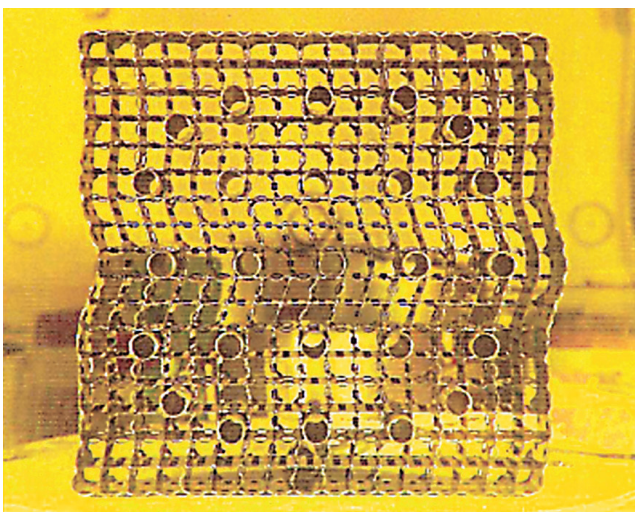

Fig. 55. Photograph of irradiated grid, subsequent to buckling test. – An illustration of the lower buckling resistance exhibited by irradiated grids.

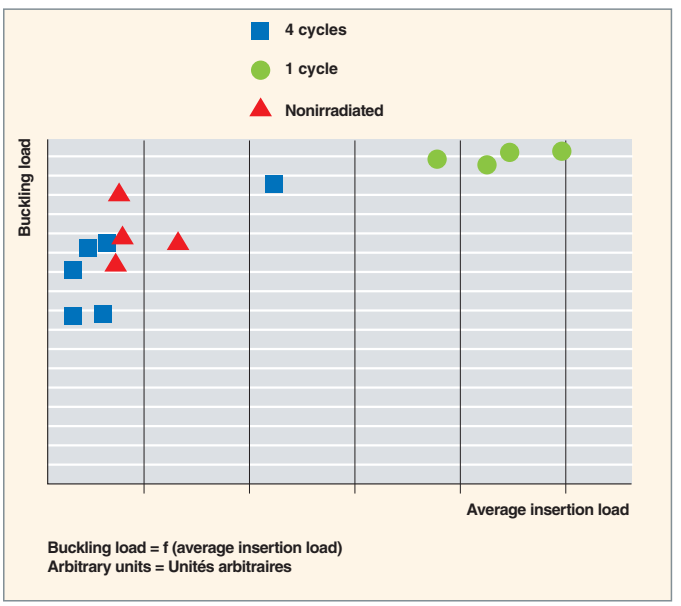


Fig. 56. Graph of buckling load, as a function of average insertion load.
Buckling load falls as the number of irradiation cycles increases – an effect of the mechanical relaxation of grid cell springs.

The R&D effort carried out at CEA is contributing to improvements in fuel assembly qualification methods, with respect to mechanical behavior. This constantly evolving endeavor seeks to secure improvements in:

- experimental protocols for the out-of-pile loop simulation of the loadings experienced by the assembly during its in-reactor lifetime, in particular through use of standard mockups, simulating the "end-of-life" state of an assembly;

- models and modeling processes, to make available tools that are qualified as design aids, or for the purposes of drawing up stronger justification reports, as regards mechanical behavior in accident conditions.

Bearing in mind rising fuel burnup values, the current R&D effort must further make it possible to ensure that structural mechanical integrity is conserved out of the core, e.g. in pool conditions, or during handling.

In the years to come, fuel will have to adjust, to cater for a wide diversity of management modes (long cycles, short cycles, adjustable-length cycles, to optimize unit outages), high burnups, and more stressful operating conditions (high local power ratings, variations in power…). At the same time, the fuel assembly needs must retain a high level of reliability, to ensure safe operation, and reactor availability.

In such conditions, the stresses imparted to the fuel assembly by its environment will be of increasing scale and intensity (irradiation, hydraulic stresses…), inducing more marked aging. The ruggedness, in terms of mechanical behavior, to be exhibited by assembly structures in normal operating conditions, or in accident situations should thus remain as a major challenge for industry, be it for designers, or operators.

## References


[1] W. Klinger, C. Petit, J. Willse, "Experience and reliability of FRAMATOME ANP's PWR and BWR fuel", IAEA (2003), *Fuel failure in water reactors: Causes and mitigation. Proceedings of a Technical Meeting held in Bratislava, Slovakia, 17–21 June 2002*, 21–29.

[2] R. Yang, O. Ozzer, H. R. Rosenbaum, "Current challenges and expectations of high performance fuel for the millennium", *Proceedings of the International Topical Meeting on Light Water Reactor Fuel Performance*, Park City, Utah (USA), 10–13 April 2000.

[3] B. Collard, "Rod cluster control assembly drop kinetics with seismic excitation", *Proceedings of the Eleventh International Conference on Nuclear Engineering*, Tokyo (Japan), 20–23 April 2003.

[4] J.-F. Archard, "Friction between metal surfaces", *Wear* 113, 1, 1986, 3-16.

[5] J. Rigaudeau, E. Morel, "Flow induced vibration analysis of PWR fuel rods validated from a variety of in-loop tests", *Proceedings of the ASME–PVP 2001 Conference – Flow induced vibration, Atlanta, Georgia (USA), 22–26 July 2001*, Vol. 420–2, Axial flow, piping systems: other topics.

[6] J. Vallory, "Methodology of PWR fuel rod vibration and fretting evaluation in HERMES facilities", *Proceedings of the International Meeting on LWR Fuel Performance*, Orlando, Florida (USA), 19–22 September 2004.

[7] B. Collard, S. Pisapia, S. Bellizzi, D. Broc, "Flow induced damping of a PWR fuel assembly", *Proceeding of the 8th International Conference on Flow Induced Vibration (FIV 2004)*, Palaiseau (France), 6–9 July 2004.

[8] D. Broc *and al.,* "Seismic behavior of PWR reactor cores: whole core model with fluid structure interaction effects", *Proceeding of the 8th International Conference on Flow Induced Vibration (FIV 2004)*, Palaiseau (France), 6–9 July 2004.

[9] P. Yvon *and al.,* "Results of crush tests performed on irradiated PWR Zircaloy-4 spacer grids", *Proceedings of the Eleventh International Conference on Nuclear Engineering*, Tokyo (Japan), 20–23 April 2003.



**Joëlle Vallory,**
*Nuclear Technology Department*
**and Thierry Forgeron,**
*Nuclear Industry Support Directorate*

| Fuel in accident situations | | |
|---|---|---|
| **Reactor operating conditions are grouped into 4 plant condition categories (PCCs):** | | |
| **PCC 1** | Normal boiler operation. | This operating mode covers variations in boiler power levels. Some transients are daily, slow, large-amplitude (up to 70% nominal power) events; others are fast, and involve low amplitudes (± 5% about average power). Such variations in power and temperature are stressful for all fuel assembly components, which must be dimensioned to cater for these events. Rod integrity is ensured. However, the primary circuit purification system does allow the reactor to be operated with a few leaking rods. |
| **PCC 2** | Moderate-frequency incidents (frequency of occurrence per reactor, per year: $0.01 < f < 1$). | Anomaly, triggering safety systems.<br>No cladding failure. |
| **PCC 3** | Low-frequency incidents ($10^{-4} < f < 10^{-2}$). | Damage to one or more containment barriers, and release of radioactive products; however, only a small fraction of rods are damaged. |
| **PCC 4** | Major, hypothetical accidents ($10^{-6} < f < 10^{-4}$).<br>Such accidents are referred to as major accidents, owing to their potential consequences, and hypothetical accidents, owing to their associated probability of occurrence (e.g. Three Mile Island). | Massive damage to barriers.<br>This covers several types of accidents:<br>• LOCA (loss of primary coolant accident, involving a rise in cladding temperature, oxidation, and production of $H_2$);<br>• RIA (reactivity insertion accident, involving a large amount of energy deposited over some 10 ms, along with release of gases occluded in the fuel);<br>• DBE (design basis earthquake). |

# Fuel in a loss of primary coolant accident (LOCA)

## Introduction to LOCA-type accident transients. – Overview of thermal–hydraulic and fuel-related aspects

Accidents of the loss of primary coolant (LOCA) type are category 4 events (PCC 4: probability of occurrence, in a power reactor, in the bracket $10^{-4}$–$10^{-6}$ per year). This class of accidents has been targeted by a major research program. In thermal–hydraulic terms, following the initial episode, involving loss of coolant, such an accident transient involves four phases, as outlined in Figure 57 (fission processes have been arrested from the start of the event, by control rod dropdown; only reactor decay heat is acting):

1. A phase involving cladding and fuel heat up, due to the effect of decay heat residual power (10–20 W/cm). The initial radial temperature gradient, occurring in the fuel rod at the end of power operation, is swiftly superseded by a near-isothermal temperature distribution. Heat up takes place in a steam environment, exhibiting kinetics of 10–20° C/s. These conditions cause external cladding oxidation, along with, in some instances, local ballooning of the cladding, under the effect of internal pressure, possibly resulting in loss of leaktightness (see Fig. 58). In the latter case, part of the readily available radioactive product inventory within the rod (i.e., in the fuel–cladding gap, open porosities, fuel grain boundary contents) is released into the primary circuit. This mainly involves isotopes of the noble gases xenon, and krypton: specific investigations have been carried out at CEA, to determine the amounts of fission gases liable to be released by fuel, in these particular conditions [1];

2. A state of equilibrium, at high temperature (900–1,200° C, depending on the rods involved), is then reached, lasting several tens of seconds. The equilibrium temperature may be modified, if, as ballooning develops, axial relocation of the fuel occurs, subsequent to fuel fragmentation, with fragments falling away: locally, prevailing residual power may then be higher than the average decay heat level;

3. A phase of abrupt rod cooling (particularly with respect to cladding, for which this is akin to "**quenching***") occurs during core reflooding by the emergency core cooling systems. In the event of an open cladding failure, rewetting causes a "washout" of internal free spaces in leaking rods, and may result in a further release of radioactive fission products: noble gases, but equally volatile isotopes (e.g. iodine, tellurium, cesium), or even nonvolatile isotopes (e.g. metallic fission products). Core cooling capabilities do depend, on the other hand, on the extent to which inter-rod spaces remain open, which may be impaired in the event of excessive cladding ballooning (see Fig. 58). This point strongly influences the accident sequence exit scenario;

4. A post-accident phase, during which, according to safety criteria, fuel elements must be amenable to cooling, and handling.

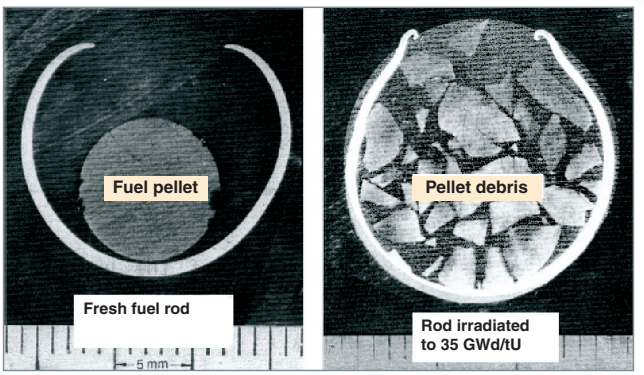


Fig. 58. Aspect of experimental fuel rods (cross-sections), subsequent to a LOCA sequence (German FR2 tests).

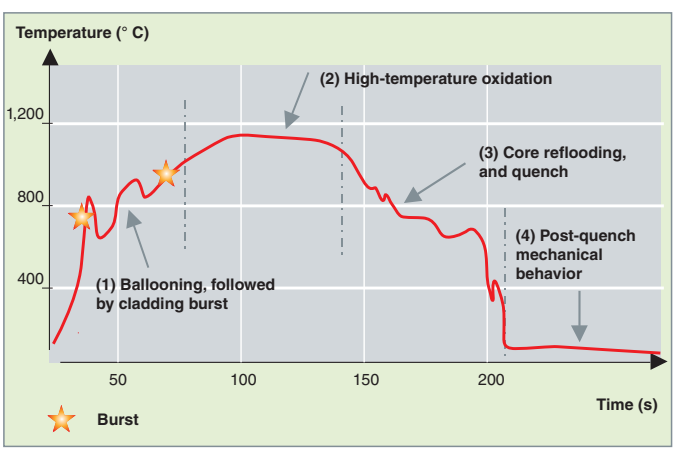


Fig. 57. Schematic of a cladding temperature transient during a loss of primary coolant accident. Impact on fuel cladding behavior.

## Incidence of LOCA transients on the thermal-metallurgical-mechanical behavior of zirconium-base alloy cladding

As cladding tubes form the first containment barrier for fuel, their integrity, during a LOCA transient, is a key parameter, and must, consequently be the object of particular investigation. In particular, aside from the cooling ability, as mentioned above, safety criteria stipulate that cladding should withstand quenching, and retain nonzero residual ductility after oxidation, up to 1,200° C, for a specified oxidation level. This issue has thus incited, for nearly three decades, researchers, at CEA and around the world, on the one hand to seek to reproduce, as best could be achieved, the most representative transients (by way of integral tests, as carried out e.g. in the Phébus reactor), through the development of associated computation codes (CATHARE); and, on the other hand, to conduct more analytical R&D work, for the purposes of understanding, quantifying, and modeling the thermic, metallurgical, and mechanical processes arising within the cladding material. It is the latter research thrust that is illustrated in what follows. The four phases typical of a LOCA event (see Fig. 57) may thus be reconsidered, along with a more precise description of their respective consequences on cladding behavior.

As regards phase 1, there must be an ability to provide a description of the ballooning–failure behavior exhibited by cladding tubes. For that purpose, CEA has developed, over the past 20 years, analytical thermomechanical test procedures (EDGAR facility), combined with investigations, and metallurgical modeling of the kinetics of the **allotropic*** alpha⇔beta phase transformation arising in the Zr-base matrix – this metallurgical transformation having a direct incidence on the material's thermomechanical response [2]. It should be noted, in this respect, that investigations of a more fundamental character, regarding creep mechanisms, in particular in the two-phase alpha–beta domain, are being undertaken in partnership with the Paris École des mines (doctoral theses: S. Fréchinet [2001], D. Kaddour [2006]). As a whole, these investigations have led to identifying thermal–metallurgical–mechanical models of internal pressure-related creep, and cladding failure criteria, in isothermal and nonisothermal conditions – models that may be integrated, ultimately, into more global LOCA computation codes.

As phases 2–4 in the transient correspond to heightened cladding oxidation, up to final cooling down, mechanical behavior must be guaranteed in terms of quench resistance, and post-quench strength. At CEA, high-temperature (HT) oxidation tests are carried out in two complementary facilities: CINOG, at Grenoble, and DEZIROX, at Saclay. Subsequent to HT oxidation, a variety of "post-quench" mechanical tests are conducted, to characterize cladding residual ductility [3]. To support these tests, metallurgical and fractographic analyses are systematically carried out, for the purposes of gaining a better understanding of the physical and microstructural parameters influencing the macroscopic behaviors observed. Currently, such investigations are leading researchers e.g. to turn to nuclear analyses, for the purposes of quantifying, and "mapping" local oxygen (and, presently, hydrogen) concentrations, across the tube thickness, as these parameters are proving critical, with respect to the embrittlement threshold of claddings subjected to HT oxidation (see Fig. 59).

It should be noted, finally, that CEA workers were the first to highlight, and quantify the impact of "service dwell time" on the LOCA behavior of claddings subjected to high rates of irradiation. Analytical investigations carried out over the past few years [4] [5] – in both cool and hot conditions – have allowed confirmation of the hypothesis that a major influencing factor, as regards in-service aging, is related to cladding hydrogen uptake (due to in-service corrosion), irradiation defects present in the irradiated material being swiftly healed, during the initial temperature rise (phase 1) involved in the LOCA transient. Figures 60 and 61 illustrate, in this respect, two major findings, recently obtained at CEA:

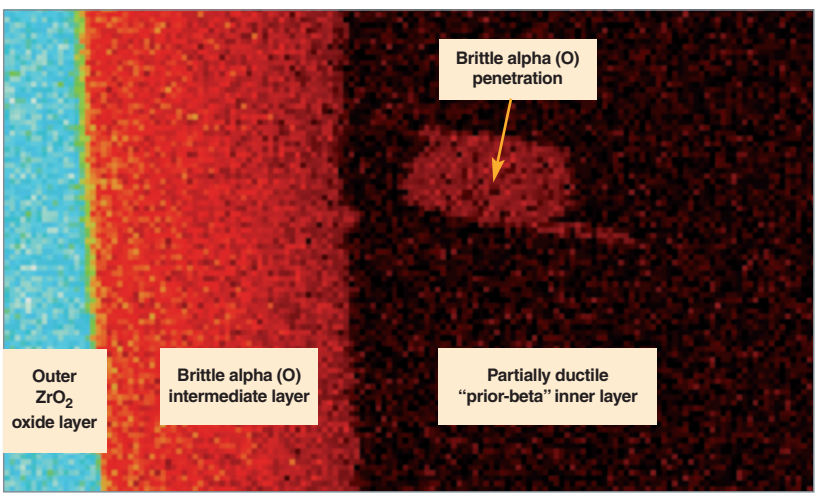


Fig. 59. Mapping of oxygen across the thickness of cladding subjected to high-temperature oxidation, obtained by nuclear microprobe – analysis pitch = 2 µm.

(*) Collaborations with DSM: Van de Graaff accelerator (INSTN), and nuclear microprobe (Pierre Süe Laboratory [CEA–CNRS]).

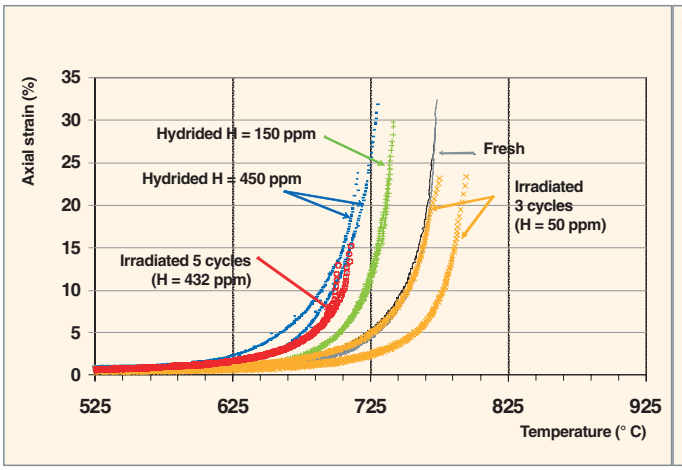


Fig. 60. Creep of pre-hydrided and/or irradiated Zy–4 during a 100° C/s ramp, when subjected to a single-axis 80 MPa loading [5].

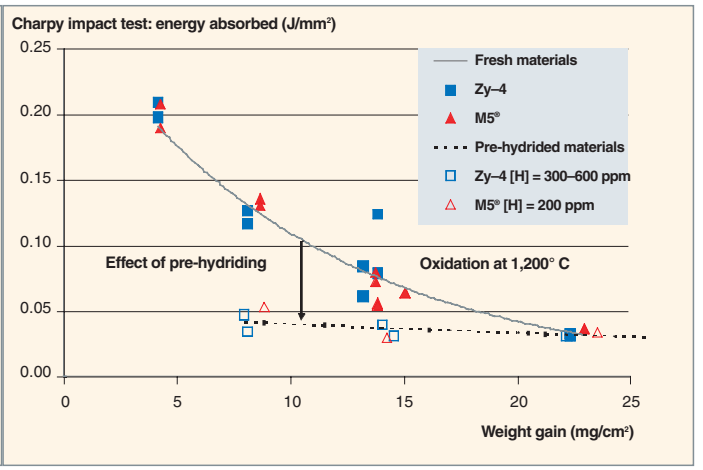


Fig. 61. Post-oxidation–quench tests. – Evolution of failure energy, as function of the level of HT oxidation – influence of pre-hydriding [5].

1. The impact of hydrogen on creep, in a dynamic ramp, as typical of the first phase of a LOCA transient. It has been shown that this effect is strongly correlated with the so-called "betagenic" effect of hydrogen, which results in lower alpha⇔beta phase transformation temperatures, as evidenced, in ramp creep curves, by a shift in failure temperatures, to lower temperatures (see Fig. 60);

2. The post-oxidation–quench embrittling effect of hydrogen, as highlighted in Figure 61, which shows the evolution of energy absorption prior to failure (Charpy-type impact tests), as a function of the oxidation level, and nominal hydrogen content. Indeed, it may be seen that the lower energy plateau – corresponding to brittle-type failure – is reached swiftly, with hydrided samples.

Currently, this issue is a topic for discussions, involving in particular, at the international level, safety authorities (NRC, IRSN, OECD–NEA, IAEA…), who are considering a revision of safety criteria, taking on board this new evidence.

## References


[1] Y. Pontillon, M.-P. Ferroud-Plattet, D. Parrat *et al.,* "Experimental and theoretical investigation of fission gas release from $UO_2$ up to 70 GWd/t under simulated LOCA-type conditions: The GASPARD programme", *Proceedings of the International Meeting on LWR Fuel Performance*, Orlando, Florida (USA), 19–22 September 2004, pp. 490–499.

[2] T. Forgeron, J.-C. Brachet *et al.*, "Experiment and modeling of advanced fuel rod cladding behavior under LOCA conditions: alpha–beta phase transformation kinetics and EDGAR methodology", ASTM STP 1354 (2000), *Zirconium in the nuclear industry, 12th International Symposium*, Toronto (Canada), 15–18 June 1998, pp. 256–278.

[3] J.-C. Brachet, J. Pelchat, *et al.,* "Mechanical behavior at room temperature and metallurgical study of low-tin Zy-4 and M5® (Zr-NbO) alloys after oxidation at 1 100° C and quenching", International Atomic Energy Agency (2002), *Fuel behaviour under transient and LOCA conditions. Proceedings of a Technical Committee meeting held in Halden, Norway, 10–14 September 2001*, pp. 139–158.

[4] J.-C. Brachet, L. Portier, L., T. Forgeron, *et al.,* "Influence of hydrogen content on the α⇔β phase transformation temperatures and on the thermal–mechanical behavior of Zy-4, M4 (ZrSnFeV) and M5® (ZrNbO) alloys during the first phase of LOCA transient", ASTM STP 1423 (2002), *Zirconium in the nuclear industry, 13th International Symposium*, Annecy (France), 10–14 June 2001, pp. 673–701.

[5] L. Portier, T. Bredel, J.-C. Brachet, V. Maillot *et al.,* "Influence of long service exposures on the thermal–mechanical behavior of Zy–4 and M5® alloys in LOCA conditions", ASTM STP 1467 (2005), *Zirconium in the nuclear industry, 14th International Symposium*, Stockholm (Sweden), 13–17 June 2004.



**Daniel Parrat,**
*Fuel Research Department,*
**and Jean-Christophe Brachet,**
*Nuclear Materials Department*

# Fuel in a reactivity insertion accident (RIA)

A reactivity insertion accident (**RIA***) is a design basis accident, classified as a category 4 event (i.e. with a frequency of occurrence evaluated at $10^{-4}$–$10^{-6}$ per reactor, per year), entailing some of the most stringent constraints, with regard to the design of pressurized-water reactors. It occurs as a result of a **rod cluster control assembly*** ejection, subsequent to the failure, and consequent depressurization of its drive mechanism housing.

Such an accident causes a very swift rise in core reactivity, inducing a power transient, with significant energy deposition in fuel rods located in the vicinity of the ejected cluster control assembly (see Fig. 62).

The first phase in the accident, due to the action of the **prompt neutrons*** yielded by fission, extends over a few tens of milliseconds. This is characterized by strong pellet–cladding mechanical interaction, owing to an expanding oxide volume, induced by adiabatic heating, and the pressure exerted by fission gases.[1] In the event of a cladding failure, during this initial phase, fuel dispersion, in the form of small fragments, may result in abrupt vaporization of the water around the rod. This prompt-neutron nuclear reaction comes to an end spontaneously, as a result of the fuel heating up, and the **Doppler*** effect.

The second phase in the accident, characterized by the thermal evolution of the system, lasts for an interval ranging from a few seconds to 10 seconds or so. This results in a significant rise in cladding temperature, with a risk of boiling crisis (departure from nucleate boiling) being reached in the water channel around the cladding; a further result is sustained high internal pressure within the rod, here again possibly impacting cladding integrity.

## Safety criteria

Current safety criteria, regarding this type of accident, were drawn up in the early 1980s, on the basis of experiments carried out in the United States (SPERT and PBF programs), and later in Japan (NSSR program), on fresh or low-irradiated (up to 30 GWd/tU) fuel. These criteria chiefly take the form of a principle of no fuel dispersion, and a limiting value for average enthalpy deposition in fuel, not to be exceeded during a transient (230 cal/g for fresh fuel, 200 cal/g for irradiated fuel), in order to guarantee there is no significant release of mechanical energy, and core cooling is preserved; and to preclude any risk of a steam explosion.

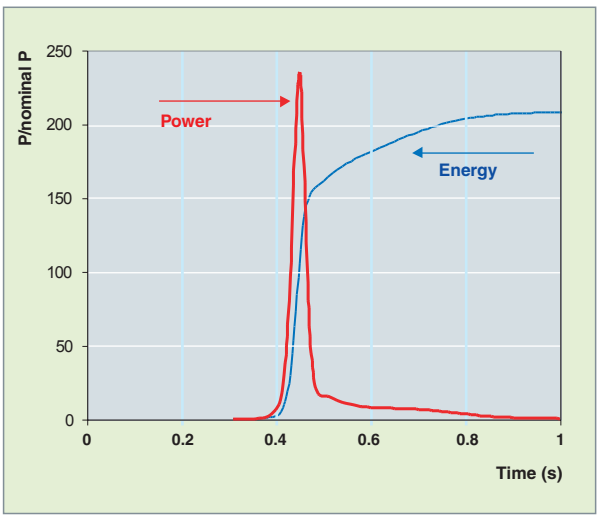


Fig. 62. Evolution of power, and energy injected during a reactivity insertion accident, as a function of time.

PWR core management optimization considerations have led the industry to go for increased assembly burnup, and the introduction of MOX fuel. These evolutions have induced CEA, and the French Nuclear Safety Institute, IRSN, to initiate new experimental programs, for the purposes of ensuring such enhanced-performance fuels are safe.

### *The CABRI research program*

As a result, the CABRI–REP Na experimental program was launched by IRSN, in the sodium loop of CEA's CABRI reactor. From 1993 to 2000, 8 tests involving high-burnup (up to 65 GWd/tU) $UO_2$ fuel, and 4 tests with MOX fuel (with burnup ranging from 28 GWd/tHM to 65 GWd/tHM) were carried out, on reconditioned, industrially manufactured rods. These tests simulated the first phase in the accident, during which strong pellet–cladding mechanical interaction occurs, with no significant cladding heating. It should be noted that the advanced transient phase, in conditions representative of the in-reactor situation (cladding heat up, strong internal pressure) will be

1. Further, more detailed information on the phenomena involved in pellet–cladding interaction may be found in the chapter on "Pellet–cladding interaction", p. 41.

addressed by the CABRI International Program (CIP), which IRSN is planning to carry out in the pressurized-water loop (BEP: *Boucle à eau pressurisée*), due to be installed in the CABRI reactor, under the aegis of a wide-ranging international collaboration, under OECD auspices, and in close collaboration with EDF and CEA.

The CABRI program has allowed the influence of various parameters to be investigated: nature of the fuel ($UO_2$, or MOX), burnup, cladding corrosion thickness, state of the corroded layer (in particular, presence or absence of spallation), cladding material (Zy4, or M5®), and power transient characteristics (energy deposition, full width of injected pulse).

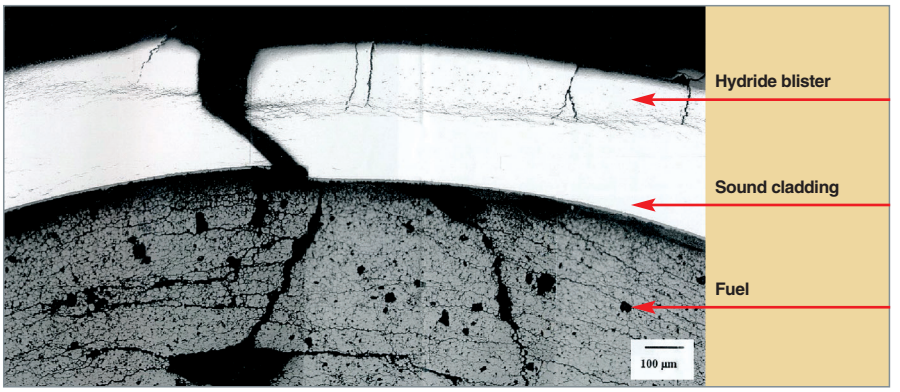


Fig. 63. Metallographic section of the REP Na8 rod, subsequent to a CABRI test, evidencing the presence of a hydride "blister" at the cladding periphery, with brittle fracture initiation, and ductile aspect in the inner region.

One further aspect of note is the development of the SCANAIR code. Its chief characteristic is the ability to cater for intimately coupled processes, to wit thermics, rod mechanics, and fission gas behavior in transients, on the basis of an initial state for the rod, as yielded by an irradiation computation. To support the development of this code, and assist in a detailed understanding of the physical processes involved, complementary analytical test programs were also carried out by CEA teams: the PROMETRA program, concerned with drawing up cladding behavior laws, in the particular stress conditions, specific to this type of accident; and the PATRICIA program, devoted to the investigation of cladding–water heat transfers, during fast cladding heat up transients.

## *The main lessons to be learnt from the CABRI program*

The immediate outcome of the fast power transient is heating up, followed by thermal expansion of the fuel, which, combined with the swelling due to fission gases (beyond fuel enthalpy of 100 cal/g), results in strong pellet–cladding mechanical interaction, mainly during the initial, prompt transient phase.

As regards $UO_2$ fuel, provided the cladding is not heavily corroded, or spalled, this mechanical interaction, even when magnified at high burnup owing to the contribution from fission gases, and fuel fragmentation in the rim region, which is most highly stressed, is not sufficient to result in cladding failure.

By contrast, when the Zy4 cladding is highly corroded, and spalled, rod failure may occur, even at low injected enthalpy levels (failure at 30 cal/g in the REP Na1 test, well below the 200 cal/g criterion). This is due to diminished cladding ductility, related to local hydride concentration, as a result of initial spalling. Indeed, hydride "blisters" form sites of brittle fracture initiation. This may progress in ductile mode into the inner, low-thickness, sound but hydrided region, once local stress equals rupture strength (see Fig. 63).

The introduction, into the PWR fleet, of the M5® alloy, far less sensitive as it is to corrosion and hydrogen pickup, provides, in this respect, a significant safety margin. As regards MOX fuel, the part played by fission gases is increased, compared to what is the case with $UO_2$, and may contribute to rod failure, even with a sound, little corroded cladding (as instanced by REP Na7). Indeed, owing to the heterogeneous structure of MOX fuel, with the presence of plutonium-rich aggregates, the amount of fission gases available at grain boundaries is higher than with $UO_2$. During a fast power transient, overpressure from gas bubbles causes grain boundaries to explode, and fuel fragmentation (see Fig. 64). This can increase cladding mechanical loading, carrying the risk of rod failure, with ejection of finely fragmented fuel.

Improving MOX fuel behavior during transients entails the development of new, higher-performance fuels, allowing a reduction in the amounts of gases precipitating into bubbles in plutonium-rich aggregates, by way of a restructuring of these aggregates.

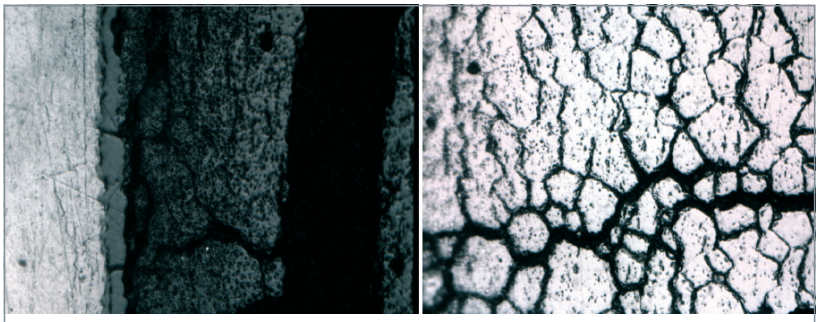

REP Na5 ($UO_2$): left: pellet rim – right: ~ 0.95 R

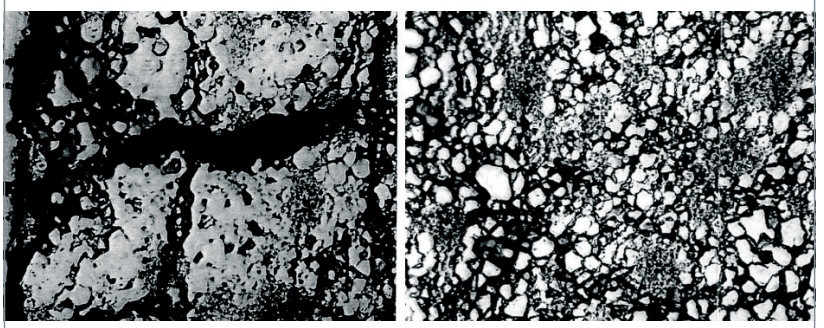

REP Na6 (MOX): left: ~ 0.98 R – right: ~ 0.95 R

Fig. 64. Fuel fragmentation, accompanied by grain boundary rupture, and decohesion, as a result of high pressure due to fission gases, during the transient.

## Bibliography


H. Bailly, D. Ménessier and C. Prunier, *The Nuclear Fuel of Pressurized Water Reactors and Fast Neutron Reactors: Design and Behaviour*, Lavoisier Publishing, Paris, 1999.

J. Papin, "The CABRI research program for study of reactivity-initiated accidents", IRSN, *Scientific and Technical Report 2002*, 53–61.

J. Papin *et al.* "Synthesis of CABRI–RIA tests interpretation", *Eurosafe Forum,* Paris, 25–26 November 2003.

E. Casanova, "Comportement des gaz de fission dans un combustible irradié lors d'un transitoire de puissance", doctoral thesis, Provence University, March 1998.



**Gérard Ducros,**
*Fuel Research Department*

# Fuel in a severe accident

The term "severe accident" refers to hypothetical situations in which, following an initiating event, e.g. a breach in the primary circuit, successive failures of protection and safeguard systems would lead to more or less complete core melt. Such situations, having a probability of occurrence of less than $10^{-5}$ per reactor, per year, are not covered as part of the design basis, however they are addressed by investigations, for the purposes of evaluating their consequences.

Following the accident that took place at the Three Mile Island nuclear power plant, in the United States, in 1979, safety organizations have extended the defense in depth system, as then implemented, to cater for such situations, through the deployment of prevention and mitigation measures, so that the consequences of a severe accident do not prove unacceptable for populations. Mention may be made, in particular, with regard to French PWRs, of the setting up of ultimate procedures, e.g. procedure U5, involving deliberate decompression of the containment, with controlled filtration of radioactive effluents.

The course of a severe accident involves the following phenomena (see Fig. 65):

- Subsequent to primary circuit draining, and core uncovery, fuel heats up under the effect of decay heat, generated by the fission products (FPs) it contains; core degradation sets in (exothermic oxidation of zircaloy rod cladding by steam, with concomitant production of hydrogen), to the point where a mixture of molten materials forms, the so-called **corium*** ($UO_2$ + $ZrO_2$ + core structural materials), which may reach 3,000° C; the corium flows through the core, and relocates at the bottom of the vessel, which it then heats up in turn;

- the pooling of fissile materials at the bottom of the vessel may induce risks of **recriticality***;

- during the core degradation phase, fission products (FPs) are released by the fuel rods: first fission gases and volatile FPs (iodine, cesium, tellurium), then a fraction of low-volatile FPs, and of the actinides;

- the aerosols that have formed, and FPs in vapor form are transported by the flow of hydrogen-rich steam into the primary circuit, and reach the containment. They may undergo partial deposition, and subsequent resuspension;

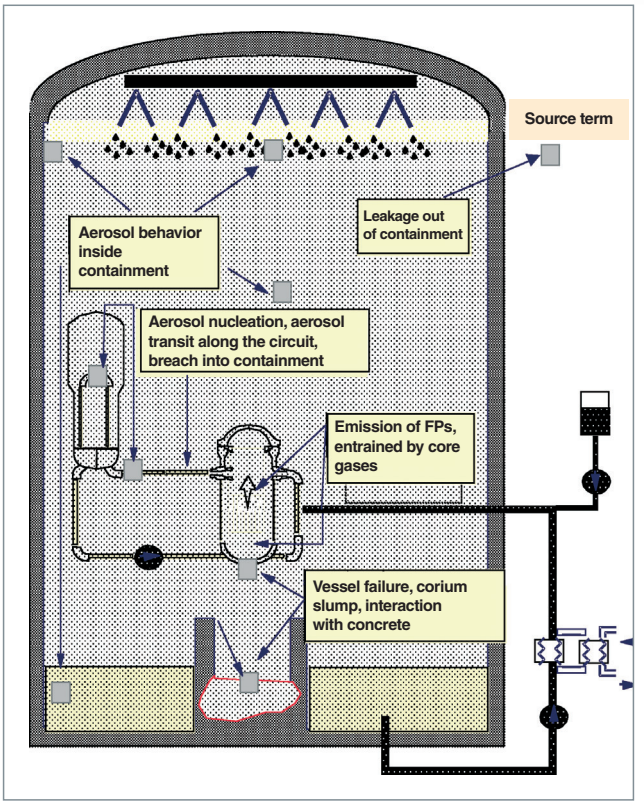


Fig. 65. The facts and events involved in a severe accident.

- following failure of the vessel lower head – should this occur – the corium is ejected into the reactor pit, due to the effect of primary circuit pressure; a fraction of this high-temperature corium may be directly drawn into the containment, and contribute to its heating up, while the corium remaining in the reactor pit interacts with the concrete basemat, resulting in concrete ablation, and release of noncondensable gases ($H_2$, CO, $CO_2$…) into the containment;

- the containment atmosphere heats up, and its pressure rises (risk of steam explosion); combustion of the hydrogen yielded by the dissociation of superheated water may occur, inducing a complementary dynamic loading of the containment (risk of hydrogen explosion);

- part of the FPs, in aerosol or gas form, may then escape the containment via a variety of leakage paths, or by venting, and cause radioactive contamination of the environment: it is this release of FPs that is taken into account by safety authorities, for the purposes of dimensioning intervention plans. Of

such FPs, iodine plays a dominant role, with regard to radiological consequences, owing to its high activity level, during the days following the accident, its high volatility, and its ability to form gaseous species, in the form of molecular iodine, or organic iodides.

All of these physical phenomena, from initiating event to radiological releases into the environment, are described, and simulated in integrated codes, known as "scenario codes," developed by safety organizations, and used, in particular, in the context of level-2 probabilistic safety analysis (PSA-2) studies. One of these, the ASTEC code, jointly developed by IRSN and GRS (a German nuclear safety organization), is on course to become the European reference code, in this area. Validation of these codes requires that they be compared with findings from experimental programs, carried out at a variety of scales. As regards more specifically fuel behavior, and FP release, mention may be made of the VERCORS analytical program, carried out at CEA, and the Phébus–FP global tests, carried out by IRSN in CEA's Phébus reactor.

## The VERCORS analytical program

The specific feature of the VERCORS program is its highly analytical character: tests are carried out in high-activity cells, on samples of actual irradiated fuel from PWRs (about 20 g of fuel), most of these being reirradiated at low power for a few days in an experimental reactor (SILOE, or OSIRIS), to reconstitute the short-lived FP inventory, such FPs being the most harmful, in radiological terms. These samples are heated in an induction furnace, in a mixed steam and hydrogen atmosphere, simulating the conditions prevailing during a severe accident. FP release is measured online, in particular by means of gamma spectrometry, aimed directly at the fuel through the accident sequence.

25 tests, carried out from 1983 to 2002, have allowed one of the most complete databases around the world to be drawn up, as regards FP release. The parameters explored, in these tests, concern the temperature levels reached (below, or above fuel melting point), oxidizing/reducing conditions in the gas environment (this playing a far from negligible role in FP release, in particular for semi-volatile FPs), burnup, type of fuel ($UO_2$ as a rule, with a few tests involving MOX), and initial fuel geometry (intact fuel, or fuel debris, to simulate the final phase in a severe accident).

Figure 66 illustrates the behavior of $UO_2$ fuel at 2,300° C in an oxidizing steam atmosphere:

- in the VERCORS 5 test (Fig. 66a), where occurrences of melt initiation were found, at contact points between the $UO_2$ and the oxidized cladding, the latter being already ruptured at a number of locations, owing to loss of ductility, and the stresses imparted by fuel swelling; the dark border around the fuel pellet rim corresponds to a region comprising large open porosities, which has been voided of most of its FPs, including some semi-volatile FPs, such as barium;

- in the VERCORS RT1 test (Fig. 66b: fuel at higher burnup), where the $UO_2$–$ZrO_2$ mixture underwent complete meltdown, filling the entire inner portion of the thoria supporting crucible.

As regards FP release, Figure 67 illustrates the various volatility classes identified by this program:

- volatile FPs, as instanced here by Cs 137, involving virtually complete release;

- semi-volatile FPs, as instanced by Ba 140, for which release is highly dependent on oxidizing/reducing conditions, and the various interactions arising between the materials present;

- low-volatile FPs, as instanced by Ru 103, involving a small but significant release, undergoing near complete retention in the hot regions of the primary circuit (including the upper vessel region);

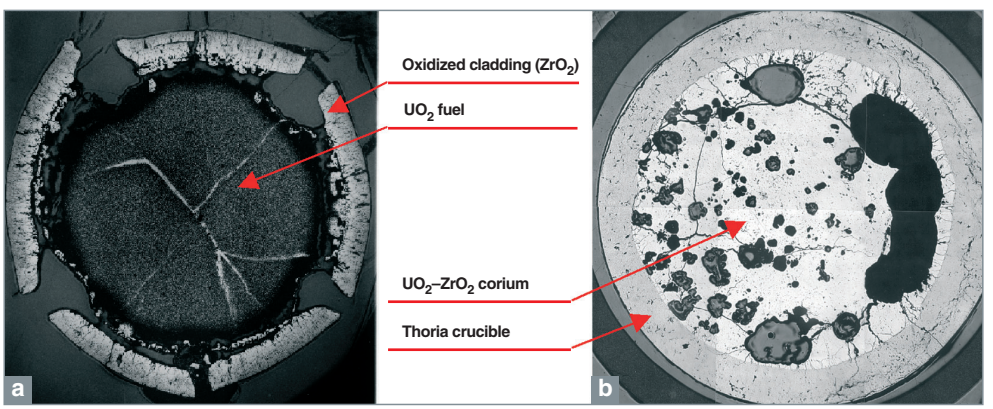


Fig. 66. VERCORS tests.
a: cross-section of fuel rod showing occurrences of melt initiation.
b: $UO_2$–$ZrO_2$ corium.

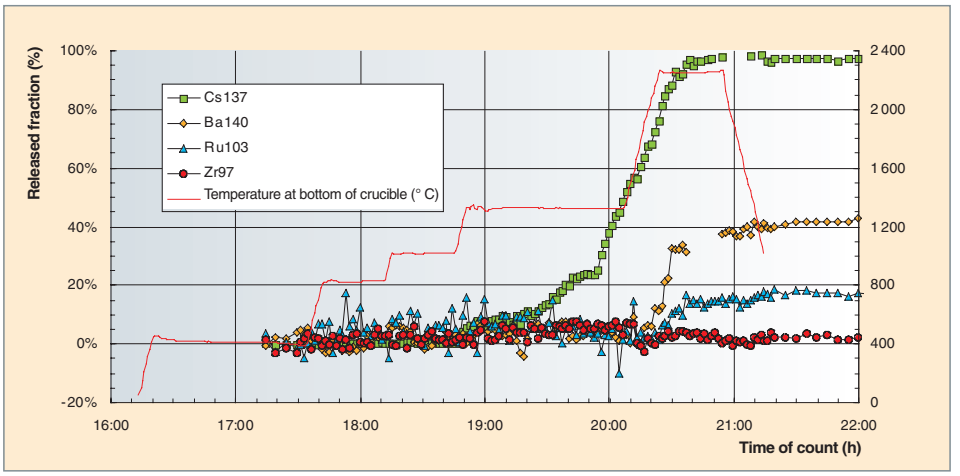


Fig. 67. Illustration of the differences in volatility exhibited by the various fission products (VERCORS tests).

- nonvolatile FPs, as instanced by Zr 97, for which release is negligible.

## The Phébus–FP global tests

The Phébus-FP facility is intended to provide conditions globally representative of a severe accident, as a complement to the analytical experiments described above. Accommodated inside and next to the core of the Phébus reactor, a neutron source used to heat test fuel, the experimental facility comprises three components: the in-pile section; an ex-core circuit simulating the primary circuit, up to the breach; and a tank, simulating the containment enclosure in the reactor building. The global scale factor stands at about 1/5,000, with respect to a 900-MWe PWR:

- the in-pile section, positioned at the center of the reactor, comprises a cluster of 20 fuel rods, and one Ag–In–Cd (AIC) or $B_4C$ absorber rod, located at the center of the cluster. Two zircaloy grids hold the rods in position, which are about 1 meter long;

- FPs, and aerosols of structural materials escaping from the cluster are transported by the gas (steam and hydrogen) flow along a vertical line, followed by a horizontal line, kept at 700° C, into a circuit representative of the main components in a PWR primary circuit, including in particular a steam generator U-tube;

- the circuit vents into a cylindrical, 10-$m^3$ tank, simulating a PWR containment. The tank walls are heated, to preclude any steam condensation, and minimize aerosol deposition. Three cylindrical, partly painted condensers simulate the surfaces of a PWR containment, and control condensation rate, and moisture. A sump, located at a lower level, containing controlled-pH water, collects condensates, and aerosols.

The experimental program as a whole covered 5 tests, carried out from 1993 to 2004:

- FPT0 (fresh fuel) and FPT1 (fuel at 23 GWd/tU), in a steam-rich atmosphere, using an AIC absorber rod, and acidic sump water;

- FPT2 (fuel at 23 GWd/tU), in a steam-poor gaseous phase, with a $B_4C$ absorber rod, and alkaline sump water;

- FPT4, involving irradiated fuel present in the form of a debris bed ($UO_2$–$ZrO_2$), to simulate the final phase in a severe accident (the sections simulating the primary circuit and containment were not included);

- FPT3 was carried out in Fall 2004, in conditions similar to those of FPT4, but with a $B_4C$ absorber rod and an evaporating, acidic sump, i.e. in conditions favoring a significant increase in gaseous iodine in the atmospheric phase inside the containment (no trapping of iodine by silver in the sump water, and potentially increased formation of organic iodides from $B_4C$ decomposition products).

These tests yielded experimental data of prime importance, in the area of fuel degradation, and FP behavior, allowing, in particular, an understanding to be gained of the coupling between the various physical phenomena involved in a severe accident (a coupling that is lacking, as a rule, in analytical tests). Among the major lessons this program has highlighted, mention should be made, in particular, of the following:

- a fuel relocation temperature that is 400–500° C lower than the melting point for uranium oxide, owing to the various interactions with structural materials, with fuel cladding in particular, and the presence of FPs within the fuel matrix;

- FP release that is in fairly good agreement with findings from analytical tests, except as regards certain semi-volatile FPs, barium in particular, owing to the strong coupling between fuel degradation, and release of these FPs;

- the complexity of iodine behavior inside the primary circuit, and containment. Large uncertainties still remain, regarding the various chemical forms for this element, in particular gaseous forms: the partitioning between molecular iodine, which is retained by the containment filtration systems, and organic iodides, which are not retained by filtration systems, is not as yet adequately known.

## Control of severe accidents in the EPR reactor

The EPR reactor (the acronym initially standing for European Pressurized-Water Reactor, now restyled as Evolutionary Power Reactor) has been designed to take over from second-generation nuclear reactors, currently being operated in Europe, and around the world. It has benefited from innovative safety provisions, in particular with respect to accidents involving core melt.

In terms of ***prevention***, first of all, the probability of occurrence of such an accident has been reduced by a factor 10, compared to the already very low value characterizing current PWRs, through the increased redundancy of safety systems, with, in particular, the presence of four independent trains of the main safeguard systems, including two trains hardened against external hazards.

The ***impacts on humans and the environment*** have, at the same time, been sharply cut back (with a source term reduction by a factor 100 for cesium, by a factor 1,000 for iodine, compared with current PWRs), through the deployment, in particular, of the following features:

- a corium catcher, located under the vessel, inside the containment, ensuring retention of all solid fission products, along with the long-term falloff, and removal of decay heat. Consequently, the risk of basemat piercing, which is taken into account for current PWRs, is precluded for EPR;

- autocatalytic hydrogen recombiners, for the purposes of preserving containment integrity in all circumstances. As a result, emergency procedure U5 (containment decompression, effluents being filtered though sandbed filters) is not required;

- high-efficiency iodine filters, having the ability to trap 99.9% of molecular iodine (and the same amount for aerosols), and 99% of organic iodine.

### References


[1] H. Bailly, D. Ménessier and C. Prunier, *The Nuclear Fuel of Pressurized Water Reactors and Fast Neutron Reactors: Design and Behaviour*, Lavoisier Publishing, Paris, 1999.

[2] J. Libmann, *Approche et analyse de la sûreté des réacteurs à eau sous pression*, INSTN–CEA, "Enseignement" series, Paris, 1988.

[3] H.J. Allelein *et al.,* "European validation of ASTEC–V1 through the EVITA project", *Eurosafe Forum*, Paris, 25–26 November 2003.

[4] G. Ducros *et al.,* "Fission product release and fuel behaviour under severe accidental conditions: synthesis of the Vercors 1–6 results", *Nuclear Engineering and Design* 208, 2001, 191–203.

[5] S. Bourdon *et al.,* "Results of initial Phebus FP tests FPT–0 and FPT–1", IRSN, *Scientific and Technical Report 2002*, 45–52.

[6] B. Clément *et al.,* "LWR severe accident simulation: synthesis of the results and interpretation of the first Phebus FP experiment FPT0", *Nuclear Engineering and Design* 226, 2003, 5–82.

[7] B. Clément, "Summary of the Phebus–FP interpretation status", *5th Technical Seminar on the Phébus–FP Programme*, Aix-en-Provence (France), 24–26 June 2003.



**Gérard Ducros,**
*Fuel Research Department*

# In-core fuel management

For the reactor, nuclear fuel provides a reserve of neutron and energy resources that varies over time, depending on operating conditions. On the one hand, this reserve becomes depleted, by fission of the **fissile*** atoms that have been loaded into the reactor; and, on the other hand, it is replenished, through neutron absorption by **fertile*** nuclei.

Fuel management thus involves optimizing the energy extracted from that fuel, while meeting a set of constraints dictated by nuclear reactor operating requirements, or safety: control of reactivity; operating flexibility; optimization of boiler power capacity; minimization of effluents, and of waste.

The loading mode selected for pressurized-light-water reactors (PWRs), as for boiling-water reactors (BWRs), involves "batch management" of fuel. The core is thus fractioned into n batches (batch fraction 1/n). At every reactor outage for refueling, the most highly irradiated fuel batch is discharged, and removed to the spent fuel storage pools, being replaced by a batch of fresh assemblies, known as the "reload." The term "**irradiation cycle***," or "campaign," is used to refer to the operating period, for a reactor, spanning two successive loadings. In France, cycle lengths stand at 12 months, and 18 months; in the United States, some irradiation cycles may be as long as 24 months. Campaign duration is also expressed in terms of effective full-power days (**EFPD***).

The reactor core is the result of the arrangement (i.e. the one-to-one correspondence of fuel assemblies, and positions within the core) selected for assemblies inside the vessel, allowing mechanical support of the unit as a whole, and coolant water circulation.

Specifying the arrangement, within the core, of fuel assemblies from the various batches involved, i.e. the loading pattern, entails investigations of reactor behavior throughout the cycle, to ensure the compliance of operating and safety parameters with those specified by the boiler design, and the design of the fuel itself. Such investigations call for very high-quality modeling of reactor physics, along with measurements carried out during operation, in the core and cooling circuits (these aspects will not be addressed in the following pages).

## Relationships between cycle length, maximum burnup, and batch fraction

It is imperative that **criticality*** be sustained in the reactor core; now, **reactivity*** falls steadily, as the energy generated (expressed in MWd/t initial heavy metal [MWd/tiHM]) increases. Cycle length is dictated by this condition, of sustained criticality. For a given cycle length, an associated batch average discharge **burnup*** value may be specified ($BU_{av-d}$), defined by:

$$BU_{av-d} = n \Delta BU_c$$

where $\Delta BU_c$ is the average core burnup increment rate, over one cycle, and $n$ is defined by the batch fraction $1/n$; these parameters result from the fuel management mode selected.

Maximum fuel element lifetime is expressed in terms of the maximum energy yielded per unit mass heavy metal (measured in MWd/t). This bounding value is dependent both on fuel design, and reactor operating mode. Obviously, the amount of energy that may be extracted from a given fuel depends on the amount of fissile nuclei it contains: maximum reload burnup is all the higher, the higher the initial enrichment value for that fuel.

Management of a reactor core may thus be optimized, in accordance with the technical or economic constraints the operator must meet, by acting on three parameters:

- irradiation cycle length;
- core batch fraction;
- fuel initial enrichment.

## Enrichment and burnable poisons

Owing to the neutronics, there are relationships linking enrichment, batch fraction (or number of batches), and cycle length (see Fig. 68).

A low number of batches, and/or lengthy campaigns entail going for increased enrichment, and hence higher excess reactivity to be controlled at the beginning of the cycle. In PWRs, this reactivity in controlled, in the course of irradiation, by diluting, to the required concentration, **boron*** (a neutron absorber), in the form of boric acid, in the primary circuit water.

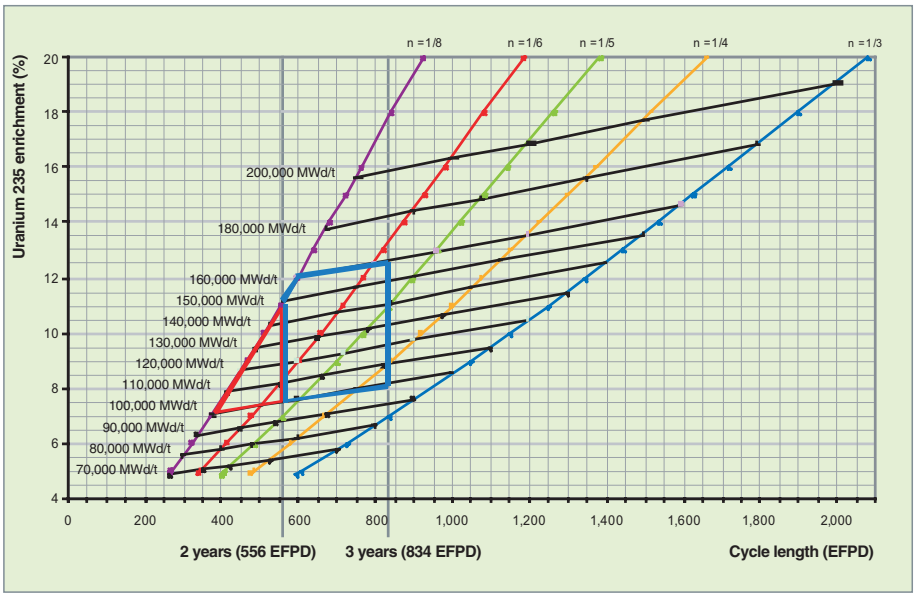


Fig. 68. Relationship between enrichment, burnup, cycle length, and core batch fraction for very high burnups:
– for a given batch fraction, feasible cycle length increases with fuel enrichment;
– for a given burnup, feasible cycle length likewise increases with fuel enrichment, though less steeply;
– for a set batch fraction, and set cycle length, the enrichment required, and burnup achieved may be derived from the diagram.

The amount of soluble boron injected is restricted by the moderator's **temperature coefficient***, at beginning of life, which must be negative, for safety reasons. Once that limit is reached, further reactivity control requires use of complementary neutron absorbers: **burnable poisons***, which vanish through neutron capture, their effectiveness declining as irradiation continues. The most widely used burnable poison is gadolinium, in gadolinia ($Gd_2O_3$) form; this is blended with uranium in some of the fuel pellets; $B_2O_3$-holding Pyrex rods were also used in early PWR cores.

Use of gadolinium as a burnable poison entails that a balance be struck between various parameters, namely gadolinia concentration, and number of gadolinia-bearing rods, and assemblies. Acting on gadolinia concentration allows poison depletion rate, and end-of-cycle residual absorption penalty to be specified; the number of gadolinia-bearing assemblies in the reload determines the amount of negative reactivity inserted at the beginning of the cycle; the number of gadolinia-bearing rods impacts the homogeneity of power distribution within the assembly.

Thus, for a given management mode (i.e. for a set cycle length, and batch fraction), the initial quantities that must be specified, and taken into account, are:

- uranium 235 enrichment (1.8–5% for current water reactors);
- uranium provenance: mined uranium, or reprocessed uranium (RU) (reprocessed uranium contains even-numbered uranium isotopes [232, 234, 236], which absorb neutrons. The fuel reactivity penalty due to these isotopes must be compensated for, by slightly higher enrichment);
- burnable poisons: number of "gadolinia" assemblies in the reload, number of "gadolinia" rods per assembly (0–20), $Gd_2O_3$ concentration (7–9%);
- plutonium concentration, and isotopic composition, in the MOX fuel case.

Cycle length, maximum assembly burnup, and batch fraction determine the enrichment required, and thus in turn the maximum boron concentration, and, if required, the amount of poisoning by means of burnable poisons.

## The impact of the nature of the fuel used, and its evolution, on the major parameters of core physics, and management

The nature of the fuel used in reactors plays a key part, with respect to certain parameters in reactor physics:

***The delayed neutron* fraction*** plays a decisive part in chain reaction control; it exhibits significant variations, depending on the kind of fuel, and fuel irradiation state (there are some two times fewer delayed neutrons with MOX fuel than with a fresh $UO_2$ fuel).

***The core's reactivity coefficient**** depends on the neutronic characteristics of the isotopes contained in the fuel. For safety reasons, the core's void coefficient must remain negative, which restricts, in effect, the plutonium content in MOX fuel, for water reactors (see Fig. 69).

***The effectiveness of absorbers***, such as soluble boron, and of rod control cluster assemblies is lower when plutonium is present; thus, for management modes involving MOX fuel, it has been found it is necessary to insert 4 extra RCCAs, to comply with safety criteria relating to absorber negative reactivity.

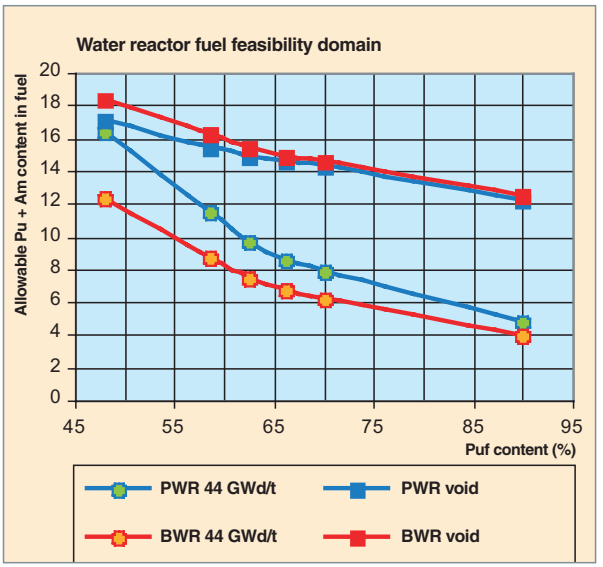


Fig. 69. When plutonium is recycled in PWRs and BWRs, fuel plutonium content must be kept within limits dictated by the minimum burnup to be achieved, and the requirement for a negative void coefficient. These limits vary, depending on the grade of plutonium used, i.e. its fissile isotope content. In practice, Pu content is restricted to about 12% in MOX, to preserve some margin with respect to these limits.

***Vessel lifetimes*** are directly dependent of the fast-neutron flux-related **fluence*** the vessel is subjected to: this fluence is due to the neutrons yielded by fission processes occurring in rod rows located at the core periphery. Figure 70 shows an image yielded by a simulation carried out with the TRIPOLI 4 Monte-Carlo neutronics code. To curb the fast-neutron flux at the periphery, the most highly irradiated assemblies must be positioned opposite the most exposed areas, and MOX assemblies must be positioned further inside the core. This strategy further allows a reduction to be achieved in neutron leakage out of the core, and contributes to extending irradiation campaigns.

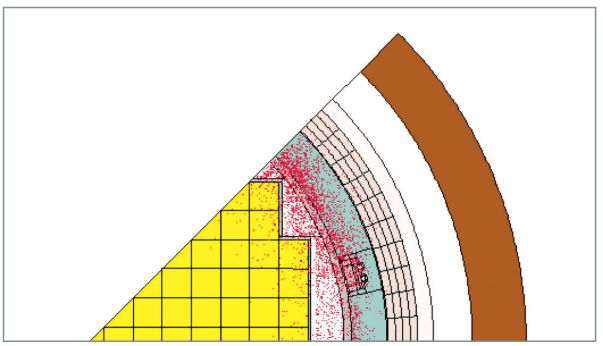

Fig. 70. Vessel fluence: meshing used for neutron transport modeling with the TRIPOLI 4 code.

***Power distribution***

The way fuel assemblies are arranged inside the core has a strong impact on power distribution; restricting the maximum power a rod may generate makes it possible to guarantee proper core behavior, in loss-of-coolant situations.

Recycling of plutonium by way of MOX assemblies has led to specifying lower-Pu-content regions at the assembly's periphery, failing which power from MOX rods would be too high. Figures 71 and 72 show the power distribution, and thermal-neutron flux in a reactor recycling plutonium.

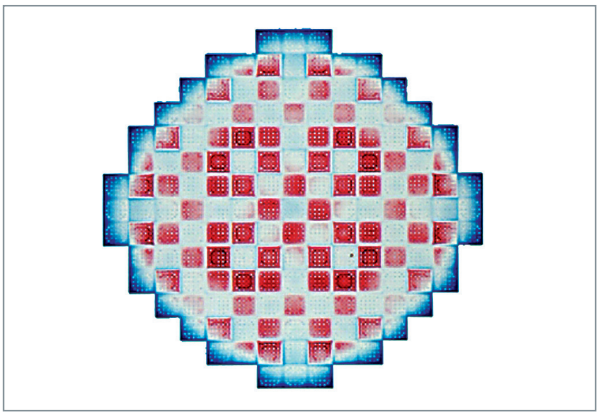

Fig. 71. Computed power distribution for a reactor recycling plutonium.

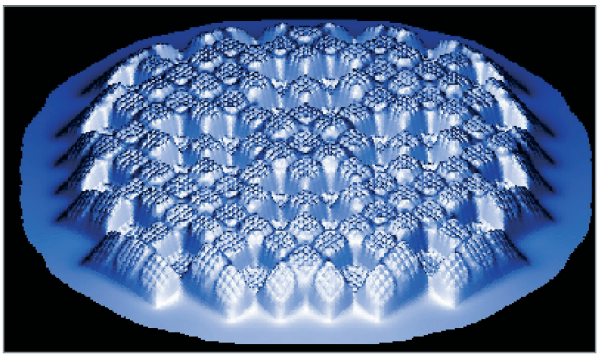

Fig. 72. Thermal-neutron flux distribution in a core loaded with MOX assemblies.

## Prospects for future trends in core management

Operators seek to optimize fuel performance, and core management performance, in order to:

- achieve increased fleet availability;
- ensure higher reliability, and enhanced operating flexibility;
- achieve savings in raw materials, by extracting a maximum amount of energy from natural uranium, while preserving (or even improving) safety levels.

On the scale of a reactor fleet, the quest for overall optimization involves a number of levels:

- scheduling unit outages to take into account seasonal demand forecasts;
- flexibility with respect to campaign duration: it is crucial to have the ability to set campaign durations by anticipation, in order to adjust capacity to match demand, and respond to the contingencies of fleet operation, over timescales of a day, or a week or so;
- reactor operating flexibility, to respond to grid load following, at timescales of the order of a minute, and to achieve, at the end of the campaign, an improved ability to operate at reduced power.

Further aspects, depending on the situations involved, may take on more or less importance. Achieving a reduction in the number of assemblies employed, per megawatt (electric) generated may be one consideration when specifying a management mode. Fuel management has a strong impact on spent fuel storage pool occupation, and on fresh, and spent fuel transportation requirements, for instance.

Fuel isotopic composition at discharge, in particular the amount, and grade of plutonium, is the outcome of a management choice that has repercussions on cycle back-end operations, in particular with regard to spent fuel reprocessing, and the recycling of plutonium in PWRs.

Currently, the thrust of investigations is along directions set by programs aimed at extending campaigns, and irradiation duration for fuel assemblies: in France, there has been an evolution from burnup of 33 GWd/t, with one-third-core refueling management, in the 1980s, to 52 GWd/t with quarter-core refueling currently. The Table below sets out the current situation.

The main investigations being conducted by EDF (see Table on opposite page) concern all units in the French operator's fleet:

**Fuel and economics**

In-core fuel management is but one element, among others, with respect to the more general issue of fuel cycle optimization.

It is true enough that fuel does not make a dominant contribution to the cost per megawatt–hour: just € 4.3/MWh, taking in all fuel cycle operations, from mine to waste. However, on the scale of a reactor fleet, any advance with respect to fuel management may swiftly translate into billions of euros annually – justifying an active research effort.

The cost factors that must be taken into account, for the purposes of techno–economic fuel optimization, are the cost of the raw material, enrichment cost, fuel element fabrication cost, reactor operating costs (which depend on irradiation cycle length), reprocessing–recycling costs, and waste management costs. All of these factors are involved, in a complex, loop manner, in the techno–economic optimization of fuel, and fuel management. For instance, supposing one seeks to make savings both on fabrication costs for the fuel elements required to generate 1 MWh, and on operating costs, this will be an incentive to go for higher burnup, and longer irradiation cycles. Thereby, the uranium inside the rod will indeed undergo better utilization, however it will also have to be more highly enriched… and thus more natural uranium will have been required, to make that rod. Ultimately, only a detailed calculation will make it possible to decide whether any gains have been made, in terms of raw material consumption, and separation work.

- PWR 900 (REP 900): MOX-parity management, initiated in 2007, with the aim of achieving comparable burnup for UOX and MOX fuels (maximum fuel assembly burnup: 52 GWd/t);
- PWR 1 300 (REP 1 300): GALICE management: 60 GWd/t by 2008, 70 GWd/t by 2015, for corresponding enrichments of 4.5%, and 4.95%, with enhanced flexibility (± 2,000 MWd/t, over the cycle duration);
- PWR 1 450 (REP 1 450): ALCADE management: by 2008, cycles to be extended from 11 months to 18 months.

**Current management modes for units in the EDF fleet**

| Reactors | Number of assemblies | Number of units | Fuel | Batch fraction | Campaign duration | Management |
|---|---|---|---|---|---|---|
| 900 MWe | 157 | 20 | UOX 3.7%<br>MOX 7.1% | 1/4<br>1/3 | 12 months, 45 GWd/t<br>12 months, 37 GWd/t | GARANCE |
| 900 MWe | 157 | 8 including 2 using RU | UOX 3.7% | 1/4 | 12 months, 48 GWd/t | |
| 900 MWe | 157 | 6 | UOX 4.2% | 1/3 | 18 months, 52 GWd/t | CYCLADE |
| 1,300 MWe | 193 | 20 | UOX 4% | 1/3 | 18 months, 47 GWd/t | GEMMES |
| 1,450 MWe | 193 | 4 | UOX 3.4% | 1/4 | 11 months, 42 GWd/t | |

The above techno–economic optimization is an instance of constrained optimization, since, as we have seen, there are technological restrictions on fuel utilization: fissile nucleus depletion, and fission product poisoning set limits, on neutronics grounds, on maximum allowable burnup, for any given fuel. At the same time, fuel in-reactor resistance is not limitless, owing to irradiation, and cladding corrosion resistance. Fuel assembly irradiation must be terminated, before potential accident situations pose a risk of cladding resistance being impaired. In practice, the fuel's characteristic parameters are set in such a way that there is not one single limiting factor, but several, acting concurrently to impose their relative restrictions: for instance, there is no point in enriching the uranium in a rod to 6%, so that it is able, in neutronic terms, to sustain a burnup of 80 GWd/t, if the rod's cladding may not withstand more than 60 GWd/t, owing to corrosion.

All techno–economic evaluations regarding fuel management [1] show there are benefits in increasing burnup to 60 GWd/t, with concomitant increases in enrichment, power density, and irradiation cycle length. Beyond 60 GWd/t, it would appear there are no further significant gains to be made, in economic terms (see Fig. 73), however cost evaluation is dependent on many parameters, in particular discount rates, and spent fuel management modes, so the situation has to be examined for each country, or even each reactor, on a case-by-case basis.

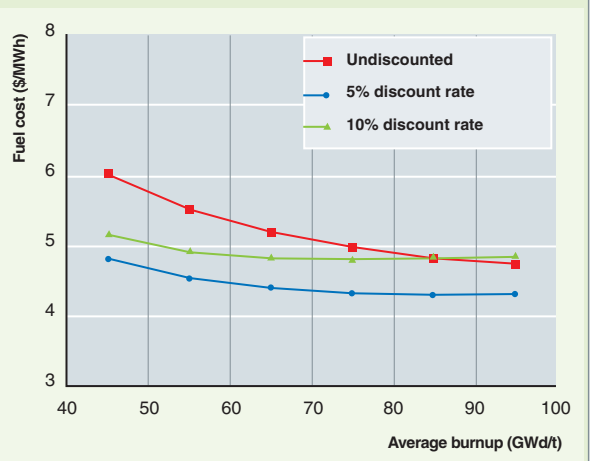


Fig. 73. Fuel cost as a function of burnup, as calculated by OECD–NEA [1]. Such a cost is highly dependent on the assumptions made. For further details, please refer to reference [1].

**Management modes being investigated for current EDF units**

| Reactors | Number of assemblies | Number of units | Fuel | Batch fraction | Campaign duration | Management |
|---|---|---|---|---|---|---|
| 900 MWe | 157 | 20 | UOX 3.7% | 1/4 | 12 months, 48 GWd/t | MOX parity |
| | | | MOX 8.6% | 1/4 | 12 months, 48 GWd/t | |
| 1,300 MWe | 193 | 20 | UOX 4.5% | 1/3 – 1/4 | 18 months, 55 GWd/t | GALICE |
| 1,450 MWe | 193 | 4 | UOX | 1/3 | 17 months, 47 GWd/t | ALCADE |

The fuel management modes being considered looking forward will result in the fuel operating in harsher conditions. This is made possible by the advances achieved with fuel ceramics, and, most crucially, cladding materials. CEA is playing its part in the evolution of these management modes, by carrying out fuel R&D programs for the purposes of suggesting, corroborating, and validating technical options, for enhanced-performance fuels.

### References:

[1] *Very High Burn-ups in Light Water Reactors*, OECD, 2006, NEA No. 6224.

**Richard Lenain,**
*Systems and Structures Modeling Department*

# Fuel cycle material balances

Two kinds, or families of fuel are used in the water reactors operated in the French nuclear power generation fleet: **UOX***, an enriched natural uranium-based fuel, and **MOX***, which is plutonium-based, on a depleted uranium carrier. Initial U 235 enrichment for the enriched uranium in UOX fuels, and initial plutonium content in MOX fuels depend on the target **burnup***, and in-reactor fuel management; for MOX, initial plutonium content is further dependent on the isotopic composition of the plutonium used.

Due to neutron-induced nuclear reactions, and radioactivity, any element present in fuel (nuclear materials, impurities, elements in assembly structural materials) undergoes, inside a reactor, nuclear transformations which alter the material balance, over the fuel's lifetime. This evolution of fuel, in the course of irradiation, is taken into account in core management studies.

Knowledge of the evolution of fuel, subsequent to irradiation, provides a major item of information, for cycle back-end operations, and waste transportation, and management. The purpose of cycle studies is the determination of material balances as a function of time, to provide pointers for policy with regard to waste recycling, storage, and long-term management.

## In-core evolution of materials

The chief nuclear reactions induced by (n, x) neutrons, and the various kinds of radioactive decay ($\alpha$, $\beta^-$, $\beta^+$) are set out in Figures 74, 75, 76 below, as applying to a radionuclide of atomic mass A, and atomic number Z (e.g. A = 235, Z = 92 for U 235): (n, f) fissions in fissile **isotopes*** cause the formation of **fission products***.

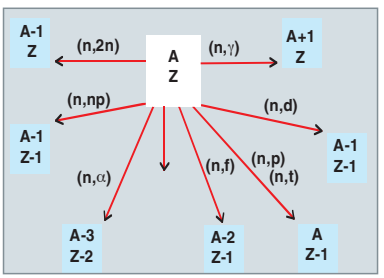


Fig. 74. Principal neutron-induced nuclear reactions, for a nucleus of atomic mass A, and atomic number Z.

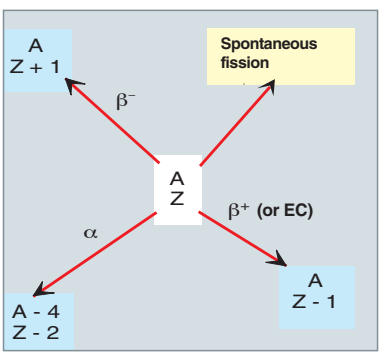


Fig. 75. Principal radioactive decay modes, liable to affect a nucleus.

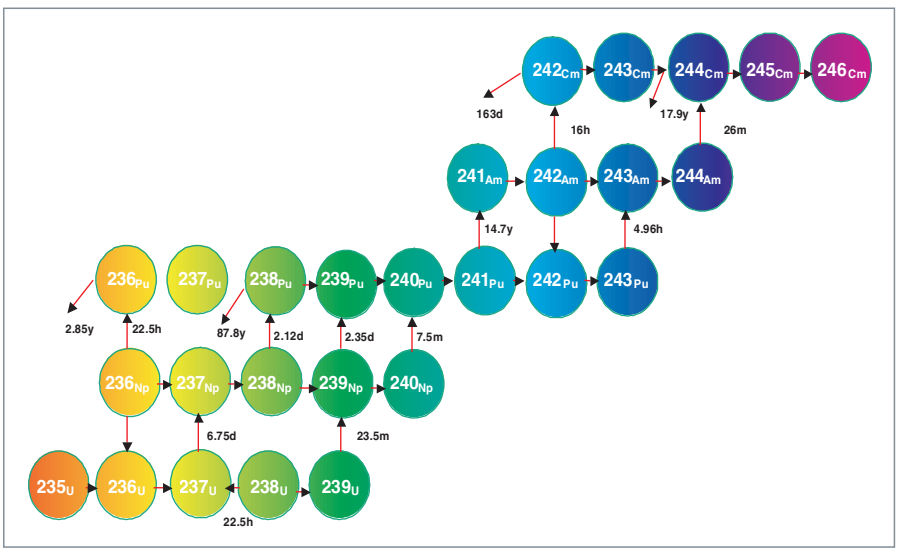


Fig. 76. Decay chain showing the actinides liable to be generated in a reactor core.

The evolution of the atom population, for each radionuclide, is governed by a differential equation, taking the following general form (N: concentration, $\sigma$: cross-section, $\lambda$: Log 2/half-life, $\gamma$: fission yield):

$$\frac{dN_i(t)}{dt} = \sigma_{k\to i} N_k(t)\phi + \lambda_{j\to i} N_j(t) - \left[\lambda_i N_i(t) + \sigma_i N_i(t)\phi\right] + \gamma_i \sigma_j \phi$$

Solving the differential system of equations of evolution governing all the relevant radionuclides makes it possible to compute material balances for the fuel; the number of radionuclides that must be considered depends on the quantity being computed; this ranges from a few tens of radionuclides, for in-core neutronic parameters, to several thousands, for core decay heat, immediately after reactor shutdown.

Figures 77 and 78, below, show, for a UOX fuel:

- the evolution of the isotopic composition of plutonium formed within the fuel – enriched to 4% U 235 – as a function of burnup; it will be noted that in-reactor Pu 239 inventory stabilizes around 40,000 MWd/t;

- actinide and fission product formation; by the end of irradiation, the fuel contains about 1% plutonium, 0.1% minor actinides, and 4% fission products.

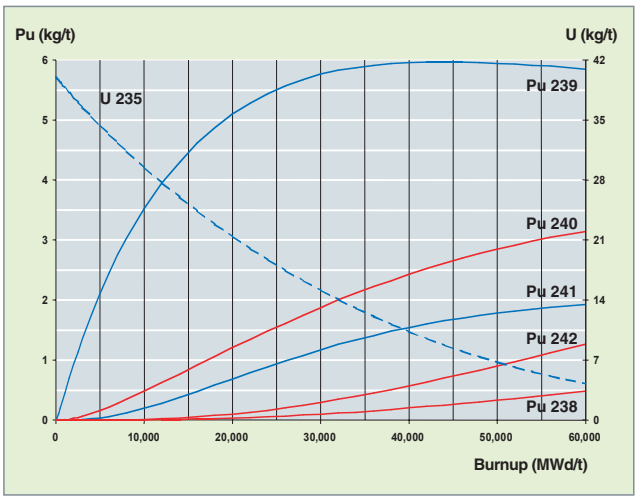


Fig. 77. The amounts of plutonium isotopes formed in a reactor core depend on burnup.

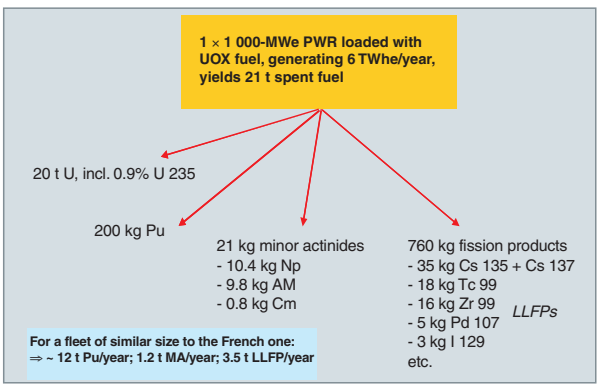


Fig. 78. Amounts of actinides, and fission products yielded in the course of UOX fuel irradiation in a water reactor.

The following table sets out actinide yields, and consumptions, for the same amount of electric energy generated, for the two types of fuel, UOX and MOX, along with plutonium isotopy, and fissile Pu (Pu 239 + Pu 241) content, this characterizing plutonium quality, with respect to reuse in the form of MOX fuel. Plutonium quality degrades during cooling time, yielding Am 241 from Pu 241 decay, as shown in Figure 79.

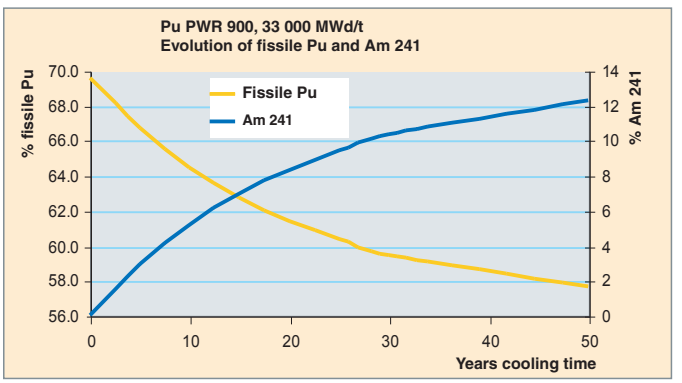


Fig. 79. The generation of americium 241 through plutonium 241 decay contributes to the degradation of the isotopic quality of the plutonium formed in reactor, i.e. the proportion of fissile isotopes it contains.

| Balance after 5 years' cooling | UOX 55 GWd/t | MOX 55 GWd/t |
|---|---|---|
| Pu (kg/TWhe) | + 26 | – 53 |
| Np (kg/TWhe) | + 1.8 | – |
| Am (kg/TWhe) | + 1.5 | + 15 |
| Cm (kg/TWhe) | + 0.3 | + 4 |
| Pu 238 (%) | 3.5 | 5.1 |
| Pu 239 (%) | 51.0 | 41.5 |
| Pu 240 (%) | 24.8 | 29.0 |
| Pu 241 (%) | 12.1 | 12.8 |
| Pu 242 (%) | 8.6 | 11.6 |
| Fissile Pu (%) | 63.1 | 54.3 |

This table shows that recycling plutonium in MOX form makes it possible to bring down plutonium inventory (a reactor loaded with 30% MOX, 70% UOX exhibits a plutonium net balance close to zero). In terms of resource management, utilization, in the form of MOX, of all of the plutonium yielded by the French nuclear reactor fleet would allow, each year, savings of some 900 tonnes natural uranium to be made, i.e. ~ 15% of annual consumption.

On the other hand, using plutonium does result in an increased content – by a factor of about 10 – in minor actinides (Am and Cm) in irradiated fuel.

## Decay heat and potential radiotoxicity

Most of the radionuclides (mainly actinides, and fission products) generated under irradiation are radioactive, with half-lives (the time interval by the end of which concentration in the element considered has been halved) that may range from a few seconds to several million years; the decay of these radionuclides involves concomitant emission of $\alpha$, $\beta$, and $\gamma$ radiation, and neutrons, from which operators must be shielded, during handling, transport, storage and disposal operations involving these materials, and which are the cause of the decay heat that must be removed.

The curves shown below (Figs. 80–83) show the evolution of decay heat in UOX and MOX fuels, along with the contribution from various elements to decay heat, and **radiotoxicity*** in MOX fuel.

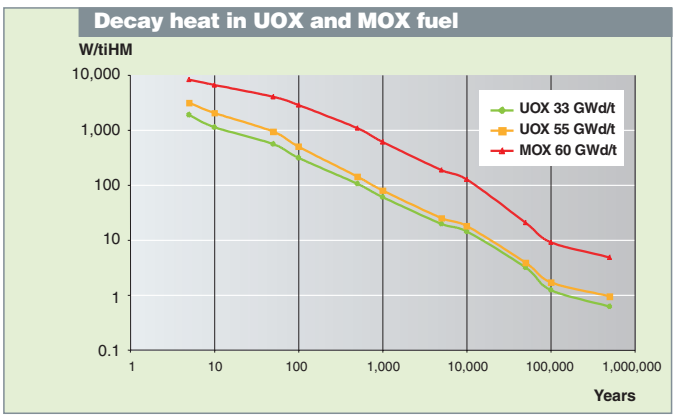


Fig. 80. The decay heat released by spent fuel (expressed here in watts per tonne of initial heavy metal) comes down as function of time. This heat being due the decay of radionuclides contained in the fuel, it is dependent on the amounts of actinides, and fission products formed, hence on burnup; decay heat is markedly larger in MOX fuel than in UOX fuel.

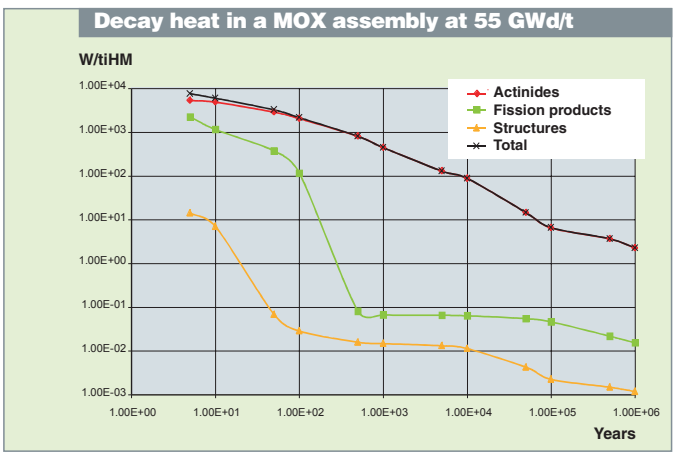


Fig. 81. The decay heat released by a spent MOX assembly involves a dominant contribution from actinides.

Beyond 5 years of cooling time, decay heat in a MOX fuel is higher than for a UOX fuel, at comparable burnup.

After 200 years' cooling time, the greater part of a fuel's decay heat is due to actinides; the same goes for radiotoxicity. After 200 years, and before 100,000 years of cooling time, the elements contributing the greater part of the heat, and radiotoxic inventory in spent fuel are, in that order: Pu > Am > Cm. To give a more precise indication, long-term radiotoxicity in a spent fuel is due, for 90%, to Pu, 10% to Am, and 1% to Cm (see Figs. 82, 83).

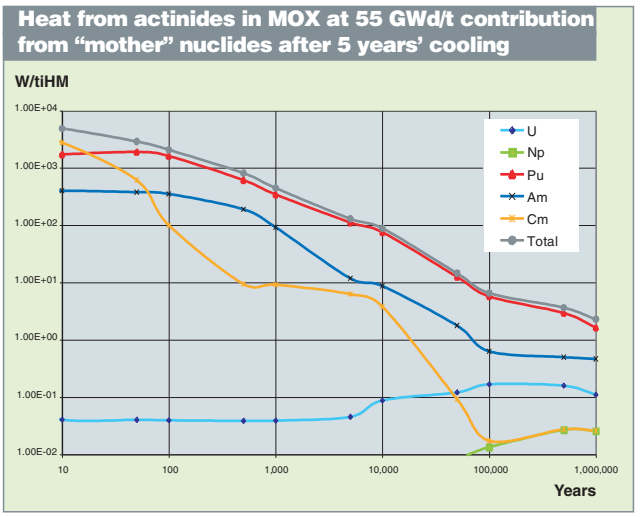


Fig. 82. Decay heat contribution from the various actinides, in spent MOX fuel, at 55 GWd/t burnup, left to cool for 5 years.

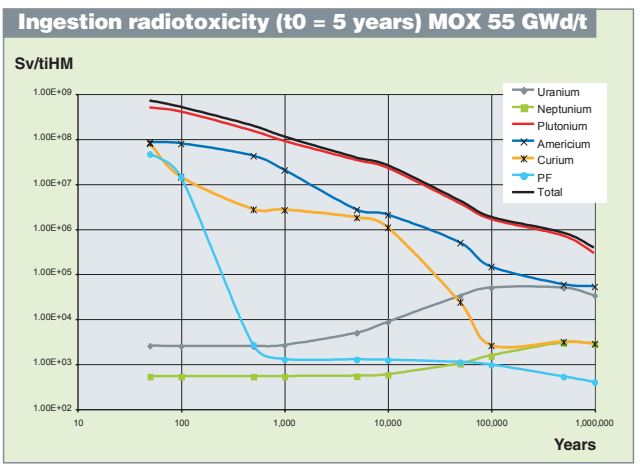


Fig. 83. Potential radiotoxicity of spent MOX fuel, as a function of time.

During spent fuel reprocessing operations, plutonium is recovered, in order to be reused, while minor actinides are conditioned, along with the fission products, in a glass matrix. R&D programs are currently ongoing to effect, in the longer term, the recovery of these actinides, at the time of reprocessing, for the purposes of transmuting them, in dedicated reactors.

## Plutonium management

It was seen earlier that using plutonium would allow savings to be made, in terms of Unat resources, along with a reduction in the potential radiotoxicity of spent fuel. Nuclear power fleet scenario studies, carried out at CEA, have shown that, compared to the open cycle (see Figure 84):

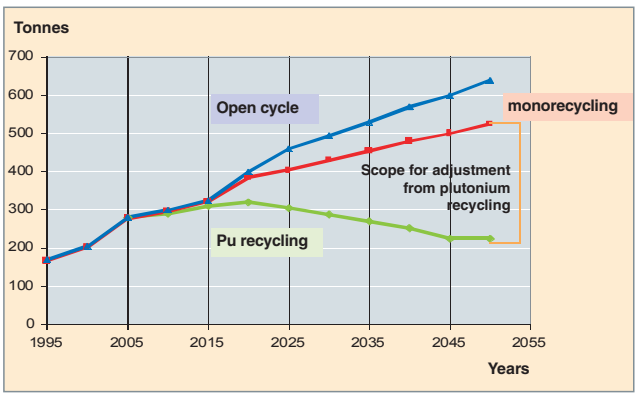


Fig. 84. Total plutonium yield from the French fleet, depending on fuel management mode.

- recycling plutonium (monorecycling, or once-through recycling) in PWRs would allow downsizing total plutonium inventory;
- multiple recycling of plutonium (a strategy that to date has not been opted for) could result in stabilizing, or even bringing down, the total plutonium inventory;
- recycling plutonium would result in a reduction in long-term potential radiotoxicity.
- As may be seen from Figure 85, retrieving minor actinides from vitrified waste packages would allow a further reduction in radiotoxicity. The transmutation of such minor actinides would be an option that could be contemplated for fourth-generation fast reactors.

**Jean-Paul Grouiller,**
*Reactor Research Department*
**and Marc Delpech,**
*Nuclear Development and Innovation Directorate*

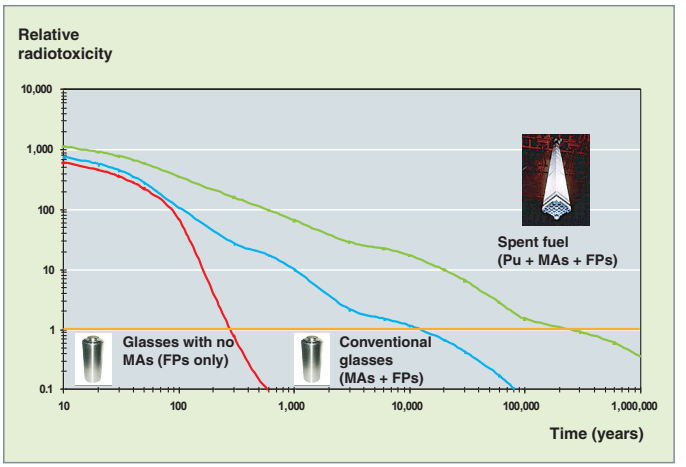


Fig. 85. Decrease in the relative radiotoxicity of spent fuel, and vitrified waste, as a function of time. Radiotoxicity, in this case, is estimated relative to that of the initial uranium (orange curve). Reprocessing–recycling of plutonium, as already implemented in France, yields a considerable reduction in relative radiotoxicity, as a first step. Retrieving minor actinides from vitrified waste packages would allow a further reduction in waste radiotoxicity.

# Long-term behavior of spent fuel

Subsequent to discharge from the reactor, a spent fuel assembly undergoes a period of **storage***. In France, this storage period takes place prior to carrying out fuel reprocessing operations. Long-term storage is being considered as one possible option, which could afford some flexibility, with respect to spent fuel management strategy. The length of such storage is a major parameter in this strategy. Now, contemplating storage of spent nuclear fuel entails gaining an understanding of, and the ability to predict the way that that fuel is liable to evolve, over timescales of centuries, as regards long-term storage, or even over several thousand years, assuming the option of deep geological **disposal*** of spent fuel were to be taken up.

The fuel rod is designed to ensure confinement of nuclear fuel materials, and nuclear fission products, over the fuel's in-reactor dwell time. Now, the $UO_2$ matrix, and the cladding degrade during irradiation, and there is a need to verify that confinement will likewise be ensured, subsequent to discharge.

## The nature of spent nuclear fuel

In the course of its in-reactor evolution, fuel undergoes physical–chemical alterations, related to the high temperatures, and fission reactions it experiences. These alterations form a major consideration, insofar as they determine the reference physical–chemical state, with respect to the long-term evolution of spent fuel.

The most significant alterations to be taken into consideration are the following:

- radial cracking of the pellet, related to a temperature gradient arising between the pellet centerline, and periphery. One may thus observe, quite commonly, some 5–7 major cracks, splitting the pellet into 15 fragments or so (see Fig. 86);

- the formation of new atoms within the material, owing to fission reactions. These may be found either in the form of solid, metallic precipitates (Mo, Tc, Ru, Rh, Pd, Ag, Cd, In…), or oxides (Rb, Ba, Cs, Te…), or immersed (in solid solution form) in the matrix (lanthanides, Sr, Zr, Nb, Y…). Among such fission products, note should be made of the particular issue of fission gases (Xe, Kr), which are partly released into the rod's free volumes (~ 2–5%), the remainder being trapped inside the pellet. This contributes to a considerable rise in rod internal pressure, which, by the end of irradiation, stands at some 40–60 bars, in cold conditions;

- damage to the matrix, with the occurrence of irradiation damage, partly healed in reactor;

- at **burnup*** values higher than 40 GWd/t, the formation, at the pellet rim, of a restructured region, featuring small grains (~ 0.2 µm), and a large proportion of closed porosity (~ 10%), whereas fabrication porosity stands at ~ 5%. A similar mechanism results, in the MOX fuel case, in the restructuring of Pu aggregates of a size greater than 10 microns or so;

- cladding damage, due to irradiation, and twin corrosion processes, external corrosion due to the effect of primary circuit water (40–100 µm oxide thickness), and internal corrosion under the effect of the fuel itself (~ 5–10 µm oxide thickness for Zircaloy 4).

Spent nuclear fuel thus exhibits a structure, and mechanical, physical and chemical properties far removed from those of a fresh fuel, the more so since its abrupt cooling, at the end of irradiation, induces major internal ruptures of equilibrium.

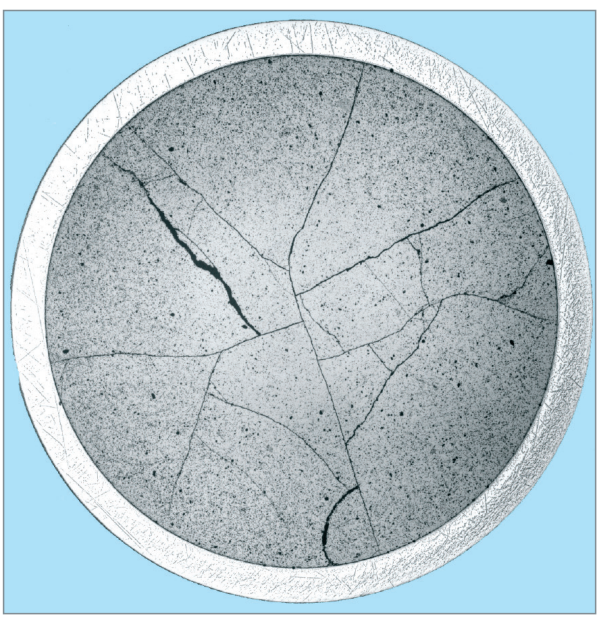

Fig. 86. Radial micrograph of spent nuclear fuel (in optical microscopy), evidencing the existence of radial cracks, arising during irradiation, as a result of temperature gradients.

## Anticipated evolution of fuel in dry storage

By definition, dry storage facilities must ensure, in nominal conditions, throughout storage time, the total confinement of spent nuclear fuel assemblies, which should not, therefore, interact with the ambient environment. In such conditions, fuel evolution is essentially due to the fuel's own internal chemical, physical, or mechanical disequilibria. What this involves is thus the fuel rod's intrinsic evolution, as it affects the pellet, on the one hand, and cladding, on the other.

### *Intrinsic evolution of the pellet*

Evolution of the irradiated fuel pellet essentially occurs under the effect of the radioactive decay of emitters present within it, resulting in an alteration of chemical inventories, and significant production of helium, due to **alpha*** decay.

To give an indication of the amounts involved, if all the helium generated within the fuel were released, this would result in an overpressure of about 125 bars in MOX fuel, 19 bars, at 19° C, in UOX fuel, after 300 years of cooling time.


Fig. 87. Evolution, as a function of time, of the volume of helium yielded (in normal temperature and pressure conditions) by UOX and MOX fuels at 47 GWd/t burnup.

It has been shown that the evolution of chemical inventories has no significant impact on the fuel pellet's oxidation state. On the other hand, alpha decay results in the accumulation of a considerable amount of helium within the pellet, especially in alpha emitter-rich fuels, such as MOX fuels (see Fig. 87). The issue is to ascertain what happens to this gas, chiefly generated as it is within fuel pellet grains: does it remain held in the $(U,Pu)O_2$ oxide, or does it rather diffuse across the grains, gradually getting released to the grain boundaries, and subsequently to the rod's free volumes? This point is all the more important since the occurrence of significant alpha irradiation in the pellets is liable to boost chemical element mobility, owing to the onset of a further mechanism, alpha self-irradiation enhanced diffusion. The fragmentary findings currently available give grounds for believing that, on the timescales involved in storage, this mechanism should not result in any significant diffusion of helium, or heavy elements. On the other hand, part of the fission gases initially trapped at the grain boundaries may be gradually released into the empty spaces, thus contributing to increased pressure inside the rod.

Finally, the fuel pellet's mechanical behavior is wholly dependent on the mechanical stability of grain boundaries. Now, it is difficult, at the present time, to demonstrate the long-term resistance of these grain boundaries, owing to the accumulation of gas bubbles, irradiation damage, and solid precipitates at these locations (see Fig. 88). One is thus led to consider them as providing a privileged path for the transport of gases, or water. Investigations are currently ongoing, to further explore this issue.

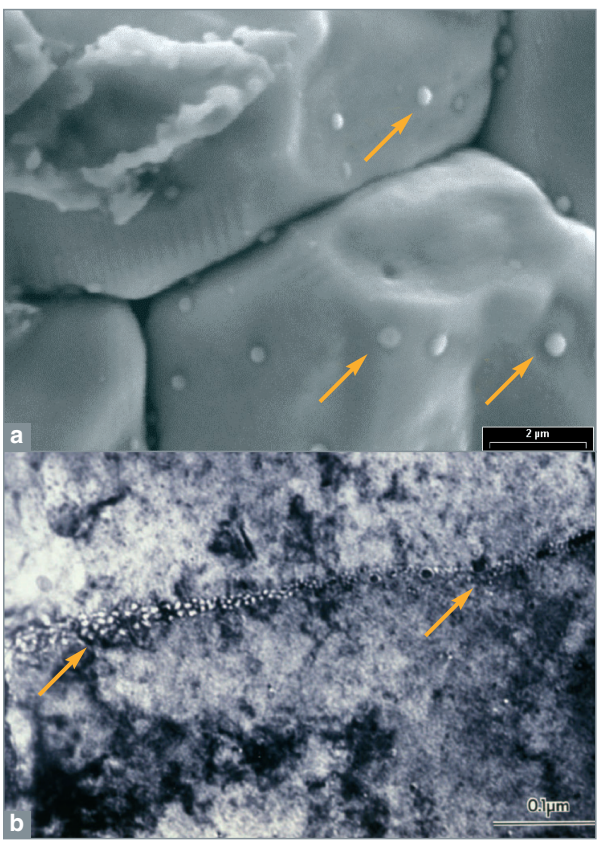


Fig. 88 (a) Micrograph of a grain boundary after irradiation, evidencing the presence of solid precipitates at this interface, and (b) micrograph, in transmission electron microscopy, evidencing the presence of numerous microbubbles at grain boundaries [1].

### *Long-term evolution of irradiated claddings*

Forming as it does the first containment barrier in storage conditions, fuel **cladding*** is subjected to considerable mechanical stress, owing to the rods' internal pressure. If the temperature is high enough, cladding undergoes gradual plastic deformation, through creep. In the long term, a risk of failure may not be ruled out, at first blush, should such deformation become too large, and exceed the material's rupture strength, which is liable itself to alter over time. In particular, investigations are being conducted to ascertain the possible influence of the hydrogen taken up within the cladding, with respect to its mechanical strength, in particular in cases involving preferential radial reorientation of hydrides, or microcracking (the "delayed hydride cracking" [DHC] mechanism). The purpose of currently ongoing investigations is thus not only to draw up long-term strain/failure models (creep model, rupture criterion), but equally to gain an understanding of, and model the evolution of mechanical properties.

The evolution over time of cladding stress, taking into account the ongoing release of gases throughout storage, has been computed at CEA. This stress is strongly dependent on the temperature scenario considered. Figure 89 shows the typical size of cladding deformation, and the margins that remain, with respect to failure, for various temperature scenarios.

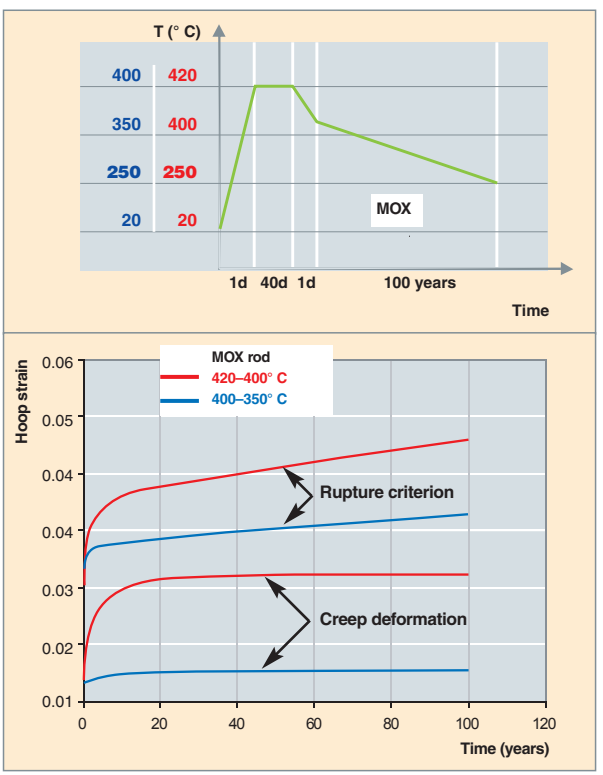


Fig. 89. Evaluation of strain, and rupture margins, for a MOX rod in storage conditions, assuming a highly unfavorable 18% initial fission gas release (though no further release).

Despite the R&D effort conducted over the past few years, and the many findings gained, such investigations do not allow, as of now, a prediction to be made, with any certainty, as to cladding evolution, over timescales of several centuries. As a consequence, it is at present deemed impossible to guarantee cladding mechanical strength beyond 100 years, and it is thus deemed unreasonable to assign to cladding a containment function beyond that timespan.

## Anticipated evolution of fuel in deep geological disposal

By contrast to long-term dry storage, deep geological disposal unavoidably involves gradual failure of the various envelopes enclosing the package (chiefly owing to corrosion), along with groundwater coming into contact with the fuel. Broadly speaking, fuel evolution, during the initial phase, of corrosion of metal envelopes, occurs while shielded from any alteration due to water from the site, i.e. as intrinsic evolution, as in storage conditions. Subsequently, in a second period, fuel undergoes alteration in the presence of water, gradually releasing around the package part of the radionuclides it contains.

### *Package evolution prior to water ingress*

In like manner to what occurs in storage conditions, fuel undergoes an intrinsic evolution, under the effect of its own internal disequilibria, and radioactive decay reactions. The chief difference, with respect to storage conditions, lies in the longer timespan involved, resulting in production of a larger amount of helium, increasing full release by diffusion to the grain boundaries, and involving further accumulation of irradiation damage. Likewise, the possible mechanical destabilization of grain boundaries becomes all the more significant, the longer the timespan involved. As a result, this microstructure is to be considered as providing a preferential path for the transport of water, and radionuclide release.

By contrast to what is the case in storage conditions, this phase in fuel evolution is relevant only inasmuch as it determines the state of the fuel, at the time of subsequent water ingress. The chief point of the ongoing investigations is thus to ascertain the evolution over time of the location of radionuclides, and surfaces accessible to water, so as to gain the ability to predict subsequent releases.

### *Instant release of radionuclides at the time of water ingress*

Water, as it comes into contact with spent fuel, dissolves all of the radionuclides present in the fuel's free spaces, and on its surfaces. This results in an instant release of radionuclides, commonly known as the "labile fraction." The amount of radionuclides thus released is thus dependent on their location, which depends on the fuel's prior intrinsic evolution, in

particular diffusion processes, and grain boundary destabilization processes. A worst-case model of diffusion under alpha self-irradiation has been developed at CEA, for the purposes of predicting the evolution over time of the labile fraction, as a function of the time when water comes into contact with the package. It is thus understood that, as regards the more mobile fission products, some 15% of the inventory is immediately available, in the event of water ingress after 10,000 years (see table below), for spent fuel at 55 GWd/t average burnup. This covers the fraction of fission gases present in free volumes, at grain boundaries, and rim porosity, at discharge from the reactor, augmented by what may have diffused from the grains to the grain boundaries (e.g. some 5% after 10,000 years).

| Radio-nuclides | Labile fraction (%) | | | |
|---|---|---|---|---|
| | Immediately after irradiation | Container failure after 1,000 years | | |
| | | 1,000 years | 10,000 years | 100,000 years |
| **C 14** | 10 | 13 | 14 | 16 |
| **Cl 36** | 11 | 14 | 15 | 17 |
| **Se 79** | 11 | 14 | 15 | 17 |
| **I 129** | 11 | 14 | 15 | 17 |
| **Cs 135** | 11 | 14 | 15 | 17 |

Evaluation of the so-called **labile*** fraction of some relevant long-lived radionuclides: proportion of the total inventory that may be deemed to be directly accessible to water, as a function of the time of water ingress into the package.

## *Alteration of fuel in disposal conditions, and release of radionuclides*

$UO_2$ is relatively stable in a deep geological environment; owing to the reducing character of the ambient medium (extremely low solubility, of ~ $10^{-8}$ mol · $L^{-1}$). However, spent fuel residual radioactivity (in particular alpha radioactivity, which is dominant in the long term) causes the dissociation of water molecules, through **radiolysis***, at the fuel–water interface (see Fig. 90). The oxidizing agents thus generated oxidize the fuel surface [oxidation of U(IV) to U(VI)], resulting in its dissolution, with the release of occluded radionuclides. Modeling these processes is highly complex, insofar as the radiolysis reactions involved are many (more than 150 reactions, in the models in common use), exhibiting fast, though diverse kinetics, and are strongly dependent on the chemistry of the ambient environment. Investigations are currently ongoing to arrive at an accurate, detailed picture of these processes as a whole, and thus gain an understanding of the manner in which materials in the environment influence fuel alteration (coupling between the package, and its environment). Thus, Swedish teams have recently highlighted the major part that would appear to be played by the hydrogen that is released by metal container corrosion processes, in these corrosion processes. The as yet fragmentary findings available in the literature would seem to indicate this hydrogen strongly restricts fuel alteration, by suppressing the oxidizers yielded by radiolysis. Likewise, it would seem likely that a fraction of the elements released through dissolution of the fuel (uranium, minor actinides, fission products) precipitate close to the fuel, in the form of new, so-called “secondary” mineral compounds. If these minerals have the ability to retain part of the radionuclides present within the fuel, then it is clear they may also contribute to the disposal facility’s confinement function.

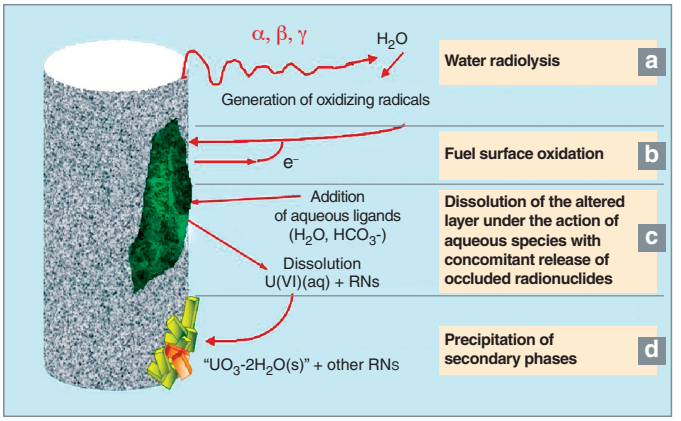


Fig. 90. General alteration mechanisms for spent nuclear fuel, in the presence of water: (a) water radiolysis due to the effects of α, β, or γ radiation; (b) fuel surface oxidation, and transformation of U(IV) to U(VI); (c) dissolution of the altered layer, under the action of aqueous species, with concomitant release of occluded radionuclides; (d) precipitation, in some instances, of secondary phases.

It will thus be seen that the phenomenology of fuel alteration, in geological disposal conditions, is a complex issue. Predicting very-long-term evolution entails, consequently, a simplification of that phenomenology, involving only retaining the dominant reactions, and ascertained facts: the effect of hydrogen, the role of which has yet to be precisely determined, is thus passed over. With this in mind, CEA has developed a worst-case model, for the purposes of describing radionuclide release through radiolytic dissolution. This model allows a prediction of maximum fuel alteration rate, as a function of time, taking into account all current uncertainties.

## Conclusion

To sum up, even though spent fuel is highly complex, the mechanisms involved in its evolution are nowadays clearly identified, and thoroughly investigated. Such findings are presently put to advantage in conservative long-term evolution models, taking on board all of the current uncertainties, and gaps in knowledge, making it possible to consider the evolution of fuels in storage, or disposal conditions. Models of releases in disposal conditions are used nowadays by **ANDRA***, to carry out its performance and safety analysis computations [2]. Concurrently, CEA is carrying forward research work, to refine its own models, by seeking to achieve improved modeling of the complex phenomenology of radiolytic dissolution, thus narrowing down the margins opted for, and by taking better account of coupling with the environment, in particular as regards the effect of hydrogen, and the role of secondary phases. Finally, a significant effort is gradually addressing the evolution of grain boundaries, in order to gain the ability to understand, and predict any significant evolution in specific surface area, which directly influences radionuclide release, in disposal conditions.

In any event, the uncertainties regarding the long-term behavior of spent fuel lead to the conclusion that a strong engineered barrier is a requirement, in all direct disposal concepts.

The powerful heat release from spent fuel will likewise dictate precautions, regarding the spacing of containers, in all concepts of direct disposal facilities in a geological environment.

### References

[1] L.E. Thomas, "Condensed-phase xenon and krypton in $UO_2$ spent fuel", in S. E. Donnelly and J. H. Evans (eds.), *Fundamental Aspects of Inert Gases in Solids, Plenum Press*, New York, 1991.

[2] ANDRA, Dossier 2005: *ANDRA Research on the Geological Disposal of High-Level Long-Lived Radioactive Waste*.

**Christophe Poinssot and Cécile Ferry,**
*Physico–Chemistry Department*

# Boiling-water reactor fuel

Boiling-water reactors (BWRs) account, the world over, for one quarter of all light-water reactors (PWRs, BWRs, VVERs). They are mainly sited in the United States, Japan, and Europe. The manufacturers involved are General Electric, Toshiba–Hitachi, Areva NP (formerly trading as Siemens), Westinghouse, and the BNFL Group (formerly ABB). There are no BWRs operating in France. It should be noted, however, that the Areva Group does produce, and reprocess BWR fuel, while Areva NP makes the ATRIUM™ BWR fuel assembly. In such a context, R&D activity at CEA is minor, compared with work relating to PWR fuel.

## Similarities, and differences with PWR fuel

As in PWRs, BWR fuel consists of **sintered*** $UO_2$ pellets, inserted into a **Zircaloy*** cladding. The height of the fissile column is comparable (3.7 m in one of the most recent boiling-water reactor models, the Advanced Boiling Water Reactor [ABWR], as against 4.2 m in a PWR of the EPR type). Rod diameter (12.3 mm in ABWR) is larger than in PWR fuel (9.5 mm). The design trend, for new fuels, is to go for smaller rod diameters. The comparison does stop here, since rod layout, enrichment distribution, and poisoning involve a fair amount of difference, between PWRs and BWRs (see Fig. 91).

Pressurized-water reactors (PWRs) use water as coolant, and neutron **moderator***, in single-phase form. Power density stands at 100 kW/l, at a pressure of 15 MPa. The density of the water used exhibits little variation as a result of thermal expansion as it passes through the core. Thus, fuel layout takes the form of open assemblies. Some positions carry guide tubes, serving to insert neutron absorbers, lowered from above; these guide tubes also form the assembly's skeleton. Use of an indirect cycle for energy transformation allows addition of boric acid into the primary circuit, to control reactivity, as the water remains constantly in liquid form. Further additives allow a fine-tuned control of chemical equilibrium.

In boiling-water reactors, the coolant and moderator is used in two-phase form. Power density, and pressure (50 kW/l, and 7 MPa) stand at half the values found in PWRs. Fluid density exhibits quite considerable variations, depending on axial elevation, and radial position within the core. This dictates a fuel layout in the form of channels, to preclude cross-flow. Thus, fuel rods are bundled inside square-section Zircaloy channel

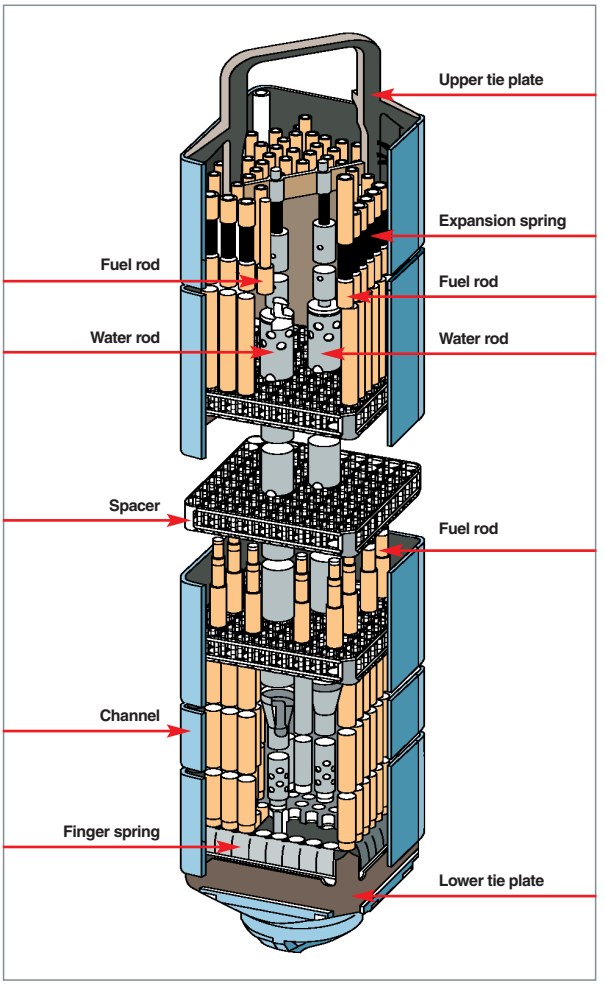


Fig. 91. A boiling-water reactor fuel assembly.

boxes (see Fig. 91). A diaphragm is positioned at the channel inlet, for the purposes of adjusting flow rate, and stabilizing the flow. Owing to in-core water boiling, it is impossible to effect further control of reactivity by means of a soluble poison. Negative reactivity is provided by addition of burnable poisons, gadolinium as a rule, in a few rods in the assembly, and by cruciform absorber rod assemblies, sliding between channel boxes (see Fig. 92). As the upper region of the vessel is taken up by steam separators, and steam dryers, insertion of the cruciform $B_4C$ rod assemblies is effected from below.

The core of General Electric's ABWR thus comprises 872 assemblies, or bundles (bundle pitch 155 mm), each compris-

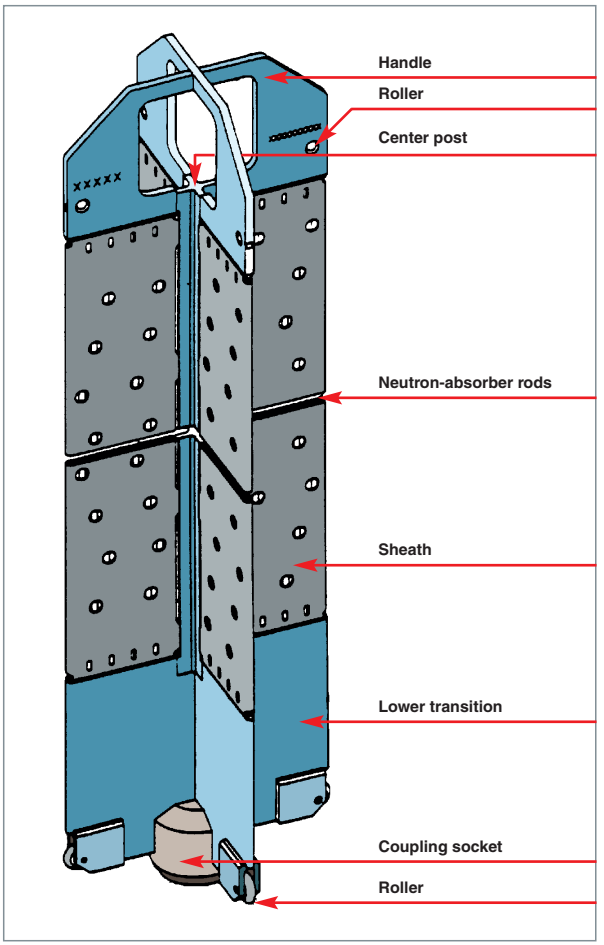


Fig. 92. Cruciform boiling-water reactor control rod assembly.

ing 10 × 10 rods, and is controlled by means of 205 cruciform absorber rods.

## Axial and radial zoning

The channel-type fuel layout results in strong neutron thermalization along the water gaps, causing locally increased power, at the bundle periphery. Such variations are counteracted through the introduction of "water holes" within the bundle, involving a variety of options, depending on manufacturers: removal of 1–2 fuel rods, a central water channel, a water cross configuration, water rods, etc. The effect is enhanced through radial modulation of U 235 enrichment in the rods (up to 9 distinct enrichment grades, depending on the manufacturer), in order to restrict, as best feasible, power peaking during the cycle. Average rod U 235 enrichment stands at about 4.5%.

The second cause of heterogeneity is due to the considerable axial variation in water density, as a result of boiling. Thus, fuel at the base of the bundle is bathed in liquid water, inducing a major neutron moderation effect.

On the other hand, in the upper region, the void ratio reaches 70%, resulting in an **epithermal*** neutron spectrum. This has a direct incidence on U 235 consumption, Pu 239 yield, and the axial power profile, during the cycle. These parameters are adjusted by way of axial U 235 enrichment zoning, and, in recent fuels, through the use of a few partial-length rods, to increase the moderator fraction in the upper region.

## Rod and channel box sizes

BWRs have the specific characteristic of involving a wide variety of designs, depending on manufacturers, from various countries, and on evolutions over time. From the 1970s, channel boxes held 7 × 7 rods, later rising to, and stabilizing at, 10 × 10 rods. This change occurred at constant box size (130 mm square, for a bundle pitch of 155 mm), on interoperability grounds, particularly in European reactors, resulting in the use of smaller-diameter rods, with a consequently increased surface/volume ratio, and improved control of enrichment and poisoning zoning, as of water hole management.

## Poisoning and reactivity control

Reactivity control involves cruciform neutron-absorber rod assemblies, inserted between bundles, and burnable **poisons***, introduced into some of the rods. The latter thus make it possible to compensate for beginning-of-cycle fuel reactivity. The cruciform control rod assemblies are used to ensure a negative reactivity margin, including in the most unfavorable case: a fresh core, in cold conditions. They are used, during operation, together with variations in core recirculation flow rate, to adjust the reactor's power level, stability margin, and axial power profile. This allows operating strategies to be specified favoring formation of Pu 239 through neutron captures in U 238 at the beginning of the cycle, in the upper region, and subsequent Pu 239 consumption at the end of the cycle. It is this operating mode that allows a significant increase in burnup to be achieved. Finally, an extended cycle may be achieved by bringing down water inlet temperature. This contrivance allows the liquid water fraction to be raised within the bundle, thus counterbalancing the fuel's loss of reactivity, by way of heightened moderation.

## Cladding specific characteristics

Nucleate boiling being an aggressive phenomenon, as regard cladding, even at temperatures lower than 300° C, BWRs use a Zircaloy–2 alloy, different from that employed in PWRs (Zircaloy–4). Zr–2 is a zirconium alloy, with 1.5% tin, containing 0.35% iron (Fe), nickel (Ni), and chromium (Cr).

To limit the number of pellet–cladding interaction-related failures, General Electric suggested, in 1981, use of cladding featuring an inside liner, a concept now taken up by most manu-

facturers. This involves a cladding made, for 9/10 of its thickness, from Zircaloy–2, the inner 1/10 consisting of pure zirconium, or a low-iron-content alloy form. This soft material is interposed at the interface between fuel pellet asperities , and the main Zr–2 cladding. This may bring down the number of failures due to pellet–cladding interaction, during power transients.

## Trends in fuel evolution

Manufacturers are working on projects for new fuel assembly architectures, with a view to achieving higher burnup – this is gradually catching up with levels achieved in PWRs – and improving operating margins, reactor availability, and fuel resource management.

The trend is, with an unchanged channel box size, to go for an increased number of rods, of lower diameter: there has been a move from 8 × 8 to 9 × 9, then 10 × 10 rods (see Fig. 93). In this manner, rod linear power may be brought down. At the same time, more degrees of freedom, in terms of design options, are thus available, as regards water hole positioning, rod poisoning, U 235 enrichment distribution. This opens the way to improved control of power distributions, and uranium consumption. Increased operating margins become feasible. Combined with improved neutronic performance, higher enrichment allows high burnups to be achieved. Fresh assemblies, now better controlled as they are, may be positioned at the center, for the purposes of low-leakage core management.

The other trend is to go, at the same time, for a larger channel box size, with a view to limiting the time required for bundle handling campaigns, during refueling (ATRIUM 12 assemblies, for Areva NP's SWR1000; or the ABWR–II project by Toshiba). Finally, Japanese studies are addressing the feasibility of using an existing boiler, or a little-modified one (the ABWR boiler) to receive 100% MOX loadings, or high-conversion-rate cores (featuring a close, triangular bundle pitch, to harden the neutron spectrum).

### References

[1] G. A. Potts, "Recent GE BWR fuel experience", *Proceedings of the International Topical Meeting on LWR Fuel Performance*, Park City, Utah (USA), 10–13 April 2000.

**Philippe Marsault,**
*Reactor Research Department*

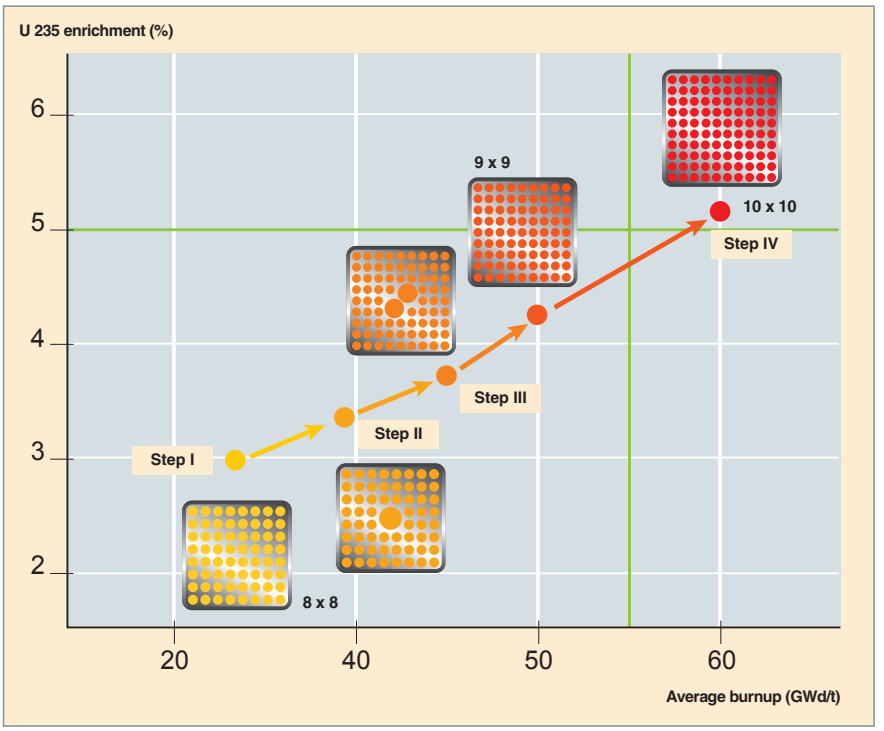


Fig. 93. Improvements in boiling-water reactor fuel performance.

# Liquid-metal-cooled fast reactor fuel

Cheap uranium resources are limited, and the resurgence of nuclear energy, currently being seen the world over, is fast consuming them. Even if spent fuel is recycled, to achieve maximum savings with respect to natural resources, second- or third-generation nuclear systems would not prove sustainable, as they do not fully utilize the energy potential from heavy nuclei. In practice, only fast-neutron breeder reactors, or fast reactors, have the ability to effect the efficient transformation of **fertile*** nuclei into **fissile*** nuclei.

By way of example, to obtain 1 GW–year of electric energy, about 1.4 tonne of material must undergo fission. To achieve this, an ordinary-water reactor (of PWR type) requires 140 tonnes of natural uranium, whereas, with a breeder system, 1.4 tonne of fertile nuclei would suffice. The saving, in terms of raw material, is patently significant.

However, the use of fast neutrons imposes very specific constraints, with regard to reactor, and fuel design. Some of these constraints stem from neutronics considerations. The low neutron **cross-sections*** prevailing, in fast-spectrum conditions, must be counterbalanced by a high concentration of fissile nuclei within the core, and a high neutron flux. The first constraint dictates a geometry that is as close as feasible, with respect to fuel elements. And, owing to the second constraint, irradiation damage is to be anticipated in core materials, and structures, from a large fast-neutron flux.

Other constraints are of a technological, and techno–economic character. High burnups are required, to recover fuel fabrication, and reprocessing costs. The plutonium (and/or U 235) inventory required for the deployment of 1 gigawatt installed electric power must be brought down, at least during the buildup of the fast-reactor fleet. Such minimization entails both high in-reactor specific power, and a short ex-reactor cycle time.

The type of reactor thus sketched out finds one first possible implementation, in a technology line that can already draw on some operational feedback, in France in particular: the sodium-cooled fast reactor line.

To demonstrate the competitiveness of the fast reactor (FR) line, with respect to light-water reactors, research efforts have persistently focused on ways to obtain high burnups, in order to bring down cycle costs [1]. Of fuel materials potentially able to fulfill this purpose, mixed oxide ($UO_2$, $PuO_2$) fuel soon made its mark as the reference material, and development of such fuels has been the lynchpin of the programs conducted over three decades at CEA [2], but equally around the world.

As regards the French experience, most of the findings in nominal operating conditions are the outcome of experimental and monitoring programs carried out in RAPSODIE (1967–83), and in the Phénix industrial prototype (1973–…), together with Superphénix (1985–88) [3]. Many tests regarding behavior in incident and accident conditions have been carried out in an international context, over more than 25 years, in the CABRI and SCARABEE reactors, at Cadarache [4].

The behavior of fast-reactor oxide fuel contrasts with that of its PWR counterpart, owing to the harsher operating conditions. The fuel's high specific power (≈ 2 kW/cm$^3$, in Phénix), combined with the mixed oxide's low thermal conductivity, results in a centerline temperature, in the fuel pellets, that is often in excess of 2,000° C. Indeed, the initial microstructure undergoes a remarkable evolution (see Fig. 94), involving a "restructuring" of the fuel in its central region, this being due to fabrication porosity migrating to the center, and the "healing" of cracks, with the concomitant formation of columnar grains, and a central cavity. Such restructuring is accompanied by a major redistribution of plutonium concentration, with increased concentration in the central region.

A high fraction of the fission gases formed is released into the fuel pin's free volumes (released fractions may reach 90% of fission gas yield) (see Fig. 95), which is a major difference between PWR fuel, and FR fuel. However, as regards the latter, no attempt has ever been made to retain fission gases within the ceramic, and only the outer region of the pellet retains part of these gases. Such high fission gas release is not, in itself, an issue, as would be the case for PWR fuel, since this situation is taken into account from the dimensioning stage, with the presence in the pins of large plenums, to cater for gas expansion: the pin is 2.7 m long, for 1 m of fissile column length. At high burnups (> 8% **FIMA***), volatile fission products (FPs) (cesium [Cs], iodine [I], tellurium [Te]), or even metallic FPs (molybdenum [Mo]) are partially released outside

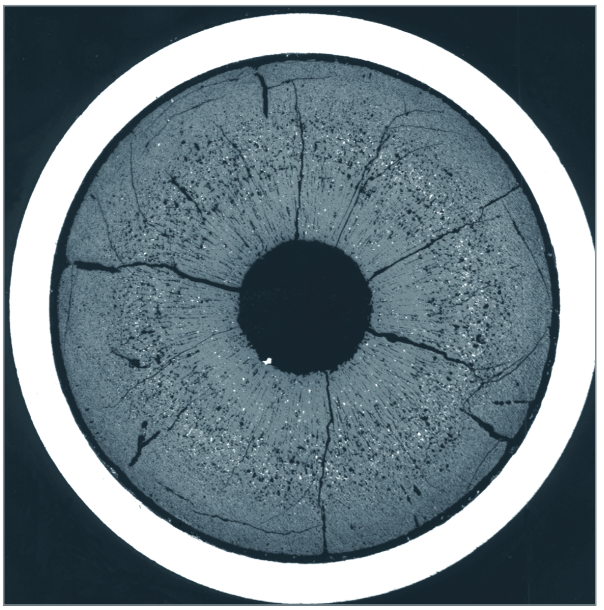

Fig. 94. Transverse metallographic section, at the maximum flux plane, of a Phénix fuel pin, showing the considerable restructuring undergone by the fuel. – Fuel: $(U_{0.8},Pu_{0.2})O_2$; cladding: 15–15 Tiε steel; max. burnup: 13.3% FIMA (125 GWd/tHM); max. dose: 115 dpa.

the fuel, ultimately forming a fuel–cladding bond, between the pellet rim and cladding.

Radial and axial migration [5] of some FPs (Te, I), combined with an increased fuel oxygen potential, this rising with burnup, results, in random fashion, in the onset of cladding internal corrosion, localized in the upper third of the fissile column (see Fig. 96).

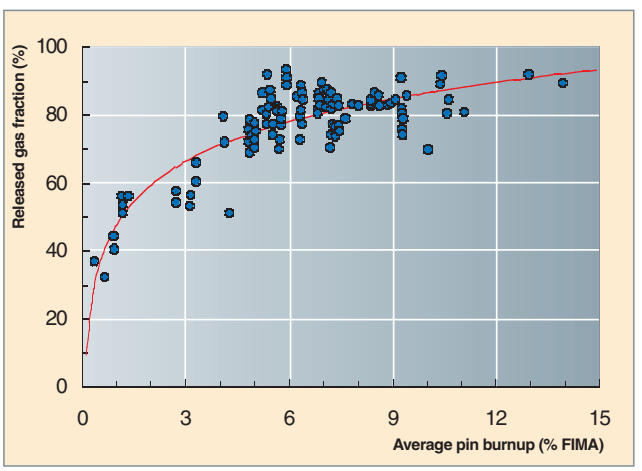


Fig. 95. Evolution, as a function of burnup, of the fission gas release rate in fuel pins taken from standard and experimental assemblies, irradiated in Phénix.

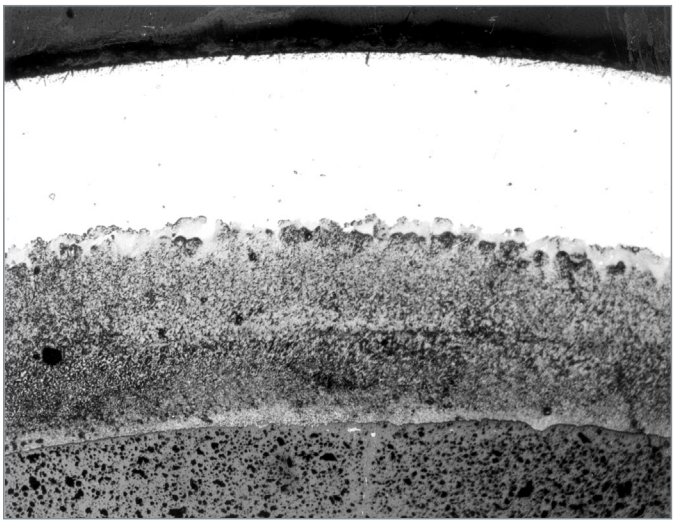

Fig. 96. An example of very extensive cladding internal corrosion (~ 40% initial thickness), in an experimental Phénix fuel element, featuring a 15–15 Tiε steel cladding, irradiated at high burnup (16.9% FIMA), corresponding to a dose of 155 dpa.

This phenomenon is seen as one of the limiting factors, as regards achieving high burnups (15% FIMA). Remedies such as the use of oxygen getters within the oxide, or the adoption of a protective coating for the inside surface of the cladding, may delay the onset of corrosion.

One further major drawback of oxide fuel is its incompatibility with sodium. However, numerous out-of-pile investigations, together with operational feedback from naturally-occurring cladding failures in the RAPSODIE and Phénix reactors, have made it possible to pin down the thermic, physical–chemical, and mechanical conditions making for the initial fault developing into an open cladding failure, and thus to suggest an adequate management mode, by the operator, for failing assemblies.

While the mixed oxide's satisfactory behavior has been proved up to very high burnups (> 15% FIMA), and during the various steps in the cycle (fabrication, storage, and reprocessing), its main drawbacks – to wit, a low heavy-atom density, and poor sodium compatibility – have led CEA teams to look to "advanced" fuels, such as metallic fuels, or carbide and nitride fuels [6].

The latter two fuel materials, refractory as they are, afford the benefits of a higher heavy-atom density, allowing a higher internal breeding gain (increased cycle duration, and larger Pu yield), and full sodium compatibility, thus avoiding unscheduled reactor outages, to discharge an assembly that has experienced a cladding failure [1].

These fuels further afford the advantage of exhibiting better thermal conductivity than the oxide, allowing lower operating temperatures, making it possible, if required, to increase operational linear power, while retaining significant margins with respect to the pellet centerline melting risk. However, these so-called "cool" fuels do exhibit swelling that is 2–3 times larger than with oxide; moreover, fission gas release, while remaining lower than with oxide, may nonetheless reach significant levels (> 50%) at high burnups (10% FIMA). The high swelling rate, combined with the lower viscoplasticity exhibited by these fuels (lower by a factor 10, compared to the oxide's), induces strong pellet–cladding mechanical interaction, once the as-fabricated gap has closed. The experience gained in this respect shows it is imperative to bring down, at the fabrication step, the packing density[2] of such fuels ($D_P < 75\% D_{Th}$), if it is intended to achieve, without incurring undue risks of cladding failure, the same burnup values as with oxide. Compared to the experience accumulated with oxide fuel, carbide, and – even more emphatically – nitride do leave, currently, many questions unanswered as to their actual potential, as fuels for sodium-cooled fast reactors. A new phase of examination, and experiment must be entered into, to evaluate not only the ability of these fuels to achieve high burnups in nominal conditions, but equally the possible advantages (or drawbacks) their behavior in accident conditions entails, together with all cycle issues associated with deployment of such fuels. In particular, do these fuels afford a better capability, or otherwise, as regards minor actinide recycling?

As regards metallic fuel, following disappointing initial attempts, in the 1950s and early 1960s, only the US teams at Argonne National Laboratory pursued a significant R&D effort, up to the early 1990s. Numerous investigations with alloy fuels enabled them to achieve, ultimately, using alloys of the U–Pu–Zr type, performance comparable to that for oxide fuel, in terms of burnup. Moreover, this experimentation was grounded on a substantial base of some 150,000 pins, irradiated in the EBR–II reactor. To be sure, this type of fuel also carries a number of drawbacks, the chief two being a risk of chemical reaction with the cladding, above 600° C (with possible formation of a eutectic), which dictates that the maximum allowable coolant temperature be brought down, in effect, in nominal operating conditions, with consequent lowering of reactor efficiency; and a cycle involving an electrochemical process, which has been deemed nonproliferating by US researchers when integrated on site – but that has yet to be demonstrated on an industrial scale (plutonium and minor actinide recycling, waste management)…

2. A fuel pin's packing density is equal to the ratio of fuel pellet cross-section, over cladding internal cross-section, multiplied by fuel density, expressed as a percentage of theoretical density.

## References


[1] H. Bailly, D. Menessier and C. Prunier, *The Nuclear Fuel of Pressurized Water Reactors and Fast Neutron Reactors: Design and Behaviour*, Lavoisier Publishing, Paris, 1999, Chapters III and VI.

[2] R. Lallement, H. Mikailoff, J.-P. Mustelier, J. Villeneuve, "Fast breeder reactor fuel design principles and performance", *Nuclear Energy* 28, 1, 1989.

[3] J.-L. Ratier, A. Chalony, G. Clottes, P. Chantoin, P. Courcon, "Behaviour of PHENIX standard fuel", *International Conference on Reliable Fuels for Liquid Metal Reactors*, Tucson Arizona (USA), 7–11 September 1986.

[4] I. Sato, F. Lemoine and D. Struwe, "Transient fuel behavior and failure condition in the CABRI-2 experiments", *Nuclear Technology* 145, 2004, pp. 115–137.

[5] M. Tourasse, M. Boidron, B. Pasquet, "Effect of clad strains on fission product chemistry in PHENIX pins at high burn-up", *International Symposium on Material Chemistry in Nuclear Environment (Material Chemistry '92)*, Tsukuba (Japan), 12–13 March 1992.

[6] J.-L. Faugère, M. Pelletier, J. Rousseau, Y. Guérin, K. Richter, G. Ledergerber,"The CEA Helium nitride fuel design", *ANP '92 – International Conference on Design and Safety of Advanced Nuclear Power Plants*, Tokyo (Japan), 25–29 October 1992.



**Michel Pelletier,**
*Fuel Research Department*

# Fast-neutron irradiation damage in structural materials

## Fast-neutron-induced damage in metals

As was emphasized in the foregoing chapter, achieving high **burnups*** entails an in-core dwell time of several years, in a fast reactor, thus subjecting assembly structural materials – fuel pin cladding tubes, and hexagonal assembly wrappers – to very large fast-neutron[3] **fluences*** (some $10^{27}$ n/m²).[4]

Such a very high flux, prevailing in the core of a sodium-cooled fast reactor [some $10^{19}$ n/(m² · s)], is the chief cause for the damage generated in claddings, and the hexagonal tubes (HTs) bundling together, and enclosing the pins of fuel assemblies [1].

Owing to the action of fast neutrons, nuclei are ejected from their equilibrium site, inducing by way of collisions the displacement of many further nuclei, thus causing a displacement cascade; this results in atoms being exchanged between sites in the crystal lattice, but equally in the formation of **point defects*** of the Frenkel pair type, comprising vacancies, and atoms in interstitial locations, in equal numbers. Moreover, certain elements have the ability to capture neutrons, giving rise to nuclear reactions. Thus, (n, $\alpha$) and (n, p) reactions lead to the formation, respectively, of helium, and hydrogen, which – whether by precipitating to form bubbles, or modifying the material's chemical composition – alter the material's properties in the course of irradiation.

The **Frenkel pairs*** generated do not remain in a stable state; instant, or delayed recombination processes arise. The material's inherent faults (dislocations, grain boundaries, porosity) play, in this respect, a major part; both interstitials and vacancies may be destroyed at these locations. The elimination of point defects at these "sinks" alters, over time, the material's microstructure: there occurs an evolution of dislocation networks, and migration of grain boundaries. At the same time, such point defects may come together, to form clusters: the coalescence of **interstitials*** yields **dislocation*** loops, whereas coalescence of **vacancies*** may either yield loops, or initiate a cavity. The latter process, of cavity nucleation and growth results in a cumulative increase in the material's volume, far greater than the saturation value due to individual, isolated defects.

Irradiation temperature has a decisive incidence on all of these processes. Low temperatures (< 0.3 $T_M$, where $T_M$ is the cladding melting point) favor a supersaturation of defects within the material, with saturation swelling not greater than 1%. Intermediate temperatures (0.4–0.5 $T_M$)[5] favor cavity nucleation and growth processes, and consequent swelling in the material. High temperatures (> 0.6 TM) result in permanent annealing of fast-neutron induced point defects.

This phenomenon of swelling in steels, through cavity nucleation and growth, was clearly evidenced by transmission electron microscopy observations, in 1967, of fuel element claddings from the DFR reactor (United Kingdom) [2]. Similar observations were made, virtually at the same time, in the United States (EBR–II), and in France (RAPSODIE). Owing to the impact of swelling, in terms of assembly lifetime, major R&D programs were then set in motion, to gain a better understanding of the mechanisms involved, and suggest solutions.

## What materials should be used?

At CEA, over the past 30 years, investigations have focused on three main families of materials, compatible with oxide fuel, and sodium: austenitic steels, based on the AISI 316 grade; nickel alloys of the Inconel family; and chromium–molybdenum ferritic–martensitic steels [3, 4].

The initial steel used in RAPSODIE, and subsequently for the first Phénix loading, for HTs and claddings, was 316 steel in hyperquenched state, allowing doses of about 50 **dpa*** to be reached. At such a dose, swelling is in excess of 10% in volume terms, which is incompatible with the functional criteria for the assembly. A remedy had to be found, regarding the metallurgical instability exhibited by austenitic steels in the 500–600° C range. The initial evolution involved work hardening of the tubes, before use, by 15–20%. The increased dislocation density achieved through this mechanical treatment favors elimination of point defects, resulting in a somewhat larger swelling incubation dose. Nevertheless, high-temperature (~ 600° C) swelling was a persistent issue. The presence

3. The fast neutron category covers neutrons with an energy higher than 0.1 MeV.

4. Codes drawn up on the basis of the binary collision model made it possible to arrive at a displacement effectiveness coefficient, taking into account lattice effects. Such computations are the basis for the most commonly used damage unit: the dpa (for steel: 1 dpa ≈ 2 · $10^{25}$ n/m²; E > 0.1 MeV). Depending on reactor neutron spectrum, this correspondence between dpa and neutron fluence varies.

5. I.e. 500–600° C for an austenitic stainless steel of the AISI 316 type.

of added elements, at low concentration (< 1%), alters point defect mobility, owing to the interaction, attractive or repulsive, arising between impurity and point defect. Of additional elements that proved beneficial, the option of titanium, combined with an optimized Ti/Si ratio, made its mark as the favored option, resulting in improved swelling resistance throughout the operating domain for claddings and HTs, while not inducing unacceptable embrittlement of the material. The "work-hardened 316 Ti" grade allowed doses of some 90–100 dpa to be achieved. However, for such good results to be achieved, the additional elements must retain all their effectiveness; to ensure this, these elements must be present in the form of a fine precipitation, which may only be obtained through thermomechanical treatments, properly controlled through all fabrication steps, from steelmaking to tube forming. Precise specifications had to be drawn up, to obtain a product that was reproducible on an industrial scale.

By further acting on the major additional elements in the steel grade (Ni, Cr), a switch was made to the "work-hardened 15–15 Ti" grade, featuring higher nickel, and lower chromium content than 316 steel, this becoming the French reference cladding material. Investigations carried out with this grade led to an optimized specification, for the European Fast Reactor (EFR) project, known as the "austenitic improved material", grade 1 (AIM1); this is currently used for the pins made in the final fabrication campaign for Phénix, and has the ability to sustain a maximum dose of 130 dpa. Figure 97 shows this evolution in swelling resistance exhibited by austenitic steel claddings for Phénix pins.

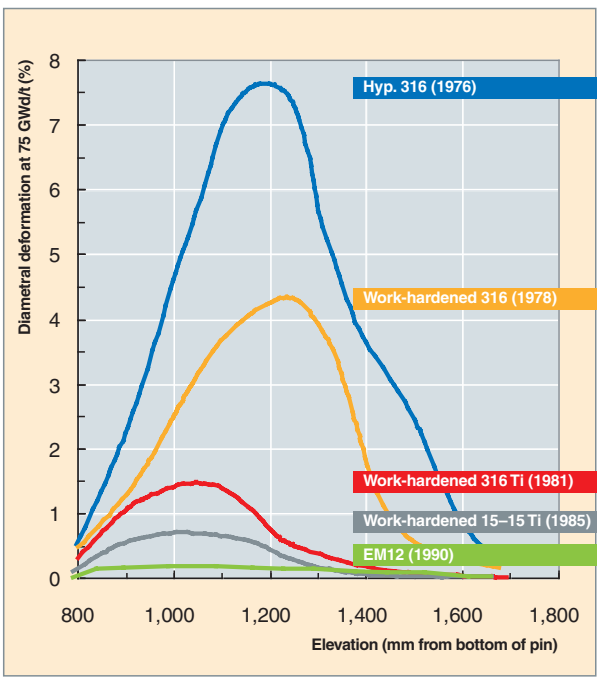


Fig. 97. Reductions achieved, at constant burnup, in maximum diametral deformation for fuel assembly claddings irradiated in Phénix, through metallurgical improvements in austenitic stainless steels. – Comparison with EM12 ferritic–martensitic steel.

The second class of materials is that of nickel alloys. Systematic irradiation tests, carried out in the 1960s, showed the major part played by nickel with respect to swelling resistance; CEA, as indeed its counterpart organizations in the United States and in the United Kingdom, thus investigated a number of alloys, including Inconel 706, and Nimonic PE16. While irradiations did confirm the low swelling exhibited by this family of alloys, at doses higher than 120 dpa, they also evidenced a marked tendency to embrittlement, in the irradiated state; the excessive brittleness arising in Inconel 706, through irradiation-induced h phase precipitation at the grain boundaries, was the cause of very extensive cladding failures in fuel pins subjected to pellet–cladding interaction, during ramping back to reactor nominal power; this state of affairs led CEA to terminate work on these materials, with only the United Kingdom persisting with optimized PE16 grades.

The body-centered cubic structure exhibited by the ferritic–martensitic class of steels endows them with high structural stability under irradiation, and good swelling resistance. However, their thermal creep resistance, poorer than that exhibited by austenitic steels, is hardly consonant with use as a cladding material, while proving suitable for HTs, for which operating temperature remains lower than 600° C. As expected, low swelling values (1–3%), depending on steel composition, and structural state, were found up to 150 dpa. EM10 (9Cr–1Mo) steel proved to be the grade exhibiting highest stability over the entire irradiation temperature domain, while EM12 steel (9Cr–2Mo–Nb–V), used for claddings, exhibited highest thermal creep resistance. Particular attention was given to the evolution, under irradiation, of the ductile–brittle transition temperature (DBTT) characterizing these ferritic materials. By contrast with the F17 (17% Cr) grade, for which DBTT rises to 250° C under irradiation, a temperature incompatible with conditions for assembly handling operations, the EM10 grade retains a DBTT lower than ambient temperature up to 100 dpa (see Fig. 98).

The weak point, for ferritic–martensitic steels, remains their high-temperature mechanical behavior. To allow their use as cladding material, at the very high doses (200 dpa) contemplated for fourth-generation fast reactors, the strengthening of their microstructure by way of a microdispersion of a hardening phase, such as oxide nanoprecipitates, has been addressed by investigations. Initial oxide-dispersion strengthened (ODS) alloy grades, based on a 13%-Cr ferritic steel containing titanium oxide or yttrium oxide nanoprecipitates, were irradiated in Phénix, in the form of fuel pin claddings, in the 1980s, in collaboration with Belgonucléaire. While examinations did confirm their satisfactory dimensional stability around 80 dpa, they also revealed unacceptable embrittlement, induced by precipitation of an embrittling phase. Nevertheless, investigations on ODSs of the martensitic (9% Cr) and ferritic

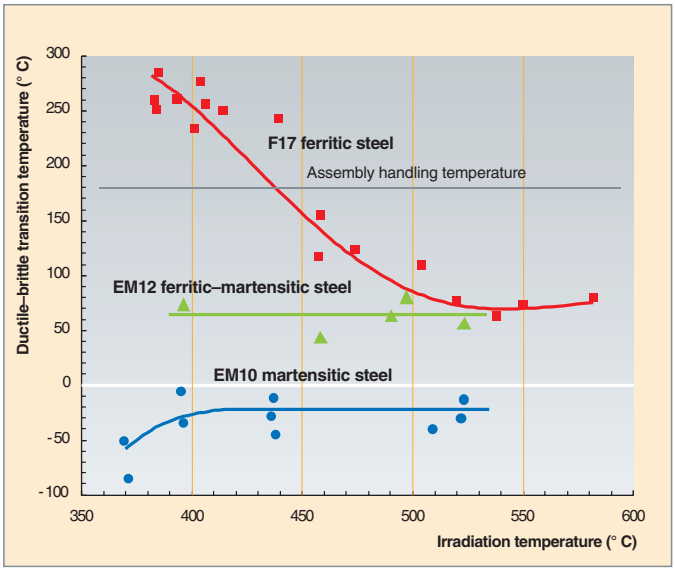


Fig. 98. Evolution of ductile–brittle transition temperature in ferritic–martensitic steels: F17, EM10, and EM12 grades, used as hexagonal tube (HT) material in fast-reactor assemblies.

(> 12% Cr) type are currently being carried forward at CEA, involving, in particular, a bilateral collaboration with Japan (JAEA), to arrive at, ultimately, a very-high-performance cladding material. However, development of these new ODSs will be a long-drawn-out effort, before a material suitable for industrial production is obtained.


Fig. 99. Evolution of the burnup performance of fuel assemblies, as a function of number of irradiation cycles in the Phénix reactor, as a result of the gradual move to structural (HT, cladding) materials exhibiting better irradiation swelling resistance.

To sum up, the constant improvements achieved with austenitic steels, along with the use of certain martensitic steels for HTs, account for the enhanced performance achieved, as regards assemblies, over the past 30 years of operation of the Phénix reactor (see Fig. 99), in terms of burnup, and dose.

Further, investigations on materials have gone hand in hand with an analysis of dimensioning rules for structural materials, in the hostile environment that is a fast-reactor core. The RAMSES II methodology [2], on the basis of the French RCC–MR standard, taking on board the specific characteristics found in irradiated materials (damage, embrittlement, rupture modes), had thus been put forward by CEA in a European context, for the erstwhile EFR sodium-cooled fast reactor project; it may be implemented for the purposes of dimensioning assemblies for the fourth-generation fast reactor prototype.

## References


[1] H. Bailly, D. Menessier and C. Prunier, *The Nuclear Fuel of Pressurized Water Reactors and Fast Neutron Reactors: Design and Behaviour*, Lavoisier Publishing, Paris, 1999, Chapter III.

[2] J. H. Kittel, B. R. T. Frost, J.-P. Mustelier, K. Q. Bagley, G. C. Crittenden and J. Van Dievoet, "History of fast reactor development", *Journal of Nuclear Materials* 204, 1993, 1–13.

[3] J.L. Seran *et al.*, "Behaviour under neutron irradiation of the 15/15 Ti and EM10 steels used as standard materials of the PHENIX fuel subassembly", ASTM STP 1125 (1992), *15th International Symposium on Effects of Radiation on Materials*, Nashville, Tennessee (USA), 17–21 June 1990.

[4] A. Maillard, M. Touron, J.-L. Seran, A. Chalony, "Swelling and irradiation creep of neutron irradiated 316 Ti and 15–15 Ti steels", ASTM STP 1175 (1993), *Effects of Radiation on Materials, 16th International Symposium*, Denver, Colorado (USA), 20–25 June 1992.

[5] RAMSES 2 Working Group, *Règles d'analyse mécanique des structures irradiées*, CEA Report CEA-R-5618.



**Michel Pelletier,**
*Fuel Research Department*

# Fuels and targets for fast-reactor transmutation

One of the directions for research, at CEA, regarding long-lived, high-level waste (chiefly minor actinides: neptunium, americium, and curium, together with some fission products, such as technetium) involves investigation of their transmutation, i.e. the transformation of such nuclides, when subjected to a neutron flux, into nonradioactive elements, or much shorter-lived nuclides.

The transmutation of a radionuclide by neutrons may be effected either by way of a fission reaction, or a neutron capture reaction. In the event of the nuclide's disappearance being due to fission, the atomic nucleus yields fission products, the greater part of which are short lived (half-life of less than 50 years). Should this be due to neutron capture, the nucleus turns into that of another radionuclide, which does not necessarily entail any significant reduction in medium- or long-term radiotoxicity. If transmutation is to be effective, the aim is therefore to favor fission reactions, rather than capture reactions.

## Fast reactors: reactors affording the ability to carry out effective actinide transmutation

The fast spectrum prevailing in fast reactors provides better conditions, as regards transmutation by fission, than the thermal spectrum in PWRs. The Table below sets out, for each radionuclide requiring transmutation, the average capture **cross-section*** $\sigma c$, and average fission cross-section $\sigma f$, together with the ratio a of these cross-sections, for three characteristic neutron spectra: a PWR spectrum, using UOX fuel; a PWR spectrum with MOX fuel; and a fast reactor (FR) spectrum with MOX fuel. The ratio $\sigma c/\sigma f$ is an indicator of the probabilities of disappearance through capture (cross-section $\sigma c$), rather than fission ($\sigma f$), at the first neutron interaction. It will be seen that this is brought down, by a factor 5 at least for most radionuclides, when a switch is made from a PWR neutron spectrum (whether thermal, or epithermal) to an FR spectrum.

## Recycling: homogeneous, or heterogeneous?

A variety of fast-reactor transmutation methods are currently being investigated. As regards minor actinides, two transmutation modes are available, each involving its own benefits, and drawbacks. The first one involves diluting minor actinides in standard fast-reactor fuel. Transmutation occurs within the fuel: this is the homogeneous mode. Advantage is then taken of the strong similarity, in crystallographic terms, found between the various actinide oxides (fluorite-type cubic structure), along with their mutual solubility. To minimize the impact of such an introduction of minor actinides on fast-reactor safety parameters, fuel minor actinide content is kept relatively low (less than 5% of heavy atoms). In such conditions, no significant evolution in fuel performance is anticipated, thermomechanical properties remaining quite close to those of standard fuel. The SUPERFACT irradiation experiment, carried out in Phénix [1], provides a good demonstration of this (see Fig. 100). The impact, however, is much higher as regards fuel fabrication plants. The powerful neutron emission, and high thermal power from americium, and, more crucially, from curium, generate additional constraints, in terms of workforce exposure, **criticality***, or new, heat release-related risks. The fabrication process must be so devised as to take place in shielded cells, using remote handling, entailing that processes be redesigned (for compactness of facilities; process robustness, and simplicity; integrated waste and scrap management), to make

**Cross-sections (expressed in barns*) for radionuclides requiring transmutation**

| Isotope | Slow-neutron reactor (PWR–UOX) | | | **Epithermal*-neutron reactor (PWR–MOX)** | | | Fast-neutron reactor (FR) | | |
|---|---|---|---|---|---|---|---|---|---|
| | $\sigma f$ | $\sigma c$ | $\alpha = \sigma c / \sigma f$ | $\sigma f$ | $\sigma c$ | $\alpha = \sigma c / \sigma f$ | $\sigma f$ | $\sigma c$ | $\alpha = \sigma c / \sigma f$ |
| **Np 237** | 0.52 | 33 | 63 | 0.6 | 18 | 30 | 0.32 | 1.7 | 5.3 |
| **Am 241** | 1.1 | 110 | 100 | 0.8 | 35.6 | 44.5 | 0.27 | 2.0 | 7.4 |
| **Am 243** | 0.44 | 49 | 111 | 0.5 | 31.7 | 63.4 | 0.21 | 1.8 | 8.6 |
| **Cm 244** | 1.0 | 16 | 16 | 1 | 13.1 | 13.1 | 0.42 | 0.6 | 1.4 |
| **Cm 245** | 116 | 17 | 0.15 | 33.9 | 5.4 | 0.2 | 5.1 | 0.9 | 0.18 |
| **Tc 99** | - | 9 | - | - | - | - | - | 0.5 | - |

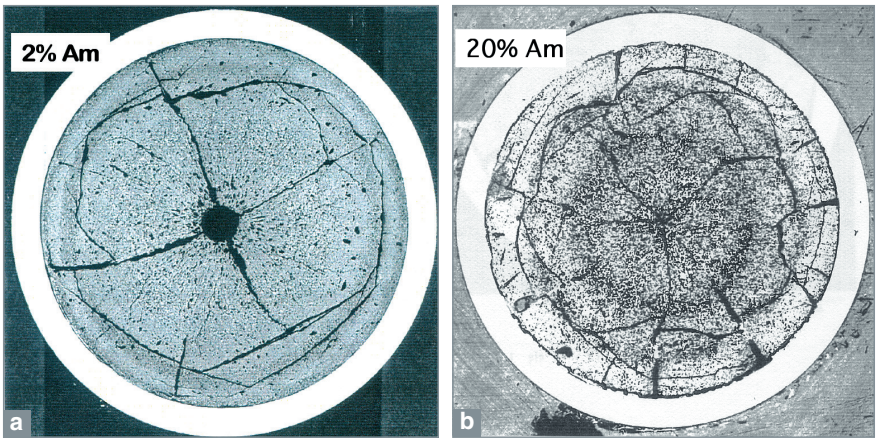


Fig. 100. Fuel from the SUPERFACT experiment, subsequent to irradiation. The fuel containing 2% americium (at left) has undergone restructuring, typical of a standard fast-reactor fuel, whereas the fuel containing 20% americium (at right) exhibits major swelling, related to the formation of a large number of helium bubbles, yielded by alpha decay of curium 242, itself generated by neutron capture in americium 241.

them suitable for more demanding, and complex handling and maintenance requirements, and minimize the resulting additional cost, in economic terms.

The second method, known as heterogeneous recycling, involves, by contrast, partitioning off minor actinide management from uranium and plutonium management. Standard fuel, and, by way of consequence, fuel fabrication plants remain uninvolved in minor actinide management. The latter nuclides are concentrated, inside the reactor core, in specific assemblies, known as "targets," which are fabricated, and/or even reprocessed in dedicated plants. The in-plant heavy metal (actinide) stream is thus restricted to the sole minor actinide streams, allowing more compact plants to be designed, better suited to the technological issues relating to the handling of americium, and curium. On the other hand, a large R&D effort is required, for the design of these new objects, and to ensure their qualification, to the same level as standard fuel.

Investigations carried out in France on long-lived, high-level waste management have given pride of place to composite targets [2]. Minor actinides, still in oxide form, this being the most stable, most easily handled form, are blended into a matrix that is inert, in neutronic terms, pressed into shape, and sintered in pellet form (see Fig. 101), as with standard fuel. Optimization of the composite is a protracted step, calling for material fabrication and compatibility tests, measurement of properties, and in-reactor tests in order to control, and gain a better understanding of, irradiation behavior. To keep to phenomena that have a significant impact on target dimensioning, and performance, the following may be noted:

1. A high production of helium, yielded by alpha decay of curium 242, which may cause strong swelling, if it remains occluded within the material, or additional pressure in the **plenum***, if released;

2. Damage to the matrix, due to fast neutrons, the recoil of fission fragments, and alpha particles yielded by nuclear decay reactions, with a resulting alteration in target material properties, in particular a marked degradation of thermal properties;

3. Pellet–cladding chemical interaction;

4. Pellet–cladding mechanical interaction.

After exploring a wide range of materials, as potential candidates for the inert matrix, such as nitrides (ZrN, TiN), or refractory metals (Mo, Cr), the options currently being looked to, as regard inert matrices, are oxide materials, exhibiting a cubic structure, such as spinel, magnesia, yttrium–aluminum garnet (YAG), or yttrium-stabilized zirconia, these exhibiting, as a whole, satisfactory thermomechanical and chemical properties, and acceptable behavior under irradiation. As regards actinide compounds, in turn, a switch is being made to complex, cubic solid solutions, such as $(An,Zr,Y)O_{2-x}$, or $Am_2ZrO_7$, potentially exhibiting better stability under irradiation, and a lower corrosion potential than simple dioxides, exhibiting a fluorite structure. Finally, a "macromass"-type composite microstructure, whereby minor actinide compounds are distributed in homogeneous fashion across the inert matrix, in the form of microspheres of 100 microns or so, allows matrix irra-

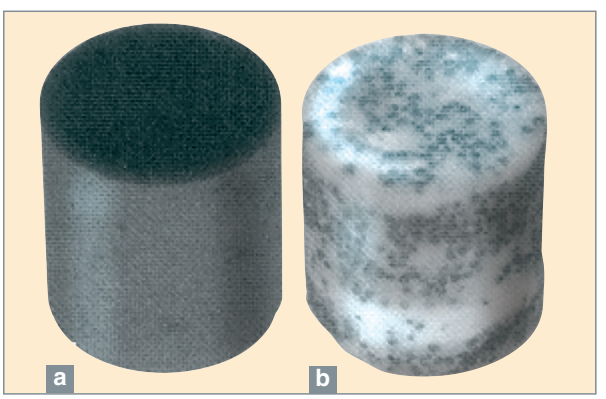


Fig. 101. Standard fuel pellet (a), and composite fuel pellet (b) used for transmutation purposes. The composite fuel, in this instance, comprises an inert spinel matrix (white), and macromasses of actinide oxide compound (black).

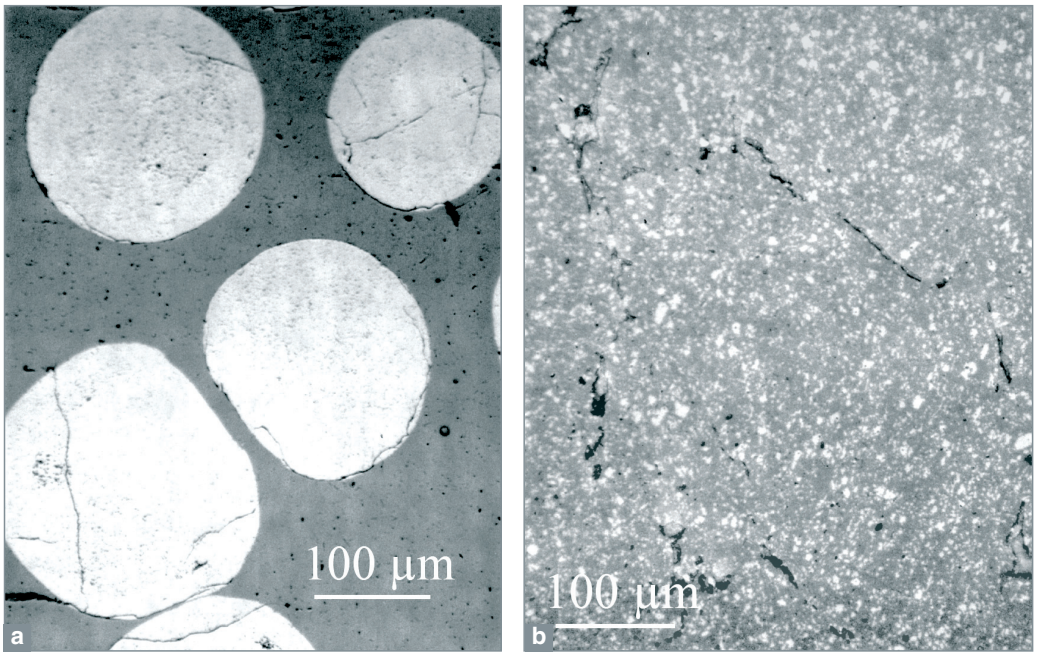


Fig. 102. Comparison of the microstructures of a "macromass" composite fuel (a), and "microdispersed" composite fuel (b). The macromass composite's inert matrix (gray) undergoes less fission fragment-related damage. The damage region is localized over 10 microns or so only, around the microspheres, whereas it covers the entire matrix in the microdispersed composite.

diation damage to be restricted to few microns around the microspheres (see Fig. 102).

Irradiation behavior of these various matrix materials was initially addressed by investigations involving ion, and neutron irradiations. In-reactor behavior of these targets was subsequently investigated by means of a number of experimental irradiations in Phénix, or in thermal-spectrum experimental reactors, allowing the main in-pile phenomena arising in such targets to be identified, and observed, in particular fission product and helium behavior, and the interactions between actinide compound, and inert matrix, depending on the materials used, amounts of actinides contained in the material, range of operating temperature undergone by the material, and targeted incineration, or transmutation rate.

This program is currently ongoing; it is anticipated these optimized structures will exhibit good dimensional stability, even over long irradiation times, which would allow high transmutation rates – higher than 90–95% – to be contemplated. In such conditions, final disposal of incinerated targets, directly after discharge from the reactor, could be envisaged, obviating the need to multirecycle them. Target cycle would thereby be greatly simplified.

Under the aegis of the recent French Act of 26 June 2006 on nuclear waste, research work is presently being directed to the homogeneous recycling of minor actinides, to be carried out in future gas- or sodium-cooled fast reactors, using however a driver fuel which, depending on reactor type, could be an actinide oxide, or a carbide, or nitride, the latter two forms exhibiting a higher heavy-atom density than standard MOX fuel.

Concurrently, novel targets, involving a uranium oxide carrier, rather than an inert matrix, are also being investigated. Such targets, positioned in the reactor's fertile blanket, would allow both actinide transmutation, and good control of core physics, while curbing proliferation risks.

## References

[1] J.-F. Babelot and N. Chauvin, "Joint CEA/ITU synthesis report of the experiment SUPERFACT 1", Transuranium Elements Technical Note JRC–ITU–TN-99/03, 1999.

[2] CEA, *Les Déchets radioactifs à haute activité et à vie longue – Recherche et résultats: Axe 1 – Séparation et transmutation des radionucléides à vie longue* (Final report, December 2005; published in March 2006 by DEN/DDIN/DPRGD).

**Sylvie Pillon,**
*Fuel Research Department*

# Particle fuel

The particle fuel concept goes back to the late 1950s. The idea then was, for thermal-neutron reactors – concurrently with studies being carried out on reactors of the natural uranium–graphite–gas (UNGG) line, in France, or the Magnox reactor line, in the United Kingdom – to investigate a form of fuel consisting of uranium finely dispersed in a graphite conducting matrix, for the purposes, in particular, of improving exchanges between gas coolant, and fuel. The concept then underwent evolution, to cater for reactor systems involving a hotter gas coolant.

## From the initial concept to the advanced TRISO particle concept

Dispersed-particle fuel concepts, and the associated fabrication processes subsequently underwent considerable evolution, depending on reactor projects. The next major innovation was to coat the millimeter-size fissile, or fertile material particles with two layers of carbon, obtained through pyrolysis from a carbon-compound precursor at high temperature: the first, porous layer having the purpose of providing a **plenum***, to accommodate fission gases, while the second, dense layer was there to ensure confinement of the fuel particle (BISO particle: see Fig. 103).

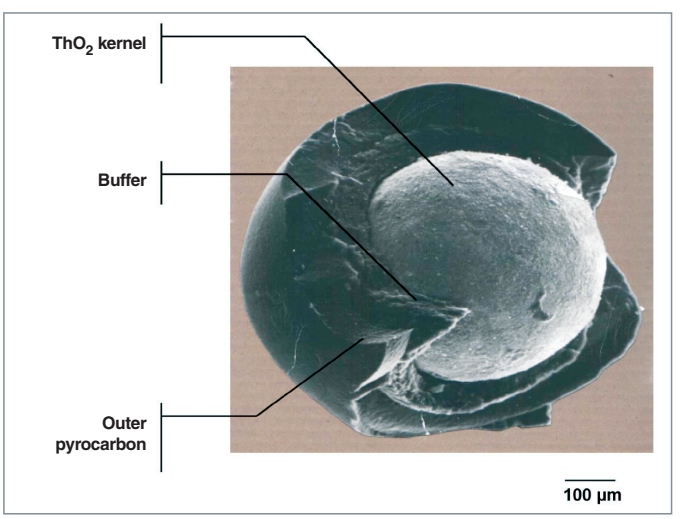


Fig. 103. Fractograph of a $ThO_2$ BISO particle.

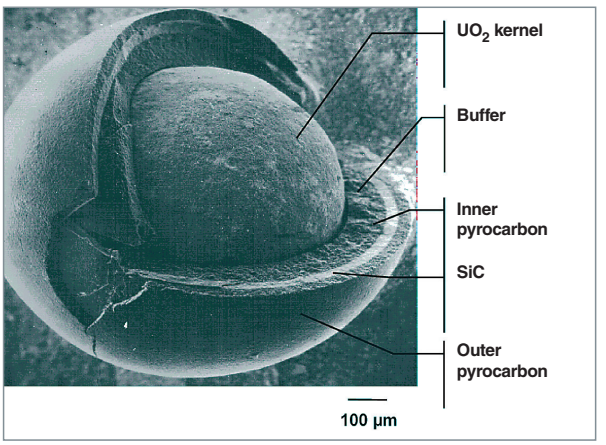


Fig. 104. Fractograph of a $UO_2$–TRISO–SiC particle.

With a view to enhance the imperviousness of particles holding fissile material, the TRISO particle concept was then developed. This particle comprises three isotropic pyrocarbon layers (hence the name "TRISO particle"), two of these forming a sandwich on either side of a ceramic material, making it possible to ensure enhanced particle leaktightness. The material chosen at the time, and subsequently proven in service, is silicon carbide (SiC): the HTR–TRISO–SiC particle was born (see Fig. 104). In terms of in-reactor behavior, as described elsewhere in this Monograph (see the chapter on "Irradiation behavior of particle fuels", *infra*, p. 109), the TRISO particle – the outcome of many years of research – stands as a brilliant invention, since, in particular:

- the dispersed fuel concept, combined with control of the **moderation ratio***, allows good control of the neutron spectrum (and of **self-shielding*** effects);
- the large specific surface area exhibited by the fissile isotope-bearing particles makes for good heat exchange with the graphite matrix, and subsequently with the coolant helium;
- the wholly refractory fuel allows high-temperature operation, a favorable condition in terms of energy conversion efficiency, further allowing a possible loss of coolant fluid to be ridden out;
- the particles' spherical shape endows the coating layers with high mechanical strength, allowing high burnups to be achieved.

| Characteristics of German reference particles (taken from [1]) | | | | |
|---|---|---|---|---|
| $UO_2$ kernel | Porous PyC (buffer) | Dense inner PyC | SiC | Dense outer PyC |
| Diameter 500 µm | 95 µm | 40 µm | 35 µm | 35 µm |
| 10.9 g/cm³ | 1.0 g/cm³ | 1.9 g/cm³ | 3.20 g/cm³ | 3.20 g/cm³ |
| Dmax/Dmin = 1.07 | | BAF = 1.06 | | BAF = 1.02 |
| Defective particle fraction: 1.5 $10^{-6}$ | | | | |

## Kernel fabrication processes

Fissile, or fertile fuel kernel fabrication processes have seen substantial evolution since the early days, depending on projects, and the knowledge gained as to fabrication processes. The process initially used, in the context of the Peach Bottom reactor program, for $UC_2$-, $ThC_2$-, or $(Th,U)C_2$-type kernels, was high-temperature (higher than 2,500° C) vacuum melting of a mixture of carbon and uranium and/or thorium carbide powders, to yield $UC_2$, $ThC_2$, or $(Th,U)C_2$ dicarbide [2]. This process was subsequently transferred to France, in the late 1970s, under the aegis of France's participation in the Dragon project, and implemented by Société française des éléments catalytiques (SFEC), at Bollène. This allowed high-quality kernels to be obtained, particularly as regards large kernels (larger than about 800 microns), and useful results to be achieved, in the context of a porous-kernel concept [3]. The process was used by CEA for the fabrication of thorium kernels, until work was terminated in this area, in the early 1980s. Subsequently, owing to German developments, and the better-quality kernels thus obtained, processes of the sol–gel type superseded the others [4], after researchers from the Italian SNAM Corporation put forward a pseudo-sol–gel process, known as the gel-supported precipitation (GSP) process. This process brought about a revolution as regards work in this area, being taken up by many research organizations, and manufacturers [4]. General Atomics (GA) used it for the fabrication of $ThO_2$ kernels for the Fort St Vrain (FSV) reactor. German teams, at NUKEM and FZJ, developed a variant of their own for AVR, and subsequently THTR reactor fuel, and further for the purposes of $UO_2$–TRISO–SiC particle development [1]. Currently, this stands as the reference $UO_2$ kernel fabrication process.

The process principle, as set out in Figure 105, involves first of all preparing a pseudo-sol (also known as a "broth") from an initial nitrate solution of the actinide involved (uranium, thorium, or plutonium). This broth is obtained through addition of a number of additives, as determined by process know-how, including a soluble organic polymer, which subsequently gels as droplets are dispersed, acting as a substrate for actinide precipitation. The formation of spherical beads is then achieved by the dispersion of calibrated droplets in a gas atmosphere containing ammonia, which induces gelation of the polymer, and precipitation of the actinide at the surface of the droplet. Such external gelation (as the process is sometimes called) allows the droplet's spherical shape to be maintained, the microspheres then dropping into an ammonium hydroxide solution, to complete gelation within the sphere. The gelled microspheres are kept some time in ammonium hydroxide to allow aging, being subsequently washed, and dried, chiefly in order to remove ammonium nitrate, and water. Further heat treatments, involving calcination, reduction, and densification, allow the microspheres to be turned into kernels of the actinide of interest.

As an alternative to the GSP process, another process may be considered, for kernel fabrication purposes; this is the HMTA or internal gelation process. The principle of this process does not involve effecting the gelation–precipitation operation by means of ammonia diffusing from the outside into the sphere's interior, rather it involves use of an internal precursor, hexamethylenetetramine (HMTA), which yields ammonia as temperature rises from 0° C to about 80° C. This process has not given rise to any industrial development, however it has been deployed on a pilot scale. It is used, in partic-

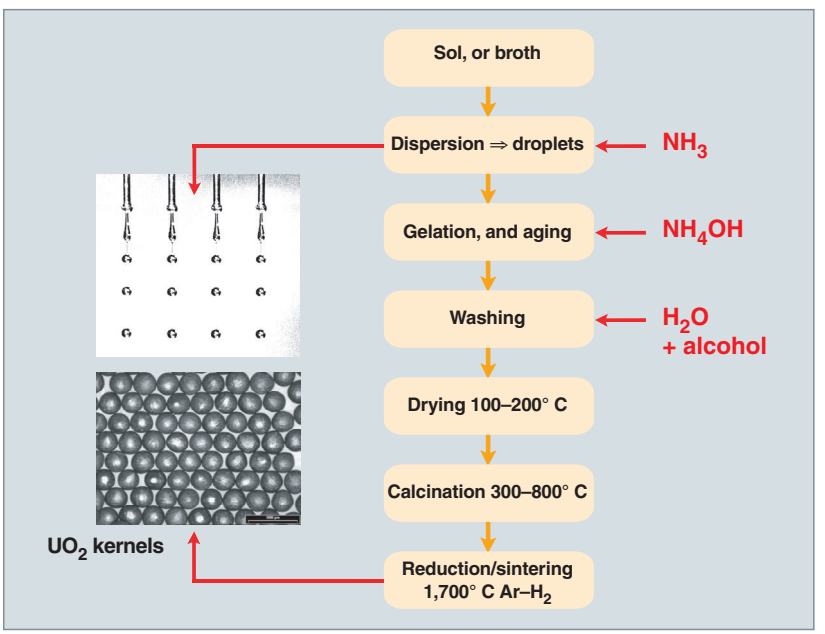


Fig. 105. Principle schematic of the GSP sol–gel process.

ular, at ORNL, in the United States, for the fabrication of UCO kernels. The respective advantages, and drawbacks of both processes have long been debated, since the 1970s [4]. It may simply be stated that both processes would appear to allow kernels of similar quality to be obtained, for diameters in the ca. 200–600 µm bracket, and that choice of process rather involves process implementation, and deployment criteria, relating in particular to precursor preparation, and management of the effluents generated.

## Particle coating by chemical vapor deposition

The principle of fluidized-bed chemical vapor deposition (CVD), through decomposition of a gaseous precursor, soon gained widespread currency (see Fig. 106), even though some preliminary studies for the Dragon project had contemplated other processes. This type of process allows the desired material quality, and deposit homogeneity to be obtained, in particular by way of the agitation of particles, and homogeneization of transfers within the fluidized bed. For pyrocarbon deposition, the precursors initially used were alkanes (methane, ethane, propane…), however, owing to the high temperatures required to effect cracking of such substances (about 1,900° C), investigations subsequently turned to alkene, or alkyne decomposition. The reference process, as currently used, involves cracking acetylene ($C_2H_2$), for the buffer, and propylene ($C_3H_6$) to obtain the dense pyrocarbons (both outer and inner layers). Decomposition reactions are carried out in a temperature domain ranging from about 1,200° C to 1,400° C, with an average deposition rate of the order of 10 µm/min (≤ 50 µm/min) for the buffer, and several µm/min (≤ 5 µm/min) for the dense pyrocarbons. The difference in deposition rates is accounted for by the properties being sought for each layer: for the buffer, the aim is to obtain a layer serving to accommodate gases, exhibiting low density, which may be deposited at high rate; whereas, for the other pyrocarbons, the aim is to obtain a dense, isotropic layer, exhibiting good mechanical strength, requiring slower deposition. For SiC deposition, methyltrichlorosilane (MTS: $CH_3SiCl_3$), a byproduct of the silicone industry, and a widely used precursor for SiC deposition, soon made its mark. Mere thermal decomposition of MTS is unable to yield pure SiC. This is obtained in stoichiometric b-SiC cubic form, by adding free carbon to MTS, in a hydrogen atmosphere. $H_2$ content must be adjusted, to preclude formation of silicon [5]. Average deposition conditions are as follows: an MTS/$H_2$ ratio of 1–5% molar, temperature of around 1,600° C, and deposition rate ≤ 1 µm/min.

A variety of technologies, and furnace sizes have been used, e.g.: conical-bottom, or porous-plate furnace; a central injector, or multiple injection; resistance, or induction heating; batch, or continuous operation; furnaces featuring crucibles of 2″ (≈ 50 mm), 3″ (≈ 75 mm), 5″ (≈ 130 mm), 240 mm, and 400 mm inner diameter [1, 3, 5]. 2″ and 3″ furnaces are generally used for laboratory facilities (< 1 kg U), while 130–400-mm furnaces have been used in pilot, or industrial facilities. However, furnace size and operating mode are also dependent on the characteristics being sought, with respect to the particles. For small kernels (≤ 300 µm), continuous operation is extremely problematical, or even impossible (owing to the thickness of the layers involved). Indeed, in the latter case, fluidized bed volume expansion is quite considerable, which dictates a reduction in the number of particles, for the final deposits. By way of example, for 300-µm kernels, on which it is desired to deposit the following layers: buffer 95 µm, PyC 40 µm (for both inner and outer layers), and SiC 35 µm, volume expansion involves a factor 13, approximately, corresponding to a final bed height of some 1.30 m, for an initial height of 10 cm!

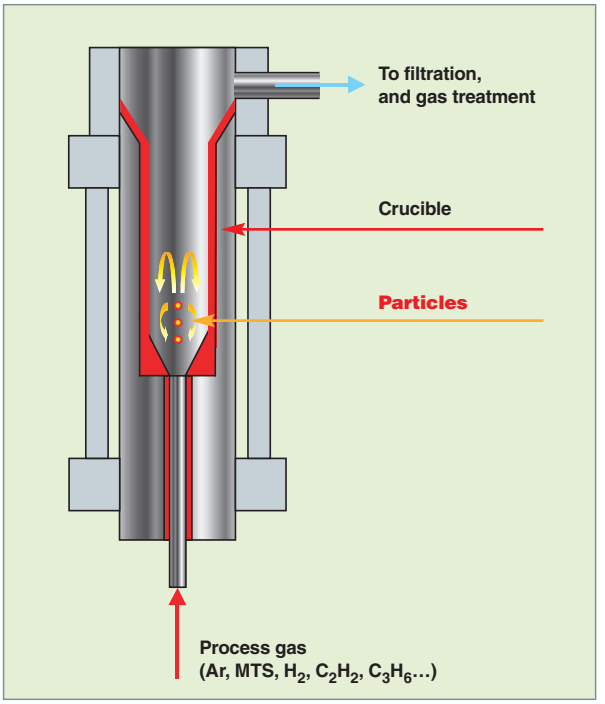

Fig. 106. Principle schematic of a CVD furnace.

## Fuel element fabrication: particle compaction

Fuel element fabrication involves the dispersion of fuel particles in a graphite matrix. This matrix is either cylindrical, in the US "prismatic block, and compact" concept, or spherical, in the German "pebble" concept. Compacts are about 50 mm high, for a diameter of 10 mm or so. A compact contains some 7,000 particles. German pebbles have a diameter of about 60 mm. The pebble comprises an outer shell, about 5 mm thick, containing no particles, and an inner region, containing some 12,000 particles. In either case, the purpose of the process is to obtain a homogeneous distribution of fuel particles across the graphite matrix, while avoiding damage to particles during fabrication, or subsequent handling operations. A number of

processes have been investigated, and used. The two reference processes are: hot injection molding, used in particular by US manufacturers for the FSV fuel; and hot pressing, used in particular by the Germans for the fabrication of AVR and THTR pebbles, and by French teams at CEA, and at the CERCA Company, for the fabrication of fuel elements, in the context of collaborations with the Dragon project, and GA in the 1970s [3, 5]. The difference between the two processes has to do chiefly with the fabrication method for "green" fuel elements, prior to the hardening and carbonization heat treatments. The green fuel element comprises fuel particles, mixed with graphite powder, and forming additives. In the injection process, the green element is obtained by injection at 150–200° C, in an appropriate mold. In the pressing process, the green element is obtained by pressing the constituents, as mixed, at a temperature of around 100–150° C. As regards these processes, a number of variants are used, depending on the type of object fabricated (cylindrical compact, or pebble[6]), but equally depending on the mixture preparation protocol implemented (e.g., overcoating fuel particles with graphite, prior to mixing, to obtain the green fuel element). The scheme set out in Figure 107 gives an overview of the various steps involved in the compaction processes.

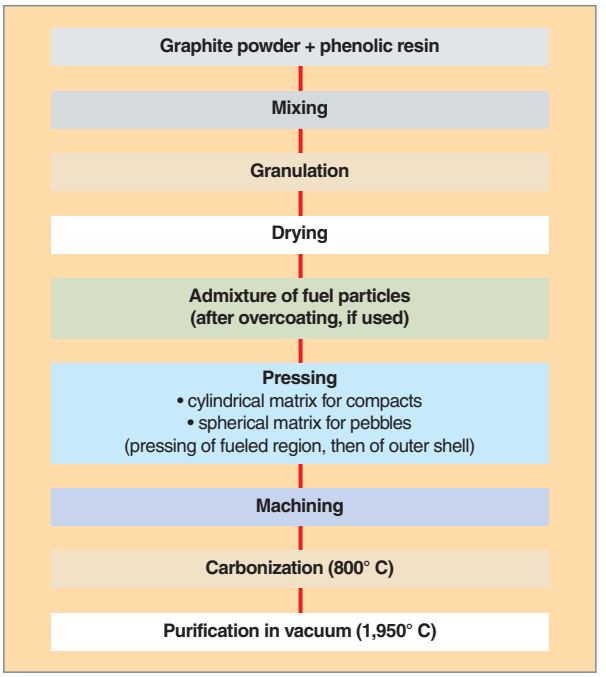


Fig. 107. Principle schematic of compaction (taken from [6]).

## Characterization of fuel particles, and elements

Fuel particle, and fuel element (compact, or pebble) characterization stands as a major component in the HTR fuel industrial fabrication process, particularly in terms of costs [6]. This is accounted for by the form the fuel takes, entailing that a large number of small objects (millimeter-size particles) be characterized; and by the type of techniques used in the 1970s, often requiring extensive manpower.

Currently, one of the challenges involved in industrial development of this type of fuel is to implement more automated methods, allowing the fast characterization of a representative number of fuel particles, and elements (compacts, or pebbles).

As regards current developments, which as a whole are at the laboratory, or pilot stage, the techniques used – still of the destructive type – include, in particular, the following [7, 8, 9]:

- automated direct-observation optical analysis, for kernel (and possibly particle) diameter, and sphericity characterization;
- automated optical analysis of metallographic sections, to measure layer thicknesses;
- optical photometric reflectance analysis, to estimate dense pyrocarbon (both inner and outer layers) isotropy;
- use of a flotation column, to measure the density of pyrocarbon and SiC layers, together with investigations to find an alternative, nondestructive method, more amenable to automation;
- the "burn-leach" test[7] method, to estimate the proportion of defective SiC layers, together with investigations to find an alternative, nondestructive method, more amenable to automation.

## From HTR fuel to VHTR and GFR fuels: the GAIA facility at CEA/Cadarache

In order to recover its expertise, with respect to HTR particle fabrication technology, and investigate fabrication of VHTR- and GFR-type fuels, CEA, in partnership with Areva, is developing, at CEA/Cadarache, a facility going under the name GAIA, for coated particle investigations, and particle fabrication [9].

The approach involved in the investigations using the GAIA facility pursues a number of directions:

6. As regards pebbles, and compacts, pressing methods differ, owing to the objects' geometry. Moreover, for pebbles, owing to the outer shell, pressing is effected in two steps: pressing of the central region, containing the particles, followed by pressing of the outer shell.

7. The "burn-leach" method involves thermal oxidation of fuel particles, or elements, followed by acid leaching, to dissolve the actinide; actinide content is then dosed, allowing the defective particle fraction to be determined.

- recovery of CEA's past know-how, in particular by way of reconfiguring the CVD furnaces at CEA/Grenoble – inherited from the collaborations with the Dragon project, and General Atomics (GA), in the 1960s and 1970s – for the purposes of particle coating;

- investigation of the elementary processes involved in fabrication processes, to identify the key steps, and decisive parameters;

- construction of a multipurpose R&D facility, known as GAIA, allowing the fabrication, and characterization of reference $UO_2$–TRISO–SiC particles, but equally of more innovative particles, for VHTR and GFR applications.

By way of example, the innovative particles being considered could include TRISO–ZrC particles (ZrC, exhibiting a higher melting point than SiC as it does, is thus a more favorable option, with respect to VHTR applications), or uranium carbide-, or nitride-based particles (closer to the concepts currently being considered for GFRs).

The refurbishment of the CVD furnaces at CEA/Grenoble, i.e. of the 3″ furnace coming from the Dragon project, and the 5″ furnace from the GA collaboration, has allowed mastery of TRISO–SiC particle fabrication to be regained (see Fig. 108). Owing to the shutdown of the facilities allowing use of uranium at CEA/Grenoble, these investigations have been carried out with yttrium-stabilized zirconia (Y–$ZrO_2$) kernels, simulating $UO_2$ kernels. They have allowed the specification of the planned GAIA facility, and will contribute to its startup. Concurrently, modeling work, along with work on identifying elementary processes, is being undertaken, in collaboration with academic laboratories, to gain an understanding of transfer processes in CVD furnaces, and deposition mechanisms for the various layers. These investigations, for the purposes of understanding, and modeling, are coupled to finescale materials characterization, to gain the ability to identify the relationships between fabrication processes, and end-use properties for the material fabricated.

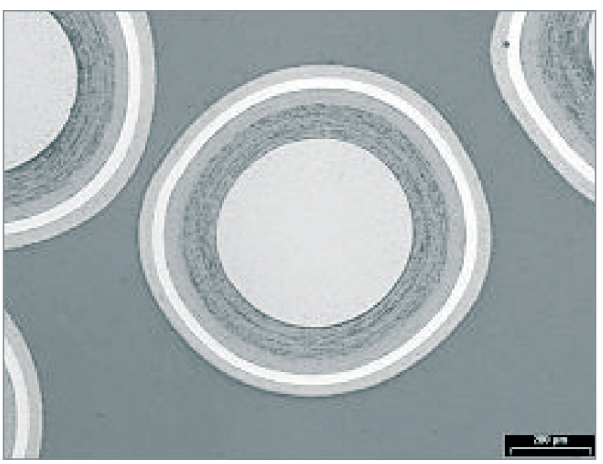

Fig. 108. Polished sections of TRISO particles.

As regards kernel fabrication, the reference, sol–gel-type GSP process was selected for the GAIA facility. The main grounds for that choice are, chiefly, more extensive industrial operational feedback (this being the German $UO_2$ kernel fabrication process), the extant knowledge, at CEA, with regard to this type of process, and the identification of outlets for the effluents yielded by the process. Owing to the process's modularity, if required, investigation of the alternative internal gelation process may also be contemplated. The work to achieve mastery of this process began with the drawing together of past knowledge (whether from within, or outside CEA), to draw on it, followed by the carrying out of tests involving small amounts of uranium-bearing material. These tests, carried out for each of the steps in the process, allowed the fabrication, at the end of 2003, of initial $UO_2$ kernels meeting the desired specifications. Nevertheless, investigations are ongoing, to achieve a better understanding of fabrication processes, and thus specify an optimum operating domain, allowing the desired material to be obtained, in reproducible fashion, with a good efficiency, with a view to future transposition to the GAIA facility.

As regards particle coating, the GAIA facility's general characteristics include, in particular, use of a 3″-type furnace, so dimensioned as to have the ability to accommodate a variety of crucibles, of 2–3″ inner diameter. Such dimensioning will allow fabrication of 50–500-g U, or even 1-kg U, batches, depending on the kernel diameters involved. The sol–gel facility is likewise dimensioned to fabricate batches of this type. Furnace loading, and unloading are planned to be carried out in glovebox, inert atmosphere (argon, or nitrogen) conditions, so that products such as carbide, or nitride kernels may be handled while shielded from the ambient, moist atmosphere (see Fig. 109). The furnace is also designed to accommodate a device catering for use of a ZrC precursor.

Concurrently, kernel and particle characterization methods are undergoing development – either by taking a cue from methods used in the past, suitably updated, or through assessment of new techniques.

As regards compaction, investigations are being carried out in partnership with the CERCA Company, who are going ahead with construction, and deployment of a compaction facility. Together, the GAIA platform, and the CERCA compaction facility will make it possible, ultimately, to achieve mastery of VHTR fuel fabrication, and to gain an understanding of the key associated processes.

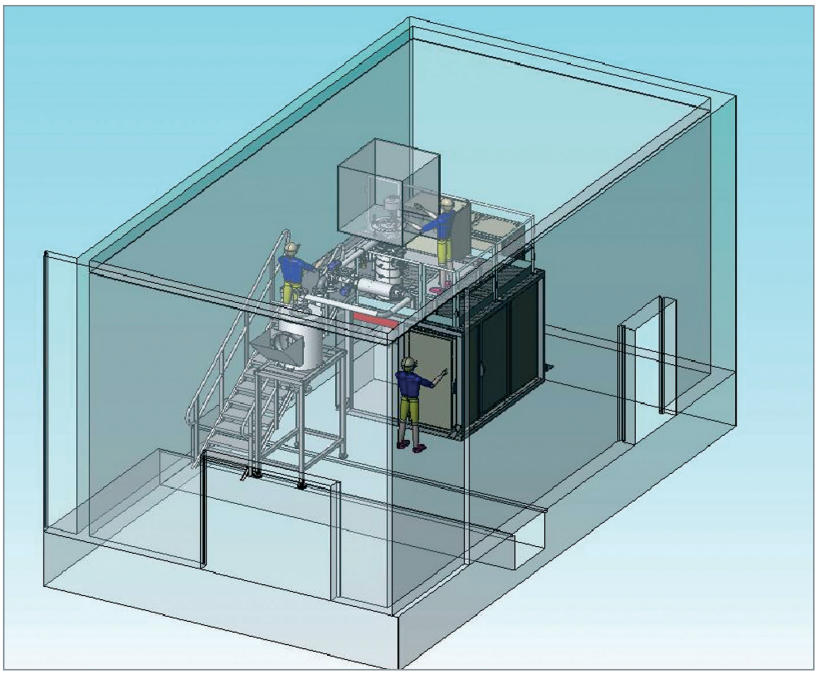

Fig. 109. GAIA facility CVD furnace unit.

## References


[1] W. Heit, H. Huschka *et al.,* "Status of qualification of high-temperature reactor fuel element spheres", *Nuclear Technology* 69, April 1985, 44–53.

[2] C. Moreau, "Fabrication de combustibles enrobés", *Technique de l'ingénieur, Génie nucléaire*, vol. BN3, No. B3640, 1983.

[3] C. Moreau, A. Ballagny, R. Bujas, J. Holder, R. Ranc et R. Soulhier, "Fabrication et performances du combustible français pour réacteurs à haute température", IAEA Symposium (IAEA CN 36/270), *Nuclear Power and Its Fuel Cycles*, Salzburg (Austria), 2–13 May 1977.

[4] IAEA (Technical Report 161, 1974), *Panel on Sol–Gel Processes for Fuel Fabrication*, Vienna (Austria), 21 May 1973.

[5] K. Minato and K. Fukuda, "Chemical vapor deposition of silicon carbide for coated fuel particles", *J. Nucl. Mat.* 149, 1987, 233–246.

[6] P. Guillermier and G. Harbonnier, "Technologie des combustibles pour RHT", SFEN Meeting, Paris (France), 10–11 December 2002.

[7] K. Sawa, S. Suzuki and S. Shiozawa, "Safety criteria and quality control of HTTR fuel", *Nuclear Eng. and Design* 208, 2001, 305–313.

[8] F. Charollais, B. Bianchini and C. Perrais, "Caractérisation de combustibles HTR par analyse d'images", *Matériaux-2002*, Tours (France), 21–25 October 2002.

[9] F. Charollais, C. Perrais, M. Perez, S. Fonquernie, C. Ablitzer, A. Duhart, O. Dugne, P. Guillermier et G. Harbonnier, "CEA & Areva HTR fuel particles manufacturing and characterization R&D program", *ATALANTE-2004*, Nîmes (France), 21–25 June 2004.



**Christophe Perrais,**
*Fuel Research Department*

# Irradiation behavior of particle fuels

## Particle fuel: a variety of failure modes for a high-strength object

Particle fuel must have the ability to withstand high temperatures, and high burnups, while not releasing large amounts of fission products. Such release of fission products by the fuel element – compact, or pebble – is mainly due to failed particles. However, since the permeation of fission products across the ceramic layers surrounding the kernel is thermally activated, intact particles are not wholly impervious for some fission products, particularly in incident situations that result in a rise in core temperature.

The core of a particle fuel-fired reactor holds several billion particles, every one of which ensures its own confinement function. The issue thus is to be able to demonstrate, on the one hand, that only a few of these have undergone failure prior to irradiation (about $10^{-5}$), that a small number fail in nominal conditions (about $10^{-4}$), or in incident conditions (a twofold increase, i.e. $2 \times 10^{-4}$), and, on the other hand, that permeability in intact particles remains acceptable, in all conditions. To carry out such evaluations, one should make the additional assumptions that failure of the ceramic layers ensuring confinement conforms to a Weibull statistical distribution, and that there is no well-defined failure limit, as is the case with metallic claddings.

The main containment barrier is the SiC layer, which provides, on the one hand, the effective diffusion barrier for most fission products, and, on the other hand, forms the structure withstanding the pressure generated by the fission gases released by the kernel, and present in the pyrocarbon buffer's open porosities.

The dense pyrocarbon layers, aside from their usefulness in easing fabrication operations, and aside from their role as additional fission product diffusion barriers, also play a major part in the SiC layer's mechanical behavior. Indeed, these pyrocarbon layers, dense as they are, compared to the buffer, though they do exhibit 15–20% porosity, undergo densification under fast-neutron irradiation, as fast-neutron **fluence*** – i.e. for neutrons with an energy higher than 0.1 MeV – may rise to several times $10^{25}$ n · m$^{-2}$, in a HTR (see Fig. 110). Bonded as they are to the SiC, which is highly rigid, they may not however densify freely. This causes, within these dense PyC layers, tangential tensile stresses, and, by way of reaction, tangential compression stresses within the SiC layer. These compression stresses delay the onset of tensile stress in the SiC layer, due to pressure from fission gases, thereby retarding SiC failure. Such stresses in the pyrocarbon layers are relieved by irradiation **creep***. This limits stress levels in the pyrocarbon layers, restricting failure of these layers at the start of irradiation. Thus, the benefit of SiC layer prestressing by the inner pyrocarbon layer may only be effective if there is strong cohesion at the interface between the two layers, and if stresses are not fully relieved. As a counterpart to such cohesion, when a crack arises in the pyrocarbon layer, there is a high probability of it further propagating into the SiC layer.

Whether it be a "compact" (a small cylinder about 10 mm in diameter, about 50 mm long), or a "pebble" (a sphere some 60 mm in diameter), the fuel element must exhibit a homogeneous particle distribution, be amenable to handling without particles incurring damage, and ensure satisfactory heat transfer between the particle, and the surrounding graphite matrix. Fuel element fabrication, whether by pressing or injection, is an operation that subjects particles to mechanical stress. The number of particles broken or damaged (e.g. with a failed outer pyrocarbon layer) during fabrication operations has a direct incidence on in-reactor behavior, in particular on the release of fission products into the primary circuit.

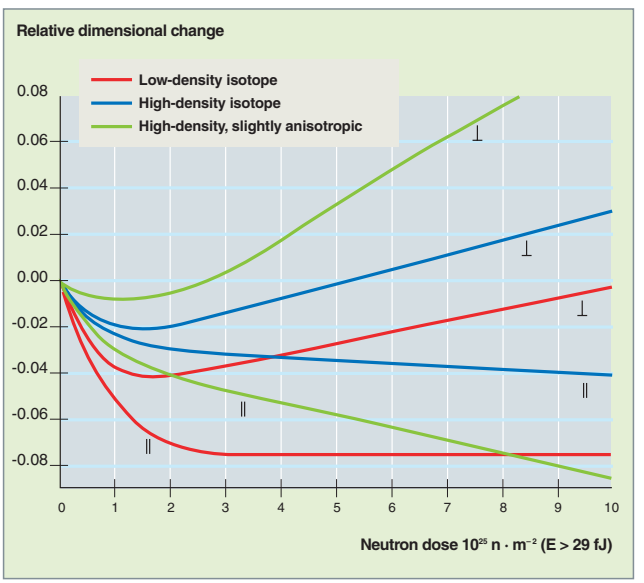


Fig. 110. Dimensional changes exhibited by various pyrocarbons, along directions parallel, and perpendicular to the deposition plane.

The distribution of particles across the fuel element, fuel element particle density, and particle power level are decisive factors, as regards fuel element behavior, and thermomechanical stresses, since they determine, in particular, the temperature gradients, and temperature levels within the particles. Thus, a "compact" is more stressful than a pebble, since it exhibits a higher particle density (the graphite blocks take up a certain volume of their own, which must be regained elsewhere), and less homogeneous distribution (particles may end up level with the compact's outer surface).

Under irradiation, the fuel element's graphite matrix shrinks. The dimensional change it exhibits, close to that for a standard graphite, stands at about 1% at the end of irradiation. Such shrinkage may subject particles to mechanical stress, chiefly at the level of the outer pyrocarbon layer, and may result in increased temperature, due to a widening gap between the graphite block, and compacts.

In the reference accident situation, the loss of cooling systems may result in fuel temperature rising to 1,600° C. At such a temperature, production of CO, through the reaction of oxygen, liberated from $UO_2$, with carbon in the buffer is heightened, resulting in increased pressure within the particle, and thus increased probability of failure. The amount of CO generated at high temperature overshadows the yield of gaseous FPs, for oxide fuels. At the same time, the rise in temperature speeds up fission product diffusion to the SiC, favoring SiC specific corrosion due to certain fission products (palladium), resulting in embrittlement. It will thus be seen that this type of fuel exhibits complex behavior, and that in-reactor failure modes are many (see Fig. 111).

## The amoeba effect

Kernel migration across the fuel particle, known as the amoeba effect, is recognized as an issue giving cause for concern, for particles exposed to steep temperature gradients. This phenomenon, which may result in complete destruction of the particle, should the kernel reach the SiC layer, is strongly dependent, on the one hand, on three operating parameters, namely kernel temperature, the temperature gradient within the particle, and burnup; and it is dependent, on the other hand, on the nature of the kernel's constituent material [1]. Initial observations of this phenomenon were made in the United States, in the 1960s, in carbide fuels. The ascertained mechanism involves the solid-phase diffusion of carbon, in a thermal gradient. Similar observations, of kernel migration going as far as to result in failure of the SiC layer, were made in the 1970s, with oxide kernel fuels. In the latter case, the mechanism is more complex, and has yet to be fully determined. It involves concurrent vapor-phase displacements of carbon, from the hot side to the cool side of the particle, owing to the presence of the carbon oxides CO and $CO_2$, but equally solid-state thermal diffusion of oxygen within the kernel.

The distance over which the kernel migrates, in oxide and carbide fuels, is often expressed in terms of an empirical expression, of the form:

$$x(t) = \int_0^t KMC\,(T)\,\frac{1}{T^2(t)}\,\frac{dT(t)}{dx}\,dt$$

where KMC (T) stands for the "kernel migration coefficient," having a value which depends on the kernel's constituent material, and irradiation temperature.

A considerable experimental database is now in place, bringing together the findings from experiments carried out by various organizations, in the United States, the European Union, and Russia. Evaluations for the kernel migration coefficient, taking the form of an Arrhenius relationship, have been suggested, chiefly for oxides (see Fig. 112).

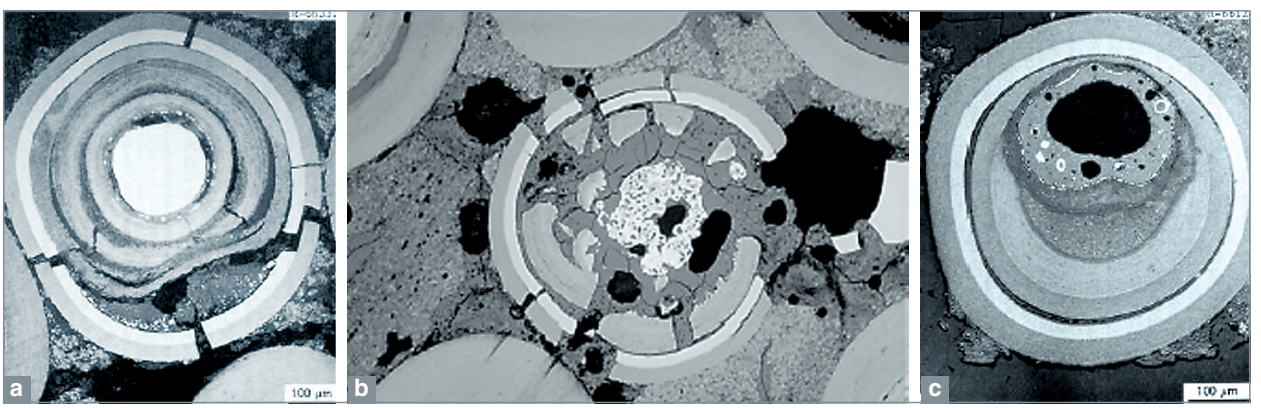


Fig. 111. Various particle failure modes: a) Accumulation of FPs; b) Overpressure; c) Amoeba effect. The amoeba effect involves kernel displacement across the buffer, due to transport of carbon atoms in the buffer from the hot side to the cool side, inside a particle subjected to a thermal gradient. The amoeba effect brings the kernel into contact with the dense pyrocarbon, resulting in particle failure.

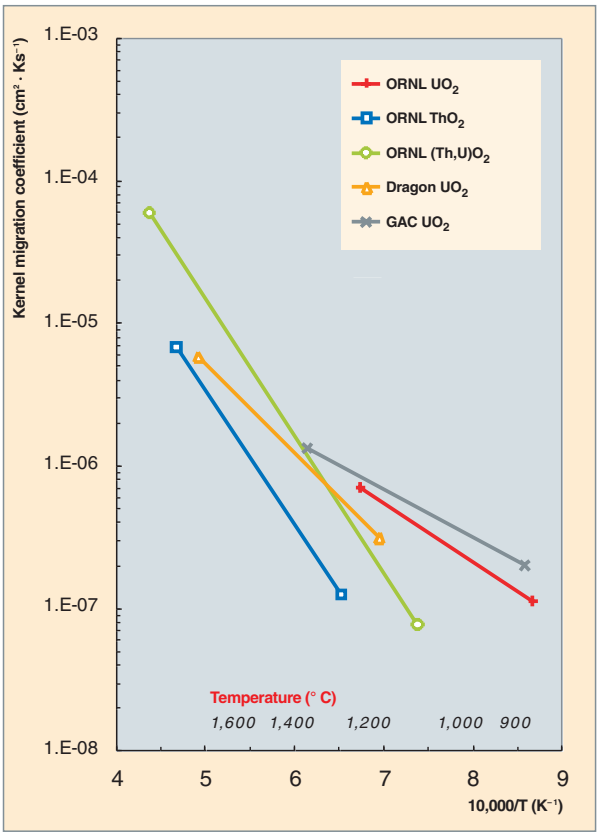


Fig. 112. Kernel migration coefficient, as a function of temperature.

Of such fission products, fission gases play a major part; while a fraction of these is retained within the kernel – depending on the temperature level within the particle, and burnup – the remainder is released into the particle's free volumes, gradually building up pressure[8]. Further, for particles involving a $UO_2$ kernel, there is the added presence of carbon oxides ($CO–CO_2$), yielded by the reaction of oxygen, liberated as a result of uranium fission, with the buffer's carbon. To preclude premature failure of the dense layers, particularly of the SiC layer, the particle must be appropriately dimensioned, by making provisions, at the fabrication stage, for an adequate buffer volume, i.e. allowing for an optimized buffer volume/kernel volume ratio, so that the onset of unacceptable tensile stress in the SiC layer is pushed back well beyond nominal burnup.

A large proportion of nongaseous fission products is retained within the kernel, in various forms: in solution within the matrix, or in the form of separate oxide phases, or of metallic precipitates, or more or less complex FP compounds. The more volatile fission products (e.g. Cs, I, Ag) tend to diffuse across the various layers in the particle. It should be noted that the switch from BISO particles, as used in initial HTR fuels, to TRISO particles has allowed quite significant gains to be achieved, in terms of FP retention, owing to the outstanding diffusion barrier, with respect to most fission products, provided by the SiC layer (see Fig. 113) [2].

Significant kernel displacements (several tens of microns) require very steep thermal gradients within the particles (several thousand degrees per centimeter). Such gradients are, in most cases, never reached in the fuel elements selected for current power reactor designs, whether they be of the "pebble bed" type (involving a homogeneous fuel distribution, and low power density), or of the "annular, prismatic-block core" type, as in General Atomics' GT–MHR project.

At the same time, since one of the factors making for carbon transport is the presence of carbon oxides in the particle's internal atmosphere, use of oxycarbide kernels, rather than $UO_2$ kernels, yielding practically no CO, is widely seen as an effective remedy to the amoeba effect.

## Fission product behavior, and diffusion in particle fuels

The release of radioactive fission products from HTR fuel particles, and fuel elements is one of the limiting factors, in terms of lifetime, for this type of fuel, in both nominal operating conditions, and accident conditions.

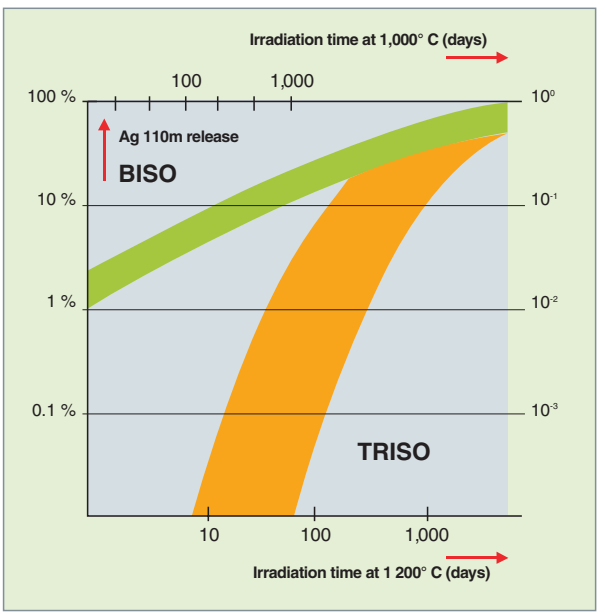


Fig. 113. Overview of Ag 110m release measurements, as yielded by irradiations of particles with low-U 235-enriched $UO_2$ kernels, of BISO and TRISO types, in the Dragon experimental reactor.

8. A small fraction of fission gases, as of other FPs, is released by direct recoil (knockout) into the buffer. For a conventional LEU TRISO particle, involving a kernel diameter of 500 microns, such recoil release accounts for 1.5% of total yield.

The best results, as regards FP retention, were achieved with **LEU***[9] TRISO particles, irradiated by German researchers in pebble-type fuels [3], at operating temperatures possibly rising to 1,300° C, burnup of 16% **FIMA***, and a fast-neutron fluence of $8 \cdot 10^{25}$ n/m². The release rates measured are moderate, in spite of fairly severe irradiation conditions; R/B ratios[10] (see Fig. 114) thus stand at less than $10^{-6}$ for Kr 85, about $10^{-5}$ for Cs 134 and Cs 137, rising to $10^{-2}$ for Ag 110m. Apart from that last element, which diffuses fairly readily across dense PyC layers, and even across SiC, the release rates measured for the other FPs, in normal operating conditions, are due to initially defective particles, or contamination of the matrix by fissile material. Which is why current fabrication specifications stipulate a heavy metal contamination rate lower than $10^{-7}$, and a defective particle fraction lower than $5 \cdot 10^{-6}$. Further, retention performance is largely dependent on fuel fabrication conditions [4]. Indeed, particles fabricated by US teams (for the NP–MHTGR fuel program[11]), involving broadly similar specifications, did not allow a comparable performance to be achieved for the resulting compacts, with release rates, for some FPs, being increased by a factor of up to 100.

The models of FP migration across the particle, and, more broadly, across the fuel element (pebble, or compact) used in software programs serving to evaluate the source term involved in fission product release in a HTR core, in normal operation, or in accident conditions, are diffusion models relying on "effective" diffusion coefficients, for each species, and each of the media being modeled.

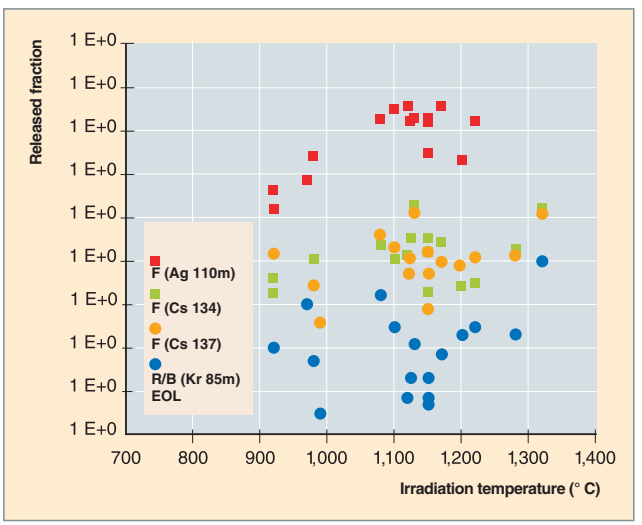


Fig. 114. Released fractions, for various types of fission products: gaseous FPs (krypton), volatile FPs (cesium), and metallic FPs (silver), as a function of irradiation temperature, from low-U 235-enriched $UO_2$ TRISO particles in German pebble elements.

9. LEU: low-enriched uranium.
10. The release rate for a fission product – whether radioactive or otherwise – is often expressed in terms of the R/B (release-to-birth) ratio, corresponding to the number of atoms released, over the number of atoms formed inside the kernel.
11. NP–MHTGR, or NPR: New-Production Modular High-Temperature Gas-Cooled Reactor.

Modeling involves solving, by analytical or numerical methods, Fick's law, which, in spherical coordinates, takes the form:

$$\frac{\partial c_i}{\partial t} = D_i^{eff}\left[\frac{\partial^2 c_i}{\partial r^2} + \frac{2}{r}\frac{\partial c_i}{\partial r}\right] - \lambda_i c_i + \dot{q}_i$$

where $D_i^{eff}$ stands for the diffusion coefficient for species i, as a rule taking the form of a, mainly temperature-dependent, Arrhenius relationship providing a global expression for the transport mechanisms[12] involved in each of the layers represented, while $\dot{q}_i$ and $\lambda_i$, respectively, are the creation term, and radioactive decay constant for the isotope being considered.

Data for effective diffusion coefficients, for the various materials, may vary widely, depending on data origin. Moreover, these coefficients do vary, depending on layer morphology. A review of the various data available was carried out recently, under the aegis of the European HTR–TN project, in order to put forward a relevant selection [5], with regard to the specifications drawn up for future particle fabrications, at CEA. Most of the software programs developed around the world use diffusion coefficient values that allow computation findings to be obtained showing good agreement with values measured experimentally, during accident simulation tests carried out with irradiated fuel elements.

While most of the fission products that diffuse across particle layers give rise to no chemical interaction with these layers, certain FPs, such as palladium, or elements in the lanthanide family[13] may corrode and damage the SiC layer (see Fig. 115). This forms one of the mechanisms for end-of-life failure. Thus, particles with oxide kernels, subjected to high power levels, involving high kernel temperatures (> 1,250° C), exhibit localized internal corrosion of SiC layers. This corrosion is accounted for, as a rule, either by palladium migration across the pyrocarbon layers, followed by chemical aggression (palladium is a metallic FP, exhibiting a much higher vapor pressure than other noble-metal FPs), or by oxidation, due to gases yielded by the reaction of oxygen, liberated as a result of fission reactions, with carbon (CO–$CO_2$ mixture).

Irradiation behavior laws, for the particle's constituent materials, would appear to be broadly dependent on their microstructure, which in turn is the outcome of the values selected for the parameters involved in the fabrication process (sol–gel, CVD: see the chapter on "Particle fuel"). Thus, so long as the correlations prevailing between these parameters, and finescale layer structure are not clearly established, it will prove difficult to extrapolate a law worked out on the basis of former fabrication runs, for an application for current materials.

12. These include bulk diffusion, intergranular diffusion, FP trapping in fabrication porosities and cracks, etc.
13. SiC corrosion by FPs in the lanthanide series (cerium, praseodymium…) has been observed chiefly in particles featuring dicarbide ($UC_2$) kernels, irradiated in the US Peach Bottom and Fort St Vrain reactors. With oxide kernels, lanthanide FPs are retained within the fuel in the form of refractory oxides, miscible with $UO_2$.

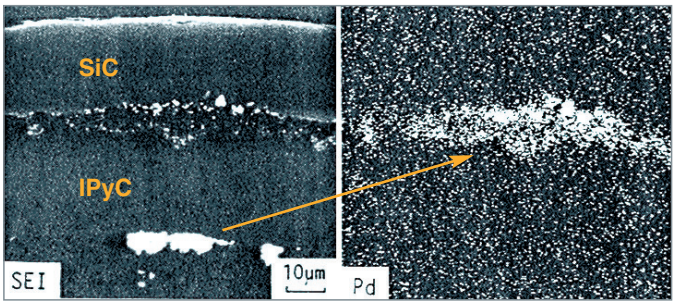


Fig. 115. Fuel particle internal corrosion due to palladium.

In the past, German teams converged to put forward a single, satisfactory technological formula, chiefly qualified in the HFR experimental reactor, and validated in the AVR prototype pebble-bed reactor, at a burnup of about 10% FIMA, with a helium outlet temperature of 850° C. Such fuels did not prove highly susceptible, in these reactors, to the failure modes outlined above. By contrast, US researchers experimented with many combinations, involving as a whole more severe loadings. Many experiments involved disappointing outcomes, evidencing the failure modes described above.

Currently, the resurgence in interest for the HTR reactor line is eliciting two types of approach. The first one, minimizing the R&D aspect, involves taking up the German concept, along with its utilization conditions. This is the approach preferred by the South Africans (PBMR) and Chinese (HTR–10), who have gone so far as to acquire sections of German fabrication facilities. The second approach seeks to make use of higher temperatures, and higher burnups, entailing a drawing away from the German concept, and, consequently, undertaking more significant R&D programs. This is the preferred way for the Japanese (HTTR), US teams (NGNP), and French teams (CEA + Areva).

As may be seen, the phenomenology of particle fuel in-reactor behavior is a complex issue. It must be said that there is as yet no precise understanding of what the limiting factors are, as regards HTR burnup levels. In spite of extensive irradiations, German experiments evidenced no particle failures. What may yet be said, as of now, is the following:

- the higher the burnup, the higher the pressure inside the particle, and the higher the probability of SiC layer failure, and thus the higher the failed particle fraction. To push back that limit, one may consider altering the reference geometry (with an increased buffer or SiC layer thickness, or a smaller kernel). At high burnup, kernel swelling would appear to be a limiting factor, since there is a risk it will interact with the dense layers, however this has not been demonstrated experimentally, and there is no agreed position on this matter among experts. Mechanical characteristics do seem to deteriorate under irradiation, however the values found in the literature are too widely scattered to allow any firm conclusions to be drawn;
- the higher the burnup, the higher the FP concentration, increasing the risks of corrosion, and of diminished envelope strength.

Gaining a better knowledge of such limitations is thus crucial, to prepare for the future: this is the purpose of two forthcoming irradiations, scheduled in the HFR reactor, in which CEA is a participant: HFR–EU1 (concerned with burnup), and HFR–EU1bis (focusing on temperature), under the aegis of European Union contracts HTR–F, and HTR–F1.

## Bibliography

D.G. Martin, “Considerations pertaining to the achievement of high burn-ups in HTR fuel”, *Nuclear Engineering and Design* 213, 2002, 241–258.

R.N. Morris, D.A. Petti, D.A. Powers, B.E. Boyack, *TRISO-Coated Particle Fuel Phenomenon Identification and Ranking Tables (PIRTs) for Fission Product Transport Due to Manufacturing, Operations and Accidents*, NRC (NUREG/CR-6844), 2004.

## References

[1] M. Wagner-Löffler, “Amoeba behavior of $UO_2$ coated particle fuel”, *Nuclear Technology* 35, No. 2, 1977, pp. 392–402.

[2] F. Homan, H. Nabielek and L. Yang, “Low enriched fuel particle performance review”, Forschungszentrum Jülich (FZJ), Report KFA-GA Jül-1502, GA-A14759 UC-77, 1978.

[3] K. Verfondern (Editor), *Fuel Performance and Fission Product Behaviour in Gas Cooled Reactors*, IAEA, TECDOC-978, November 1997, Chapter 3.

[4] D. Petti, J. Maki, J. Buonjiurno, R. Hobbins and G. Miller, *Key Differences in the Fabrication, Irradiation and Safety Testing of US and German TRISO-coated Particle Fuel and Their Implications on Fuel Performance*, INEEL/EXT-02-02300, 2002.

[5] A collaboration of work performed by BNFL, CEA, FRAMATOME–ANP and FZJ, *Selection of Properties and Models for the HTR Coated Particle*, HTR-F–0312-D-3.2.1; first version deliverable No. 12, 2003.

**Mayeul Phelip and Michel Pelletier,**
*Fuel Research Department*

# Mechanical modelling of particle fuel

One of the great assets of particle fuel lies in its ruggedness. Its design endows it with the ability to withstand high mechanical, and thermomechanical stress levels. Such stresses may be due to a variety of causes: the accumulation of fission products inside the envelopes, the deformation of materials under irradiation, or owing to the temperature field, coupled with thermal expansion. In order to take full advantage of the margins provided by this ruggedness, it is indispensable that a high-quality model be available, of particle fuel mechanical behavior.

Mechanical modeling involves, first of all, ascertaining the phenomena involved, and understanding them, on the basis of accrued experience, in particular by way of post-irradiation examinations of the outcomes of previous experiments, in order then to be able to simulate them, by means of the equations of mechanics.

Numerous investigations have been carried out over the past few decades, in various countries – the United States, Germany, the United Kingdom, France, Russia, and, more recently, China, and Japan – on the irradiation behavior of fuel particles. Owing to the large number of particles held in a reactor core, such investigations, and the most successful models that have been associated to them were mostly grounded on statistical methods. Such statistical methods do as a rule rely, on the other hand, on deterministic thermomechanical models.

Put simply, the principle of particle fuel mechanical modeling is to compute the evolution of a particular stress (e.g. tangential stress, in a given layer) as a function of **fast fluence***, or **burnup***, and associate to this a probabilistic model (which may take into account e.g. the statistical distribution of thickness in the various layers, the Weibull-type distribution of ultimate tensile strength in the layer subject to computation, and the distribution of temperature, burnup, and fluence loadings), to arrive at a computed failure probability, associated to that stress variation (see Figs. 117, 118). The simplest probabilistic model, often used as an initial approximation, involves considering only a global, Weibull-type statistical distribution. The (cumulative) failure probability for the ceramic layer subjected to stress $\sigma$ may then be expressed as:

$$P_R(\sigma) = 1 - e^{-\ln(2)\left(\frac{\sigma}{\sigma_m}\right)^m}$$

where $\sigma_m$ and $m$ stand for, respectively, the ultimate tensile stress median value (i.e. corresponding to a probability of 1/2), and the Weibull modulus of the ceramic of interest. The latter quantities are, as a rule, expressed as a function of temperature, and fluence, to take into account material degradation due to irradiation. By multiplying $P_F$ by the number of particles being considered (corresponding e.g. to an irradiation experiment), the expected average number of failed particles is obtained.

Particle fuel modeling has given rise to a fair number of computation codes. Mention may be made of the German PANAMA and CONVOL codes; the British STRESS3 code, associated, for the statistical side, to the STAPLE code; the US SORS (General Atomics) and PARFUME (INEEL) codes; the Russian GOLT code; and one French code, CORMORAN. The STRESS3 and CONVOL codes evolved as variations on a common formulation. Mention may also be made of the Japanese code used to compute the fuel particles for the HTTR experimental reactor, which was drawn up on the basis of PANAMA and CONVOL.

Most of the above-mentioned codes make use of analytical formulations that involve considering the particle, in simplified form, as a pressure vessel (withstanding the pressure generated by gaseous fission product release, and CO formation), solely comprised of the three following layers: inner pyrocarbon (IPyC) layer, SiC layer, and outer pyrocarbon (OPyC) layer (see Fig. 116). The loadings imparted to the particle that are then considered are gas pressure, and the fast-fluence-induced deformation of PyC layers.

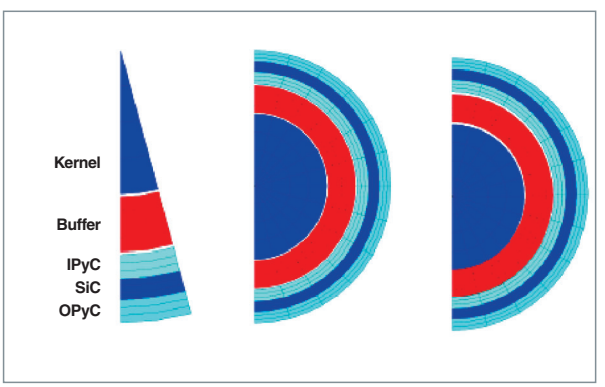


Fig. 116. Examples of finite-element models used for the mechanical modeling of particle fuel, with the ATLAS application, developed at CEA (1-D, 2-D concentric, 2-D non-concentric models).

Simplifying assumptions are made: thin shell approximation, perfectly rigid SiC, undergoing no deformation.

SiC irradiations show that this layer remains stable under irradiation, up to the maximum doses contemplated for **HTRs***. At the same time, in mechanical terms, it is 10 times more rigid than PyC (Young's modulus E stands at 400,000 MPa for SiC, as against ~ 30,000 MPa for PyC). As a result, mechanical stresses induced by SiC layer dimensional changes under irradiation are negligible, compared to stresses induced by gas accumulation, and fast-fluence deformation of the PyC layer.

By way of example, the following is a simplified formula for tangential stress in the SiC layer, as arrived at by Williamson and Horner (1971) [1]:

$$\frac{2t_2}{r}\sigma_2 \cong P + \frac{\dot{g}_1}{K_1(1-\nu_1)}\frac{2t_1}{r} + \frac{\dot{g}_3}{K_3(1-\nu_3)}\frac{2t_3}{r}$$

where $\sigma_2$ is the tangential stress in the SiC layer, $r$ is the average radius of the SiC layer, $P$ is pressure, $t_1$, $t_2$, $t_3$ respectively stand for IPyC, SiC, and OPyC layer thickness, $K_1$, $K_3$ are the respective irradiation creep coefficients for the IPyC and OPyC layers, $\nu 1$, $\nu 3$ are the respective creep Poisson ratios for the IPyC and OPyC layers, and $\dot{g}_1$, $\dot{g}_3$ are the respective irradiation-induced strain rates in the IPyC and OPyC layers. It will be seen that, if $\dot{g}_1$, $\dot{g}_3$ have zero value, the formula reduces to the classical formula for tangential stress in a pressurized sphere:

$$\sigma_2 = P\frac{r}{2t_2}\cdot$$

Feedback from experience of using these codes shows that results are highly sensitive to the behavior laws for the materials involved, and that such laws are not easily arrived at. To date, it has invariably proved highly problematical to achieve reliable predictions.

The main drawback of these codes is that they do not cover particle thermics, and that they do not allow for representations of the kernel, or buffer layer. Banking on its experience in the area of thermochemical, thermic, and mechanical fuel modeling, CEA decided to develop an integral uranium oxide-based particle model, making use of a finite-element method, by way of the ATLAS application [2], in the PLEIADES simulation platform.

Modeling fuel kernel irradiation behavior takes on board the following phenomena:

- the evolution over time of neutron power, fission density, and burnup;
- fuel thermal and mechanical behavior (associated laws: $\rho$, $C_P$, $\lambda$, $\alpha$, E, $\nu$);
- the formation rate, and release rate of fission gases Xe + Kr, along with the evolution of the fuel O/M ratio, and CO/$CO_2$ formation;
- structural evolution under irradiation, as characterized by densification, solid and gas swelling, and creep.

Modeling the coating layers' irradiation behavior takes into account the following phenomena:

- thermal and mechanical behavior ($\rho$, $C_P$, $\lambda$, $\alpha$, E, $\nu$);
- corrosion of the SiC layer, due to metallic FPs emanating from the irradiated fuel, and to CO;
- structural evolution under irradiation, as characterized by irradiation-induced deformations, and thermal and irradiation creep;
- the evolution under irradiation of ultimate tensile strength, as characterized by the Weibull distribution for brittle materials $\sigma(\theta, \phi t)$.

The application is currently undergoing development; Figures 116–118 show the models used, along with findings, in terms of stresses, and failure probability.

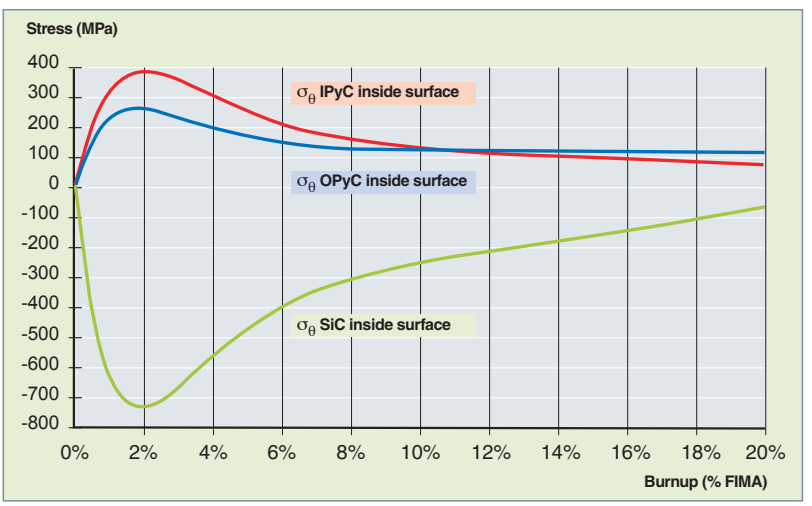


Fig. 117. An example of the computation of tangential stress evolution in the IPyC, SiC, and OPyC layers.
At the beginning of irradiation, the pyrocarbon shrinks, inducing compression stresses in the SiC. Subsequently, accumulation of gaseous FPs causes a buildup of pressure in the particle, and the SiC undergoes a switch to tensile stress. It is these tensile stresses, rather than compression stresses, that cause failure of this layer. In the instance shown above, the SiC stays in compression up to 20% FIMA, however, depending on scenarios, particles may switch to tensile stress earlier, with increased risks of failure.

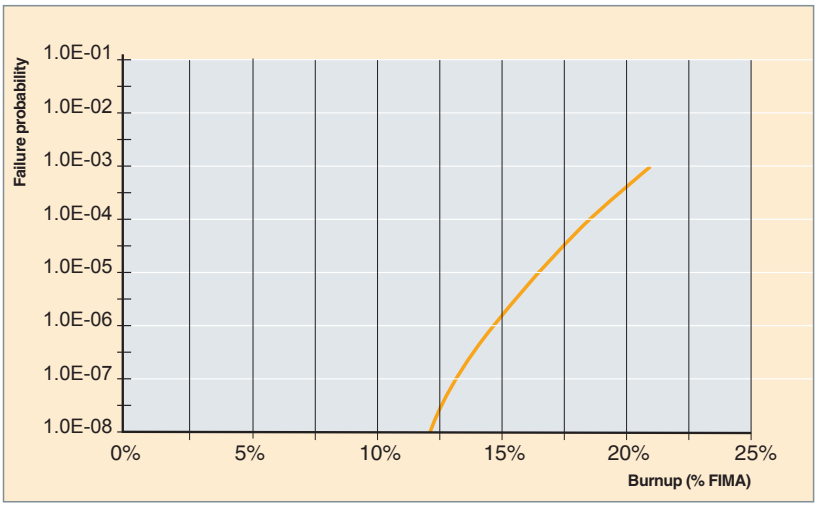


Fig. 118. An example of the computation of particle fuel failure probability, as a function of burnup.

## References

[1] D. G. Martin, "Considerations pertaining to the achievement of high burn-ups in HTR fuel", *Nuclear Engineering and Design* 213, 2002, 241–258.

[2] F. Michel, P. Mailhe, "ATLAS, a code for V/HTR fuel performance evaluation", American Nuclear Society, 2006 ANS Annual Meeting (ANS-2006), Reno, Nevada (USA), 4–8 June 2006.

**Mayeul Phelip,**
*Fuel Research Department*

# Very-high-temperature reactor (VHTR) fuel

The thermal-spectrum, very-high-temperature reactor (VHTR) [1] is one of the candidate reactor concepts for the fourth generation of electricity generating nuclear reactors. The coolant helium, involving as it does a very high core outlet temperature (1,000° C, rather than 850° C for a conventional HTR), makes it possible to consider VHTRs for cogeneration applications, i.e. combined very-high-temperature heat, and power production.

However, this significant increase in core outlet temperature will not only have an impact on materials for the intermediate heat exchangers, but will also result in the fuel being hotter, in nominal operation, than in the HTRs so far considered. In the foregoing chapters, it has been shown that particle fuel, involving particles coated with pyrocarbon (PyC) and silicon carbide (SiC) layers, does not rise above a maximum temperature of about 1,250° C, in normal operating conditions, or 1,600° C, in the event of a loss of coolant accident.

In order to ensure satisfactory mechanical, and thermomechanical particle behavior, in both nominal and accident conditions, at maximum operating temperatures higher by about 150–250° C, while keeping to targets, in terms of burnup, similar to those for conventional HTR fuels, i.e. ~ 200 GWd/t[14], R&D will address, on the one hand, fuel element geometry, to specify a new design for compacts, and hexagonal blocks, allowing a lower D T to be achieved, between the hottest fuel particle, and the helium channel; and/or address, on the other hand, altering the fuel particle's constituent materials (kernel, and coating layers).

The consequences of such increased temperature, as regards the irradiation behavior of a conventional particle, with a $UO_2$ kernel, are many [2]:

First of all, there will be a rise in thermally activated phenomena; mention may be made, in no particular order, of the following: increased fission gas release; accelerated diffusion of volatile, and metallic fission products, such as cesium, or silver; and heightened formation of carbon monoxide, and dioxide, due to the reaction arising between oxygen atoms from the kernel, liberated as a result of fission processes, and carbon in the low-density pyrocarbon buffer layer. Further, should the temperature gradient inside the particle be steep, the higher temperature will favor carbon transport, from the hot to the cold region in the particle, by way of vapor-phase, and solid-phase migrations, resulting in the phenomenon known as the "amoeba effect" (see the chapter on "Irradiation behavior of particle fuels").

One further possible consequence is an alteration of irradiation densification and swelling kinetics for the dense inner pyrocarbon (IPyC), and outer pyrocarbon (OPyC) layers, encasing the silicon carbide layer on either side. Measurements of pyrocarbon strain rates, obtained at various irradiation temperatures, and various neutron doses, show that increased temperature does result in larger strain rates, and increased material anisotropy. Indeed, the desired equilibrium arising between layers, to keep the SiC layer in compression as long as feasible, could be compromised, impacting particle lifetime.

To meet these challenges, the intention is, of course, to keep the TRISO particle concept, which is a proven one, however the idea is to alter, to some extent, the particle's constituent materials, by using constituents better suited to very-high-temperature operation. As we have seen, a number of phenomena liable to lower particle lifetime may be attributed, in part, to the $UO_2$ kernel. Mention may be made, among others, of the release of fission gases, and metallic, or volatile fission products, along with the generation of carbon oxides. Consequently, solutions must be looked to, with a view to curbing such events, involving use of other materials than $UO_2$, such as, e.g., uranium oxycarbide (UCO), or the addition of inhibiting agents in the $UO_2$, or the buffer, to restrict the formation of carbon oxides, and limit the risk of "amoeba effect."

The most significant experience, as regards UCO fuel, comes from the investigations carried out by US laboratories for the NP–MHTGR program, from the 1970s on, at ORNL[15] in particular. The chief consideration underlying their choice of UCO as reference HTR fuel is based on its satisfactory physical–chemical behavior, at first blush, with respect to fission products. The simultaneous presence of oxide and carbide phases[16] stabilizes the system's oxygen potential, up to

14. This is the target specific burnup for high-quality **LEU*** $UO_2$ fuel coming from the German program. As regards high-enriched (**HEU***) fuels, burnups higher than 750 GWd/$t_{HM}$ have been achieved in the past.

15. ORNL: Oak Ridge National Laboratory (United States).

16. The "UCO" terminology in fact refers to a composite, comprising $UO_2$ and $UC_2$ phases. The respective proportions for these phases may vary over a wide range of makeups.

the very high burnups (75% **FIMA*)** previously achieved with high-U 235-enriched fuels.

The $UC_2$ phase present in this composite fuel reacts with a fraction of the oxygen liberated, as a result of the fission of a uranium nucleus, from the $UO_2$ phase, to yield back $UO_2$, in accordance with the following reaction:
$UC_2 + O_2 \rightarrow UO_2 + 2\,C$.

As a result, the atmosphere stays at a low oxygen potential – P ($O_2$) – level, stabilized throughout irradiation, thus strongly restricting carbon oxide formation. The chief consequences are diminished kernel migration across the particle ("amoeba effect"), and lower potential SiC layer corrosion owing to such gas. An initial content of 10–20% $UC_2$ would appear to be adequate to preclude generation of CO, at the target burnups contemplated for current, LEU- (low-enriched uranium) type fuels. Experiments carried out in conditions representative of those prevailing in prismatic-block cores (more stressful for fuel than pebble-bed cores) have confirmed the absence of any significant migration of UCO kernels.

Fabrication of such UCO kernels, using gelation techniques, has been evaluated at CEA. By way of modifications, with respect to the fabrication principle involved in the sol–gel route for $UO_2$ kernels, from the initial solution preparation step (introduction of carbon black) to the final heat treatment steps, of calcination and sintering, involving different options as regards the temperature and gases employed, kernels of this type may be obtained.

The UCO kernel, involving as it does a $UC_2$ volume fraction lower than 20%, exhibits a thermomechanical behavior similar to that of a $UO_2$ kernel. Further, estimated excess solid swelling, compared with $UO_2$, remains low, when referred to kernel fabrication diameter allowances. On the basis of the current state of knowledge, regarding the microstructure of UCO fabricated by the sol–gel route, release of fission gases into the particle's free volumes, in nominal operating conditions, is believed not to be significantly different from that for $UO_2$.

Such UCO, involving a $UC_2$ phase fraction lower than 20%, does not exhibit less satisfactory behavior than $UO_2$, as regards lanthanide[17] retention; on the other hand, the lower metallic FP (Ag, Cs, Pd) retention ability exhibited by the $UC_2$ phase may result in diffusion of such FPs, that is all the greater, the larger the volume fraction for this phase in UCO.

From these findings, it may be seen that use of UCO should afford some advantages, compared with $UO_2$; the positive aspects involve, chiefly, a lowering of internal pressure in the particle, owing to the absence of CO production, thus resulting in diminished failure risks related to such loading, along with the curbing of the "amoeba effect" risk, in the event of particularly severe operating conditions. A fairly similar behavior to that of $UO_2$ may be anticipated, with respect to lanthanide FP diffusion, kernel swelling, and fission gas release. On the other hand, far from trivial issues may be foreseen, as regards fabrication, in particular quality issues with respect to microstructural homogeneity, owing to the admixture of carbon black with the initial sol–gel solution. Under irradiation, increased diffusion of metallic FPs – such as Ag, Pd – out of the fuel may be feared, in both nominal and accident conditions.

To mitigate that weak point, strengthening must be sought, for the particle coating, with respect to diffusion.

To that end, a number of means may be contemplated. The first one involves trapping such fission products in the particle's inner layers, before they can reach the inside surface of the SiC layer. This may be achieved by means of so-called "sacrificial" layers, i.e. layers a few microns thick, playing no part in particle mechanical behavior, but having the purpose both of trapping a maximum amount of free oxygen, and equally of retaining such fission products as would be liable to diffuse across the main SiC layer, or subject it to chemical aggression. Such particles have already been fabricated, in small quantities, in the past, using zirconium carbide (ZrC) deposited directly onto the kernel; even though this layer does degrade during irradiation, it does afford a substantial advantage, as regards retention of such elements as silver, or europium, compared with the SiC–TRISO particle.

A second option is to go for a material exhibiting a better ability than SiC to retain metallic fission products, in the harsher nominal, and accident conditions prevailing in VHTRs. A material that would appear to meet these criteria is zirconium carbide [3]. This ceramic is particularly refractory; its melting point of 3,450° C may be referred to the 2,000° C taken to be the temperature for initiation of SiC chemical decomposition. The benefits ZrC may afford, as a structural material, with respect to SiC, for the TRISO particle, involve preserving its integrity at very high temperatures, in the accident situations that may be contemplated in VHTRs; and the ability to fabricate compacts featuring a higher-density graphite matrix, obtained by heat treatment at higher temperature (> 2,000° C), allowing, ultimately, a gain in terms of compact thermal conductivity, and maximum operating temperature. At the same time, ZrC exhibits no reaction for most of the fission products emanating from the kernel. Finally, diffusion of such fission products in ZrC is, for a given temperature, lower than in SiC.

The use of particles featuring a ZrC layer is, at present, far less widespread than that of conventional SiC–TRISO particles. Such particles have undergone only "laboratory" fabrication –

17. $UC_2$-kernel fuels have been much investigated, and used in HTR reactors developed in the United States. One of the main drawbacks of $UC_2$ is low retention, within the fuel, of fission products of the lanthanide (rare-earth) type, with a consequent high risk of SiC layer corrosion by such FPs.

in particular in the United States (Los Alamos Scientific Laboratory, General Atomics), Japan (Japan Atomic Energy Research Institute [JAERI]), and Russia – followed by experimental irradiations, and out-of-pile tests. Fabrication, by way of fluidized-bed chemical vapor deposition, may be achieved by two methods: sublimation of zirconium chloride powder; or *in-situ* generation, from zirconium "sponge," in a halogen gas (chlorine, iodine, or bromine) atmosphere, of zirconium halide. In either case, the gaseous zirconium compound is mixed, in appropriate proportions, with methane, hydrogen, and argon, to obtain deposition of ZrC [3]. A series of experiments, involving yttrium-stabilized zirconia simulant kernels, was recently carried out at CEA. Many tests, for the purposes of adjusting deposition parameters (gas injection temperature, flow rates), were required, to achieve an acceptable initial result. Macroscopic observations (see Fig. 119) show good cohesion between the dense PyC, and ZrC layers, as characterized by a clean, undeflected failure at the PyC–ZrC interface.

Optical microscopy observations of polished sections (see Fig. 120) show up microstructural variations, correlated with chemical composition gradients across the thickness of the ZrC layer. At the surface, over a thickness of about 8 µm, the layer exhibits a compact, if stratified appearance. Further down, the layer appears to be granulated, exhibiting slight variations in color, indicating variations in chemical composition, or grain size. The ZrC deposition process still needs to be optimized. Improvements being considered should allow better control of zirconium chloride and hydrocarbon distribution.

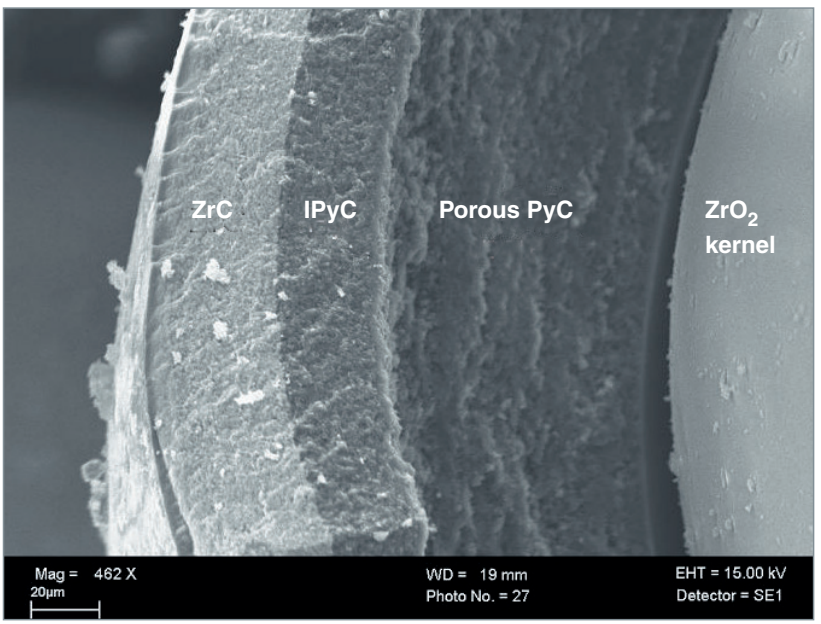


Fig. 119. Scanning-microscopy fractograph of a particle, showing its morphology, subsequent to the ZrC layer deposition step (DRT/LITEN).

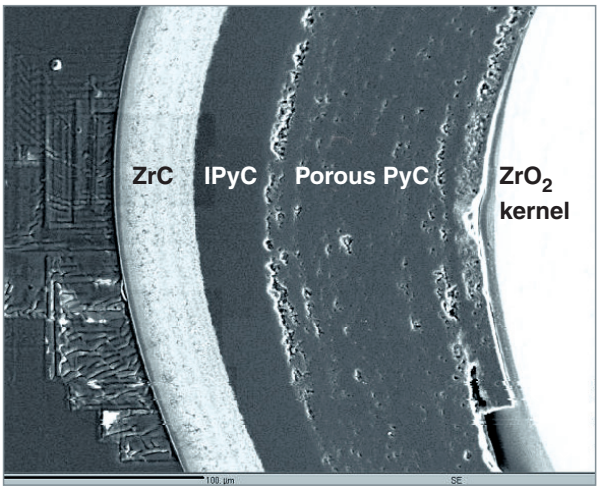


Fig. 120. Optical micrograph, obtained on a polished section, showing variations in microstructure, correlated with chemical composition gradients across the thickness of the ZrC layer (DRT/LITEN).

While the feedback from experience with ZrC–TRISO particles, in normal operating conditions, and in conditions representative of accident situations, is much smaller than for their SiC-layer counterparts, promising results have already been achieved. Thus, it has been confirmed that ZrC has a better retention ability than SiC, with respect to some fission products, such as cesium (see Fig. 121), and silver; on the other hand, other fission products, lanthanides in particular, diffuse more readily. Nevertheless, the ZrC layer does prove less liable to chemical aggression by palladium, and more resistant to the "amoeba effect" than SiC. At the same time, ZrC–TRISO particles were able to withstand, with a breakage fraction lower than 1%, post-irradiation heating tests, up to 2,400° C [3].

A number of relevant solutions, as regards a VHTR application, are thus already available; they do require, however, industrial-scale validation, if a higher-performance TRISO particle is ultimately to be obtained, compared to the current, reference SiC–TRISO particle, such as to allow a substantial gain, with respect to employment temperatures, in both nominal and accident conditions, while safeguarding reactor safety.

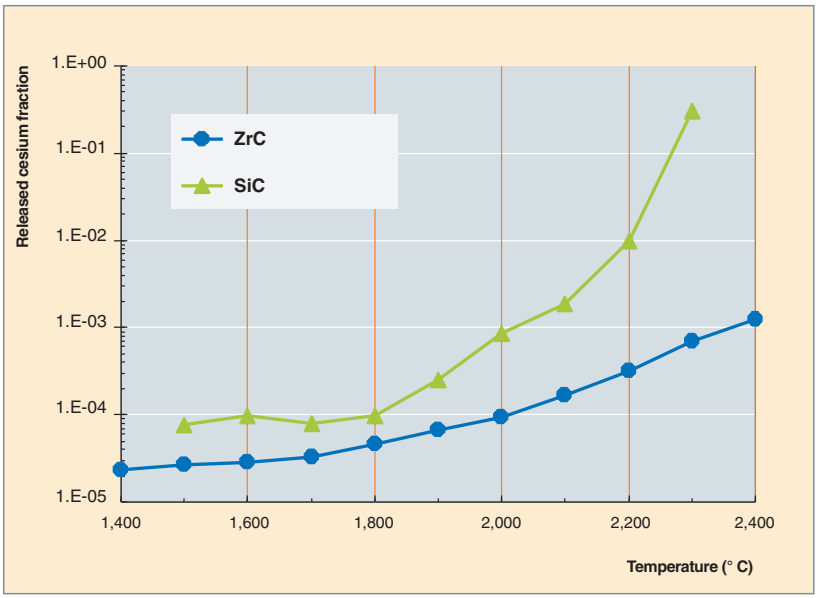


Fig. 121. Comparison of releases of isotope Cs 137, from particles coated with SiC, and ZrC layers, during post-irradiation heating, over 2 hours.

## References

[1] M. Lecomte, "Le réacteur à gaz à très haute température (VHTR)", *Revue générale nucléaire*, year 2003, No. 4 (July–August), pp. 69–72.

[2] J.-P. Nabot, P. Martin, M. Pelletier, S. Pillon and N. Chauvin, "Technologies du combustible et du cycle associé pour les différents concepts Génération IV", *Revue générale nucléaire*, year 2003, No. 4 (July–August), pp. 98–104.

[3] K. Verfondern (Editor), *Fuel Performance and Fission Product Behaviour in Gas Cooled Reactors*, IAEA, TECDOC-978, November 1997, Chapter 7.

**Michel Pelletier,**
*Fuel Research Department*

# Gas-cooled fast reactor (GFR) fuel

Fast reactors allow an outstanding neutron economy to be achieved, however they do require a large fissile material inventory, owing to the small **cross-sections*** prevailing at high energies. By way of fertile **capture*** in uranium 238, they make it possible to ensure the best value-added use of natural resources, in the context of a closed cycle. In fast spectrum conditions, fission and capture cross-sections, in the main **actinide*** isotopes, favor fission, allowing the recycling of minor actinides (Np, Am, Cm), and consequently a drastic downsizing in terms of long-lived radioactive elements requiring to be consigned to waste. Fast-neutron reactors – fast reactors – thus stand, patently, as attractive reactors for the future, with regard to all aspects of the cycle. This will prove to be all the more so, if the cycle may be closed by means of a treatment process catering for the group management of all actinides (uranium, plutonium, minor actinides), thus enhancing the cycle's proliferation resistance.

Aside from these benefits, which are common to all fast-spectrum reactors, gas-cooled reactors (GCRs) open the way to applications other than electric power generation, in particular hydrogen production, made possible by the high core outlet temperatures reached by the coolant. The gas-cooled fast reactor (GFR) concept may further draw on gas coolant technology that is already available, for thermal-spectrum reactors. The GFR thus stands, in a manner of speaking, as a "sustainable variant" of the high-temperature reactor (HTR).

## The specifications for GFR fuel

Such aims do entail, however, as a precondition, the requirement to develop a suitable fuel. The chief difficulty arises from the fact that the gas involved (helium, in effect) is a low-density coolant fluid, which must thus take up a considerable volume fraction in the core (about 40%), if it is to ensure heat removal, consequently restricting the volume that may be allocated to fuel, fuel containment barriers, and assembly structures.

The core design, for gas-cooled fast reactors, further entails the following specifications, for fuel:

- the ability to incorporate plutonium, up to a content of 15–20%, and minor actinides, with contents ranging from 2% (for equilibrium recycling in fast spectrum conditions) to some 5% (if it is intended to recycle the minor actinides yielded by thermal-spectrum reactors);
- a high heavy-atom density, dictating a dense fissile material (such as carbide, or nitride);
- the ability to undergo reprocessing, and refabrication by way of remotely handled operations, in the context of a closed cycle for all actinides, involving controlled, minimized waste production;
- satisfactory behavior, exhibiting a high radioelement containment level, over a temperature range of about 1,000–1,200° C, in nominal operating conditions;
- a slight degradation of behavior in accident conditions (in the event of depressurization, in particular), when temperatures may rise to 1,600° C;
- the ability to achieve **burnups*** guaranteeing, ultimately, adequate cycle economy (5 at.% **FIMA*** initially, 10 at.% FIMA subsequently), i.e. a fast **fluence*** of $2 \cdot 10^{27}$ n/m$^2$.

Such specifications entail a number of consequences, as regards the choice of fuel element materials, and the various physical properties these must exhibit.

## GFR fissile material

The fissile material should exhibit the highest heavy-atom density feasible. This entails going for an actinide carbide, or nitride, exhibiting a higher density than oxide (× 1.23, and × 1.30, respectively, for the same fabrication porosity, with mixed U–Pu compounds), and better heat conduction (with about 7 times higher thermal conductivity), thus making for a "cool" fuel, with a better ability to retain its own fission products, thus subjecting the first containment barrier to lower stress levels.

The choice between carbide, and nitride stems from the following considerations:

- ***performance:*** carbide affords the best performance, in terms of core volume, and immobilized fissile material. Indeed, the nitrogen present in the nitride gives rise to a neutron capture process ([n,p] reaction in N 14, yielding C 14); for nitride to achieve a performance equivalent to that of carbide, the cycle has to include a step of nitrogen enrichment (to at least 50%) with the N 15 isotope (natural nitrogen contains some 0.5% N 15). At the same time, nitride requires management of the C 14 generated, and further yields helium (by way of a [n,a]

reaction in N 14), this accounting for about 20% of fission gas volume;

- ***irradiation behavior:*** swelling rates under irradiation are about the same for carbide, and nitride fuel: some 1.4–1.6%/at.%, so long as temperatures do not exceed 1,200° C (such temperatures further making for fairly low fission gas release). Nitride, which could possibly exhibit a slightly lower swelling rate, does exhibit, on the other hand, at high temperatures, signs of dissociation of the (U,Pu)N phase, with concomitant precipitation, in the fuel–cladding gap, of the plutonium-rich metallic phase;

- ***cycle safety:*** carbide and nitride compounds may ignite spontaneously in air, when in powder form: management of such pyrophoricity must thus be ensured, for all cycle steps.

The balance would rather appear to tip in favor of carbide, however, before a final choice is made, a number of points will require investigation, in particular the ability of the carbide and nitride compounds to incorporate significant fractions of minor actinides, while retaining a satisfactory behavior under irradiation.

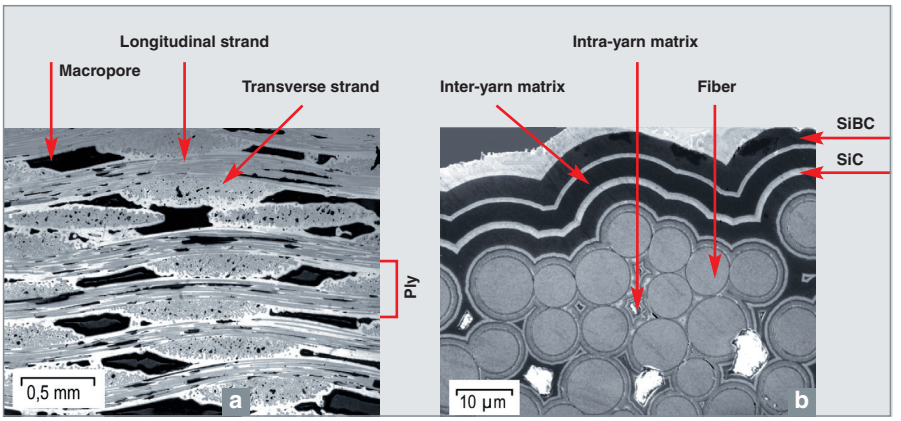


Fig. 122. SEM images of SiC-fiber-reinforced SiC (SiC–SiCf) ceramic composite (LCTS, Bordeaux).

## First containment barrier materials

Strict compliance with the specifications entails use of ceramic materials as constituents for the fuel element structure, and first containment barrier. Indeed, refractory-metal alloys (i.e. Mo, Nb, Ta, W alloys) exhibit a very high neutron absorption capacity, and would degrade core performance.

The main ceramics that have been identified are carbides, and nitrides (SiC, TiN, ZrC, TiC, ZrN), all being amenable to association with either actinide carbide, or nitride. In particular, silicon carbide exhibits acceptable behavior under a neutron flux, in the range where this has been ascertained (up to 80 dpa SiC, i.e. over practically half of the desired range), and at the temperatures contemplated, at which swelling remains low.

However, initial investigations have shown that use of monolithic ceramics, such as silicon carbide, may not be considered, on account of their **toughness*** being too low: any fuel element structural component, indeed, needs must exhibit a minimum amount of **ductility***. It thus becomes necessary to turn to reinforced ceramics, these being the only materials liable to yield the desired tradeoff between thermic, neutronic, and mechanical properties.

Use of long-fiber-based composites, such as SiC-fiber-reinforced SiC (SiC–SiCf) composites (see Fig. 122) may provide the desired solution: owing to the characteristics of their fiber reinforcement, they prove tolerant, to some extent, to deformation, and damage. On the other hand, they do not exhibit sufficient imperviousness to fission gases, or the coolant helium; it thus proves necessary, in order to guarantee the function assigned to the first containment barrier, to resort to liners, or impervious coatings, consisting of a small thickness of refractory metal alloys. This requirement makes for singularly more complex fabrication for such fuel elements, compared with those for other reactor lines, such as sodium-cooled fast reactors (SFRs), involving use of metallic claddings ensuring the twin functions of imperviousness, and mechanical strength.

## GFR fuel element concepts

Initially, attempts were made to adapt, to meet fast spectrum requirements, the HTR ***particle concept***, ensuring as it does confinement of fission products as close as possible to the fissile kernels where they are generated, by means of a multilayer coating. This concept, proving highly rugged as it does, when dimensioned as in HTR reactors (with a 4-layer design), had to be abandoned for GFRs, as it carries the drawback of a low fissile material volume fraction, and thus does not allow GFR fuel specifications to be met. At the same time, certain materials basic to this concept (pyrolytic carbons, in particular) exhibit poor resistance to high fast fluence.

Initial dimensioning studies resulted in two concepts emerging, meeting specifications:

- ***the*** cylindrical ***pin concept***, involving pellets held in a cladding, harks back to a conventional design. The challenge to be met then switches to pin dimensioning, and development of the cladding. The cladding could consist of a reinforced ceramic (such as SiC–SiCf), with a metallic liner.

The life-limiting phenomenon, for such GFR pins, is fuel–cladding interaction. Carbide or nitride fuel swelling rate is about twice that of oxide, and, at the temperatures at which it will operate, it does not creep readily. The ceramic cladding (even when fiber-reinforced) exhibits too little ductility to accommodate, without incurring unacceptable damage, strong mechanical interaction. Such low ductility further dictates that pins be short (maximum length around 1 meter).

The design for such pins will thus involve ensuring they operate out of mechanical interaction conditions for as long as possible, which comes down to finding the best tradeoff between an ensemble of fabrication and operating parameters, such as diameter, initial fuel–cladding gap, as-fabricated fuel porosity, together with stability under irradiation for such porosity, maximum linear power, etc.;

- ***the macrostructured plate concept***, recently put forward at CEA/Cadarache, provides an original solution (see Fig. 123), allowing the various constraints highlighted above to be met, as relating to the specifications, and material properties. In this concept, the plate's core structure consists of a ceramic matrix, formed in a honeycomb shape, while the fissile phase takes the form of cylindrical compacts, positioned in each cell of the honeycomb matrix. Two plates, likewise made of ceramic material, ensure cell closure, and thermal exchange with the coolant gas. These fuel plates are inserted, in three stacks, set at 120 degrees from each other, into the hexagonal-section assembly casing. Preliminary dimensioning of these plates results in a thickness lower than 10 mm, width of 120 mm, and length of about 250 mm.

The theoretical advantages afforded by this concept are as follows:

- optimized heat transfer, from power source to coolant, with minimal thermal resistance between fuel compact and cladding, and maximal exchange surface area between cladding and coolant; the design further allows good fuel temperature control, whatever the levels of fission gas release inside the cells;

- the presence, in every cell, of a space surrounding the fuel compact (due to the bringing together of cylindrical, and hexagonal geometries) allows gaseous fission products to collect, while limiting any pressurization of these products, in all operating conditions;

- good plate mechanical strength, with respect to pressure loadings, and mechanical interactions between fuel and cladding: compact–cell interaction is restricted to the sole dimension perpendicular to the plane of the plate, allowing stresses to be minimized, by accommodating the distortion imposed by fuel swelling, through cladding sag, and radial deformation of the compact, by way of an irradiation creep mechanism; using fuel compacts of a cambered, bulging shape further allows gradual contact to take place, thus precluding stress concentration.

Owing to the stringent specifications stipulated for them, GFR fuel elements are unquestionably those for which development, and qualification will set the strongest challenge. Currently ongoing investigations at CEA are seeking to meet this challenge: solutions have been put forward on paper, and fabrications are being undertaken for both concepts, pin, and plate. Experimental irradiations are planned, in Phénix in particular (FUTURIX irradiations), or in BR2 (IRRDEMO experiment). Specific modeling is also being developed: this involves the CELAENO application, in the PLEIADES platform. The aim is to demonstrate, by 2012, the feasibility, and viability of these GFR fuel element concepts.

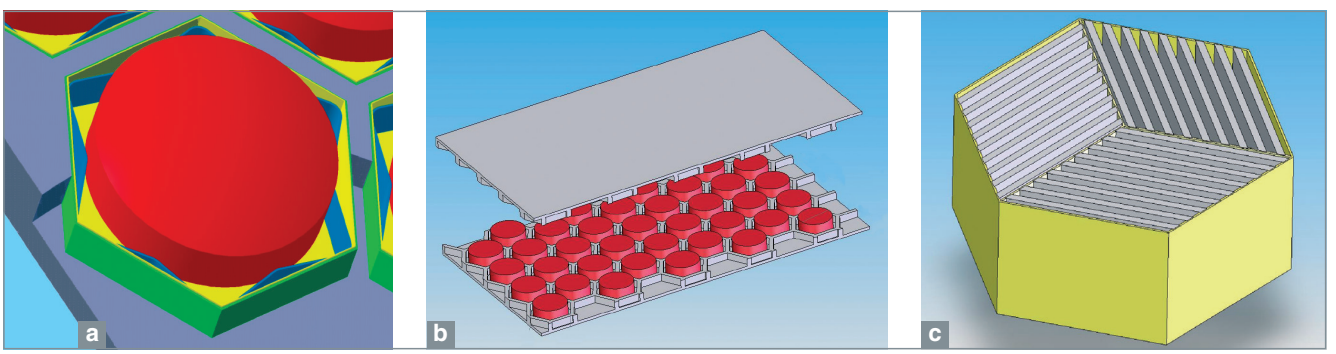


Fig. 123. Schematics showing a fuel compact in its cell (a); a macrostructured plate (b); and stacked plates in a hexagonal casing (c).

## Bibliography

P. Martin, N. Chauvin, “Gas cooled fast reactor system: major objectives and options for reactor, fuel and fuel cycle”, GLOBAL 2005, Tsukuba (Japan), 9–13 October 2005.

J.-C. Garnier, J.-C. Bosq, T. Cadiou, N. Chauvin, O. Cioni, P. Dumaz, D. Lorenzo, F. Morin, A. Ravenet, P. Richard and A. Tosello, “Status of GFR pre-conceptual design study”, ICAPP 2007, Nice (France), 13–18 May 2007.

A. Ravenet, “Macrostructured plate fuel element”, French patent No. 0552488 (2005).

**Yannick Guérin and Michel Pelletier,**
*Fuel Research Department*

# Research reactor fuels

## A considerable feedback from experience

Research reactor fuel design underwent virtually no evolution after these research reactors were commissioned, in the early 1960s. Indeed, the very high power density characteristic of these reactors – up to 1,500 kW/liter core (HFIR, United States) – dictates use of a highly divided fuel, in the form of thin plates about 1 mm thick, mostly comprised of aluminum (selected for its good thermal conductivity). The reference industrial process (see Fig. 124), which involves roll-milling together the fuel meat, or fissile core (a blend of aluminum alloy and aluminum powders), and the cladding (aluminum alloy plates), meets that goal particularly well. This process can draw on considerable feedback from experience, since nearly all experimental reactors use this type of fuel. The process has seen large-scale implementation with NUKEM, in Germany, UKAEA, in the United Kingdom, CERCA, in France, and Babcock, in the United States. The standard fuel thus produced is a UAl (or $UAl_x$) powder-based fuel, involving uranium enriched to 93% U 235 – i.e. high-enriched uranium (HEU) fuel.

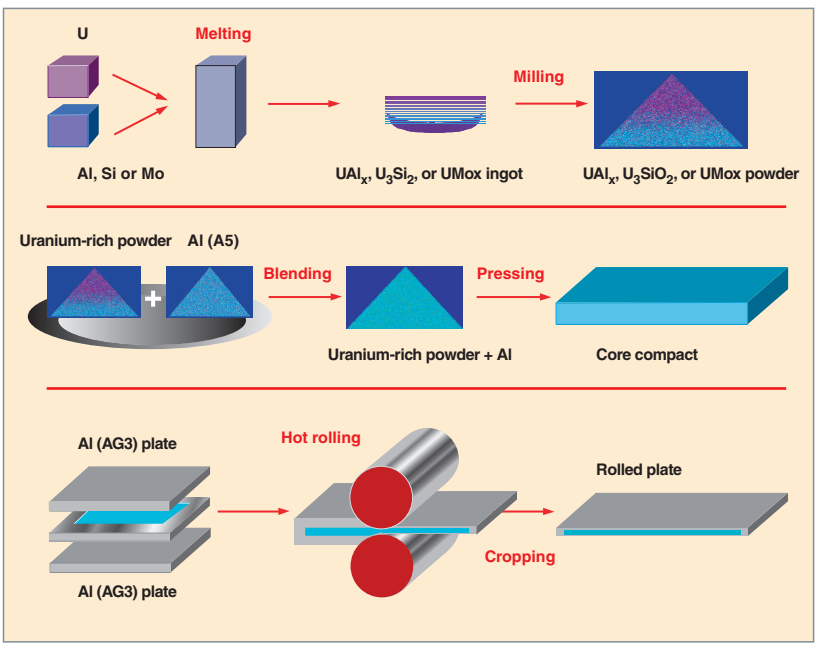


Fig. 124. Principle of the "co-rolling" fuel plate fabrication process.

In the late 1970s, the United States took the decision no longer to export highly enriched uranium (> 20% U 235). This decision was the outcome of a recommendation from Working Group 8 of the International Fuel Cycle Evaluation (INFCE) Program, setting at 20% the limit for uranium enrichment, above which enriched uranium would be deemed to be proliferating [1]. Subsequent to that evaluation, launched by President Carter in 1977, a program for the conversion of research reactors to use of low-enriched uranium (**LEU***) was set in place. In 1978, the US Department of Energy (DOE) charged Argonne National Laboratory (ANL) with this remit. The Reduced Enrichment for Research and Test Reactors (RERTR) program was initiated in 1978, with strong participation from CEA, the organization hosting the second RERTR meeting at Saclay, in 1979.

Such evolutions in research reactor fuel design as have taken place, since 1980, are the result of the implementation of these directives. In particular, new alloys had to be found, involving a higher uranium content, to make up for the shortfall in terms of uranium enrichment, and the new products required qualification under irradiation. The issue is still very much present, and stands at the core of the approach involved in designing the fuel for the Jules Horowitz research reactor, the future European instrument that will be used for neutron irradiation experiments, which should achieve initial criticality at Cadarache (France), by the beginning of 2014 [2].

## Conversion of French reactors to low-enriched (≤ 20% U 235) $U_3Si_2$ fuel

CEA has made an active contribution to qualification of $U_3Si_2$ fuel, in particular through irradiations of miniplates, carried out in the SILOE reactor, and subsequently of full-size plates in the IRIS device, specifically designed to allow accurate measurement of changes in plate thickness, at the end of each cycle.

The ensemble of data required for the purposes of reactor conversion was

published in 1988 by the US Nuclear Regulatory Commission (NRC), under reference NUREG-1313 ($U_3Si_2$ being qualified for a uranium density of 4.8 gU/cm³).

### *Moderate-performance reactors*

***OSIRIS:*** This reactor, which had been using, since the 1970s, Caramel fuel ($UO_2$ enriched to 7%, Zircaloy cladding), was not strictly concerned by the conversion process itself, switching experimental reactors to LEU fuel. However, it was deemed opportune to switch to use of $U_3Si_2$ fuel, qualified as this was to world standards, and fabricated on a large scale by Areva–CERCA.

The conversion process could not be initiated before 1994, owing to specific issues raised by the French safety authority. Thus, specific experiments, such as EPSILON, carried out in the SILOE reactor, were carried out to provide information as to fission product release in accident situations; and irradiation of an instrumented plate was effected to calibrate computation results obtained with FLICA, the CEA reference code for fuel element thermal–hydraulics.

Conversion of the OSIRIS reactor was completed stepwise, by replacing over time spent Caramel fuel elements with $U_3Si_2$ elements.

### *High-performance reactors*

***ORPHEE:*** the computations carried out showed that switching from HEU (high-enriched uranium) $UAl_x$ fuel to silicide (LEU) fuels, which are denser, would result in a major curtailing of core lifetime, by a factor of about 2, along with a hardening of the spectrum, with consequently reduced effectiveness of emergency shutdown systems. On those grounds, it was decided not to proceed with ORPHEE reactor conversion.

***HFR*** (High-Flux Reactor, Grenoble): for the same reasons, and as computations carried out by ANL, regarding HFR, showed that a fuel exhibiting a density of 7.9 gU/cm³ would be required, HFR conversion has been put back to a later date.

The HEU (93%) required for operation of these reactors has been supplied by Russia, since 1997.

## Conversion of all reactors: R&D requirements for high-performance reactors

The main in-service (or planned) reactors concerned by the issue of conversion to LEU, and development of new fuels are set out in the following Table. There are in fact 129 reactors around the world (as of beginning of 2007) using HEU fuel, and targeted by a conversion program.

Moderate-performance reactors, such as OSIRIS, Studsvik, and HFR (Petten) recently (May 2006), have undergone conversion to LEU without any major difficulty being encountered.

Currently, the following may be noted:

- high-flux reactors, in particular HFR (Grenoble), ORPHEE, BR2, ATR, FRM–II, and JHR, may not use LEU $U_3Si_2$ fuel at 4.8 gU/cm³ – the only truly qualified fuel – without incurring a significant downfall in flux performance, or fuel "overconsumption;"
- continued noncompliance, with no set deadline, with enrichment reduction directives is deemed unacceptable, in political terms;
- the issue of the cycle back-end has become critical, since the United States made it known, in 1996, that it would no

**The main research reactors around the world**

| Reactors | Country | MW | Conversion to LEU qualified as of now (E < 20%) |
|---|---|---|---|
| **OSIRIS** | France | 70 | yes |
| **ORPHEE** | France | 14 | no |
| **JHR** | France | 100 | (project: requires qualification of a high-density LEU fuel) |
| **HFR** | France | 57 | no |
| **FRM–II** | Germany | 20 | no (planned use of medium enrichment) |
| **BR2** | Belgium | 100 | no |
| **HFR/Petten** | Netherlands | 45 | yes |
| **Studsvik** | Sweden | 50 | yes |
| **MARIA** | Poland | 30 | partly converted |
| **ATR** | United States | 250 | no |
| **HFIR** | United States | 85 | no |
| **HANARO** | Korea | 30 | yes |
| **JMTR** | Japan | 50 | yes |
| **PIK** | Russia | 100 | (project: planned use of HEU) |
| **MIR** | Russia | 100 | no |
| **SM2** | Russia | 100 | no |
| **RSG–GAS** | Indonesia | 30 | yes |
| **ANSTO** | Australia | 20 | (project: planned use of LEU) |

longer agree to take back high-enriched fuels from other countries, after 2006. As a result, it has become crucial, for countries operating experimental reactors, to find solutions, in particularly by opting for an easily reprocessable fuel, whereas $U_3Si_2$ fuel is deemed "difficult to reprocess."

In this new context, as it emerged in the late 1990s, a reassessment and research process was set in motion, under the aegis of DOE and ANL, with the aim of selecting, and qualifying, by 2006 (this target date having now been pushed back to 2010), a new fuel, to meet the following targets:

- significantly increased density, to allow conversion of all reactors, including those run by DOE;
- ease of fuel reprocessing.

On the basis of these criteria, UMo7–9 (a uranium–molybdenum alloy with 7–9 wt.% Mo) was selected as the best candidate. Indeed, this fuel allows a gain in uranium density of some 40%; and it is recognized as being easily reprocessed, subsequent to the feasibility study carried out by Areva NC and CEA.

The international community, in particular the United States (ANL), Canada, France, Russia, Korea, and Argentina, has come together to organize its contribution to the qualification of this novel fuel.

In France, such investigations are being carried out under the aegis of a collaboration between Areva (more specifically its subsidiary CERCA, a fuel supply leader) and CEA, the latter planning on constructing a large test reactor: the Jules Horowitz Reactor (JHR). The findings from these investigations are shared and analyzed internationally, with ANL in particular. The aim of the French UMo development program is to achieve qualification of a UMo fuel exhibiting a density of up to 8 gU/cm$^3$, for the purposes of:

- meeting flux requirements for so-called "high-performance" reactors – first and foremost the requirements of the future Jules Horowitz Reactor;
- having the ability to supply operators lacking a cycle back-end solution with a substitute, easily reprocessed LEU fuel, as an alternative solution to $U_3Si_2$ fuel.

This program addresses all aspects of the fuel cycle: fabrication, irradiation behavior, code development, reprocessing treatment process validation. Development and qualification work is being carried out on full-size plates.

## An "advanced" research reactor fuel: UMo

### Investigations carried out at CEA regarding UMo, from 1999 to 2003

A five-party agreement, set up between CEA, Cogema, Technicatome, Framatome, and CERCA, served as framework for these investigations, over the years 1999–2003. The main outcomes from this initial phase are outlined in the following paragraphs.

#### *Fabrication process*

For its fabrications of UMo fuel, CERCA uses its so-called "advanced" process, developed and fine-tuned in the course of $U_3Si_2$ fuel fabrication runs, involving densities of up to 6 gU/cm$^3$. The volume fraction taken up by UMo particles invariably stands at about 50%, however fuel zone porosity depends on the nature of the UMo powder used: porosity is higher than 10% for machined and milled powders, lower than 2–3% for powders obtained by the atomization process.[18] The uranium density obtained is slightly higher than 8 gU/cm$^3$. Inspection of the plates (X-radiography, ultrasounds, micrography) has shown these plates meet specifications.

In an initial stage, UMo powders were fabricated by the standard crushing–milling process (the conventional practice for $U_3Si_2$). However, the ductility exhibited by UMo – whereas $U_3Si_2$ is brittle – makes this a resource-intensive step, and unacceptably so, in any event – unless specific development work comes in – for the purposes of industrial-scale production. Initial investigation prototypes were fabricated in this manner (IRIS–1 and UMUS experiments: see the following Table). For subsequent irradiations (FUTURE and IRIS–2), plates were fabricated using atomized powders. The atomization process, on the other hand, has proved industrializable.

#### *The irradiation program*

Qualification of UMo fuel entails demonstrating its satisfactory behavior under irradiation. The irradiation program, involving full-size plates, comprised 4 experiments during the initial phase of the study (1999–2003) [3], involving increasing cladding temperatures. The irradiation conditions used for this program are set out in the following Table, with a comparison shown in Figure 125. The experiments were chiefly designed to determine the effects of high specific power levels (rising from ~ 140 W/cm$^2$ to ~ 340 W/cm$^2$) on the irradiation behavior of UMo–Al particle fuel. The aim was to achieve a maximum

18. This process involves the atomization of liquid UMo over a rotating disc, followed by fast quenching in an argon atmosphere. The particles thus obtained are quasi-spherical. The atomization process is deemed to be the most promising, in terms of industrial production.

| Summary of French experiments carried out under the five-party framework (1999–2003) | | | | |
|---|---|---|---|---|
| **Experiments** | **IRIS–1** | **UMUS** | **IRIS-2** | **FUTURE** |
| **Reactor** | OSIRIS (Fr) | HFR (NL) | OSIRIS (Fr) | BR2 (B) |
| **Year** | 2000–2001 | 2000 | 2002 | 2003 |
| **Number of full-size plates** | 3 | 2/2 | 4 | 2 |
| **Type of UMo powder** | mach.–milled | mach.–milled | atomized | atomized |
| **Enrichment (% U 235)** | 19.75 | 19.75/35.00 | 19.75 | 19.75 |
| **Uranium density (gU/cm³)** | 8.0 | 8.0 | 8.0 | 8.0 |
| **Fabrication porosity (%)** | 11–13 | 11–13 | 1–2 | 1–2 |
| **Max. surface heat flux at BOL (W/cm²)** | 140 | 175/250 | 240 | 340 |
| **Max. cladding temperature at BOL (° C)** | 75 | 90/110 | 100 | 130 |
| **Coolant velocity (m/s)** | 9 | 8 | 9 | 12 |
| **Test status** | complete | terminated after failure | premature termination | premature termination |
| **Number of irradiation cycles** | 10 | 2 | 4 | 2 |
| **Total duration (EFPD)** | 240 | 48 | 60 | 40 |
| **Average burnup (% U 235) at EOL** | 50 | 15 | 30 | 25 |
| **Max. local burnup (% U 235) at EOL** | 67 | 20 | 40 | 33 |

local burnup (BU) of 70%,[19] for each test. As a rule, whichever reactor core management mode is implemented, maximum end-of-life (EOL) local burnup never exceeds 80%.

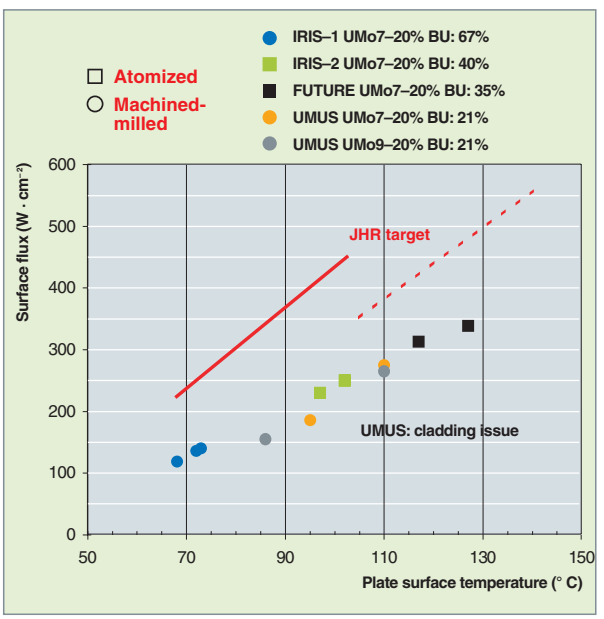


Fig. 125. Evolution of surface flux, as a function of cladding external temperature.

19. Burnup is expressed, here, in terms of the fraction of initial U 235 atoms consumed. Burnup, as expressed in GWd/t, is approximately equal to {936.06*[(0.8232ε + 0.0028) a + 0.031 (1 – ε) a²]}, where a stands for the U 235 depletion fraction, and e for enrichment (from 0 to 1). Burnups of 50%, or 70%, for a fuel enriched to 20% U 235, are equivalent, respectively, to ~ 84 GWd/t, and ~ 120 GWd/t.

Inside OSIRIS, the IRIS device (see Fig. 126) allows, at every end of cycle, measurement of plate thickness, along the entire length of the plates. Thus, IRIS–1 and IRIS–2 plates were measured along 5 axial profiles, and 1 transversal profile, at the level of maximum flux. For the other experiments, UMUs, carried out in HFR (Petten), and FUTURE, in BR2, measurements were taken only at the end of irradiation. A comprehensive program of destructive tests is systematically carried out at the end of irradiation (optical micrography, SEM, microprobe…).

Figure 127 shows the increase (in microns) in plate thickness, as a function of burnup. In the IRIS–1 irradiation, all post-irradiation examinations confirmed the highly satisfactory behavior of high-uranium-loading plates, using machined and milled UMo7 and UMo9 (8 gU/cm³), exhibiting moderate swelling up

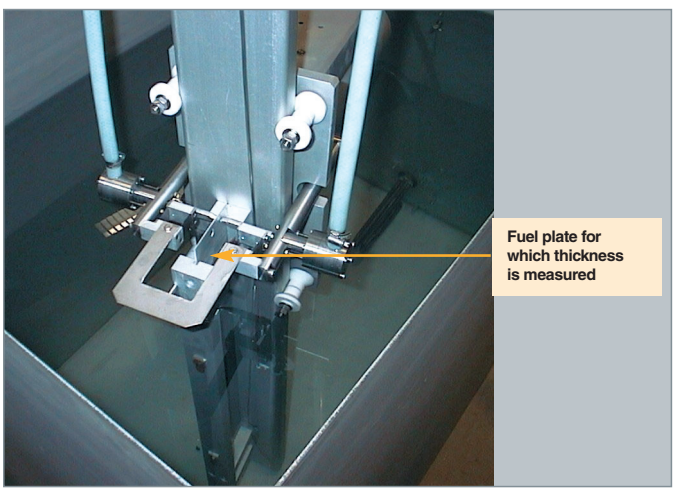


Fig. 126. IRIS device, for the measurement of plate thickness along the entire plate length.

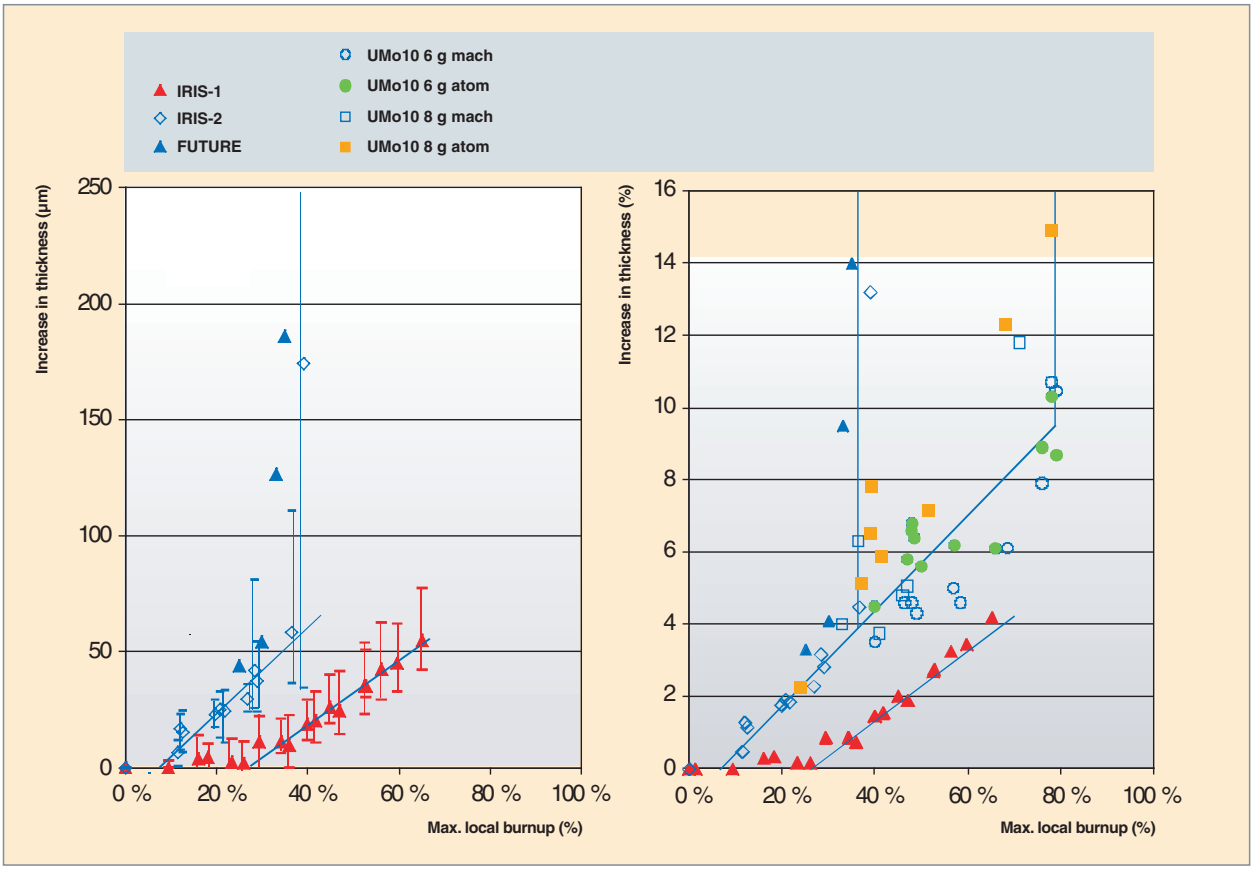


Fig. 127. Increase in plate thickness, as a function of burnup:
a) French tests; b) tests taking into account ANL findings.

to a burnup of 67% (i.e. 240 effective full-power days). No increase in plate thickness was found in the 0–25% burnup range, probably owing to relatively high fabrication porosity (~ 12%). At higher burnups, plate thickness varies in linear fashion, namely 1.4 micron (0.10%) per percent burnup.

The UMUS experiment, carried out in HFR (Petten), was terminated prematurely, after only two cycles, owing to a failure occurring in plates enriched to 35%. This failure was due to excessive cladding oxidation, and consequent fuel overheating. This irradiation showed that the bounding operating conditions for UMo are related to the thickness of the oxide (boehmite) layer.

For the two most stressful irradiations, IRIS–2 and FUTURE, an abnormal increase in plate thickness (see Fig. 127) led to termination of these experiments, after 4 cycles (max. BU 40%), and 2 cycles (max. BU 33%), respectively. At low burnup, the increase in plate thickness varies in linear fashion (up to a burnup of 35–40%), by 1.8 micron (0.13%) per percent burnup, i.e. ~ 30% more than in IRIS–1. Pillowing of the plates is subsequently observed, at the plate hot spots. Fission rate stood at ~ $4.8 \cdot 10^{14}$ f/cm³/s in IRIS–2, $6.5 \cdot 10^{14}$ f/cm³/s in FUTURE.

Metallographic examinations carried out on both types of fuel, IRIS–2 fuel [4] and FUTURE [5], are quite similar. The cause of pillowing is understood, as of now, to involve two concurrent phenomena:

1. An interaction arising between UMo and the surrounding Al matrix (see Fig. 128), this exhibiting unsatisfactory properties under irradiation (thermomechanical properties, fission gas retention…). On the other hand, the satisfactory intrinsic behavior of UMo is confirmed;

2. Formation of coarse porosity at the interface between the interaction region and Al, in which fission products, mainly gases, accumulate. This porosity coalesces, to the point where it forms a cavity, damaging the fuel meat (tearing). Gas pressure is certainly decisive in this respect.

Similar findings were obtained by ANL, on miniplates irradiated in ATR, particularly at high temperature. These findings led to a thoroughgoing reappraisal of the qualification program for UMo fuels, as it had been planned by French and US researchers, if a reprocessable fuel was yet to be provided by the 2010 target date.

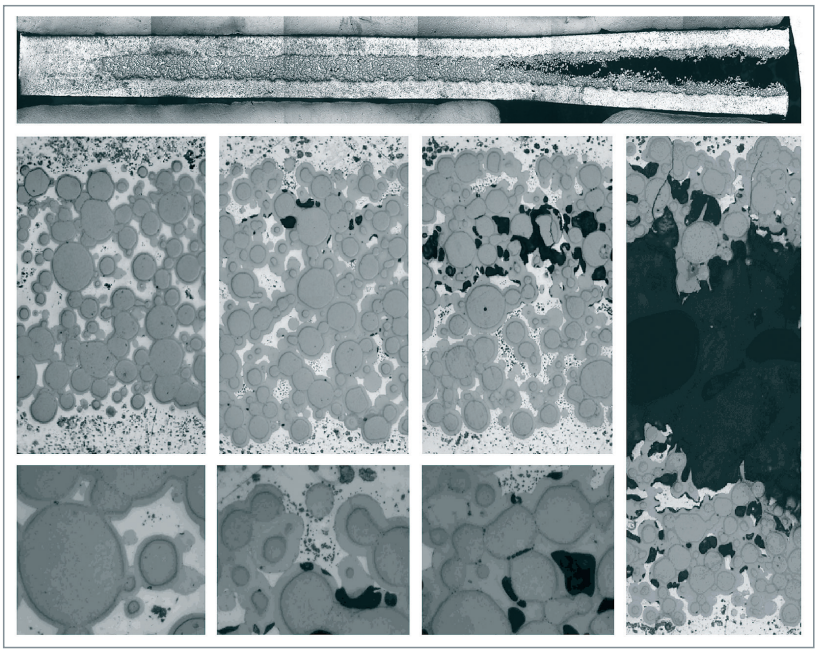

Fig. 128. Metallographic examinations, carried out in the plane of maximum flux, on an irradiated IRIS–2 plate.

### *Irradiation behavior computation codes*

CEA has developed the MAIA application, allowing the thermomechanical and physical–chemical simulation, in normal, incident, or accident irradiation conditions, of fuel plates intended for experimental reactors. The processes modeled include fuel thermics, neutronics, mechanics, and physico-chemistry (external cladding oxidation, formation of an interaction compound, fission product formation). The code is used to support interpretation of experiments, or verification of certain fuel behavior criteria in incident/accident situations.

A program of experimental data acquisition (thermal and mechanical properties), from fuel examined before and after irradiation, makes it possible to modify the laws and models taken into account, and validate the code. This validation is further carried out in the context of a benchmark, known as PLATE, developed by ANL. Argentinian teams are likewise developing their own code, PLACA.

The MAIA code has undergone gradual evolution, to cater for better representation of JHR fuel plates: curved plate, nature of the materials, move to 3D modeling, in order to have the ability to take into account boundary conditions, covering in particular the mechanical effects due to stiffeners.

### *Reprocessing of UMo fuel*

Areva NC have demonstrated the feasibility of UMo reprocessing, compliant with internationally drawn up regulations, as regards specification of glasses. Investigations, and development work are ongoing, with technical support from CEA, in order to confirm, and optimize the process for industrial purposes. Tests carried out in the ATALANTE facility with irradiated plates have confirmed the reprocessability of UMo fuel [6].

### Investigations carried out at CEA regarding UMo, since 2004

UMo in a pure Al matrix, as initially considered for qualification purposes, had shown its limitations, during this first project phase. An R&D program (both in pile and out of pile) was therefore set in motion, with the aim of restricting and/or modifying the characteristics of the interaction arising between UMo particles, and the aluminum matrix.

CEA is thus conducting research work along the four following directions, which also involve international collaborations:

- modification of the Al matrix: use of additives (Si, Ti…), dispersion of various species to trap fission gases…;
- modification of UMo particle composition, or microstructure: ternary alloys (involving Si, Zr, Nb), grain size, Mo homogeneity…;
- ensuring the presence of a diffusion barrier at the UMo–Al interface: coatings, thermochemical treatments…;
- complete elimination of the Al matrix: monolithic concept.

The R&D drive thus launched [7] has the purpose of selecting promising concepts, affording some benefits, to be tested under irradiation. Recent, or ongoing in-pile experiments are beginning to yield encouraging results.

Of the remedies tested, addition of silicon in the Al matrix is the most extensively investigated path. Two new French experiments (see the following Table) have thus allowed its influence to be investigated: IRIS–3 (atomized UMo-based fuel), and IRIS–TUM[20] (machined–milled UMo-based). Plate behaviors, in terms of thickness variations, are compared in Figure 129.

The positive effect of Si is chiefly found in fuels fabricated from atomized powders (IRIS–3), though this requires sufficient amounts of Si (≥ 2 wt.% in Al). The effect is less apparent when the fissile compound is machined and milled. Indeed, the behavior of such fuel is found to be satisfactory, even in a pure

20. An experiment carried out on behalf of the Technical University, Munich (TUM) [Germany].

| Summary (as of mid-2007) of French experiments carried out since 2004 | | |
|---|---|---|
| **Experiments** | **IRIS–3** | **IRIS–TUM** |
| **Reactor** | OSIRIS (Fr) | OSIRIS (Fr) |
| **Year** | 2005–2006 | 2006–2007 |
| **Number of full-size plates** | 4 | 4 |
| **Type of UMo powder** | atomized | mach.–milled |
| **Enrichment (% U 235)** | 19.75 | 49.5 |
| **Si content in Al matrix (wt.%)** | 0.3 or 2.1 | 0 or 2.1 |
| **Uranium density (gU/cm³)** | 8.0 | 8.0 |
| **Fabrication porosity (%)** | 1–2 | 8–9 |
| **Max. surface heat flux at BOL (W/cm²)** | 196 | 250–260 |
| **Max. cladding temperature at BOL (° C)** | 83 | 103 |
| **Coolant velocity (m/s)** | 9 | 9 |
| **Test status** | complete | complete |
| **Number of irradiation cycles** | 7 | 8 |
| **Total duration (EFPD)** | 131 | 147 |
| **Average burnup (% U 235) at EOL** | 49 | > 56 (equivalent) |
| **Max. local burnup (% U 235) at EOL** | 59 | > 74 (equivalent) |

Al matrix, as the IRIS–1 experiment had shown, this being corroborated, on the other hand, by the IRIS–TUM experiment, for high-irradiation conditions (maximum surface flux of ~ 260 W/cm²).

These findings gave grounds for looking into another avenue, explored during out-of-pile investigations, and deemed to be promising: the presence of an oxide layer at the UMo–Al interface. Indeed, machined and milled powders are oxidized during the mechanical milling operation. This parameter could have a favorable effect under irradiation, by altering the kinetics, and nature of the interaction phase. Future post-irradiation examinations will allow better understanding of this issue. A new irradiation (IRIS–4), to test this oxide solution, is indeed scheduled for the end of 2007. This will involve testing the influence of a controlled (in terms of thickness, nature…) peripheral oxide layer, formed by thermochemical treatment of atomized UMo particles.

Finally, the monolithic concept stands as an alternative to the UMo–Al dispersed concept. This involves a clad UMo foil, to restrict UMo–Al exchange surface areas (the Al, in this case, being the cladding). This concept is encountering issues of a technological nature, chiefly as regards UMo foil fabrication, and cladding of the element. New fabrication processes have been developed, from 2005, by Areva–CERCA, with support from CEA. Irradiation of full-size monolithic UMo plates should be initiated at the end of 2007, in OSIRIS, with the IRIS–5 experiment. So far, only miniplates (a few square centimeters large) have been tested under irradiation, by ANL.

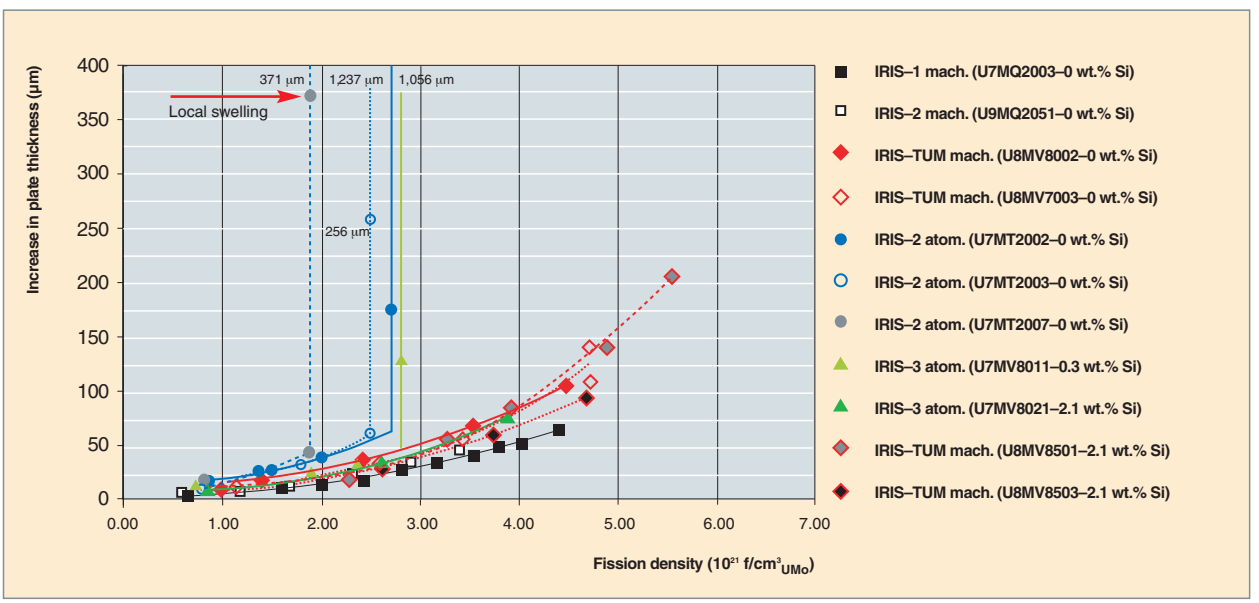


Fig. 129. Comparison of plate thicknesses, for plates testing remedies for dispersed fuel, or involving no remedy [8].

## The startup fuel for the Jules Horowitz Reactor (JHR) will still be $U_3Si_2$–Al

The evolution of research reactor fuels has chiefly occurred as the result of implementation of the nonproliferation directives. For moderate-power reactors, such as OSIRIS, it has proved feasible to use $U_3Si_2$ fuel, qualified to world standards. For high-performance reactors, fuel density must be raised significantly (to around 8 gU/cm$^3$). UMo alloy stands, to date, as the best candidate, owing to its undoubted inherent qualities, such as density, reprocessability, fission product retention capability. It is thus seen as the fuel of the future, both in order to meet the requirements of high-performance reactors, and to secure an industrial cycle back-end for all reactors opting for this solution.

However, UMo maturity is insufficient to ensure startup in JHR, if the target of initial criticality by 2014 is to be met. Consequently, the JHR project, which entered the development stage in 2006, opted [2] to select, as startup fuel, $U_3Si_2$ (dispersed in an Al matrix), this being already in widespread use, in many reactors (OSIRIS, HFR [Petten], JMTR…). Its satisfactory behavior has to be demonstrated, in the specific conditions prevailing in JHR. The uranium loading, and enrichment opted for are, respectively, 4.8 gU/cm$^3$ (this being the density qualified in NUREG-1313), and 27% U 235 (to compensate for the lower density). A qualification program, in normal JHR operating conditions, together with a justification program, for incident and accident conditions, have been launched. The initial experiment for the qualification program has been successfully carried out, at JHR hot spot temperature (140° C): SHARE experiment, in BR2. Construction of a hydraulic loop inside BR2 (EVITA loop) is also going ahead, for the purposes of tests scheduled for 2008–10.

### References


[1] A. Glaser, "About the enrichment limit for research reactor conversion: why 20%?", *27th International Meeting on Reduced Enrichment for Research and Test Reactors (RERTR 27)*, Boston, Massachusetts (USA), 6–10 November 2005.

[2] D. Iracane, "JHR project status", *11th International Topical Meeting on Research Reactor Fuel Management (RRFM 2007) and Meeting of the International Group on Research Reactors (IGORR)*, Lyon (France), 11–15 March 2007.

[3] J.-M. Hamy, P. Lemoine, F. Huet, C. Jarousse, J.-L. Emin, "The French U–Mo group contribution to new LEU fuel development", *9th International Topical Meeting on Research Reactor Fuel Management (RRFM 2005)*, Budapest (Hungary), 10–13 April 2005.

[4] F. Huet, J. Noirot, V. Marelle, S. Dubois, P. Boulcourt, P. Sacristan, S. Naury, P. Lemoine, "Post-irradiation examinations on U–Mo full-sized plates: IRIS–2 experiment", *9th International Topical Meeting on Research Reactor Fuel Management (RRFM 2005)*, Budapest (Hungary), 10–13 April 2005.

[5] A. Leenaers, S. Van den Berghe, E. Koonen, C. Jarousse, F. Huet, M. Trotabas, M. Boyard , S. Guillot, L Sannen a, M. Verwerft, "Post-irradiation examination of uranium–7 wt% molybdenum atomized dispersion fuel", *Journal of Nuclear Materials* 335, 2004, 39–47.

[6] N. Herlet , G. Ferlay, J.-P. Dancausse, A. Juvenelle,"Reprocessing U–Mo spent fuels: dissolution experiments on non-irradiated and irradiated materials", *9th International Topical Meeting on Research Reactor Fuel Management (RRFM 2005)*, Budapest (Hungary), 10–13 April 2005.

[7] S. Dubois, F. Mazaudier, J.-P. Piron, P. Martin, J.-C. Dumas, F. Huet, H. Noël, O. Tougait, P. Lemoine, C. Jarousse, "Out of pile French research program on the U–Mo/Al system: first results", *9th International Topical Meeting on Research Reactor Fuel Management (RRFM 2005)*, Budapest (Hungary), 10–13 April 2005.

[8] S. Dubois, J. Noirot, J.-M. Gatt, M. Ripert, P. Lemoine, P. Boulcourt, "Comprehensive overview on IRIS program: irradiation tests and PIE on high density U–Mo/Al dispersion fuel", *11th International Topical Meeting on Research Reactor Fuel Management (RRFM 2007) and Meeting of the International Group on Research Reactors (IGORR)*, Lyon (France), 11–15 March 2007.



**Alain Ballagny, Patrick Lemoine,**
*Simulation and Experimental Instruments Directorate*
**and Sylvie Dubois,**
*Fuel Research Department*

# An instrument for fuel research: the Jules Horowitz reactor (JHR)

The behavior of nuclear fuels in power reactors is an area of R&D of major importance, calling for instrumented experiments, involving the ability to mimic the fissions, and damage these fuels experience, on the scale of one rod, or a few rods. Such experiments are carried out in research reactors, also known as “materials testing reactors” (MTRs).

Subsequent to the shutdown of the SILOE reactor (Grenoble), France has just one reactor of this kind: OSIRIS (at Saclay), which is due to be shut down in the early 2010s, owing to its technical obsolescence (it first went critical in 1966). For that reason, CEA has been studying, in close contact with its main partners, in France and around the world, a new research reactor: the Jules Horowitz Reactor (JHR), named after the great French nuclear physicist. This reactor will be sited at Cadarache, with initial criticality scheduled for the end of 2013. Operating in conjunction with sample preparation and examination laboratories (LEFCA, LEFCA–STAR), the JHR reactor will provide a crucial research platform, for the purposes of ensuring the optimization, and safety of existing fuels, and for the development of the innovative fuels required for the systems of the future.

Jules Horowitz was one of the great scientists of the present era. Acting in turn as a researcher, politician, and industrialist, he devised the major French nuclear projects. This Polish emigrant, who became a French national, passionately attached to securing energy independence for his adopted homeland, was a major figure in nuclear energy, on the world scene. Already in 1948 a high-flying physicist, he published the first theoretical account of mu meson decay. Subsequently, he built up reactor physics from scratch, with more specific regard to thermal-neutron reactors. He was one of the initiators, alongside other CEA and EDF engineers, of development for the natural uranium–graphite–gas (carbon dioxide) reactor line. He found it hard, indeed, loyal as he was to his first passions, to accept the discontinuation of that reactor line, however he soon came round to advocating the new options, with equal enthusiasm.

## Fuel irradiation experiments in JHR

For the purposes of fuel development, and qualification, two types of experiment may be distinguished. The first type is concerned with the inert materials used to ensure containment of the fissile material (PWR fuel claddings, particle fuel ceramic coatings). The second type addresses the system comprising the fissile material, together with its containment materials.

### *Experiments concerning containment materials*

The purpose of these experiments is to establish macroscopic mechanical behavior laws for metallic claddings, or coating ceramics, subjected at the same time to three kinds of stresses, mechanical, thermal, and irradiation stresses.

The advances achieved in the understanding of the mechanisms involved make it possible to complement macroscopic tests with more finescale experiments, enhancing, when combined with numerical simulation, the ability to extrapolate findings.

A major industrial, and scientific challenge is set by the investigation of the viscoplastic behavior of such materials under irradiation. Within the parameter space of deformation rate, temperature, radiation flux intensity, the coupling of mechanisms involved in the production, and diffusion of heterogeneities determines the creep laws, these in turn being crucial with regard to fuel lifetime, and management of incident or accident transients.

Post-irradiation tests are essential, however the coupled character of the mechanisms involved further entails that experiments be carried out under flux, in a research reactor.

By way of illustration, to take the case of fuel claddings, investigations of irradiation creep have led to the proposal that JHR feature – to complement conventional tests, which remain a requisite – an experimental device, allowing:

- the setting up, under flux, of a biaxial stress (this being required by the anisotropic character of such materials as zirconium);
- online monitoring and control of this mechanical stress, the aim being to vary, and measure this stress on line, to explore the various microstructural states the material goes through;

• the rigorous control of thermal gradients, as the necessary precondition for the proper interpretation of data. Such control of gradients sets a strong technological challenge, considering the high irradiation rates being aimed for (some 15 dpa [displacements per atom] per year), owing to adventitious heating processes, due to the ambient gamma flux. A forced-circulation NaK coolant technology, to be mounted in the device itself, is being developed (see Fig. 130).

With respect to pressurized-water reactors, and boiling-water reactors, corrosion stands as one further coupling parameter, which, if it is to be taken into account, requires precise control of temperature, irradiation conditions (as regards both sample, and coolant, owing to the effects of radiolysis), and mechanical stresses. The specification of relevant protocols, and the development of instrumentation to measure local chemistry, and crack propagation are being addressed by collaborations with European partners.

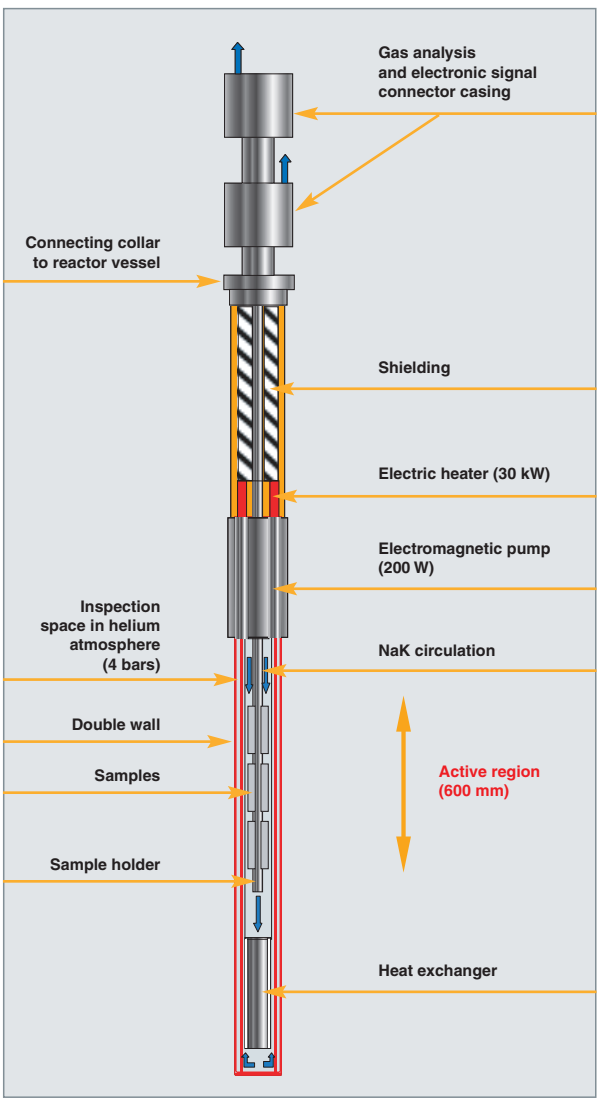


Fig. 130. A viscoplasticity experiment, involving online control of biaxial mechanical stresses.

In the area of high-temperature materials (e.g. SiC–SiC ceramics), the aim initially is to carry out tests in high temperature ranges (1,000° C and above), entailing technological developments as regards instrumentation. In the longer term, experiments involving online monitoring and control of mechanical stresses will also be required.

### *Experiments concerning the fuel system*

The aim, in this case, is to ascertain fuel behavior at the end of life (i.e. at high **burnups***), and during the various incident and accident transients. The devices, and experimental loads used to carry out fuel irradiations in JHR will be designed, in particular, to allow:

• catering for fuel base-irradiated in reactor, and reconditioned in an experimental load. The fuel, and its sample-holder, may be instrumented (thermocouples, pressure sensors, profile measurements…);

• speeding up experiments, in order to achieve rapidly the target burnup, or **fluence*** values, while not disturbing the relative magnitude, and importance of the physical processes governing fissile matrix evolution. For the purposes of materials physics, rather than focus on representativity of the neutron spectrum, the point is to reproduce actinide fission rate, and the damage rate (**dpa***) in inert materials. In many situations, arising with PWRs, VHTRs, or GFRs, it is crucial that the proper burnup-to-dpa ratio be ensured, if the experiment is to be representative of the interaction between fissile, and inert materials. Control of that ratio dictates the experimental location within JHR, and device design. Converter devices may be used, to effect local modification of the neutron spectrum "experienced" by the experimental load;

• mimicking, at the level of the experimental load, the range of environmental conditions the fuel may experience in reactor (neutron flux, and spectrum; volumetric power, and/or temperature; coolant chemistry, nature, pressure, and velocity, etc.). This range is to be reproduced, around the sample, by means of programmed, gradual variations of such parameters (transients, cyclings…). Here again, good experiment quality entails extremely precise control, e.g. of thermal gradients at the level of the fuel sample;

• favoring online instrumentation (temperatures, pressures, monitoring of fission gases emanating from the fuel rod…). Such online monitoring of measurements is an essential component in the JHR design, the reactor featuring a dedicated control room, for experimenters.

Depending on fuel type, irradiation will be carried out in the reactor reflector (the reflector, made up of beryllium blocks, surrounds the core, to limit neutron leakage), or in the core (e.g., for investigations concerning fast-neutron reactor lines, when a high dpa level is required). Power may be adjusted,

either by moving the load relative to the core, or by means of an absorber screen. This screen may also serve to adjust neutron spectrum balance, to ensure the proper dpa/burnup ratio.

Fuel experiments, in JHR, will be able to draw on specific analytical resources – complementing irradiation test resources – such as the fission product analysis laboratory, gammagraphy and neutronography inspection benches, and hot cell for (non-destructive) fuel examination.

To take the example of water reactors, such resources make for effectiveness, when conducting the experiments detailed in the following paragraphs.

### Fission gas distribution, and release

Knowledge of the mechanisms governing the migration of fission products (gases in particular), as a prerequisite for a mechanistic approach of the phenomena, is a key point for the optimization of in-reactor fuel utilization, more particularly with respect to fuel lifetime. Measurement of the amounts of fission gases – whether stable, or radioactive – released from the matrix in steady operating conditions, together with measurement of emission kinetics during transients, or cycles (in terms of power, and/or temperature), are privileged tools, for the purposes of obtaining either a "snapshot" of the microstructural state, or a master clock, by which phenomena may be paced.

Such measurements are usefully complemented by destructive post-irradiation examinations (release of gases held in the matrix through heat treatments, microprobe analyses, etc.).

### Thermomechanics of the experimental load

The physical processes governing the evolution of the fissile matrix under irradiation, at the microscopic scale, are, as a rule, highly temperature-dependent. Accumulation of fission gases at the grain boundaries, and their release to free volumes are key instances in point. The resulting gas distribution determines the macroscopic evolution of fuel geometry over time, due to densification, gas and solid swelling, and, ultimately, interaction with the cladding (or coating) forming the first fission product containment barrier.

### Fuel–coolant interaction and fission gas release in the event of loss of integrity in the first barrier

The import of this issue is, first and foremost, an operational one. This issue is decisive for power reactor operation, by way of the technical operating specifications concerning primary coolant circuit activity. Knowledge of the fission product activity levels that will be reached in that circuit is, indeed, of crucial importance as regards reactor operation – with respect to the dosimetry of workforce exposure levels, intervention conditions during unit outages, control of the activities rejected in effluents, and, ultimately, installation decommissioning.

Also, understanding the behavior of fuel "element" (rod, particle…) internal free spaces, in situations involving interaction with the coolant further makes it possible to specify the physico-chemical reactions arising at the surface of the fuel, and quantify a possible degradation kinetics, which may involve concomitant release of fissile material (at the irradiation, or disposal stage).

### Behavior during certain incident situations (power "ramps"), or accident situations (loss of coolant accident)

Separate-effect experiments allow the requisite investigations to be carried out, for the purposes of industrial reactor safety. The aim is to mimic the mechanisms involved in reactivity and/or heating transients. Even though incident or accident parameters are not fully reproduced, such tests allow the activation of a limited number of physical mechanisms, in order to quantify their individual effects, and evidence the various couplings that arise. Interaction between fuel and first barrier, along with the kinetics of fission gas release, and its possible effect on fuel mechanical strength are privileged topics for investigations carried out by way of such experiments.

As regards gas-cooled reactors, online measurement of fission products is a central tool, for the purposes of fuel development, and qualification, entailing as these do statistical approaches to loss of confinement.

With regard to gas-cooled fast reactors, experiments with particle fuels in the JHR core will allow simulation of the proper level of both fast, and thermal flux. This will require inserting screens, to restrict the intensity of the thermal-neutron flux.

## *The contribution of a fission product laboratory to the investigation of nuclear fuel behavior*

The online availability of a fission product laboratory provides an essential complement, as regards JHR's experimental capability.

Nuclear fuel, whichever reactor line is considered, is a product that undergoes far-reaching evolution in the course of its dwell-time in the neutron flux. Fission products are highly diverse chemical elements (gaseous; volatile and nonvolatile solids), involving content levels much higher than what might be termed impurities. Of these, noble gases (xenon, and krypton) play a specific part, owing both to their abundance (about 1/3 of all fission products), and to their behavior in the fuel. Indeed, they diffuse readily across the material, due to local thermal conditions, forming either nano- or microbubbles within grains, or bubbles at grain boundaries. A small fraction escapes from the fuel, becoming available in open porosities, and the fuel element's internal free volumes.

The amount, and distribution of such fission gases are decisive factors, limiting in-reactor fuel lifetimes. Their effects chiefly involve:

- the formation of thermal barriers, owing to their high insulation capacity (accumulation of bubbles, opening up of gaps), causing an increase in fuel temperature;

- a rise in internal pressure, resulting in mechanical stresses imparted to the first barrier;

- the formation of a source term, in the event of accident, owing to the instant availability, and radioactive character of a fraction of these noble gases.

Nuclear fuel optimization (increasing lifetime, enhancing fission product retention, in the event of accident…) entails, primarily, improved control of the mechanisms governing fission gas behavior (distribution, migration). A privileged experimental strategy, to gain an understanding of these mechanisms, involves setting up an external stress to which the fuel material is subjected, such as a power or temperature transient, and analyzing the material's response to that stress. The measurement then relies:

- either on the radioactive character of some of these gases, this providing a natural clock. Indeed, the correlation law, between release level and radioactive half-life, makes it possible to identify the mechanisms involved;

- or on the overall released fractions of stable fission gases, allowing identification of the gas "vessels" voided under stress (see Fig. 131).

The fission product laboratory associated to JHR thus provides an ensemble of analytical resources, required for the purposes of gaining such knowledge, set up in cells, in bunkers inside the reactor building. The sample undergoing irradiation is fitted with a short internal scavenging line, allowing the recovery of released radioactive gases having a half-life longer than a few minutes. The composition of the mixture, in terms of its various nuclides, may then be ascertained either by gamma spectrometry (on line, on the piping; or delayed, using traps), or chromatography and mass spectrometry.

The laboratory further allows measurement of released fission products, other than gases, along with activation products, in that part of the irradiation device's cooling fluid is diverted through the facility. Measurements are chiefly based on gamma spectrometry of this fluid. Circuit purification equipment allows fission products to be separated according to physical–chemical nature, and kept for the purposes of further, complementary analyses (beta or alpha spectrometry, absorption spectrometry…). Areas of investigation as diverse as the release of activity from fuel in a loss of tightness situation, component corrosion under a neutron flux, measurement of specific elements (tritium, helium…), or activity balances inside a device, after the experimental load has been subjected to an accident sequence, become accessible, through the fission product laboratory.

The experiments to be carried out in JHR, and its associated laboratories will partly come under the aegis of common-interest, international research programs, partly under research projects on behalf of manufacturers in the European Union, or from around the world.

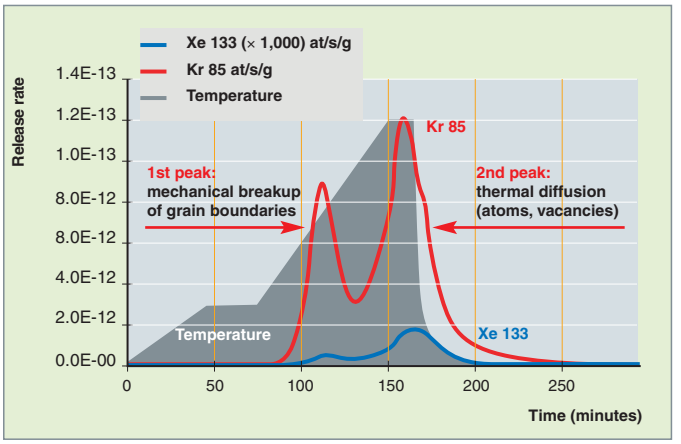


Fig. 131. Fission gas release rate, as a function of fuel temperature.

## JHR: a flexible instrument

JHR, initial criticality for which is scheduled for 2013, is a pool-type, pressure-vessel reactor. It will have a thermal power of 100 MW. The highly compact core (a cylinder 60 cm in height, and diameter) comprises a pressure vessel enclosing a rack, holding about 40 fuel elements. The latter take the form of cylinders, 600 mm high and 95 mm in diameter, consisting of curved plates (3 × 8 plates per element), assembled together, allowing space for the channels required for coolant water circulation. The water-moderated core will be fitted with beryllium reflectors (see Fig. 132).

Coolant water, circulating from base to top, is injected at a pressure of 14 bars, and a temperature of 25° C, exiting at a pressure of 5 bars, and a temperature of 35° C.

To achieve the required performance, while using low-enriched uranium, the fuel, currently being developed, will involve uranium–molybdenum (8% Mo) alloy-based plates, the alloy being dispersed in an aluminum matrix, with an aluminum-alloy cladding.

The core has the capability to deliver high fast-neutron (i.e. neutrons with energies higher than 1 MeV), and thermal-neu-

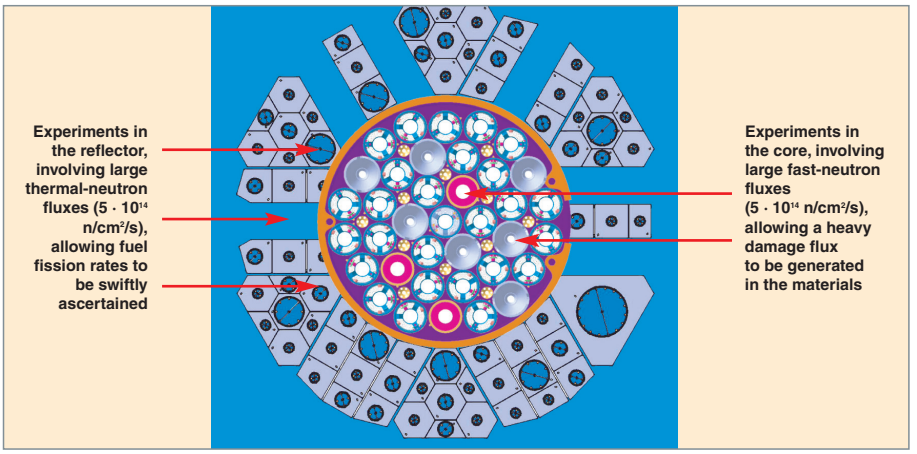


Fig. 132. The JHR core is contained in a cylinder some 60 cm in diameter, and height.

tron (with energies lower than 1 eV) fluxes; either flux may reach $5 \cdot 10^{14}$ n/cm²/s. Locally, addition of driver fissile material makes it possible to modify, and increase the neutron flux received by the experimental load.

JHR may accommodate some 20 experiments simultaneously, involved in optimization of materials, and fuels, whether in use, or being developed for the nuclear systems of the future.

By selecting the position for the experiment, and by way of local contrivances in the core, or reflector, the thermal-neutron, fission-inducing flux, and the fast-neutron flux – and thus the damage to materials used for fissile material containment – may be adjusted to simulate fuel behavior for the various technology lines. The JHR core's power density makes it possible to deliver a fast-neutron flux much higher than that generated in thermal-neutron reactors, of the same order of magnitude as that prevailing in gas-cooled fast reactors. With respect to sodium-cooled fast reactor technology, the highly instrumented experiments carried out in JHR will complement those, of a more global character, carried out in reactors belonging to that technology line, such as Phénix, or Monju. Test loops (pressurized-water loops, boiling-condition water loops, gas, or sodium loops) allow the local mimicking of environmental conditions for the various power reactor lines.

The design of the reactor building (see Fig. 133) gives pride of place to a large experiment area, used to carry out irradiation experiments. Fuel behavior, in experiments simulating normal conditions, but equally incident or accident situations, will be monitored by means of extensive instrumentation. Coupled with modeling, such instrumentation makes it possible to extrapolate findings to situations inaccessible to direct experiment. JHR is designed to carry out, as a standard procedure, online measurement of fission products yielded by experimental fuel loads.

Online measurements, together with the setting up of realistic environmental conditions, with respect to various reactor lines, dictate the use of a set of bunkers, located over three levels inside the reactor building, as close as possible to the irradiation area.

The nuclear island (see Fig. 134) comprises the reactor building, associated to a nuclear ancillaries building, allowing conduct of the experiment as a whole: preparation of the load in the experimental device, irradiation, management of the post-irradiation part of the experiment (nondestructive measurements), retrieval of the experimental load – possibly stressed to failure point – to direct it to the analysis laboratories (LECA–STAR…).

**Daniel Iracane,**
*Simulation and Experimental Instruments Directorate*
**and Daniel Parrat,**
*Fuel Research Department*

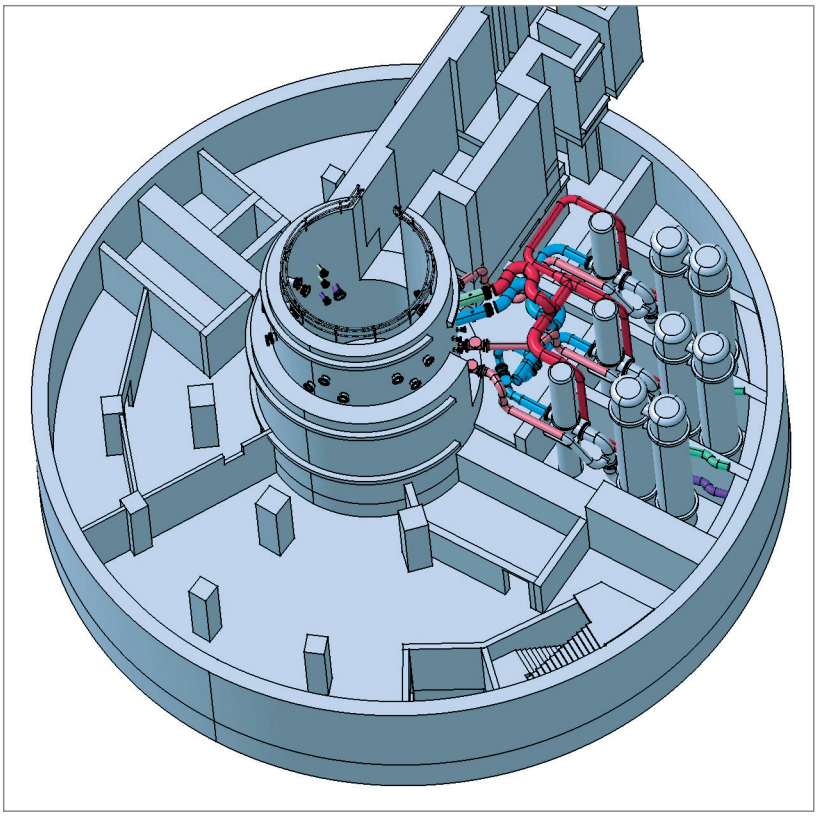

Fig. 133. The reactor building.

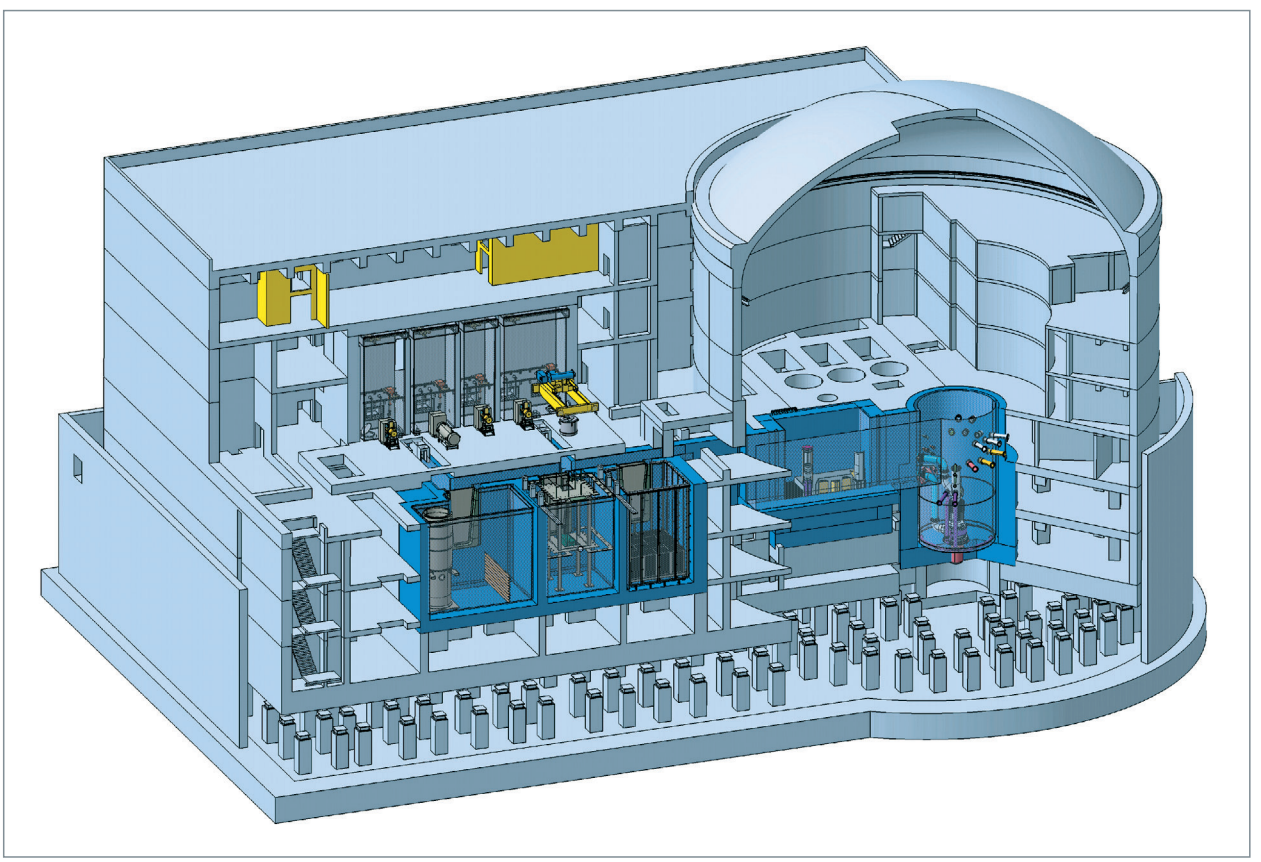

Fig. 134. The nuclear island.

# Glossary – Index

**Actinides:** rare-earth elements, having atomic numbers ranging from 89 to 103. This group corresponds to the filling up of subshells 5f and 6d. Actinides exhibit very similar chemical properties to one another. 7, 8, 31, 34, 77–81, 84, 93, 99, 100, 101, 123, 124.

**Activation:** the process whereby certain nuclides, particularly within structural materials in reactors, are made radioactive, through neutron bombardment, or bombardment by other particles. 21, 33, 38, 138.

**Additive** (sintering)**:** a chemical element added to a powder, in order to control the sintering process, and the **microstructure*** of the sintered material. 15, 47, 49.

**Amoeba** (effect)**:** the migration of the kernel in a fuel particle, under the effect of a temperature gradient. 110, 111, 119–121.

**ANDRA:** the French National Agency for Radioactive Waste Management (Agence nationale pour la gestion des déchets radioactifs). 5, 85.

**Assembly** (fuel)**:** in the core of a water reactor, fuel **rods*** are grouped into bundles exhibiting adequate stiffness, precisely positioned within the reactor core. It is that structure as a whole, comprising from 100 rods or so to several hundred rods, loaded as a unit into the reactor, which is known as a **fuel element***, or assembly. 7–13, 35, 36, 38, 51–57, 71–75, 87–89, 95–97.

**Barn:** the unit used to measure **cross-sections*** (1 barn = $10^{-24}$ cm$^2$). 99.

**Boiling-water reactor (BWR):** a reactor in which water boils directly inside the core. 12, 13, 16, 42, 71, 73, 87, 88.

**Boron:** an element used, among other applications, as a neutron absorber in nuclear reactors. 71, 72, 107.

**Buckling:** the collapse of a mechanical structure, owing to a loading that makes it unstable. 55, 56.

**Burnup:** strictly speaking, this refers to the percentage of heavy atoms (uranium, and plutonium) that have undergone **fission***, over a given time interval. This term is commonly used when evaluating the amount of thermal energy, per unit mass of **fissile*** material, yielded in reactor, from the time of loading, to discharge of the fuel; it is then expressed in megawatts–day per tonne (MWd/t). **Discharge burnup*** is the value for which the fuel assembly, after several irradiation cycles, must be finally discharged. See the Monograph as a whole. 71-75, 93, 113, 117, 119.

**CABRI:** a research reactor, used for investigation of accident situations. 63–65, 91, 93.

**Capture:** the capture of a neutron by a nucleus. Capture is said to be “radiative,” if it is immediately followed by emission of gamma radiation. It is said to be “fertile,” if it yields a fissile nucleus. 17, 19, 35, 72, 88, 95, 99, 100, 123.

**Cladding:** an envelope, encasing the fuel material, having the purpose of ensuring fuel isolation and mechanical strength inside the reactor core. 9–11, 16–18, 35–47, 59–68, 93, 95–97, 100, 109, 124, 125, 128, 130, 131, 133, 135, 137.

**Control rod:** a movable rod, or group of rods moving as an integral unit, containing a neutron-absorbent material, and which, according to its position in the core of a nuclear reactor, influences its reactivity. See **Rod cluster control assembly***.

**Conversion:** the chemical transformation of uranium, for the purposes of enrichment, storage, or nuclear fuel fabrication. 13, 103, 34.

**Coolant:** the fluid (a gas, or liquid) used to remove the heat generated by **fissions***. In a **pressurized-water reactor***, water plays the role both of coolant, and moderator. 7, 35, 41, 52, 93, 103, 119, 123–125, 136–138.

**Core melt:** a nuclear accident in which the nuclear fuel is brought to a sufficiently high temperature for it to melt, and pool together in the form of a corrosive magma (the **corium***), at the bottom of the reactor vessel. 70.

**Corium:** a mixture of molten materials, yielded by the accidental meltdown of a nuclear reactor core. 67, 68, 70.

**Creep:** the gradual deformation of a solid body, due to a stress field, applied over extended time intervals. Creep may be activated by heat (this is then known as “thermal creep”), and/or irradiation. 18, 20, 36, 37, 41, 43, 44, 47, 48, 52, 54, 60, 61, 83, 96, 109, 116, 125, 135.

**Critical:** this refers to a medium in which a fission chain reaction is self-sustaining, i.e. where the same number of neutrons are yielded, as disappear. 42, 60, 136.

**Criticality:** the characteristic state of a mass of material containing fissile elements, and, as the case may be, other elements, in such a configuration – composition, proportions, geometry – that a fission chain reaction may be self-sustaining within the material. 67, 71, 99.

**Cross-section:** the measure of the probability of interaction between a particle and a target nucleus, expressed in barns (1 barn = $10^{-24}$ cm$^2$). In the case of the **neutron***, for instance, this defines its probability of interaction with nuclei in the material. 17, 35, 77.

**Delayed neutrons: neutrons*** released by **fission*** fragments, with a delay, on average, of a few seconds after fission has occurred. Though accounting for less than 1% of neutrons released, they ultimately allow reactors to be controlled. See also **Effective beta***. 77, 100, 101, 107, 123–125.

**Dislocation:** a defect affecting the array of atoms, in a crystalline solid. A distinction is made between dislocations involving insertion of an extra half-plane of atoms in the crystal (edge dislocations), and those involving the crystal lattice being cut along a half-plane, with atoms in the crystal shifted parallel to, and on either side of the half-plane (screw dislocations). 14, 31, 33, 36, 37, 95, 96, 135.

**Disposal** (of nuclear waste)**:** a disposal facility is an installation where waste is held, with no notion of retrieving it at a later date. Retrieval would nonetheless be feasible, in the reversible disposal case (see also **Storage***). 79, 81, 83–85, 101, 137.

**dpa:** the number of displacements per atom, induced in a material under irradiation. This is an appropriate unit to quantify irradiations in metals. 92, 95–97, 124, 136, 137.

**Ductility:** the ability of a material to undergo plastic deformations. 36, 60, 64, 68, 124, 125, 129.

**EFPD:** a unit of operating time, for a nuclear reactor, expressed in terms of "effective full-power days." 71, 72, 130, 133.

**Enrichment:** a process which, in the case of uranium, allows, by various means (gaseous diffusion, ultracentrifugation, selective laser excitation), an increase in the concentration of isotope 235, relative to isotope 238, which is predominant in natural uranium. 13, 71, 72, 74, 75, 77, 87–89, 111, 112, 124, 127, 128, 130, 133, 134.

**Epithermal** (neutrons)**:** neutrons having an energy in the 10 eV–20 keV range (approximately), thus endowed with a velocity higher than that of thermal neutrons. 17, 19, 99.

**Eutectic:** the melting point of a binary mixture depends on the proportions of its constituents. It may be considerably lower than the melting point of either constituent, in pure form, reaching a minimum value for a so-called "eutectic" composition. 7.

**Fast reactor (FR):** a reactor using no **moderator***, in which most fissions are caused by fast neutrons, i.e. neutrons exhibiting energies of the same order as that they are endowed with when yielded by fission. 8, 91, 93, 95–97, 99–101, 124, 136.

**Fertile:** term used to refer to a material the nuclei of which yield, by neutron absorption, **fissile*** nuclei. This is the case of uranium 238, which yields plutonium 239. A material is said to be "sterile," when this does not occur. 71, 91, 101, 103, 104, 123.

**FIMA** (fission per initial metal atom)**:** a unit of burnup for nuclear fuels, expressed in terms of the fraction of fissions occurring in a population of atoms. The correspondence with specific burnup (MWd/tM), which is the preferred measure used by reactor operators, stands at 1% FIMA ≈ 9,500 MWd/tM. This may be compared with the nominal burnup for PWR $UO_2$ and MOX assemblies, which currently stands at 52,000 MWd/tM (5.5% FIMA). 92, 93, 112, 113, 116, 117, 120, 123.

**Fissile** (nucleus)**:** a nucleus liable to undergo **fission*** through **neutron*** absorption. Strictly speaking, it is not the so-called "fissile" nucleus that undergoes fission, rather it is the compound nucleus formed subsequent to a neutron capture. 71, 75, 91, 124.

**Fission:** the splitting of an atomic nucleus into two fragments. This transformation, which is a particular case of radioactive decay, occurring for certain heavy nuclei, releases a considerable amount of energy, with concomitant emission of neutrons, and gamma radiation. Fission of so-called "fissile" heavy nuclei may be induced by collision with a neutron. See the Monograph as a whole.

**Fission products: nuclides*** yielded either directly, by nuclear **fission***, or indirectly by the **decay*** of fission fragments. See the Monograph as a whole.

**Fission spike:** fission fragments travel, on average, 5–8 µm in the fuel, before they are stopped. Along their paths, atoms are very strongly excited, and thousands of point defects are generated by elastic collisions by the end of their travel. Some 5,000 Frenkel pairs remain in the crystal after each fission. It is this region of disorganized material that is known as a "fission spike." 17.

**Fluence:** a measure of dose, used to quantify the irradiation of materials. The number of incoming particles (e.g. neutrons) per unit surface, during irradiation. 73, 95, 109, 112, 115, 116.

**Frenkel pair:** see **Point defect***.

**Fretting:** the wear occurring in a material, under the combined effect of friction, and corrosion (the term is used more particularly to refer to the wear arising in a fuel rod, at the point where it is in contact with the support grid, in the assembly). 21, 51, 54, 55, 57.

**Fuel cycle:** the ensemble of steps undergone by fuel, from ore extraction to waste disposal. 7, 8, 74.

**Fuel element:** see **Assembly***.

**Fuel:** a constituent material, in the **core*** of a nuclear reactor, containing **fissile*** elements sustaining a **chain reaction*** within the material. See the Monograph as a whole.

**GAIA:** a particle fuel fabrication facility, at CEA's Cadarache Center. 107, 108.

**GFR:** gas-cooled fast reactor. 123–126, 136.

**HEU** (high-enriched uranium)**:** uranium enriched to more than 20% uranium 235. 119, 127, 128.

**Interstitial:** (see **Point defect***).

**Irradiated fuel:** fuel assemblies taken out of a nuclear reactor, after a time of useful energy production. Also known as "spent fuel." 26, 27, 63, 65, 69, 78, 82, 116.

**Irradiation cycle:** the time interval over which a reactor is operated, between two successive loadings. 9, 17, 71–74.

**Isotopes:** forms of one and the same chemical element, for which the nuclei have the same number of protons, but different numbers of neutrons. Uranium 238 and uranium 235 are isotopes of uranium. 7, 21, 23, 59, 72, 73, 77, 78, 103.

**Jules Horowitz Reactor (JHR):** see in particular the chapter on "An instrument for fuel research: the Jules Horowitz Reactor (JHR)". 129, 134, 135.

**Labile release:** a fraction of the radionuclide inventory liable to undergo instantaneous release, when water comes into contact with irradiated fuel. This chiefly involves soluble fission products, dissolved into the water, and is independent of the containment properties exhibited by the various layers in the irradiated fuel. It is chiefly dependent on water accessibility, and the amounts of FPs segregated, or sorbed on the fuel's outer surface. 84.

**LEU** (low-enriched uranium)**:** uranium enriched to less than 20% uranium 235. 111, 112, 119, 120, 127–129, 134.

**LOCA:** loss of primary coolant accident. This type of accident is included as part of the design basis, for safety purposes, in water reactors. 51, 58–61.

**MARGARET:** a model describing fission gas behavior in fuel pellets. 29, 30.

**Martensitic** (structure)**:** a body-centered cubic crystal structure, found in certain metal alloys, certain steels in particular. 95-97.

**METEOR:** a model describing the behavior of a fuel rod under irradiation. 29, 30, 43.

**Microstructure:** as applied to nuclear fuel, or a metallic material, this term refers to the conformation, size and configuration exhibited by a polycrystalline material. 18–21, 23, 25, 26, 36–38, 46–49, 83, 91, 95, 96, 100, 101, 113, 120, 121, 132, 136, 137.

**Minor actinides:** heavy nuclei, yielded, inside a reactor, by successive neutron captures, from nuclei in the fuel. The isotopes chiefly involved are neptunium (237), americium (241, 243), and curium (242, 244, 245). 8, 78–80, 84, 93, 99–101, 123, 124.

**Moderation ratio:** in a reactor, the ratio of the quantity of moderator material (water, as regards **PWRs***, in particular), over the quantity of fuel. This ratio governs average neutron energy. 103.

**Moderator:** a material consisting of light nuclei, slowing down **neutrons*** by way of elastic scattering. This is used is slow-neutron nuclear reactors, to increase the probability of interaction between neutrons, and heavy nuclei in the fuel; the moderator should have a low capture capability, to avoid neutron "wastage," and be sufficiently dense to ensure effective slowing down. 72, 87, 88.

**MOX** (mixed oxides)**:** a mixture of (natural, or depleted) uranium oxide, and plutonium oxide. See the Monograph as a whole, and more particularly: 14, 25, 48, 74, 78–80.

**Neutron flux:** the number of neutrons passing across a unit surface, per unit time. 35, 43, 73, 91, 99, 124, 137, 139.

**Neutronics:** the study of the paths followed by **neutrons*** in **fissile***, or nonfissile media, and of the reactions they induce in matter, in particular inside nuclear reactors, with regard to their multiplication, and the initiation, and control of the **chain reaction***. 7, 30, 35–38, 42, 51, 71–73, 75, 78, 87–89, 91, 95, 99, 100, 103, 116, 119, 123, 124, 127, 132, 136–138.

**Nitride:** 7, 8, 34, 92, 93.

**ODS** (oxide-dispersion-strengthened)**:** an alloy strengthened by oxide nanoparticles. 96, 97.

**ORPHEE:** a French research reactor. 128.

**OSIRIS:** a French research reactor. 42, 45, 49, 52, 68, 128, 130, 133–135.

**Particle fuel:** see the chapter on "Particle fuel". 103.

**PCI:** pellet–cladding interaction. 30, 41–43, 45, 47, 48.

**Pellet:** a small cylinder of uranium- or plutonium-based ceramic, or ceramic involving other actinides, used as nuclear fuel. See the Monograph as a whole, and more particularly: 10, 13–16, 18–20, 41–46, 100.

**PHEBUS:** a research reactor, used for investigation of accident situations. 69.

**PHENIX:** a prototype sodium-cooled **fast reactor***. 91–93, 95–97, 139.

**PLEIADES:** a dedicated fuel computation software platform. 30, 43, 46, 116, 126.

**Plenum:** in a fuel rod, the plenum is a free volume within the rod, holding no fissile material. This space serves to confine fission gases released by the fuel, preventing such release from causing too much increased pressure in the rod. 10, 47, 85, 100.

**Plutonium:** an element generated through neutron capture in uranium, inside nuclear reactor cores. The unevenly-numbered **isotopes*** are **fissile***, plutonium consequently being a recoverable nuclear material, for value-added purposes, e.g. for use in the form of **MOX*** fuel. See the Monograph as a whole, and more particularly. 9, 14, 25, 47, 71-80.

**Point defect:** a defect localized at a single point in a crystal lattice, owing either to a missing atom (**vacancy***), or to a supernumerary atom, located between normal atom positions (**interstitial***), or yet to an extraneous atom, substituted for one of the atoms in the lattice. A **Frenkel pair*** is generated by the displacement of one atom out of its site in the crystal, thus yielding one vacancy, and one interstitial. 31–33, 96.

**Poisons** (neutron)**:** elements exhibiting a high neutron capture capability, used to counteract, at least in part, excess **reactivity*** in **fissile*** media. Four natural elements are particularly neutron absorbent: **boron*** (due to its B 10 isotope), cadmium, hafnium, and gadolinium (due to isotopes Gd 155, and Gd 157). Some poisons are known as "burnable" poisons, as they vanish gradually during burnup. Certain **fission products*** are neutron poisons. 22, 71, 72, 87, 88.

**Potential radiotoxicity** (of a given quantity of radionuclides, e.g. in waste)**:** potential radiotoxicity, defined as the product of the **radionuclide inventory***, multiplied by the ingestion dose factors for these radionuclides, is an indicator of the harmful potential of this quantity of radionuclides, in an accident situation. 79, 80.

**Pressurized-water reactor (PWR):** a reactor in which heat is transferred from the core to the heat exchanger by water kept at high pressure in the primary circuit, to prevent its boiling. See the Monograph as a whole.

**Pyrocarbon**, or **pyrolytic carbon:** amorphous carbon, yielded by the high-temperature decomposition of a gaseous hydrocarbon. Pyrocarbon is used as a coating layer in the makeup of fuel particles. 103, 105, 106, 109, 110, 112, 115, 116, 119.

**Pyrophoric:** this refers to a material liable to ignite spontaneously in air. 13, 124.

**Radioactive decay:** the transformation of a radionuclide into a different nuclide, by spontaneous emission of alpha, beta, or gamma radiation, or electron capture. The end product is a nucleus exhibiting lower energy, and more stable. Every radioactive decay process involves a well-defined half-life. 82, 83, 112.

**Radioactivity** (radioactive)**:** the property, exhibited by certain natural or artificial elements, of spontaneously emitting $\alpha$ or $\beta$ particles, or $\gamma$ radiation. More broadly, this term is used to refer to the emission of radiation concomitant with the **decay*** of an unstable element, or **fission***. 77, 84.

**Radiolysis:** the decomposition of matter by ionizing radiation. 22, 38, 84, 136.

**Radionuclide inventory:** the amount of fission products and actinides contained in an irradiated fuel, as a rule expressed in becquerels per gram initial heavy metal, or grams per tonne initial heavy metal (Bq/giHM, or g/tiHM). These amounts, and the associated isotopic spectra depend on a number of parameters, such as the nature of the fuel, and irradiation conditions (burnup…). Average inventories are computed, for a given point in time, by means of computation codes, whereas inventory distribution, depending as it does on irradiation conditions, and fuel thermics, requires use of characterization resources (electron microprobe…). 59, 68, 78–80, 82, 84.

**Reactivity:** a dimensionless quantity, used to evaluate small variations in the multiplication **factor*** $k$ around the critical value, and defined by the formula: $\rho = (k-1)/k$. Its value being very small, it is as a rule expressed in percent millirho (**pcm** unit). In a reactor, there is zero reactivity when the reactor is **critical**; reactivity is positive when it is **supercritical**, and negative when it is **subcritical**. 9, 35, 58, 63–65, 71–73, 87, 88, 137.

**Reactivity coefficient:** a variation in the **multiplication factor***, due to reactor operation, i.e. resulting from changes in temperature, and composition, due to the release of energy, and **neutron*** irradiation. 72.

**Release fraction:** as applied to fuel, this terms refers to the ratio of the quantity of fission products released from the fuel ceramic, over the total quantity yielded by fission reactions. 19, 22, 23, 92, 112, 138.

**RIA:** reactivity insertion accident. 63.

**Rim:** the region, at the periphery of a fuel **pellet***, that undergoes restructuring due to irradiation and thermal gradients. 19, 27, 29, 43, 84.

**Rod:** a small-diameter tube, closed at both ends, used as a component of a nuclear reactor core, holding fissile, fertile, or neutron-absorbent material. When it holds fissile material, the rod is a **fuel element***. 7–13, 16–19, 21–23, 28, 29, 35, 47–49, 51, 54, 55, 57–59, 63, 64, 67–69, 81–83, 87–89.

**Rod cluster control assembly (RCCA):** see **Control rod***. 11, 51–53, 63.

**SCANAIR:** a code having the chief characteristic of catering for such closely coupled processes as rod thermics, and mechanics, and fission gas behavior during a transient, on the basis of a rod initial state, as yielded by an irradiation computation. 64.

**Self-shielding:** the process whereby neutrons are preferentially absorbed by peripheral heavy atoms, in a fuel mass. Depending

on fuel geometry, such absorption may diminish, to a greater or lesser extent, penetration of neutrons into the inner regions of the fuel. 17, 103.

**SIMS** (secondary-ion mass spectroscopy)**:** this method, used for the analysis of the surface of materials, involves bombarding the sample with an ion beam, and analyzing the ions stripped from the surface, by means of a mass spectrometer. 27, 28, 30.

**Sintering:** an operation involving the welding together of grains of a compacted metal or ceramic powder, by heating it to a temperature lower than the melting point of the material. 13, 15, 47, 49, 104, 120.

**Sorbed:** see **Sorption***.

**Sorption:** the weak, reversible bonding of an atom, or molecule on a solid surface. 21.

**Specific burnup** (or **Burnup***, or "burnup fraction")**:** the total amount of energy yielded, per unit mass, in a nuclear fuel. This is generally expressed in megawatts–day per tonne (MWd/t). 71–75, 93, 113, 117, 119.

**Storage** (nuclear waste)**:** a storage facility is an installation in which waste is held, with a view to retrieving it at a later date (see also **Disposal***). 13, 36, 51, 71, 74, 77, 79, 81–83, 85, 92.

**Superphénix:** a prototype sodium-cooled fast reactor. 91.

**Swelling:** a phenomenon arising in materials under irradiation. 13, 18, 20, 25, 29, 32, 36, 41–44, 64, 68, 93, 95–97, 100, 113, 116, 119, 120, 124, 125, 131, 137.

**Temperature coefficient:** a coefficient expressing the variation in the **multiplication factor***, in a reactor, as its temperature varies. A negative temperature coefficient is an important criterion of core stability. 72.

**Toughness:** a characteristic quantity, for a material, expressed in $MPa \cdot m^{1/2}$, a measure of its resistance to crack propagation. 124.

**TOUTATIS:** a 3-D fuel application, developed from CEA's CAST3M finite-element code. 43.

**Transmutation:** the transformation, by means of a **neutron***-induced nuclear reaction (capture, **fission***), of one **isotope*** into another, and, more particularly, the transformation of a long-lived **radioactive*** isotope into a short-lived, or stable isotope. 7, 8, 79, 80, 99–101.

**TRIPOLI:** a Monte-Carlo-type computation code, used to model neutron transport. 73.

**TRISO:** a type of fuel particle, comprising a fissile, or fertile material kernel, coated with 4 successive layers: porous pyrocarbon, dense pyrocarbon, SiC, dense pyrocarbon. 103, 104, 107, 111–113, 119–122.

**UOX:** the standard **light-water reactor*** fuel, consisting of uranium 235-**enriched*** uranium oxide. 74, 75, 77–79, 82, 99.

**Uranium:** the heaviest natural element, having atomic number 92.

**Vacancy:** (see **Point defect***).

**VERCORS:** an analytical software program, developed at CEA, for the investigation of fuel behavior, and FP release. 68–70.

**Zircaloy:** an alloy of zirconium and one or more other metals (tin, iron, chromium, nickel), exhibiting particularly good mechanical strength, and chemical resistance. It is used in fuel cladding designs. 8, 10, 16, 36-39, 42, 57, 67, 69, 87–89, 128.

Contributors to the present volume:

Yannick Guérin (Topic Editor)
Jean-Luc Guillet (Topic Editor)
Alain Ballagny
Jean-Luc Béchade
Bernard Bonin
Jean-Christophe Brachet
Marc Delpech
Sylvie Dubois
Gérard Ducros
Cécile Ferry
Michel Freyss
Didier Gilbon
Jean-Paul Grouiller
Daniel Iracane
Sylvie Lansiart
Patrick Lemoine
Richard Lenain
Philippe Marsault
Bruno Michel
Jean Noirot
Daniel Parrat
Michel Pelletier
Christophe Perrais
Mayeul Phelip
Sylvie Pillon
Christophe Poinssot
Joëlle Vallory
Carole Valot

… together, of course, with all the members of the DEN Monographs Editorial Committee:

Bernard Bonin (Editor in chief), Alain Vallée (CEA Saclay Center), Martine Dozol (CEA Cadarache Center), Michaël Lecomte (CEA Valrho Center), Bernard Bouquin (Communications Division), Michel Beauvy, Georges Berthoud, Mireille Defranceschi, Gérard Ducros, Yannick Guérin, Yves Limoge, Charles Madic, Gérard Santarini, Jean-Marie Seiler, Pierre Sollogoub, Étienne Vernaz.